

Arild Kjølle

Microbiologically induced calcite precipitation as a method for ground improvement in granular and cohesive soils

Master's thesis in Geotechnics
Supervisor: Professor Rao Martand Singh
July 2021


Arild Kjølle

Microbiologically induced calcite precipitation as a method for ground improvement in granular and cohesive soils

Master's thesis in Geotechnics
Supervisor: Professor Rao Martand Singh
July 2021

Norwegian University of Science and Technology
Department of Civil and Environmental Engineering



<p>Project title:</p> <p>Microbiologically induced calcite precipitation as a method for ground improvement in granular and cohesive soils.</p>	<p>Date:</p> <p>09.07.2021</p> <p>Number of pages:</p> <p>222</p> <p>Number of appendix:</p> <p>0</p>
<p>Author:</p> <p>Arild Kjølle</p>	
<p>Department at NTNU:</p> <p>Department of Civil and Environmental Engineering</p>	
<p>Degree:</p> <p>Master of Science in engineering (Msc.)</p> <p>Master i ingeniørfag / Sivilingeniør</p>	
<p>Study programme:</p> <p>Civil and Environmental Engineering, specialization in geotechnics</p> <p>Bygg- og Miljøteknikk, fordypning i geoteknikk</p>	
<p>Supervising Professor:</p> <p>Professor Rao Martand Singh</p>	
<p>Key search words:</p> <p>Microbiologically induced calcite precipitation (MICP) by <i>S. pasteurii</i></p> <p>MICP in granular soils and cohesive soils</p> <p>MICP in cold climate ground conditions</p> <p>Norwegian University of Science and Technology (NTNU)</p>	
<p>Norwegian University of Science and Technology Department of Civil and Environmental Engineering</p>	

Preface

This thesis is conducted as an extensive literature review on the research conducted on microbially induced calcite precipitation (MICP). The thesis is the finalization of the master's degree programme in civil and environmental engineering and conducted as part of the course TBA4900 at NTNU. The main supervisor of the study has been Prof. Rao Martand Singh at the department for civil and environmental engineering at NTNU.

This study is conducted with the aim to evaluate the viability of MICP using *S. pasteurii* as an alternative and more sustainable method for ground improvement, including cold climate ground conditions. The extended aim of the thesis is to contribute to the work being conducted by researchers around the world to develop suitable strategies for implementation of MICP and to address the challenges facing the implementation in situ. The work is aimed at an audience within geotechnical engineering and others that work with or have an interest in ground improvements. I would like to express gratitude for the guidance and support of Prof. Rao Martand Singh throughout the spring semester.

Trondheim 09.07.2021

Arild Kjølle

Arild Kjølle

Summary

Microbiologically induced carbonate precipitation (MICP) have the potential to be an alternative and more sustainable method for ground improvement, which can reduce the use of cement products, is less intrusive to the soil and have a lighter footprint on the terrain. MICP uses bio-mineralization induced by ureolytic bacteria through ureolysis which leads to precipitation of calcium carbonate (CaCO_3) usually in the form of calcite. This mineral act as a binder that cement the particle contacts and increase the shear strength and stiffness of the soil or reduce the porosity and permeability of the soil. The major part of the studies on MICP have been conducted on granular soils, while a smaller number on cohesive soils. The work of this thesis have been conducted as an extensive literature review on MICP, where the research aim is to evaluate the viability of MICP with *S. pasteurii* as a method for ground improvements including its viability in cold climate ground conditions. The evaluation is conducted on the basis of the research objectives, which are to research *S. pasteurii* suitability for MICP in soils, the factors affecting the MICP process, the achieved enhancement of shear strength in MICP-treated granular and cohesive soils, the resulting residual permeability in MICP-treated granular soil and the challenges facing the in situ implementation of MICP.

The findings show that ureolysis by *S. pasteurii* and consequent precipitation is viable in both granular and cohesive soils under oxic conditions and at temperatures in the range 4-50°C. For MICP-treated granular and cohesive soils, the shear strength is significantly increased with increasing calcium carbonate concentration (CCC), where the relation is exponential in MICP-treated sands. The degree of reduction in permeability of MICP-treated sands increases with increasing CCC, particle size and porosity, while dilatancy and brittleness at low strain increases with increasing CCC. Strain-hardening behaviour in MICP-treated clay increases with increasing CCC, while brittleness increases with increasing CCC in silty clay. The research show that the implementation of MICP in situ faces some challenges, where potential solutions are indicated for uniform spatial distribution of CaCO_3 binder, removal of NH_4^+ in granular soils and controllability of the precipitation rate, which govern the cementation pattern and hence the residual permeability post-treatment in granular soils. The cementation pattern is however indicated to be affected by degree of saturation, independent of the precipitation rate. The research do not provide indications on viability for precipitation or cell growth under anoxic conditions, removal of NH_4^+ through rinsing or low pressure injections in

cohesive soils or distribution of CaCO_3 binder across low permeability layers in stratified deposits with varying permeability. Further studies on the long-term durability of CaCO_3 binder under cyclic FT is needed for a proper evaluation of the viability of MICP in cold climate ground conditions.

This thesis conclude that MICP is evaluated to be viable using *S. pasteurii* in regions without cyclic FT under oxic conditions in granular soils. Ureolytic activity and consequent precipitation under oxic conditions is found to be viable in cohesive soils, while MICP at the current stage of development, is evaluated to not be viable in cohesive soils such as fine silt and clay. This is due to the lack of strategies that can enable distribution of fluids through low pressure injections in low permeability soils nor rinsing of NH_4^+ through injection and extraction of rinse solution in low permeability soils. This thesis suggests an evaluation of two proposed approaches to adress uniform distribution of binder in MICP-treated granular soil and injection and distribution of binder in cohesive soils.

Sammendrag

Indusert mikrobiologisk utfelling av kalsiumkarbonat (MICP) har potensiale til å bli en alternativ og mer bærekraftig metode for grunnforsterkning som kan redusere bruken av sementbaserte bindemidler, er mindre forstyrrende for grunnen og har et lettere avtrykk på terrenget. MICP anvender bio-mineralisering gjennom hydrolyse av urea som leder til utfelling av kalsiumkarbonat (CaCO_3), som oftest i form av kalkstein som binder jordpartiklene sammen og øker skjærfasthet og stivhet eller reduserer porøsiteten og permeabiliteten i den behandlede jorden. Majoriteten av forskningen på MICP er utført med hensyn på friksjonsjordarter, og et mindretall på kohesjonsjordarter. Arbeidet med denne studien har blitt utført som et omfattende litteraturstudie av tilgjengelig forskning relatert til MICP, med det forskningsmål å evaluere egnetheten til MICP med *S. pasteurii* som metode for grunnforsterkning, inkludert anvendelse av metoden under grunnforhold i kaldt klima. Evalueringen er utført på basis av objektivene i denne studien, som er å undersøke *S. pasteurii* sin egnethet som utøvende bakterie i MICP, de påvirkende og drivende faktorene i MICP prosessen, oppnådd skjærfasthet i MICP-behandlet friksjons- og kohesjonsjord samt reduksjon av permeabilitet i MICP-behandlet friksjonsjord.

Resultatene i denne studien viser at hydrolyse av urea med *S. pasteurii* og påfølgende utfelling av CaCO_3 kan skje ved 4-50°C under forhold med tilgjengelig oksygen i både friksjons- og kohesjonsjord. For MICP-behandlet sand og kohesjonsjordarter så øker skjærfastheten betraktelig med økende konsentrasjon av kalsiumkarbonat (CCC), hvor økningen er eksponentiell for sand. Graden av reduksjon i permeabilitet for MICP-behandlet sand øker med økende CCC, kornstørrelse og porøsitet, mens det observeres økende sprøhet ved lav tøyning og økende dilatans med økende CCC. For MICP-behandlet leire så observeres økende kontraktant oppførsel og skjærfasthet ved økende CCC, mens MICP-behandlet siltig leire viser økende sprøhet med økende CCC. Funnene i denne studien tilsier at implementering av MICP in situ står ovenfor noen utfordringer. For friksjonsjord så indikerer forskningen mulige løsninger og gjennomførbarhet for uniform distribusjon av CaCO_3 , fjerning av NH_4^+ etter behandling og kontroll av utfellingsraten som er styrende for mønsteret på sementeringen i.e restpermeabiliteten. Det bør noteres at det er funnet indikasjoner på at mønsteret på sementeringen kan påvirkes av graden av vannmetning, uavhengig av faktorene som kontrollerer utfellingsraten.

Det er ikke funnet noen indikasjoner i forskningen på gjennomførbarhet for hydrolyse av urea eller cellevekst under forhold med begrenset tilgang til oksygen, fjerning av NH_4^+ i kohesjonsjord, injeksjon og distribusjon av bakterie- og sementeringsløsning i kohesjonsjord eller distribusjon av CaCO_3 på tvers av lag med lav permeabilitet i lagdelte masser med varierende permeabilitet.

Konklusjonene er at MICP med *S. pasteurii* er evaluert til å være egnet i friksjonsjord som ikke er gjenstand for sykliske fryse og tine (FT) prosesser under forhold med tilgang til oksygen. Det er behov for videre undersøkelser rundt effekten av syklisk FT over tid på CaCO_3 for evaluering av egnetheten til MICP i kaldt klima. På nåværende tidspunkt i utviklingen, så er MICP evaluert til å være uegnet i kohesjonsjord som fin silt og leire, grunnet mangel på tilnærminger som kan realisere distribusjon av flytende løsninger ved injeksjoner under lavt trykk i jord med lav permeabilitet samt fjerning av NH_4^+ etter behandling i jord med lav permeabilitet. Denne studien foreslår en evaluering av to tilnærminger som muligens kan løse utfordringer ved uniform distribusjon av CaCO_3 i friksjonsjord samt injeksjon og distribusjon i kohesjonsjord.

List of contents

PREFACE	II
SUMMARY	IV
SAMMENDRAG	VI
LIST OF FIGURES.....	XI
LIST OF TABLES.....	XXV
1. INTRODUCTION	1
1.1 BACKGROUND	1
1.2 RESEARCH AIM AND OBJECTIVES	2
1.3 THESIS OUTLINE	3
2. SOILS.....	4
2.1 PARTICLE SHAPE AND SURFACE TEXTURE	4
2.2 GRAIN SIZE.....	4
2.3 POROSITY AND RELATIVE DENSITY	6
2.4 GRADING AND COMPACTION.....	8
2.5 FLOW THROUGH POROUS MEDIA	9
2.5.1 Permeability.....	9
2.6 STRUCTURAL STABILITY OF SOILS	11
2.7 SOIL FABRIC.....	13
2.8 MINERALOGY	17
2.8.1 Clays	17
2.8.2 Granular soils.....	19
2.9 PORE SIZE DISTRIBUTION IN FINE GRAINED SOILS.....	20
2.10 STRESS HISTORY	22
2.11 RESPONSE TO LOADING.....	23
2.12 INTERPARTICLE FORCES.....	25
2.13 FREEZE AND THAW CYCLES	28
2.14 PLASTICITY OF COHESIVE SOILS	29
2.15 ANISOTROPY	31
2.16 SHEAR STRENGTH	32
2.17 STRESS-STRAIN AND SOIL STATES.....	38
2.18 TRIAXIAL SHEAR TEST.....	40
2.19 UNCONFINED COMPRESSION TEST.....	41
2.20 SOIL ENHANCEMENT WITH BINDERS.....	42

3. MICROBIOLOGICALLY INDUCED CALCITE PRECIPITATION (MICP)	46
3.1 BACTERIA IN SOILS	46
3.2 BACTERIAL TRANSPORT WITHIN THE SOIL	47
3.3 GEOMETRIC COMPATIBILITY.....	49
3.4 DRIVING FACTORS FOR MICP	50
3.5 UREOLYTIC BACTERIA	52
3.6 BIOCHEMICAL REACTIONS.....	54
3.6.1 Ureolysis and precipitation	54
3.6.2 CO ₂ in ureolysis	56
3.6.3 Ammonium as a byproduct	56
3.7 UREASE ACTIVITY.....	58
3.8 FACTORS AFFECTING THE UREASE ACTIVITY.....	61
3.8.1 Soil properties.....	61
3.8.2 Anoxic conditions.....	66
3.8.3 Cell growth	69
3.8.4 Cementation solution.....	73
3.8.5 pH.....	74
3.8.6 Temperature	75
3.9 CELL SURFACE CHARGE.....	79
3.10 CEMENTATION.....	80
3.10.1 Precipitation of CaCO ₃	80
3.10.2 Effect of particle size distribution	85
3.10.3 Effect of particle shape and surface texture.....	86
3.10.4 Calcium carbonate crystals.....	88
3.10.5 Residual permeability post-treatment	95
3.10.6 Cementation patterns.....	96
3.11 CURING TIME	98
3.12 IN SITU APPLICATION OF MICP	100
3.12.1 Injection strategies	100
3.12.2 Liquid flow and bacteria retention	104
3.13 SCALED UP MICP EXPERIMENTS.....	106
3.14 CHALLENGES WITH UPSCALING.....	110
3.15 COMPARISON OF METHODS.....	112
4. IMPROVEMENT OF ENGINEERING PROPERTIES	114
4.1 GRANULAR SOILS	114
4.1.1 Unconfined compression strength.....	114
4.1.2 Durability under cyclic freeze and thaw	119
4.1.3 Durability under wetting and drying cycles	120

4.1.4 Durability under acidic rain exposure	121
4.1.5 Triaxial shear strength and volumetric response.....	122
4.1.6 Direct shear in silty sand	130
4.1.7 Reduction of permeability	131
4.2 COHESIVE SOILS	135
4.2.1 Unconfined compression strength UCS.....	135
4.2.2 Shear strength and volumetric response.....	141
5. DISCUSSION.....	143
5.1 FACTORS AFFECTING MICP	143
5.1.1 Cell growth.....	148
5.1.2 Urease activity	151
5.1.3 Ammonium as a byproduct.....	160
5.1.4 Geometric compatibility.....	162
5.1.5 Precipitation of CaCO ₃	165
5.1.6 Calcium carbonate crystals	170
5.1.7 Effect of particle characteristics.....	174
5.1.8 Cementation pattern.....	176
5.1.9 Flow and bacterial retention	178
5.1.10 Injection strategies and spatial distribution of CaCO ₃ binder	180
5.1.11 Comparison of methods	185
5.2 MICP-TREATED GRANULAR SOILS	186
5.2.1 Unconfined compression strength.....	188
5.2.2 Triaxial shear strength and volumetric response.....	191
5.2.3 Permeability.....	194
5.3 MICP-TREATED COHESIVE SOILS.....	197
5.3.1 Unconfined compression strength.....	198
5.3.2 Triaxial shear strength and volumetric response.....	199
5.4 S. PASTEURII AS A CAUSATIVE AGENT FOR MICP IN SOILS.....	201
5.5 VIABILITY AND CHALLENGES FOR MICP AS A METHOD FOR GROUND IMPROVEMENT	204
5.6 VIABILITY OF MICP IN COLD CLIMATE GROUND CONDITIONS.....	214
6. CONCLUSIONS	216
6.1 RESEARCH OBJECTIVES.....	216
6.2 VIABILITY OF MICP WITH S. PASTEURII	219
6.3 FURTHER WORK	221
7. BIBLIOGRAPHY	223

List of figures

Figur 1. Shows graphic describing sphericity and roundness of grains. Graphic from (Powers, 1953)	4
Figur 2 Illustration of well graded soil with uniformly shaped particles. Illustration from (Sandven et al., 2017)	6
Figur 3. Illustrates the states of density in relation to the relative density. Illustration from (Sandven et al., 2017).	7
Figur 4. Illustrates degree of compaction as a function of grading. Illustration from (Sandven et al., 2017).	8
Figur 5. Illustrate soil fabric of soils deposited as single grains. Illustration from (Holtz et al., 1981).	11
Figur 6. Show the particle structure in lacustrine clays. Illustration from (Sandven et al., 2017).	12
Figur 7. Show the particle structure in marine clays. Illustration from (Sandven et al., 2017).	12
Figur 8. Show the different elements of a soil fabric proposed by Collins and McGrown (1974) . Illustration from(Chang et al., 2011)	13
Figur 9. Show elementary particle arrangements of different soils. Illustration from (Collins and McGown, 1974).....	14
Figur 10. Show schematic representations of particle assemblages. (a,b,c) connectors, (d) irregular aggregations by connector assemblages, (e) irregular aggregations in honeycomb, (f) regular aggregation interacting with particle matrix, (g) interweaving bunches of clay, (h) interweaving bunches of clay with silt inclusions, (i) clay particle matrix and (j) granular particle matrix. Illustration from (Collins and McGown, 1974).	15

Figur 11. Shows particle associations in clays. a) dispersed and deflocculated, (b) aggregated but deflocculated FF association or paralell oriented aggregation, (c) EF flocculated but dispersed, (d) EE flocculated but dispersed, (e) EF flocculated and aggregated, (f) EE flocculated and aggregated (g) EF and EE flocculated and aggregated. Illustration from (Mitchell and Soga, 2005).....	16
Figur 12. Show schematic representations of pore space groups. Illustration from (Collins and McGown, 1974).....	17
Figur 13. Show silicon tetrahedron and silica tetrahedra arranged in a hexagonal network. Illu-stration from (Mitchell and Soga, 2005).....	18
Figur 14. Show octahedral unit and sheet structure of octahedral units. Illustration from (Mitchell and Soga, 2005).....	18
Figur 15. Show the forming process of clay mineral groups. Illustration from (Mitchell and Soga, 2005).....	19
Figur 16. Show differential pore volumes versus equivalent pore diameter derived from Nitrogen adsorption method. Data adapted from (Zaffar and Sheng-Gao, 2015).....	21
Figur 17. Show pore size distribution in the clays. Data adapted from (Chen et al., 2019).....	22
Figur 18. Show the effect of OCR on peak shear strength and change in volume during shear. Illu-stration from (Budhu, 2008).....	23
Figur 19. Illustrate the effects of drained and undrained conditions on volume change. Illustration from (Budhu, 2008).....	24
Figur 20. Show idealized stresspaths and stress-strain curves for dilatant and contractant soils. Illustration from (Sandven et al., 2012).....	25
Figur 21. Shows different failure mechanisms or stress response in soils. Illustration from (Mitchell and Soga, 2005).....	25

Figur 22. Show different interparticle forces divided into groups. Illustration from (Santamarina, 2003).....	26
Figur 23. Show the process of aggregation in fine particles. Illustration from (Zhang et al., 2016b).....	29
Figur 24. Show the fracturing process in coarse particles due to frost. Illustration from (Zhang et al., 2016b).	29
Figur 25. Show consistency changes as a function of water content in cohesive soil. Illustration from (Sandven et al., 2017).....	30
Figur 26. Illustrate the Tresca failure criterion for undrained shear strength and the equilibrium conditions.. Illustrations from (Emdal et al., 2009)	33
Figur 27. Show effect of increased confining pressure on undrained shear strength. Illustration from (Holtz et al., 1981).....	33
Figur 28. Show correlation between undrained shear strength and water content in Norwegian clays. Illustration from (Sandven et al., 2017).....	34
Figur 29. Illustrate the Mohr columb failure criterion for effective shear strength and the equilibrium conditions. Illustration from (Emdal et al., 2009).....	35
Figur 30. Show effects of dilation on the Columb's failure envelope and the different soil states . Illustration from (Budhu, 2008).	37
Figur 31. Show the response of different types of soils to shear. Illustration from (Holtz et al., 1981)	39
Figur 32. Show sketch of the unconfined compression test rig and strees conditions acting upon the sample during uniaxial shear. Illustration from (Sandven et al., 2017).	41
Figur 33. Show different applications for DSM columns. Illustration from (Covicorp, 2020).	42

Figur 34. Show example of mixing pattern with MSM. Illustration from (Covicorp, 2020).	43
Figur 35. Show stabilizing ground under planned retaining wall with MSM. Illustration from (Covicorp, 2020).	43
Figur 36. Shows MSM/DSM used to reduce permeability under flood protective constructions. Illustration from (Covicorp, 2020).	43
Figur 37. Show soil enacement under road and rail embankments. Illustration from (Covicorp, 2020).	44
Figur 38. Show MSM applied over cemented columns in soft top layer below a road embankment. Illustration from (Covicorp, 2020).	44
Figur 39. Show DSM used to cut off contaminated flows. Illustrations from (Covicorp, 2020).	44
Figur 40. Show principle for jet grouting to enhance soil. Illustration from (Van Passen et al., 2010)	45
Figur 41. Shows applied pressures during jet grouting in cohesive soils. Illustration from (grouting, 2021).....	45
Figur 42. Shows compatability for effective particle size (d_{10}) in relation to size of organism. The bounded region in the diagram represent the range of geometric compatability between pore size and bacteria size. Illustration from (Mitchell and Santamarina, 2005b).....	49
Figur 43. Show limitation boundaries in terms of effective particle size (d_{10}) and depth. Illustration from (Lin, 2016).	50
Figur 44. Show measured urease activity for different ureolytic bacteria. Data adapted from (Duraisamy, 2016)	53
Figur 45. Show Scanning Electron Microscopy (SEM) image of <i>S.pasteurii</i> bacteria. Image from (Ma et al., 2020b).....	53

Figur 46. Show SEM image of percipitated CaCO_3 on and in between sand particles. Image from at left side from (Choi et al., 2020a) and image at right from (Cheng et al., 2017)	55
Figur 47. Show final NH_4^+ removal as a function of distance from injection point. Data adapted from (Lee et al., 2019b)	57
Figur 48. Show sorbed NH_4^+ remaining after rinsing of MICP-treated soil. Data adapted from (Lee et al., 2019b).	58
Figur 49. Shows the effect of pH on urease activity. Data from Stocks-Fischer et Al. 1999 (■) and Whiffin 2004 (□). Illustration from (Van Paassen, 2009a)	59
Figur 50. Show normalised urease activity as a funtion of temperature for different cementation solutions. Data adapted from (Whiffin, 2004).	60
Figur 51. Show urease activity for different soils as a funtion of carbon content in the soil. Data adapted from (Gillman et al., 1995).	62
Figur 52. Show urease activity at different temperatures as a function of pH in natural soils. Data adapted from (Vahed et al., 2011).....	63
Figur 53. Show urease activity at different temperatures as a funtion of organic content in natural soils. Data adapted from (Vahed et al., 2011)	63
Figur 54. Show rise in pH in MICP-treated organic soil as an indication of urease activity. Data adapted from (Sidik et al., 2014).	64
Figur 55. Show urease activity as a function of urea concentration. Data adapted from (Moyo et al., 1989).....	65
Figur 56. Show urease activity as a function of temperature. Data adapted from (Moyo et al., 1989).....	65
Figur 57. Show the increase in density due to precipitation over time, in sands with a variation in dominating minerals. Data adapted from (Montoya, 2012)..	66

Figur 58. Show bacterial density as optical density at 600 nm (OD ₆₀₀) of S.pasteurii under aerobic and anaerobic conditions, as a function of time. Data adapted from (Mitchell et al., 2019).....	68
Figur 59. Show bacterial density and corresponding urease activity for S.pasteurii at 30°C . Data adapted from (Van Paassen, 2009a).....	70
Figur 60. Show the effect of urea on bacterial density of S. pasteurii, as a function of time. Data adapted from (Ma et al., 2020b).....	71
Figur 61. Show the effect of urea on urease capacity during cell growth of S. pasteurii, as a function of time. Data adapted from(Ma et al., 2020a)	71
Figur 62. Show effect of temperature and inoculation solution on growth of S.pasteurii. Data adapted from (Verba et al., 2016)	72
Figur 63. Show effect of temperature on bacterial density over time. Adapted with data from (Nayanthara et al., 2019).	73
Figur 64. Show effect of different salts on the urease activity of the S. pasteurii urease. Data adapted from (Gorospe et al., 2013).	74
Figur 65. Show normalized urease activity under varying values of pH. Data adapted from (Nayanthara et al., 2019)	75
Figur 66. Show regional average annual (1985-2014) temperatures in Norway. Illustration from (2021).....	76
Figur 67. Show groundwater temperatures in the nordic countries. Illustration from (NVE, 2021).	77
Figur 68. Show urease activity as a funtion of time for different temperatures. Data adapted from (Peng and Liu, 2019b).	78
Figur 69. Show urease activity as a function of time for different curing temperatures. Data adapted from (Nayanthara et al., 2019).....	78

Figur 70. Show measured zeta potential for <i>S. pasteurii</i> . Data adapted from (Williams et al., 2017).....	79
Figur 71. Show negative electric charge of cell membrane of <i>S. pasteurii</i> over time. Data adapted from (Ma et al., 2020b).	80
Figur 72. Show measured zeta potential for <i>S. pasteurii</i> . Data adapted from (Keykha et al., 2017)	80
Figur 73. Show equilibrium between precipitation and dissolution for CaCO_3 at 25°C. Data adapted from (De Moel et al., 2013)	81
Figur 74. Show percipitated CaCO_3 as a function of time for different temperatures. Data adapted from (Peng and Liu, 2019b).	82
Figur 75. Show comparison of amounts of percipitated CaCO_3 for different ureolytic bacteria. Adap-ted with data from (Nayanthara et al., 2019).....	83
Figur 76. Show precipitation of <i>S. pasteurii</i> in sand and silt. Data adapted from (Kim et al., 2014).....	84
Figur 77. Show precipitation of CaCO_3 as a function of magnesium ion concentration. Adapted from (Nayanthara et al., 2019).....	85
Figur 78. Show cementation as a function of particle size in different soils. Data adapted from (Rebata-Landa, 2007)	86
Figur 79. Show SEM images of grain size and shape used in the study. Image from (Nafisi et al., 2018).	87
Figur 80. Show SEM images of cementation on and between grains post-treatment. Image from (Nafisi et al., 2018)	87
Figur 81. Show the principle of paralell bond in particle to particle cementation, Illustration from (Nafisi et al., 2018).....	88

Figur 82. Show loss of mass (CaCO_3) as a function of number of WD cycles, for MICP-treated samples of poorly graded sand with different CCC. Data adapted from (Gowthaman et al., 2021). 89

Figur 83. Show the process of erosion of CaCO_3 mass during wetting. Illustration from (Gowthaman et al., 2021). 90

Figur 84. Show CaCO_3 crystal size as a function of biomass (bacterial density). Data adapted from (Al-Thawadi and Cord-Ruwisch, 2012)..... 91

Figur 85. Show cubic (left) CaCO_3 crystal formatio) at low cell concentration and spherical (right) at high concentrations. Image from(Cheng et al., 2007)..... 92

Figur 86. Shows a) weak CaCO_3 coating from high urease activity and effective CaCO_3 bridging of the grains from low urease activity. Image from (Cheng et al., 2016). 92

Figur 87. Show morohology of precipitated CaCO_3 by *S. pasteurii* at different temperatures. Images from (Jianyun, 2005) 93

Figur 88. Show morphology of CaCO_3 precipitated by *S. pasteurii* under different pH. Images from (Tang et al., 2020) 93

Figur 89. Shows crystal growth or size, as a function of cementation solution. Data adapted from (Al-Thawadi and Cord-Ruwisch, 2012)..... 94

Figur 90. Show SEM images of the morphology of percipitated CaCO_3 crystals at different ratios of Mg^{2+} and Ca^{2+} . Image from (Nayanthara et al., 2019). 95

Figur 91. Show effect of rising phreatic line (water table) in a slope. Illustration from (borders, 2021) 96

Figur 92. Show individual patterns and a combination of cementation patterns. Illustration from (Nayanthara et al., 2019). 97

Figur 93. Show classification of calcite (CaCO_3) crystals. Images from (Cui et al., 2017a). 98

Figur 94. Show UCS for increasing curing time for MICP-treated silty clay. Data adapted from (Teng et al., 2020) 99

Figur 95. Show UCS as a function of curing time for MICP-treated fine grained soil with different CCC. Data adapted from 99

Figur 96. Show UCS as a function of curing time for MICP-treated high plasticity clay. Data adapted from (Godavarthi Rajani, 2020)..... 100

Figur 97. Show concentration and distribution of CaCO_3 for one and two phased injection methods. Data adapted from (Cheng et al., 2019)..... 103

Figur 98. Show achieved UCS for one and two phased injection methods. Data adapted from (Cheng et al., 2019). 104

Figur 99. Show cementation for varying treatment strategies in coarse gravel. Images from (Van der Star et al., 2011)..... 106

Figur 100. Shows drilling through cemented mass (left) and drilled pathway (right). Images from (Van der Star et al., 2011) 107

Figur 101. Show grid of injection wells on top of projected pathway for pipeline (left) and stabilized gravel (right). Images from (Van der Star et al., 2011) (left) and (DeJong et al., 2014) (right).. 107

Figur 102. Resistivity mapping for soil profile before and after MICP-treatment. Illustration from (DeJong et al., 2014) (Deltares). 108

Figur 103. Show setup for larger scale MICP experiment in sand. Image from (Paassen, 2009) 109

Figur 104. Show the exposed cemented sand body. Image from (Paassen, 2009) 109

Figur 105. Show CaCO_3 concentration and distribution along the longitudinal centre line of cemented mass. Injection well at 1.5 m and extraction well at 6.5 m.. Plot and image from (Paassen, 2009). 110

Figur 106. Show UCS as a function of curing time for samples treated with lime and samples treated by MICP. Data adapted from (Umar et al., 2019) 112

Figur 107. Show hydraulic conductivity as a function of curing time for samples treated with lime and samples treated with MICP. Data adapted from (Umar et al., 2019)..... 113

Figur 108. Show comparison of acheived UCS between treatment with MICP, ash and cement in soil as a function of percentage additives for different curing times. Data adapted from (Oyediran and Ayeni, 2020) 113

Figur 109. Show acheived UCS as a function of CCC in sands, compiled from different studies. Data adapted from (Choi et al., 2020a). 114

Figur 110. Show acheived UCS as a function of CCC in sands, compiled from different studies. Data adapted from (Rahman et al., 2020a)..... 115

Figur 111. Shows acheived UCS in MICP-treated medium sand for different concentrations of cementation solutions. Data adapted from (Shahrokhi-Shahraki et al., 2015). 115

Figur 112. Show acheived UCS in two MICP-treated medium sands with different bacterial concentrations, with *S. pasteurii*. Data adapted from (Shahrokhi-Shahraki et al., 2015) 116

Figur 113. Show acheived UCS as a function of CaCO₃ content for different temperatures in MICP-treated sand. Data adapted from (Cheng et al., 2016). 116

Figur 114. Show acheived UCS as a function of CaCO₃ content for different levels of urease activity. Data adapted from (Cheng et al., 2016)..... 117

Figur 115. Show acheived UCS as a function of CaCO₃ content for differently graded MICP-treated sands. Data adapted from (Cheng et al., 2016)..... 117

Figur 116. Show acheived UCS as a function of CaCO_3 content for MICP-treated sand with different share of clay. Data adapted from (Cheng and Shahin, 2015) 118

Figur 117. Show acheived UCS in MICP-treated sand as a function of CaCO_3 content for different concentrations of cementation solution. Data adapted from (QABANY and Soga, 2014) 118

Figur 118. Show acheived UCS as a function of CaCO_3 content for varying degree of saturation in MICP-treated coarse sand. Data adapted from(Cheng et al., 2013) 119

Figur 119. Show UCS as a function of CaCO_3 content for MICP-treated uniform and well graded sands during FT cycles. Data adapted from (Cheng et al., 2016). 119

Figur 120. Show UCS as a function of FT cycles with varying number of treatment cycles of cementation solution in MICP-treated sand. Data adapted from (Sharma et al., 2021) 120

Figur 121. Show reduction in UCS as a function of number of WD cycles for MICP-treated poorly graded sand with different CCC. Data adapted from (Gowthaman et al., 2021)..... 120

Figur 122. Show UCS as a function of corrosion of CaCO_3 in MICP-treated sand with different CCC, due to acidic flushing. Data adapted from (Gowthaman et al., 2020). 121

Figur 123. Show change in friction angle as a function of CCC in MICP-treated sands, compiled from different studies. Data adapted from (Choi et al., 2020a) 122

Figur 124. Show measured friction angle as a function of CCC in MICP-treated sand with different degree of compaction. Data adapted from (Cui et al., 2017a).	123
Figur 125. Show measured cohesion as a function of CCC in MICP-treated sand with different degree of compaction. Data adapted from (Cui et al., 2017a). ..	123
Figur 126. Show change in friction angle as a function of CaCO ₃ content in MICP-treated sands with varying grading and degree of saturation. Data adapted from (Cheng et al., 2013).	124
Figur 127. Show undrained shear strength for MICP-treated sand with different CCC. Data adapted from (Cui et al., 2017a).	125
Figur 128. Show undrained failure modes under triaxial shear in MICP-treated sand with different CCC. Image from (Cui et al., 2017a)	125
Figur 129. Show brittleness index as a function of CCC in MICP-treated sand with different CCC. Data adapted from (Cui et al., 2017a).....	126
Figur 130. Show drained shear strength and strain response for MICP-treated sand with different particle shape. Data adapted from (Nafisi et al., 2018).....	127
Figur 131. Show drained volumetric response for MICP-treated sand with different particle shape. Data adapted from(Nafisi et al., 2018).....	127
Figur 132. Show drained shear strength and strain response for MICP-treated 50-70 Ottawa sand at different confining pressure and CCC, compiled from different studies. Data adapted from (Rahman et al., 2020a).	128
Figur 133. Show drained shear strength and strain response for MICP-treated 20-30 Ottawa sand at different confining pressure and CCC, compiled from different studies. Data adapted from (Rahman et al., 2020a).	129

Figur 134. Show drained volumetric response for MICP-treated 20-30 Ottawa sand at different confining pressure and CCC, compiled from different studies. Data adapted from (Rahman et al., 2020a).....	129
Figur 135. Show drained volumetric response for MICP-treated 50-70 Ottawa sand at different confining pressure and CCC, compiled from different studies. Data adapted from (Rahman et al., 2020a).....	130
Figur 136. Show undrained shear strength and strain response in MICP-treated sand with different degree of silt content. Data adapted from (Zamani and Montoya, 2015).....	130
Figur 137. Show undrained porepressure response for MICP-treated sand with different degree of silt content. Data adapted from (Zamani and Montoya, 2015).	131
Figur 138. Show permeability post-treatment as a function of CCC in different MICP-treated sands. Data adapted from(Rahman et al., 2020b)	131
Figur 139. Show normalized permeability post-treatment as a function of CCC for different concentration of cementation solution (CaCl ₂ /urea) in MICP-treated sand. Data adapted from (QABANY and Soga, 2014).	132
Figur 140. Show normalized permeability post-treatment as a function of CCC in MICP-treated sands with varying relative density. Data adapted from (Choi et al., 2020b)	132
Figur 141. Show normalized permeability post-treatment as a function of CaCO ₃ content for different levels of urease activity in MICP-treated sand. Data adapted from (Cheng et al., 2016)	133
Figur 142. Show UCS as a function of reduction in permeability in MICP-treated sand for different concentrations of cementation solution. Data adapted from (Shahrokhi-Shahraki et al., 2015).	133

Figur 143. Show acheived dry density as a function of CaCO_3 for increasing number of treatment cycles in MICP-treated sand.Data adapted from (Cui et al., 2017a).	134
Figur 144.Show permeability post-treatment as a function of CaCO_3 content for different levels of saturation and different grading in MICP-treated sand. Data adapted from (Cheng et al., 2013)	134
Figur 145. Show UCS in MICP-treated silty clay for different concentrations of cementation solution ($\text{CaCl}_2/\text{urea}$). Data adapted from (Teng et al., 2020).....	135
Figur 146. Show UCS in MICP-treated high plasticity clay for different concentration of cementation solution and curing time. Data adapted from (Godavarthi Rajani, 2020).....	136
Figur 147. Show acheived UCS as a function of concentration of cementation solution ($\text{CaCl}_2/\text{urea}$) for the MICP-treated fine grained soil with varying degree of fines and sand. Data adapted from (Sharma and Ramkrishnan, 2016).	137
Figur 148. Show acheived UCS and degree of reduction in water content for different concentrations of cementation solution ($\text{CaCl}_2/\text{urea}$) in MICP-treated soft clay. Data adapted from (Xiao et al., 2020).	137
Figur 149. Show UCS as a function of pH for different volumes of bacterial suspension in MICP-treated clay (<i>S.pasteurii</i>). Data adapted from (Keykha et al., 2017)	138
Figur 150. Show UCS as a function of clay content for different CCC in soil treated by stimulating indogenous bacteria in the soil (bio-stimulation). Data adapted from (Islam et al., 2020).	139
Figur 151. Show UCS as a function of water content in MICP-treated clay and clay treted with only cementation solution ($\text{CaCl}_2/\text{urea}$).. Data adapted from (Bing, 2015).	140

Figur 152. Show UCS for MICP-treated clayey silt at different percentage of max dry density. Data adapted from (Soon et al., 2013)..... 140

Figur 153. Show drained shear strength and strain response for MICP-treated clay and clay treated with only cementation solution (CaCl₂/urea) for different confining pressure. Data adapted from (Bing, 2015)..... 141

Figur 154. Show drained failure envelope for MICP-treated clay and clay treated with only cementation solution (CaCl₂/urea). Data adapted from (Bing, 2015).
..... 141

Figur 155. Show drained volumetric response for MICP-treated clay and clay treated with only cementation solution (CaCl₂/urea) for different confining pressure. Data adapted from (Bing, 2015)..... 142

List of tables

Tabell 1. Lists denotation of particles based on particle size. Data adapted from (Sandven et al., 2017) 5

Tabell 2. Lists denotation of soils as a function of size distribution. Data adapted from (Sandven et al., 2017). 5

Tabell 3. Lists denotations for morain as a function of silt content. Data adapted from (Sandven et al., 2017) 6

Tabell 4. Lists typical porosities for different Norwegian soils. Data adapted from (Sandven et al., 2017). 6

Tabell 5. Lists notations for degree of uniformity in a soil, based on coefficient of uniformity. Data adapted from (Sandven et al., 2017). 9

Tabell 6. Lists typical range of permeability in Norwegian soils. Data adapted from (Sandven et al., 2017). 10

Tabell 7. Lists main groupings of macrofabric elements in soils proposed by Collins and McGrown (1974). Data adapted from (Collins and McGrown, 1974).	14
Tabell 8. Lists plasticity and share of fines in the different clays in the study. Data adapted from (Zaffar and Sheng-Gao, 2015).	21
Tabell 9. Lists classification and range of plasticity index in Norwegian clays. Data adapted from (Sandven et al., 2017).	31
Tabell 10. Lists range of friction angle for different soils. Data adapted from (Budhu, 2008).	38
Tabell 11. Lists common nutrients for bacterial growth. Data adapted from (Mitchell and Santamarina, 2005b).	47
Tabell 12. Listsintended geotechnical applications for different bacteria used in previous studies. Data adapted from (Choi et al., 2020a).	52
Tabell 13. Lists degree of correlation between urease activity in indegenous soil bacteria and different soil properties at 16°C and 24°C. Data adapted from (Vahed et al., 2011).	62
Tabell 14. Lists compounds by ratio for proposed oxygen releasing mixture. Data adapted from (Chen et al., 2012).	69
Tabell 15. Lists previous findings of optimal pH range for S.pasteurii. Data adapted from (Crowley et al., 2019).	75
Tabell 16. Lists gradation for the Ottawa sands. Data adapted from (Covicorp, 2020).	128
Tabell 17. Lists soil properties of samples in the study. Data adapted from (Sharma and Ramkrishnan, 2016).	136
Tabell 18. Lists properties of the clays used in the study. Data adapted from (Bing, 2015).	139

1. Introduction

1.1 Background

Soil is a natural material made up of mineral constituents of variable size, which differ from the parent materials in their morphological, physical, chemical, and mineralogical characteristics (Hamza and Anderson, 2005). As part of civil engineering, it is often the case that the soil at locations where there are plans for development of infrastructure or buildings, do not possess satisfactory geotechnical engineering properties to support the added load from the planned structures. Roads and railways are subject to settlements and instability in saturated soft cohesive soils or loose granular soils. Dikes, dunes and slopes can experience a reduction in or loss of stability, coastlines and riverbanks are exposed to erosion, while earthquakes can cause liquefaction in loose saturated sediments and damage structures. In other cases, existing structures on soils that have experienced a reduction in its initial engineering properties which can affect the stability of foundations or slopes, needs to be reinforced. Some times it is necessary to reduce the permeability in the ground to reduce or limit diffusion of polluted liquids from ground deposits, into the groundwater system. In other cases, there is a need to control the flow of water into or around structures to maintain stability.

To increase the strength and stiffness or reduce the permeability of soils, methods such as cement grouting, mass stabilization mixing (MSM) or deep soil mixing (DSM) with cement, lime or chemical binders, are often applied. These binders, bridge the particles together through cementation and reduce the voids in the material, hence making the material stronger, stiffer and denser. However, these methods for ground improvement have a high carbon footprint, are invasive to the soil, are energy demanding and in general less sustainable for the environment. Cement is an integral part in most of the existing grouting and soil mixing methods and the production of cement is according to (Andrew, 2019), assumed to contribute to as much as 8% of the global CO₂ emissions. To achieve the collective goal of reducing CO₂ emissions, the construction industry needs access to innovative and more sustainable methods for ground improvement that will contribute to reaching this goal. A path to reduce the adverse effects of ground improvement with heavy machinery and cement based binders, is to develop a

viable and more sustainable technique adapted from naturally occurring phenomena such as bio-mineralization.

Microbiologically induced carbonate precipitation (MICP), is a relatively new technology that uses bio-mineralization through hydrolysis of urea (ureolysis) to increase the stiffness and strength or reduce the permeability or porosity of soils. This process involves ureolytic bacteria that produce the urease enzyme, which degrade urea and in the presence of sufficient concentrations of dissolved calcium ions (Ca^{2+}) and carbonate (CO_3^{2-}), precipitate calcium carbonate (CaCO_3) usually in the form of calcite, which act as binder between the soil particles. The CO_2 released from bacterial respiration during ureolysis is sequestered through the bio-mineralization process. However, ammonium (NH_4^+) and ammonia (NH_3) is generated as part of ureolysis and need to be removed from the treated soil.

The method has still not been widely applied in the industry as a commercial solution for enhancement of engineering properties in soils, where the implementation of MICP in situ faces some challenges such as achieving uniform distribution of CaCO_3 binder within the treated area as well as injection of solutions and flow of liquid in low permeability soils, treatment in anoxic conditions below the watertable, controllability of cementation pattern and residual permeability as well as removal of byproducts from the treated soil. There have been conducted several studies on MICP with a collective aim to identify and address these challenges. For MICP to be a viable and competitive alternative to the traditional use of cement based binders, these challenges need to be addressed.

1.2 Research aim and objectives

The degree of enhancement in shear strength and reduction in permeability or porosity that can be achieved using MICP in granular soils have been extensively studied, while fewer studies have been conducted on cohesive soils. Some of the factors affecting the MICP process such as effects of pH, temperature, bacterial density, concentration of cementation solution as well as effects of urease activity, temperature or pH on precipitation, have been extensively studied. There are few studies addressing the effects of anoxic conditions, clay minerals and restricted pore space on urease activity. Most of the research is conducted as lab studies, while a few studies have been conducted as large scale field studies in granular soils, whereas none in cohesive soils. Although several ureolytic

bacteria have been investigated for the purpose of MICP, *S. pasteurii* seem to be the most frequently used and is found to be the most robust and suitable causative agent for this purpose. The research aim of this thesis is to evaluate the:

- ***Viability of MICP with *S. pasteurii* as a method for ground improvement in granular and cohesive soils, including viability in cold climate ground conditions.***

The evaluation is conducted on the basis of the research objectives of this thesis, as listed below:

- ****S. pasteurii* as a causative agent for MICP in soils.***
- ***Factors affecting the MICP process***
- ***Achieved enhancement of shear strength and residual permeability in MICP-treated granular soil***
- ***Achieved enhancement of shear strength in MICP-treated cohesive soils.***
- ***Challenges for implementation of MICP in situ***

Limitations:

Due to restrictions tied to handling of bacteria, the planned lab investigations on MICP at low temperatures in sand and cohesive soils, could not be conducted. Given the low number of studies in the literature addressing MICP at low temperatures, results from those studies would have contributed to a stronger basis during evaluation of the viability of MICP in cohesive soils as well as in cold climate ground conditions.

1.3 Thesis outline

The introduction in chapter 1 describes the background for the thesis, the research aim and objectives as well as limitations of the work, while chapter 2 describes soil properties and mechanical behaviour of soils, geotechnical applications of cement and lime based binders as well as requirements for viability of MICP as a commercial solution for ground improvement. In chapter 3, bacteria in soils, ureolytic bacteria, geometric compatibility of soil and bacteria, hydrolysis of urea (ureolysis), factors affecting MICP, precipitation, crystal morphology, cementation pattern, curing time, injection strategies and bacteria retention, are described. Chapter 3 further show comparisons of treatment with MICP

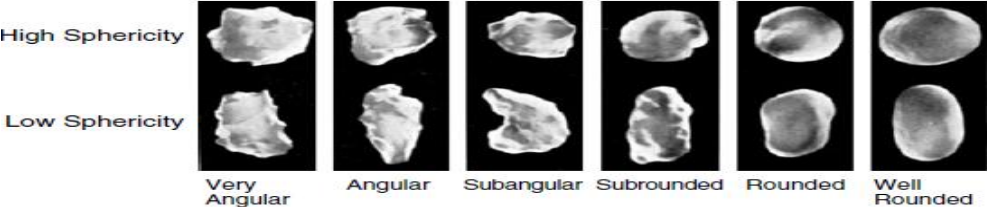
and cement or lime and it further describes larger scale field studies with MICP in granular soils.

Chapter 4 describes results for shear strength, volumetric response and reduction in permeability as well as the effect of cyclic freeze and thaw, wetting and drying cycles and exposure to acidic rain, on the shear strength in MICP-treated granular soils. Chapter 4 further describes results for shear strength and volumetric response in cohesive soils. In chapter 5, the results of the research in this thesis are discussed in respect to the research aim and objectives, while chapter 6 seek to give a conclusion on the research aim of the thesis through the stated research objectives. Chapter 6 further state recommendations for further work, while chapter 7 is assigned to the bibliography.

2. Soils

2.1 Particle shape and surface texture

It is noted by (Sandven et al., 2017), that the shape or morphology of the soil particles can be characterized as rounded or angular, while the surface by smoothness or roughness. (Mitchell and Soga, 2005) describes the particle morphology as spherical, rounded, blocky, bulky, platy, elliptical or elongated, where sphericity depend on the elongation and roundness on the angularity. (Sandven et al., 2012) further note that rock fragments transported under glaciers, result in sharp and angular grains with a rough surface, whereas rock fragments transported in water results in more rounded grains with a smoother surface. Historically, particle morphology in soil mechanics are described by comparing single grains against standard charts, such as the graphic presented below.



Figur 1. Shows graphic describing sphericity and roundness of grains. Graphic from (Powers, 1953)

2.2 Grain size

The particles in soils display large differences in size due to factors such as mineralogy, structural strength of original rock and processes of erosion and

abrasion. The conditions during sedimentation, will according to (Sandven et al., 2012) decide the distribution of coarser and finer particles in a given soil.

Soil particles are identified according to their size, as presented in the table below.

Tabell 1. Lists denotation of particles based on particle size. Data adapted from (Sandven et al., 2017)

Principal denotation	Sub-denotation	Grain size [mm]
<i>Block</i>	-	> 60
<i>Cobbels</i>	-	600-60
<i>Gravel</i>	Coarse	60-20
	Medium	20-6
	Fine	6-2
<i>Sand</i>	Coarse	2-0,6
	Medium	0,6-0,2
	Fine	0,2-0,06
<i>Silt</i>	Coarse	0,06-0,02
	Medium	0,02-0,006
	Fine	0,006-0,002
<i>Clay</i>	-	< 0,002

Soils are described on the basis of their grain size distribution, as presented in the table below (Sandven et al., 2012).

Tabell 2. Lists denotation of soils as a function of size distribution. Data adapted from (Sandven et al., 2017).

Particle content	Description of soil
> 30% clay	clay
15-30% clay	clay + adjective of other fractions
5-15% clay	clayey
> 45% silt	silt + adjective of other fractions
15-45% silt	silty
> 60% sand, gravel or cobbel	sand/gravel/cobbel+ adjective
20-60% sand, gravel or cobbel	Sandy/gravelly/ cobbly

Morain (till) is a well graded mixed glacial deposit, which can contain grain sizes from clay to block. Classification based on material < 0,06 mm, is used to

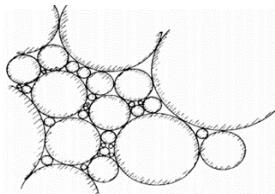
describe the morainic material and calculated as weight percentage of the material fraction < 20 mm. The notations are presented in the table below.

Tabell 3. Lists denotations for morain as a function of silt content. Data adapted from (Sandven et al., 2017)

Particle content	Notation of morain
> 15 % silt	Gravelly moraine
15 - 35 % silt	Sandy moraine
> 35 % silt	Silty moraine

2.3 Porosity and relative density

It is noted by (Nimmo, 2004) that the porosity will affect the free movement of water, air, nutrients, chemicals and bacteria within the soil. A granular soil with uniform particle size and shape, will have a higher porosity than one with particles of different sizes and shapes, where smaller particles fill the voids between the larger particles. The sketch presented below, illustrate a packed and well graded soil.



Figur 2 Illustrate well graded soil with uniformly shaped particles. From (Sandven et al., 2017)

The porosity (n) is defined as the fraction of the total soil volume that is taken up by the pore space, and can be calculated as:

$$n = \frac{V_p}{V_s} = \frac{\gamma}{\gamma_s(1+w)} \cdot 100 \quad [-] \quad \text{Eq. 2.3.1}$$

where V_p [m^3] is the pore volume, V_s [m^3] the volume of solid particles, γ [KN/m^3] the unit weight, γ_s [KN/m^3] the unit weight of solids and W [%] the natural water content. Typical values for porosity in norwegian soils are listed in the table below.

Tabell 4. Lists typical porosities for different Norwegian soils. Data adapted from (Sandven et al., 2017).

Soil	n [%]
Sand	30-50
Silt	40-55
Clay	40-60
Moraine	30-50
Peat	60-100

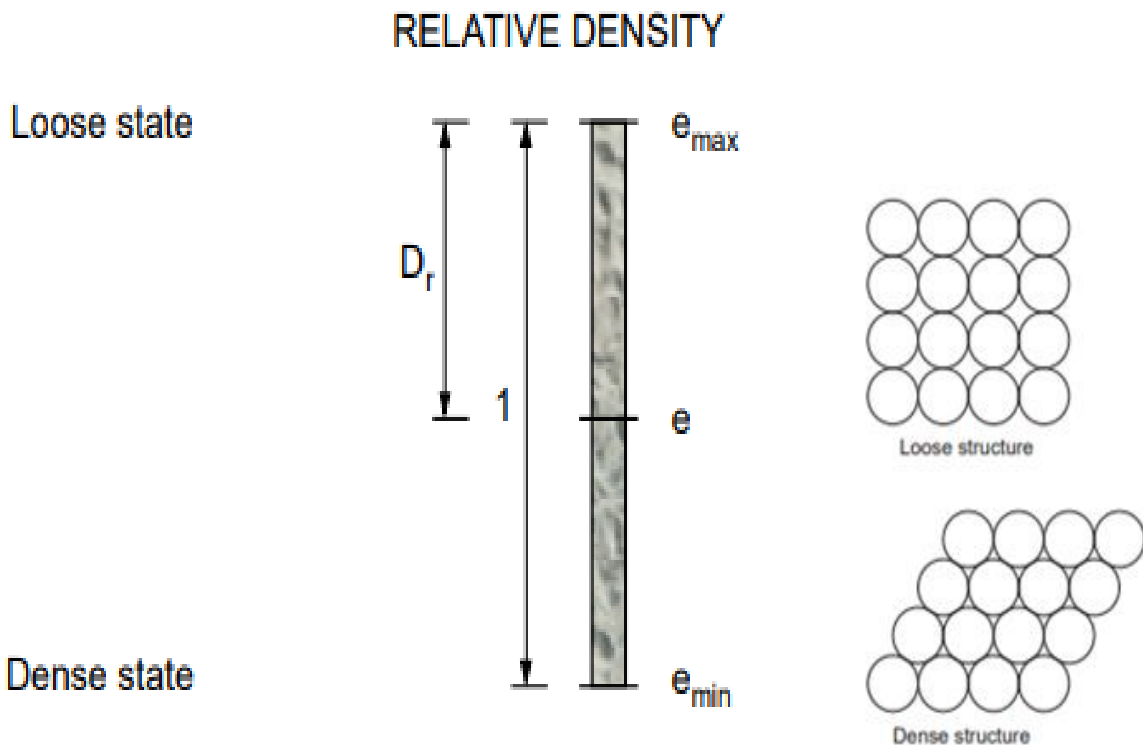
The void ratio (e) is commonly used for clays and is defined as the ratio between the pore volume and the volume of solid particles, where e exceed 1, when $V_p > V_s$ in a soil. Typical values for e in Norwegian clays are 0,6-1,5 and is calculated as:

$$e = \frac{V_p}{V_s} = \frac{\gamma_s (1+w)}{\gamma} - 1 \quad [-] \quad \text{Eq. 2.3.2}$$

For fully saturated soils:

$$e = \frac{w \cdot \gamma_s}{\gamma_w} \quad [-] \quad \text{Eq. 2.3.3}$$

In their work, (Mitchell and Soga, 2005) note that the packing range of particles in a given soil, is often related to the maximum and minimum void ratios, representing the loosest and densest states, respectively. Poorely graded soils tend to have a narrower range of possible densities compared to well graded ones, while soils with angular shape particles tend to be less dense than soils with more rounded particles. Relative density (D_r), is a measure of the current void ratio (e) in relation to the maximum (e_{max}) and minimum (e_{min}) void ratios. As illustrated below, e_{max} represents the loosest state, while e_{min} the densest state.



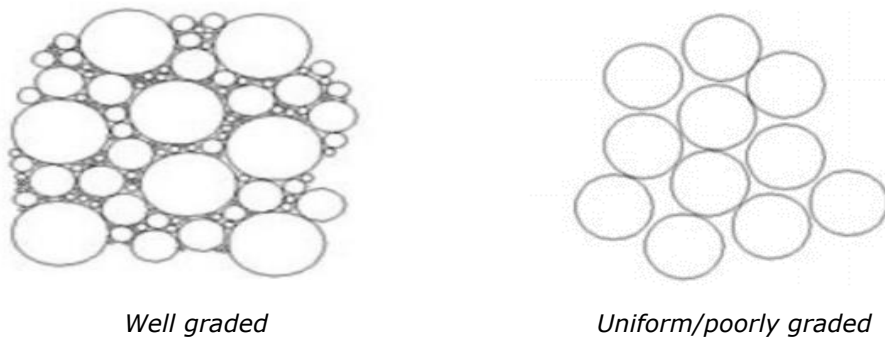
Figur 3. Illustrate states of density in relation to the relative density. Illustration from (Sandven et al., 2017).

The relative density together with the applied effective stresses, governs the mechanical behaviour of granular soils (Mitchell and Soga, 2005). D_r is defined as:

$$D_r = \frac{e_{max} - e}{e_{max} - e_{min}} \cdot 100 \% [-] \quad \text{Eq. 2.3.4}$$

2.4 Grading and compaction

Soil is a three-phase material, where the soil volume consists of solids, water and air, where (Knappett and Craig, 2012) note that solid particles and water can be considered as incompressible, whereas air is highly compressible. This enables a rapid reduction of soil volume during loading by rearrangement of particles in dry or partially saturated soils, whereas in saturated soils with low permeability the volume change will take much longer time, due to the water not being able to drain from the pores. In their work, (Sandven et al., 2017) state that a well graded soil will achieve a higher degree of compaction, whereas a more uniform or well sorted soil, will achieve a lower degree of compaction. The figures below illustrate examples of well and poorly graded soil matrices.



Figur 4. Illustrates degree of compaction as a function of grading. Illustration from (Sandven et al., 2017).

Poorly graded soils are usually sorted by water or wind, soils with a particle size range missing (gap graded soils) are sorted by water, while well graded soils such as glacial tills, are the product of bulk transport processes (Budhu, 2008). The slope of the distribution curve of a given soil, indicate the gradation of the material, expressed by the uniformity coefficient C_u (Sandven et al., 2017):

$$C_u = \frac{d_{60}}{d_{10}} [-] \quad \text{Eq. 2.4.1}$$

Where d_{10} and d_{60} are the particle diameters for which 10% and 60% of the particles are finer and is obtained from the distribution curve generated by the

results from mechanical sieving and hydrometer ($d < 63 \mu\text{m}$). The effective particle size d_{10} is important when regulating the flow of water through a soil, where a higher d_{10} translate to increased particle size and permeability in the soil. The d_{10} can indicate if coarser particles float in a matrix of fines, where the coarser particles may not be in effective contact with each other. The table below lists notations of uniformity in granular soils based on the derived C_u value.

Tabell 5. Lists notations for degree of uniformity in a soil, based on coefficient of uniformity. Data adapted from (Sandven et al., 2017).

Uniformity coefficient C_u	Gradation
> 15	Well graded
5-15	Medium graded
< 5	Uniformly or poorly graded

2.5 Flow through porous media

2.5.1 Permeability

Permeability is defined as the property of a porous material which permits the passage of fluids through its interconnecting voids. High permeability in a soil means that fluid can flow through at a higher velocity [m/s] and with a higher degree of ease, whereas low permeability indicates a lower flow velocity and lower degree of ease. It is noted by (Sandven et al., 2012), that the knowledge or determination of the permeability in soils within geotechnical engineering, is relevant for foundations, slope stability, seepage and internal erosion through earth dams, drainage under retaining walls and containment of polluted soil deposits among other geotechnical considerations.

In their work, (Mitchell and Soga, 2005) note that coarse soils will generally have a network of continuous pores which provide a better flow of fluids, where a poorly graded (uniform) sand will have higher permeability than a well graded sand, due to finer particles filling the voids between the larger particles in the well graded sand. Increased share of fine particles in a soil, will increase the available surface area for water to attach, where the retained water will not contribute to the fluid flow. (Mitchell and Soga, 2005) note that the water in clays is partly free water contributing to fluid flow and partly retained water adsorbed to the particle surfaces. Clays and fine silt have very low permeability, where fissures in clay increase its permeability, while coarse silt will have lower

permeability than that of fine sand. The permeability is related to particle size distribution, density and pore size distribution. (Yang et al., 2001) state that the pore channels in silt, are large enough for water to move relatively freely, but small enough to have capillary effects, which renders silts prone to frost heave in cold climate ground conditions. (Knappett and Craig, 2012) note that in stratified soil deposits, the permeability for flow parallel to the direction of stratification, is higher than for flow perpendicular to the direction of stratification.

The coefficient of permeability (k) also referred to as the hydraulic conductivity of a soil, describe the degree of ease for flow through the soil. This factor can be affected by the density and viscosity of a liquid, where k is a proportionality factor in Darcy's law and can be defined as the flow velocity at a gradient (i) equal to 1. The velocity (v) of the water flow can be calculated as (Sandven et al., 2017):

$$v = k \cdot i \text{ [cm/s]} \quad \text{Eq. 2.5.1.1}$$

The table below lists typical values for permeability in norwegian soils.

Tabell 6. Lists typical range of permeability in Norwegian soils. Data adapted from (Sandven et al., 2017).

Soil	Permeability k [cm/s]
Gravel	> 1
Homogenous sand	$1-10^{-3}$
Homogeneous silt	$10^{-3}-10^{-6}$
Moraine	$10^{-4}-10^{-7}$
Clay	$10^{-6}-10^{-9}$

The permeability of a soil, depends according to (Sandven et al., 2017) on the composition and distribution of grains as well as the quality of the fluid flowing through the pores. This relationship can be expressed as:

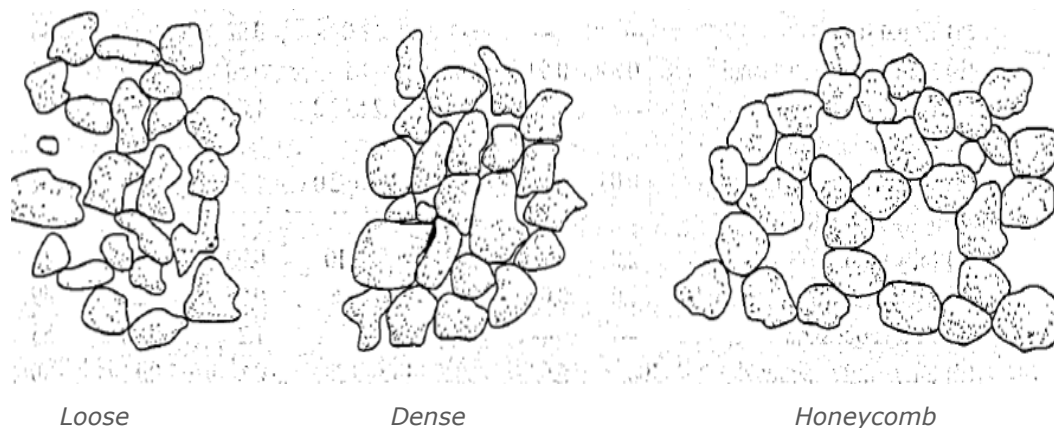
$$k = \frac{g}{\eta \cdot K} \quad \text{Eq. 2.5.1.2}$$

Where g is gravity [cm/s^2], η is kinematic viscosity [cm^2/s] and K is an empirical coefficient [cm^2] related to the grain size distribution, pore volume and soil density, while the ratio g/η represent the quality of water and varies with temperature.

2.6 Structural stability of soils

The structure of the soil skeleton will depend on conditions during sedimentation, particle size distribution and shape, minerals and organic matter among others. In their work, (Sandven et al., 2017) note that till often will be well graded with a dense structure, where the share of fines in the till will depend on the transportation and deposition of the material in the glacier. Tills are generally considered stable with good mechanical strength and they have decreasing permeability and increasing compressibility with increasing share of fines.

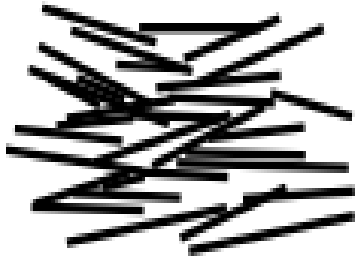
In their work, (Holtz et al., 1981) note that some single grained fabrics ($d > 0,01$ mm) have a very open structure with a very high void ratio, described as «honeycomb» fabric. Such a fabric is metastable, where the structure can support static loads, but is very sensitive to collapse under vibration or dynamic loading. Loose and poorly graded sands have according to (Sandven et al., 2017) an open and porous structure, making them more permeable and compressible as well as potentially unstable, whereas well graded sands have a denser packing, are less permeable and compressible as well as more stable. Although the single grain fabric of soils are more complex, an idea of the structure of single grained fabrics, can be seen in the illustration presented below.



Figur 5. Illustrate soil fabric in different states of density in soils deposited as single grains. Illustration from (Holtz et al., 1981).

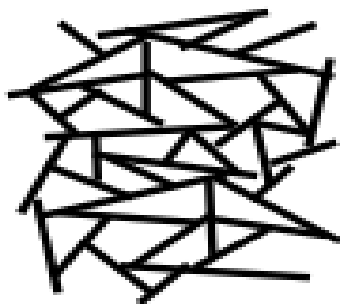
In their work, (Lin et al., 2016) note that the fabric structure of silts and sands is governed by the self-weight of the particle, thus it is relatively stable with changes in stress, whereas the fabric structure in clays is controlled by electrostatic interactions and the structure is subject to significant volumetric change with increasing confinement. (Sandven et al., 2017) state that lacustrine or fresh water clays, have a dense grain structure with particles oriented in parallel direc-

tions during sedimentation, due to the low number of ions in the fresh pore water. They have low permeability and high compressibility, where undrained shear strength properties will depend on cohesion, water content and stress history. Illustration below shows the structure of fresh water clays.



Figur 6. Show the particle structure in lacustrine clays. Illustration from (Sandven et al., 2017).

Marine clays and fine silts have an open and porous structure, where the particle contact points are of van der Waal character and have a card house structure. The strength of marine clays would generally depend on the same factors as fresh water clays, except the bonding between the particles is a function of remaining salt concentration in the pore water. This bonding will be very weak if the salt concentration in the porewater due to leaching, decreases below 0,5%. At this salt content the soil skeleton would be prone to collapse when disturbed, liquifying the soil and reducing the residual shear strength of the soil to almost zero. Illustration below shows the open structure of such marine sediments.



Figur 7. Show the particle structure in marine clays. Illustration from (Sandven et al., 2017).

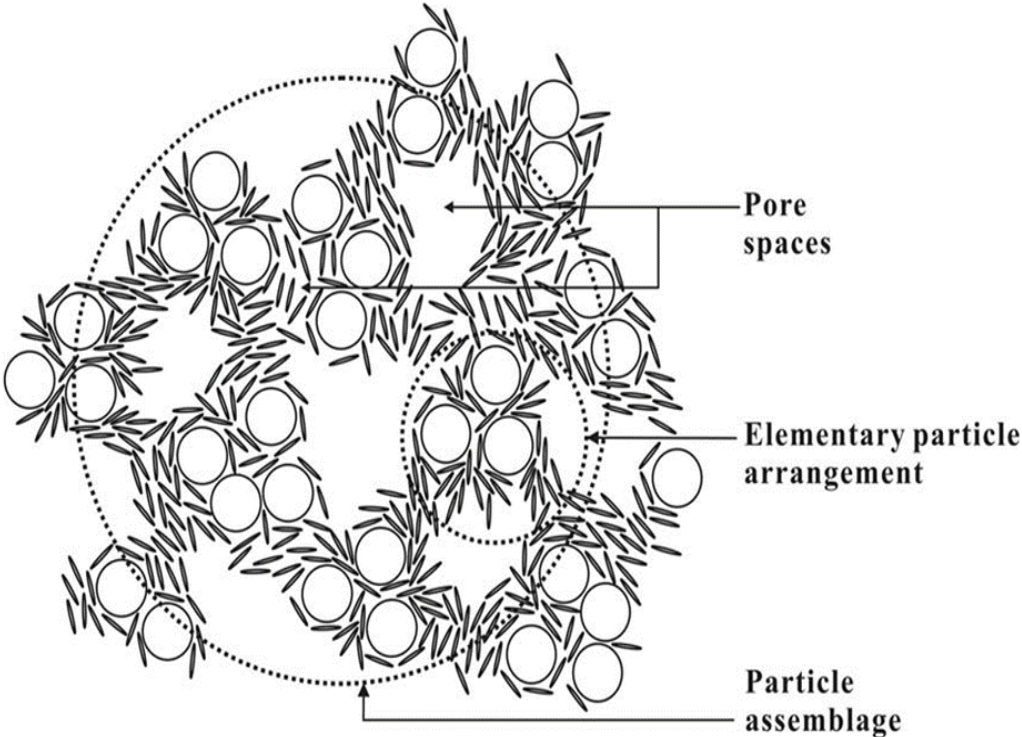
According to (Holtz et al., 1981), the macrofabric have a significant influence on the engineering behavior of fine grained soil deposits, where joints, fissures, intermediate silt or sand layers and channels left behind from decayed roots, will often govern the entire soils mass response to external loading or stress. The strength of a soil mass is significantly reduced along a crack or fissure and if unfavorably oriented in relation to applied stress, instability or failure may occur.

Intermediate layers of thin sand or silt within a thick clay deposit can influence the drainage properties of the clay deposit and may cause uncorrect calculated rates of settlement, if missed during initial investigations.

2.7 Soil fabric

It is noted by (Mitchell and Soga, 2005), that the fabric of a soil may be considered on three different levels of scale, where the *microfabric* consists of the regular aggregations of particles and the very small pores (0,1-0,3 μm), *minifabric* containing aggregations of microfabric and the interassemblage pores (100-200 μm) between them and the *macrofabric* containing cracks, fissures and root holes which correspond to transassemblage pores.

The *macro-* and *minifabrics* govern the hydraulic conductivity and thus the primary consolidation in fine grained soils, while the microfabric affect secondary settlement (creep). The macro fabric of soils can according to work by (Collins and McGown, 1974), be described as comprising three distinct elements, where soils are composed of one or some of these fabric elements. The features are shown in shown in the illustration presented below.



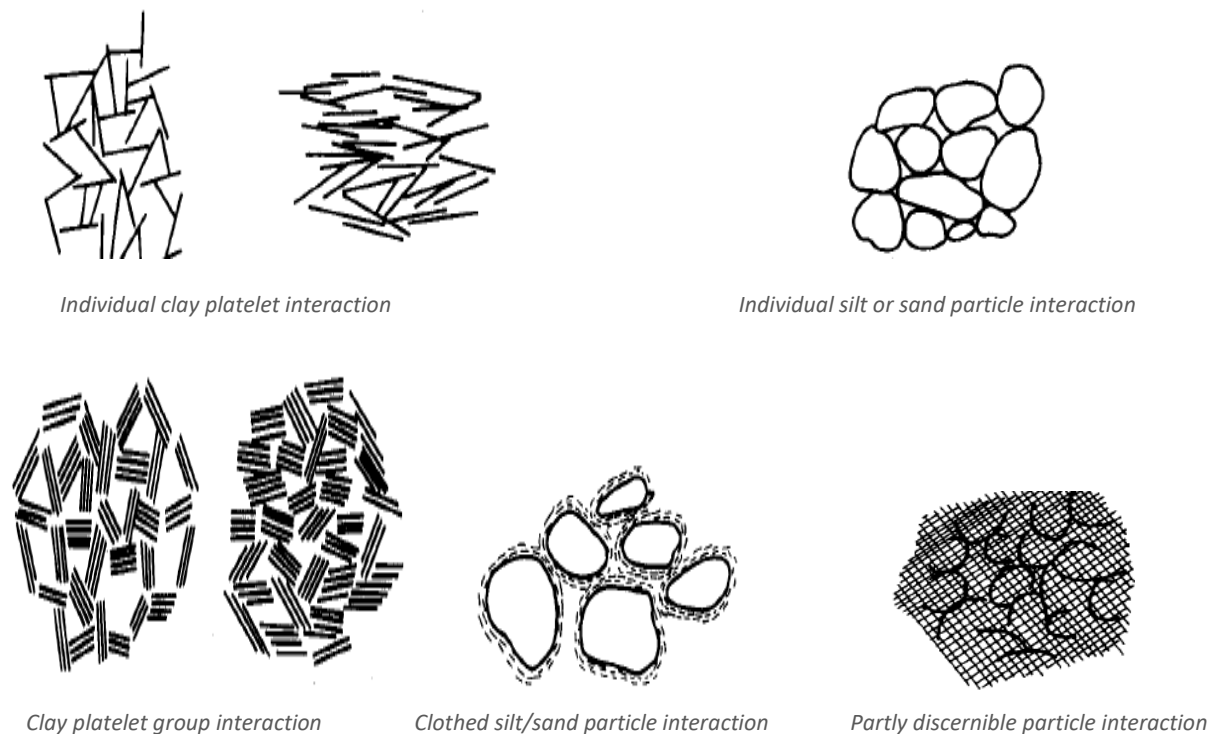
Figur 8. Show the different elements of a soil fabric proposed by Collins and McGrown (1974) . Illustration from(Chang et al., 2011)

The element groups proposed by (Collins and McGown, 1974), are described in the table below.

Tabell 7. Lists main groupings of macrofabric elements in soils proposed by Collins and McGown (1974). Data adapted from (Collins and McGown, 1974)

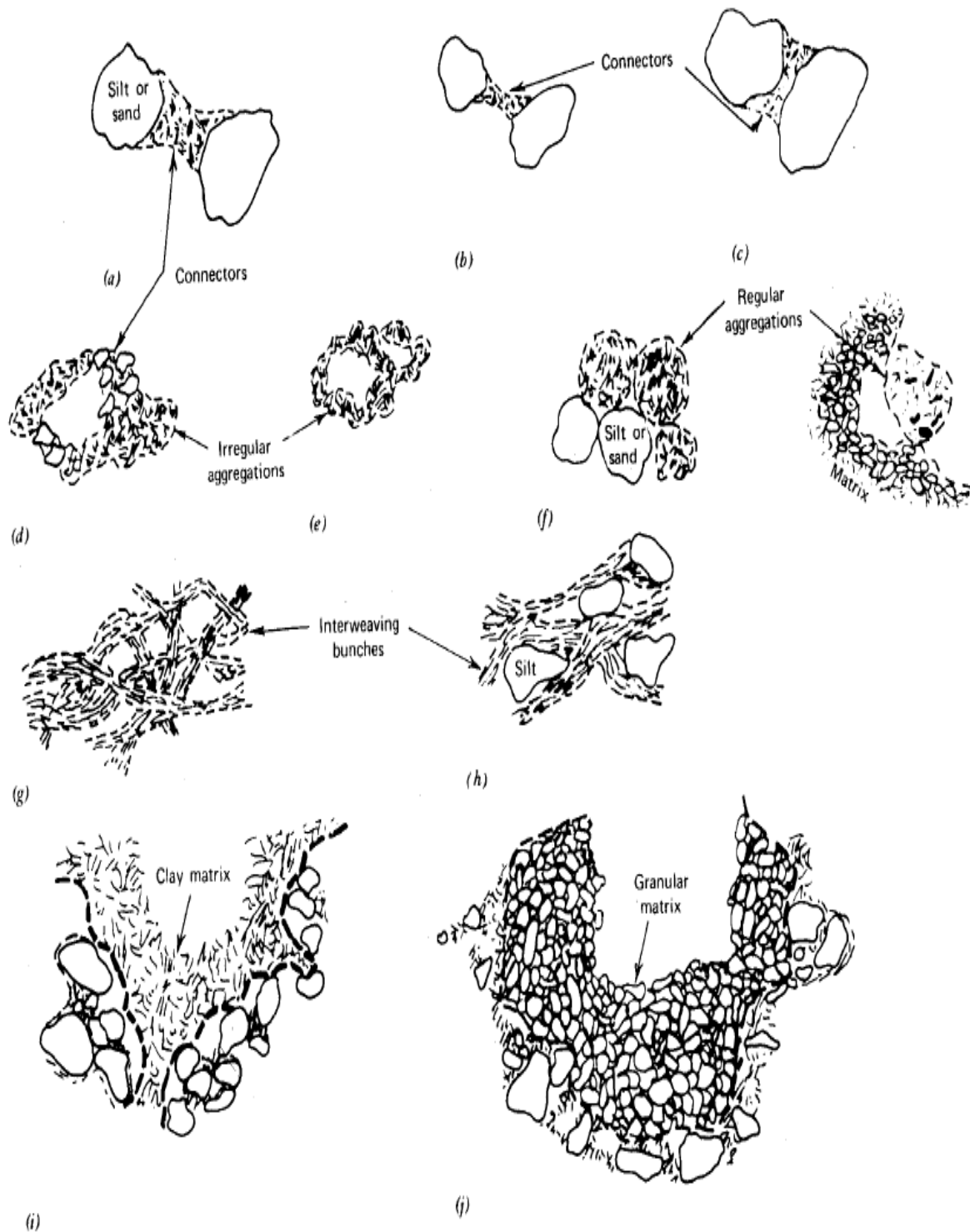
Element group	Description
<i>Elementary particle arrangements</i>	Single (individual) forms of particle interaction at the level of individual clay, silt or sand particles.
<i>Particle assemblages</i>	Units of particle organization having definable physical boundaries and a specific mechanical function, which consist of one or more forms of the elementary particle arrangements.
<i>Pore spaces</i>	Fluid and/or air filled voids within the soil fabric

Fine grained soils usually consist of multiparticle aggregates, while sand and gravel particles are sufficiently large and bulky, and usually behave as independent units (Mitchell and Soga, 2005). Below is a schematic representation of the elementary particle arrangements group, suggested in work by Collins and McGown (1974).



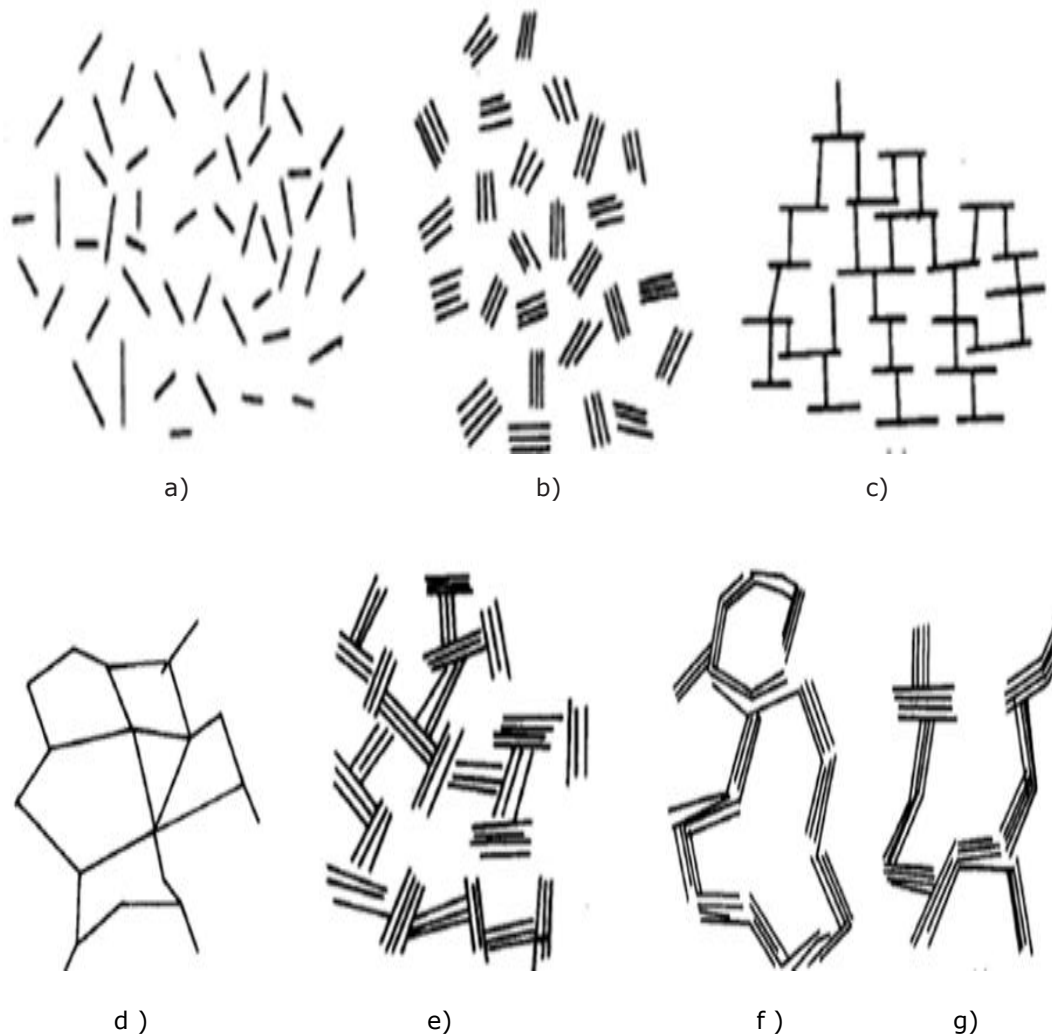
Figur 9. Show elementary particle arrangements of different soils. Illustration from (Collins and McGown, 1974).

Particle assemblages group, consist of one or more forms of the elementary particle arrangements (Collins and McGown, 1974). A schematic presentation of the particle assemblages group is presented in the illustration below.



Figur 10. Show schematic representations of particle assemblages. (a,b,c) connectors, (d) irregular aggregations by connector assemblages, (e) irregular aggregations in honeycomb, (f) regular aggregation interacting with particle matrix, (g) interweaving bunches of clay, (h) interweaving bunches of clay with silt inclusions, (i) clay particle matrix and (j) granular particle matrix. Illustration from (Collins and McGown, 1974).

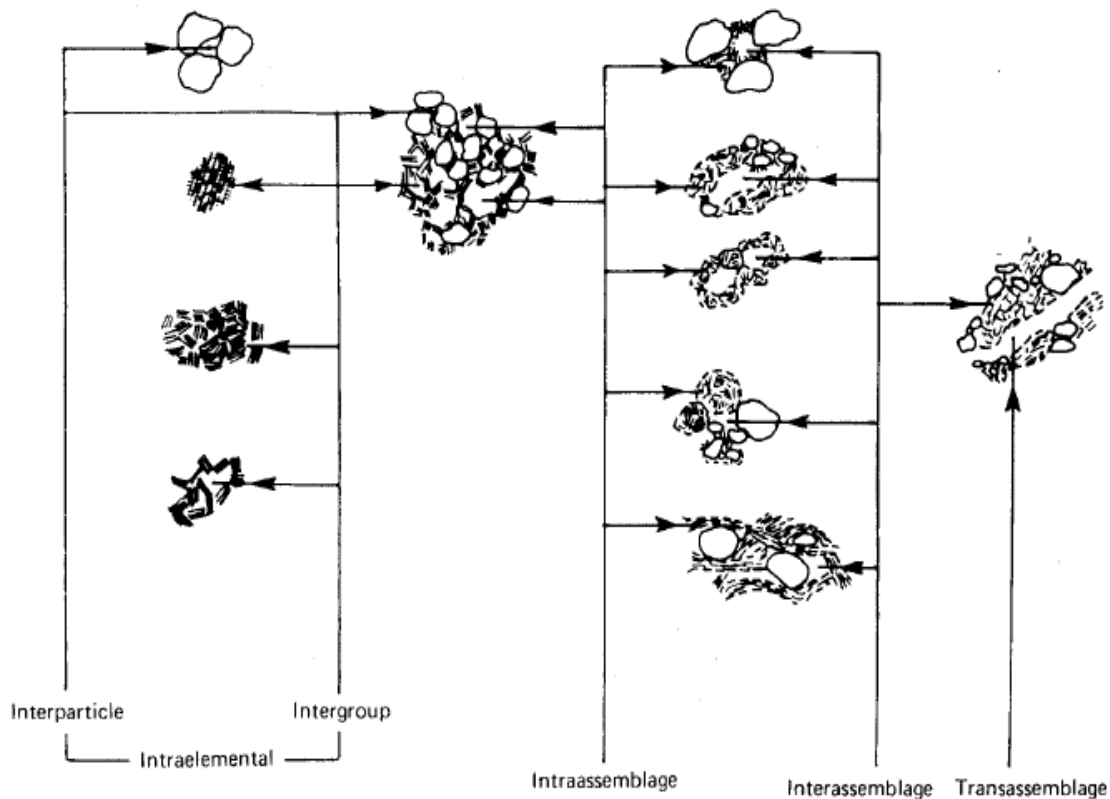
According to (Mitchell and Soga, 2005), clay sediments are often formed by the deposition from flowing or still water, and can be in the form of multiparticle assemblages (flocculated/ aggregated) or independent single particles or particle groups (deflocculated/dispersed). The thicker and larger particles are formed from face-to-face (FF) association, while edge-to-face (EF) and edge-to-edge associations can form cardhouse structures found in quick clays. Particle associations in clay suspensions are presented in the illustration below:



Figur 11. Shows particle associations in clays. a) dispersed and deflocculated, (b) aggregated but deflocculated FF association or paralell oriented aggregation, (c) EF flocculated but dispersed, (d) EE flocculated but dispersed, (e) EF flocculated and aggregated, (f) EE flocculated and aggregated (g) EF and EE flocculated and aggregated. Illustration from (Mitchell and Soga, 2005)

In their work, (Mitchell and Soga, 2005) state that the pores and voids determine the fluid and gas conductivity properties of the soil. These in turn govern the rate of fluid and chemical transport, development of excess pore pressures during deformation, the ease and rate of drainage or consolidation rate, capillary pressure development and potential for liquefaction under dynamic loading.

A schematic presentation of the pore spaces group suggested by (Collins and McGown, 1974) are presented in the illustration below.



Figur 12. Show schematic representations of pore space groups. Illustration from (Collins and McGown, 1974).

2.8 Mineralogy

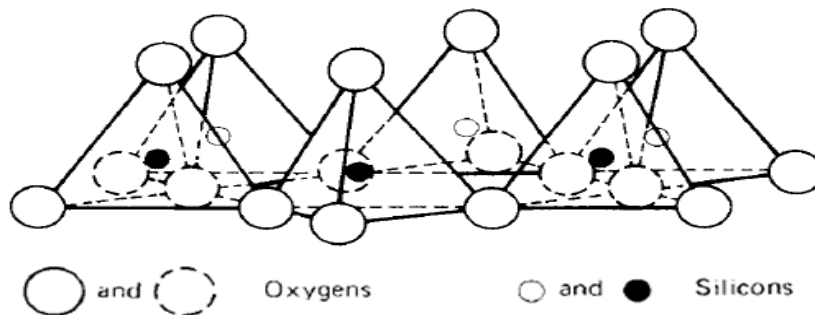
2.8.1 Clays

In work by (Al-Ani and Sarapää, 2008), it is noted that clay consists of minerals in the form of layer silicates, generally formed through chemical weathering and erosion of rock silicate minerals. Some of the more common clay minerals are illite, chlorite, montmorillonite, vermiculite and kaolinite. Illite and chlorite is common in cold climate regions with current or historic glacial activity, while in warmer regions with acidic ground conditions kaolinite which have lower ability to absorb ions, is common. Montmorillonite which is prone to swelling in the presence of water, can often be found within crushing zones in rock faults.

In their work, (Mitchell and Soga, 2005, Al-Ani and Sarapää, 2008) note that the negatively charged surface of a clay particle will attract positive ions (cations) at an interface that is termed as the diffuse double layer. The properties of this layer is dependent on clay mineral as well as the chemistry of the pore water,

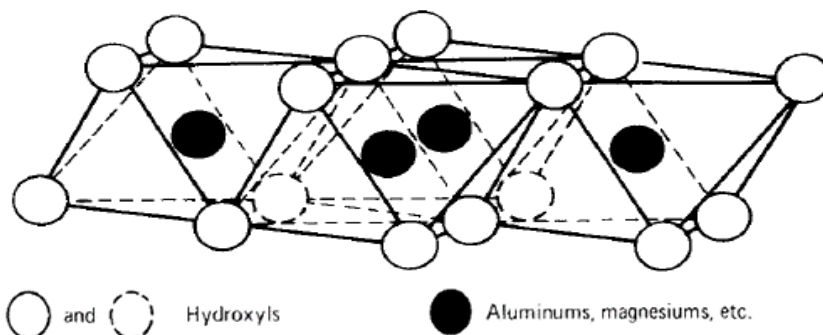
where the inner most layer of water in the doublelayer is strongly adsorbed water, which is more viscous than free pore water. (Al-Ani and Sarapää, 2008) note that the strength of the bonding between the negatively charged particle surfaces and cations, vary from weak (Van der Waals) to moderate electrostatic bonds, to strong chemical bonds.

According to (Mitchell and Soga, 2005), the clay minerals are built up with polymeric layers of silica tetrahedral sheets joined with octahedral sheets of Al, Mg, Fe, O and OH-. It is further noted that the silica *tetrahedra* are interconnected in a sheet structure, where three of the four oxygens in each tetrahedron are shared, forming a hexagonal net. The bases of the tetrahedra are all in the same plane, where all the tips point in the same direction, as can be seen in the illustration presented below.



Figur 13. Show silicon tetrahedron and silica tetrahedra arranged in a hexagonal network. Illustration from (Mitchell and Soga, 2005).

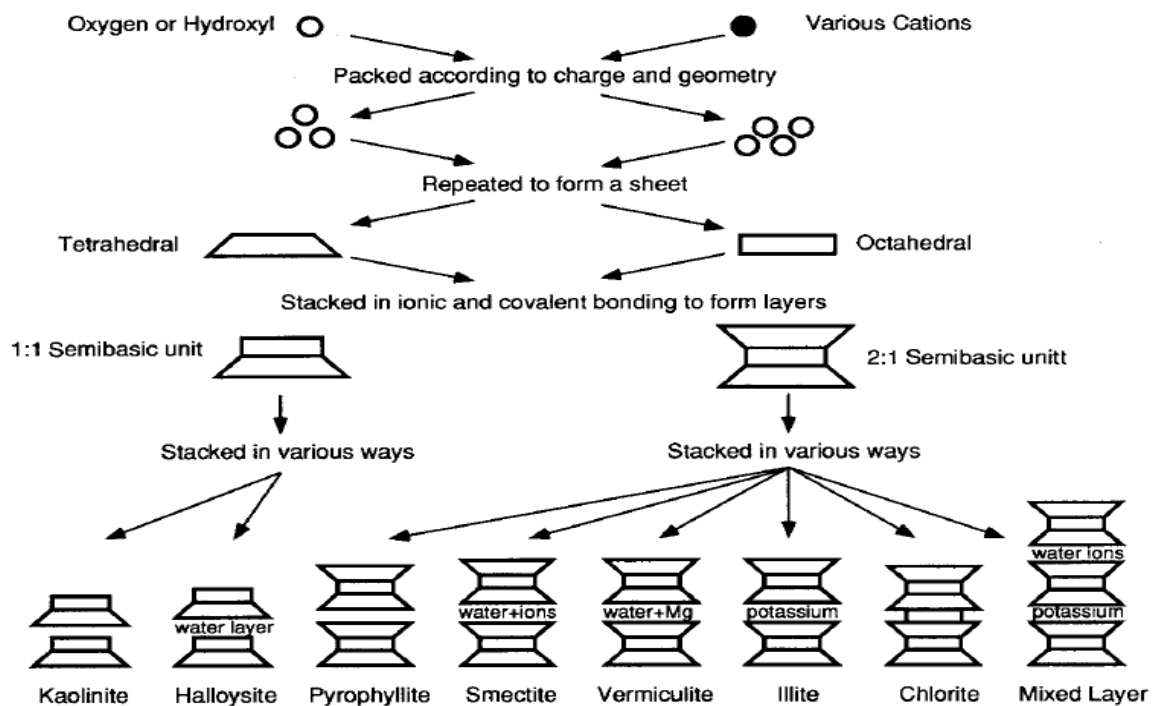
The *tetrahedra* structure has the composition $(Si_4O_{10})^{4-}$ and can replicate indefinitely. Replacement of four oxygens by hydroxyls or by joining with a sheet of different composition and that is positively charged, will obtain electrical neutrality. The *Octahedral* sheet structure is composed of magnesium or aluminium in octahedral coordination with oxygens or hydroxyls, as can be seen in the illustration presented below.



Figur 14. Show octahedral unit and sheet structure of octahedral units. Illustration from (Mitchell and Soga, 2005)

It is further noted by (Mitchell and Soga, 2005), that cations such as Fe^{2+} , Fe^{3+} , Mn^{2+} , Ti^{4+} , Ni^{2+} , Cr^{3+} and Li^{+} , can replace Al^{3+} and Mg^{2+} in an octahedral sheet structure. If the cation is trivalent, 2/3 of the cationic spaces are filled, and the structure is termed dioctahedral. When aluminum ($Al_2(OH)_6$) is combined with silica sheets in clay mineral structures, it is referred to as a *gibbsite* sheet, while when the cation is divalent, the structure is referred to as *trioctahedral*, whereas a magnesium ($Mg_3(OH)_6$) octahedra sheet, is termed a *brucite* sheet.

Members of the same clay mineral group, generally possess similar engineering properties. Most clay minerals in Norwegian soils are illite in a 2:1 structure and these clays are often sticky and have a high plasticity, whereas 1:1 structures form a clay with weaker bonding and lower plasticity. The manner in which atoms are assembled into tetrahedral and octahedral units as well as the formation of sheets and the stacking of layers forming the different clay mineral groups, is explained in the illustration presented below.



Figur 15. Show the forming process of clay mineral groups. Illustration from (Mitchell and Soga, 2005).

2.8.2 Granular soils

According to (Mitchell and Soga, 2005), the hardness and resistance to physical and chemical breakdown, are determined by the mineral composition of a given soil. Most soils are weathering products of rocks and soils, where quartz is the most abundant mineral, with smaller amounts of feldspar and mica. It is further noted that quartz is composed of silica tetrahedra that form spirals with their

oxygens bonded to silicon. This provide a stable structure with strongly bonded ions, high mineral hardness and without cleavage planes. This make it a highly resistant material and hence its abundance in many soils.

In their work, (Mitchell and Soga, 2005) further note that feldspars can be present in smaller amounts in granular soils. Feldspars are silicate minerals with a 3D structure, where the structure is more open, have poorly bonded units and cleavage planes, where the mineral have low hardness and low resistance against the breaking down of particles. These properties account for the relative low presence of feldspars in soils. Mica can be present in small amounts in granular soils and are composed of tetrahedral and octahedral units joint together in a sheet structure with an electrostatic bond of moderate strength. Due to the thin plate morphology of mica flakes, sands and silts with a few percent mica, may display high compressibility under loading and swelling during unloading.

2.9 Pore size distribution in fine grained soils

In their work, (Nimmo, 2004) note that porosity in soils can be conceptually divided into textural and structural porosity. The textural porosity refers to the porosity value at a random arrangement of the particles and is related to the pore size distribution (PSD) of the medium. The structural porosity is the pore space between micro-aggregates and between aggregates, which contains macropores such as interparticle voids, biopores and cracks. Both structural and textural porosity, have a significant influence on the soils capacity for water retention.

(Nimmo, 2004) further note that a distinction is made between the wider pore bodies and more narrow pore openings, also called pore throats. For a sand dominated by textural pore space, the pore bodies are the spaces between the particles wich are relatively closed of, but can empty or fill up with water, while the structural (macropores) pore space form a network of channels, directly contributing to fluid flow. Macropores could be formed as a result of clay particles and organic matter cementing together into individual aggregates or from biogenic channels left by decayed roots or tunneling worms. In work by (Zaffar and Sheng-Gao, 2015), it is noted that in clayey soils:

- pores $< 0,01 \mu\text{m}$ are located in the interlayer spaces within the clay
- pores $0,01-0,1 \mu\text{m}$ are located between clay platelet bundles

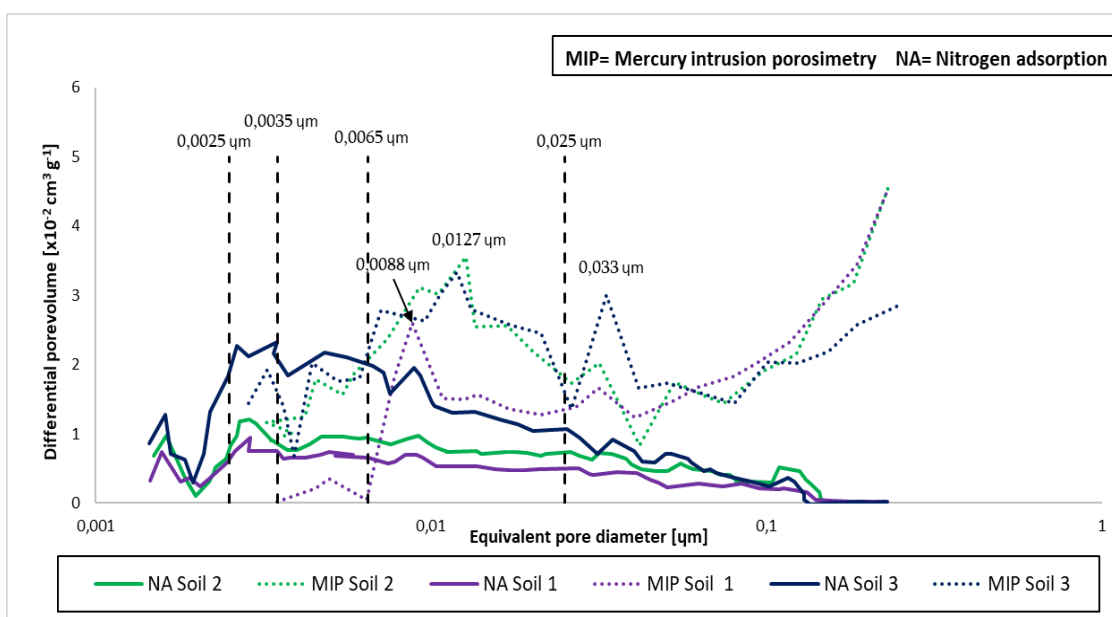
- pores > 1 μm are located between aggregates of particles

According to (Kuila and Prasad, 2013), Cameron and Buchan (2006) proposed classifying pores as macropores (> 75 μm), mesopores (75–30 μm), micropores (30–5 μm), ultramicropores (5–0.1 μm), and cryptopores (0.1–0.007 μm). As part of a study on the effect of organic matter on the pore size distribution (PSD). In their work, (Zaffar and Sheng-Gao, 2015) measured the PSD of three different clays. Some of the clays properties are listed in the table presented below.

Tabell 8. Lists plasticity and share of fines in the different clays in the study. Data adapted from (Zaffar and Sheng-Gao, 2015).

Parameter	Soil 1 [%]	Soil 2 [%]	Soil 3 [%]
d < 0,002 mm [%]	44,77	50,57	43,87
Plasticity index [%]	15,94	19,38	14,22

The PSD of the clays was determined by Nitrogen adsorption (NA) method as well as Mercury Intrusion Porosimetry (MIP). The results from the NA test, show that the clays have a large share of pores < 0.05 μm , where 50 % of the pores were < 0.01 μm and 30 % within 0.01–0.05 μm . The PSD measured by MIP, was systematically higher than that by NA, particularly at around 0,1 μm . It is noted that the MIP method is more suitable for analyzing materials with larger pore size and provides relatively low accuracy for the smaller pores, due to fracturing in the material under high intrusion pressure. The results for the two types of tests are presented in the plot below.

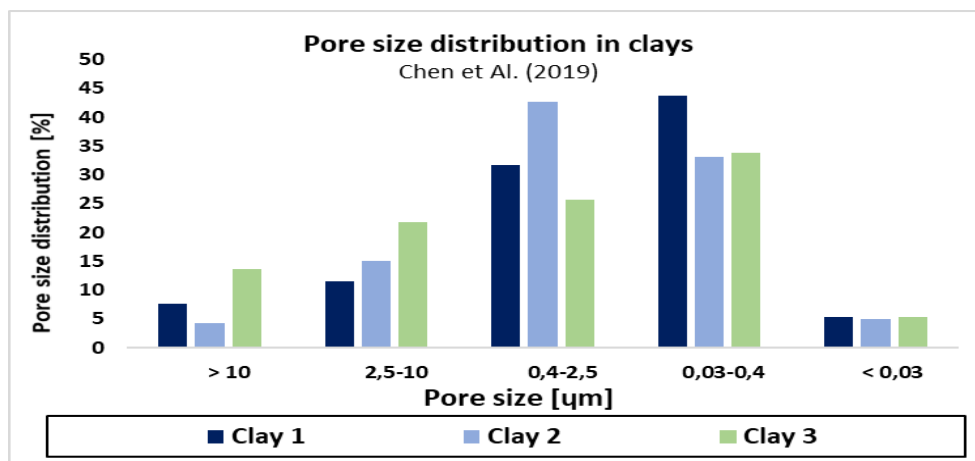


Figur 16. Show differential pore volumes versus equivalent pore diameter derived from Nitrogen adsorption method. Data adapted from (Zaffar and Sheng-Gao, 2015).

The pore volume range of the three tested clays was:

- 35 % ultramicropores (5–0.1 μm)
- 31,4 % macropores ($>0,05 \mu\text{m}$)
- 16,0 % cryptopores (0.1–0.007 μm)
- 9,7 % micropores (30–5 μm)
- 7,3 % mesopores. (0,002-0,05 μm)

As part of a study on the effect of pore size on seepage in clays, (Chen et al., 2019) determined the PSD of three natural clays. The study found that 64,6 - 80,8% of the pores were $< 2,5 \mu\text{m}$, 11.6-21.3% between 2,5-10 μm and 4,2-13,6% $>10 \mu\text{m}$. The pore size range for the three natural clays are presented in the diagram below.



Figur 17. Show pore size distribution in the clays. Data adapted from (Chen et al., 2019)

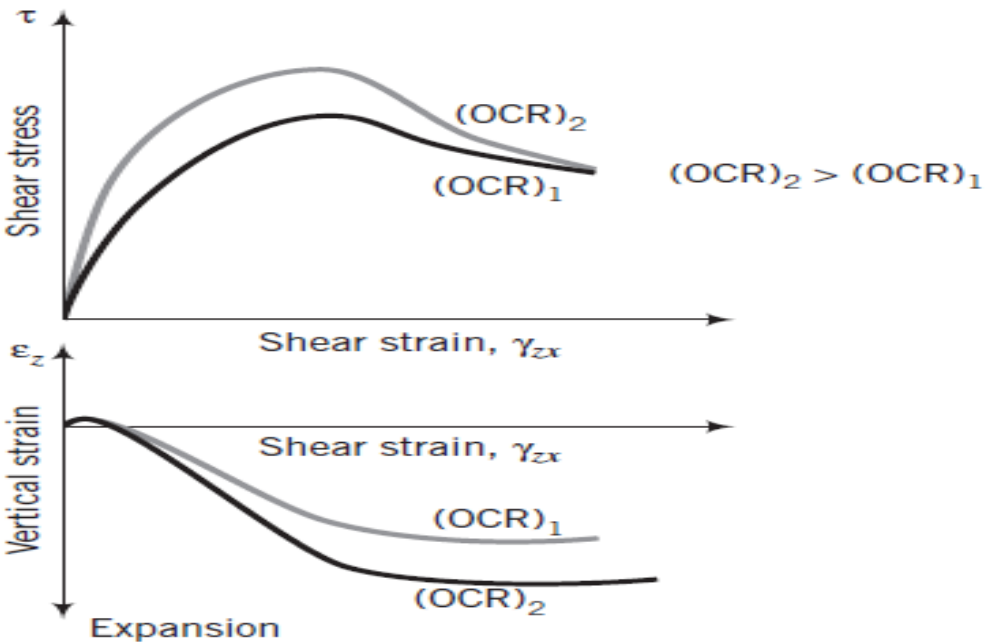
2.10 Stress history

The stress history of a given soil refers to the highest stress that the soil has previously been exposed to, which have a significant effect on the soils behaviour during loading or induced stress. Soils are defined as either normally consolidated (NC) or overconsolidated (OC). According to (Sandven et al., 2017), a NC soil has only been exposed to or consolidated for its own current overburden effective stress (σ'_{vo}). When loaded in an oedometer, the NC soil will experience small deformations until the applied stress exceeds σ'_{vo} , where the deformation will increase. OC soil have been exposed to and consolidated for previous stress or preconsolidation stress (σ'_c) greater than σ'_{vo} . The σ'_c of the OC sediment can be due to previous overlaying glaciers that later have melted, soil masses that later have been eroded away, capillary suction, creep or effects of ageing. In OC

soils, the weakest parts of the soil structure has already been broken down due to the previous stress exposure. This gives the soil a significant resistance to deformations for loading up to σ'_c and a distinct increase in deformation when applied stress exceeds σ'_c . (Holtz et al., 1981) adds that for applied stress below σ'_c , the soil can be assumed to have an elastic behaviour, whereas for stress above σ'_c , the soil would behave like an elastoplastic material. The overconsolidation ratio (OCR), is defined as:

$$\text{OCR} = \frac{\sigma'_c}{\sigma'_{v0}} \tag{Eq. 2.10.1}$$

(Budhu, 2008) notes that higher OC given the same soil homogeneity of soil and mineralogy, will generate higher peak strength and under drained shear a higher volume expansion, compared to soil with lower OCR. This is illustrated in the plots presented below.



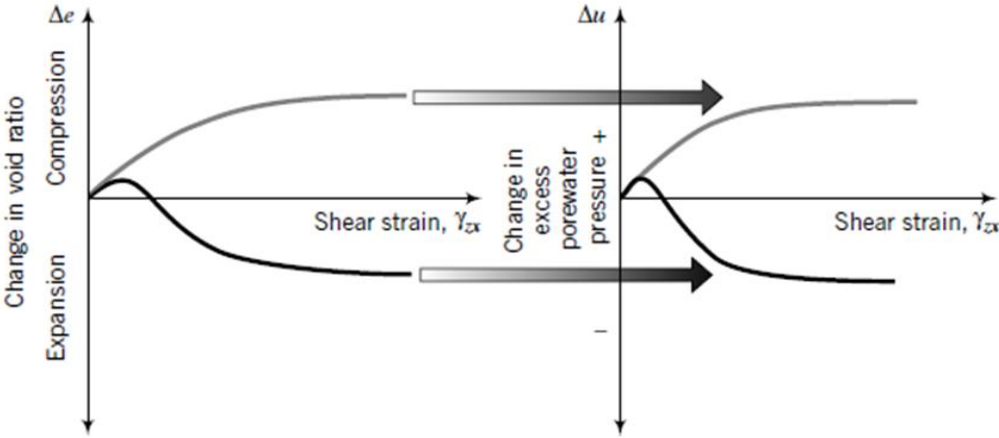
Figur 18. Show the effect of OCR on peak shear strength and change in volume during shear. Illustration from (Budhu, 2008)

2.11 Response to loading

It is noted by (Sandven et al., 2012), that when subjected to external loading, the internal stress in the soil will change to maintain an equilibrium in the new stress state. In granular soils with high permeability, the added stress ($\Delta\sigma$) from external loading is taken as an increased particle contact or effective stress (σ'), where any short term increase in pore pressure, dissipates in a rapid manner due

to rapid evacuation of water in the pores. On the contrary, when fine grained soils with low permeability such as clays and fine silts are loaded, the water can not escape the pores and this generate excess pore pressure (Δu). In geotechnical engineering, the former is refered to as a drained response to loading, while the latter is refered to as an undrained response. Some silts can according to (Yang et al., 2001), display partially drained loading, where Δu develops simultaneously with dissipation, which leads to a short-term increase in pore pressure.

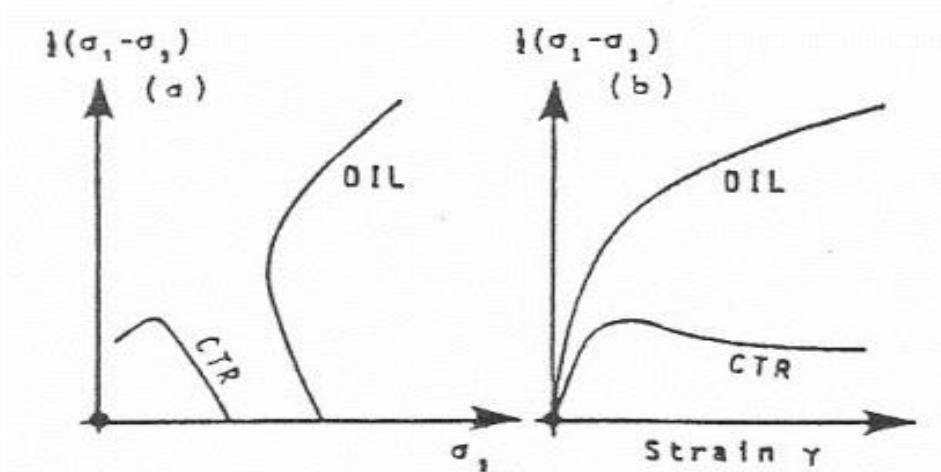
It is noted by (Sandven et al., 2012) that under drained shear in densly packed soils, the particles will seek to climb over each other, causing a volumetric expansion (dilation), while under undrained loading this type of soil will according to (Holtz et al., 1981), generate a negative Δu (suction) which increases the particle contact and hence increases σ' . In soils with a loose or lower degree of packing, the particle structure will seek to compress under drained shear, causing a volumetric reduction (contraction) and generate a positive Δu during undrained shear, which reduces the particle contact and hence reduces σ' . The plots below illustrate the soils tendency to change their volume during drained shear and corresponding response of Δu during undrained shear.



Figur 19. Illustrate the effects of drained and undrained conditions on volume change. Illustration from (Budhu, 2008)

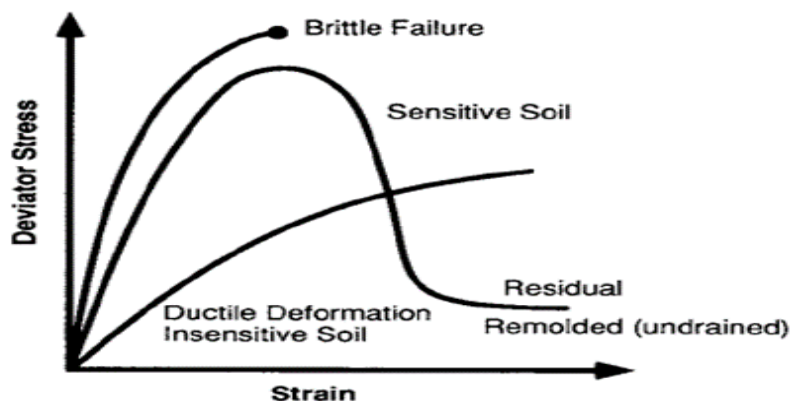
(Sandven et al., 2012) note that dilative behaviour is common in non-cohesive soils but can also occur in highly OC clays or low sensitivity clays under low consolidation stress, while contractive behaviour is common in soft or NC clays as well as loose silts. Dilitant (DIL) behaviour with strain-hardening response to

stress induced shear and contractive (CTR) behaviour with strain-softening response are illustrated in the idealized curves presented below.



Figur 20. Show idealized stresspaths and stress-strain curves for dilatant (DIL) and contractant (CTR) soils. Illustration from (Sandven et al., 2012)

It is noted by (Sandven et al., 2012), that the failure in dilative soils take time to develop, and such soils will generally display early warning signs in situ before failure. Contractive soils will usually develop sudden failures, often at low strains, where the soil may loose much of its initial strength down to a very low residual strength, and in extreme cases liquefy (quick clays). Brittle failure in OC clay, quick clays, cemented soils and dense sands occur momentary, whereas in some silts, NC clays and loose sands, a ductile failure is common. The plot below illustrate failure mechanisms in idealized stress-strain curves.

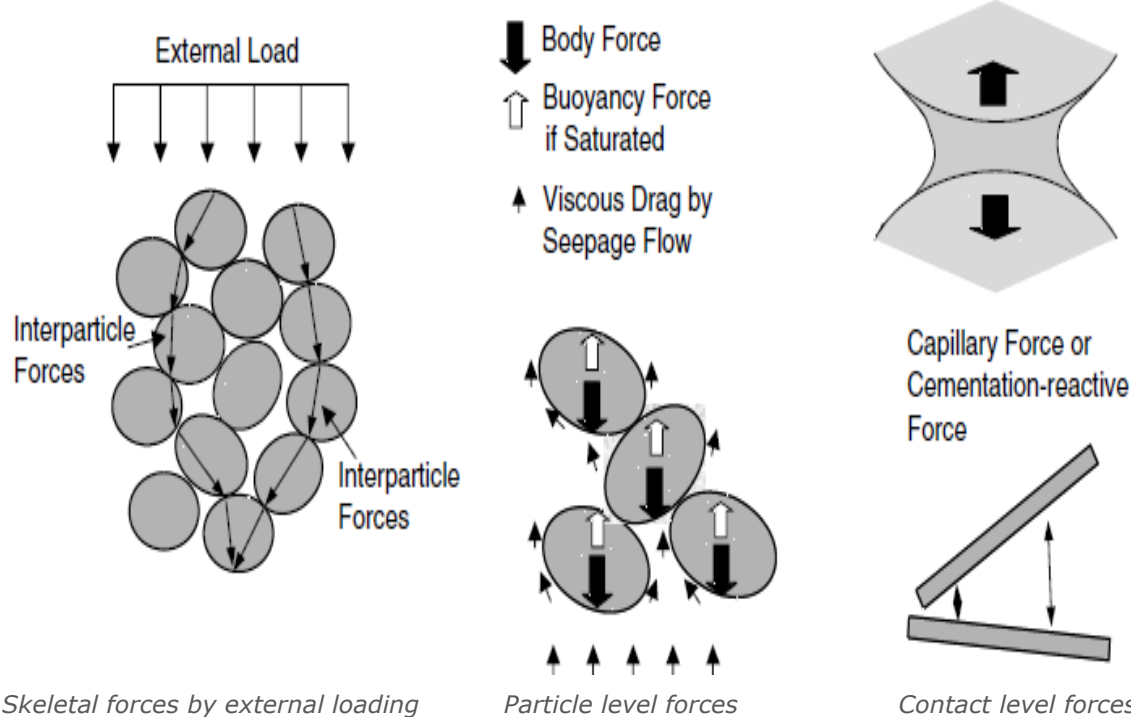


Figur 21. Shows different failure mechanisms or stress response in soils. Illustration from (Mitchell and Soga, 2005)

2.12 Interparticle forces

In work by (Yang et al., 2001), it is stated that sands behaviour is influenced by the soil fabric, clay behaviour by electro-chemical bonding forces between the soil particles, while both these mechanisms may influence the behaviour of silts.

The interparticle forces at the microscale can according to (Santamarina, 2003), be divided into *skeletal forces* due to external loading, which are transferred from the load and through the particles and *particle level forces* that are caused by self weight, buoyancy (submersion) and seepage forces. The last category is *contact level forces* such as electrostatic bonding, cementation and capillary suction, which over time generate interparticle cohesion. The illustration presented below show the different interparticle forces divided into groups, acting on the soil skeleton.



Figur 22. Show different interparticle forces divided into groups. Illustration from (Santamarina, 2003)

It is noted by (Mitchell and Soga, 2005), that both normal and tangential forces develop at particle contacts when external loading is applied. Each particle will experience different forces on the skeleton depending on the position relative to the adjacent particles, but the strongest particle forces will generally develop in the direction of the major principal stresses. It is further noted that the development and distribution of the interparticle skeletal forces, determine the stress-strain behavior, volumetric response to induced shear and the shear strength in the soil.

In their work, (Mitchell and Soga, 2005) further note that the weight of the particle, act as a body force in dry soil and contribute to skeletal forces, whereas the effective weight of the particle is reduced in submerged soils, due to the

uplift force from buoyancy. This leads to smaller skeletal forces for submerged soil, compared to dry soil. Seepage forces from externally added water pressure, produce hydrodynamic forces which act upon the particles and alters the skeletal forces.

Van der Waals forces can according to (Anandarajah and Chen, 1997), be explained as electromagnetic waves emanating from interacting atoms, causing an attraction force between molecules or colloids. The magnitude of the attraction depends on the spatial distribution of separation distance between the molecules as well as the medium in which the waves move through. These interparticle forces are generally considered as a weaker form of bonding. However, (Mitchell and Soga, 2005) note that although van der Waals bonds are weak, they are strong enough to determine the final arrangements of groups of atoms in some solids, and may have a minor contribution to the cohesion in fine grained soils.

The capillary properties of a given soil will affect the interparticle mechanisms of a soil skeleton above the saturated zone, where (Mitchell and Soga, 2005) note that suction can develop when saturated soil begins to dry, due to surface tension in the water phase and retained water on the particle surfaces. The suction will increase the particle contact, hence increasing the effective strength of the soil skeleton. This is a temporary effect that can dissipate if the soil is either dried out or saturated. (Mitchell and Soga, 2005) adds that true cohesion in soil, is shear strength in excess of that generated by frictional resistance from particle sliding as well as rearrangement and crushing of particles. The contribution to true cohesion from interparticle attractive forces are considered minor, whereas contribution from cementation is considered as significant.

The cementation in soils can develop naturally from precipitation of calcite, silica, aluminaoxides, ironoxides or artificially by stabilizers such as cement and lime. The degree of cementation between the particles in a soil, contribute directly to the soils effective strength. (Mitchell and Soga, 2005) note that the behaviour of a cemented soil depend on when the cementation occurred in respect to time of loading, where artificially cemented soils are loaded after cementation have occurred and the contact forces within the cemented particle bonding can become negative, depending on the tensile resistance of the bond. This makes the distribution and magnitude of forces acting on the skeleton and the bonding,

affected by particle arrangement within the skeleton and the bonding between particle contacts.

The cementation in natural soils develops during or after overburden loading, where the contact forces caused by loading are developed before the cementation. This suggests according to (Mitchell and Soga, 2005), that cementation possibly can contribute to the magnitude of forces at particle contacts and that the stiffness and strength of a soil, might differ depending on when and how cementation bonds were developed.

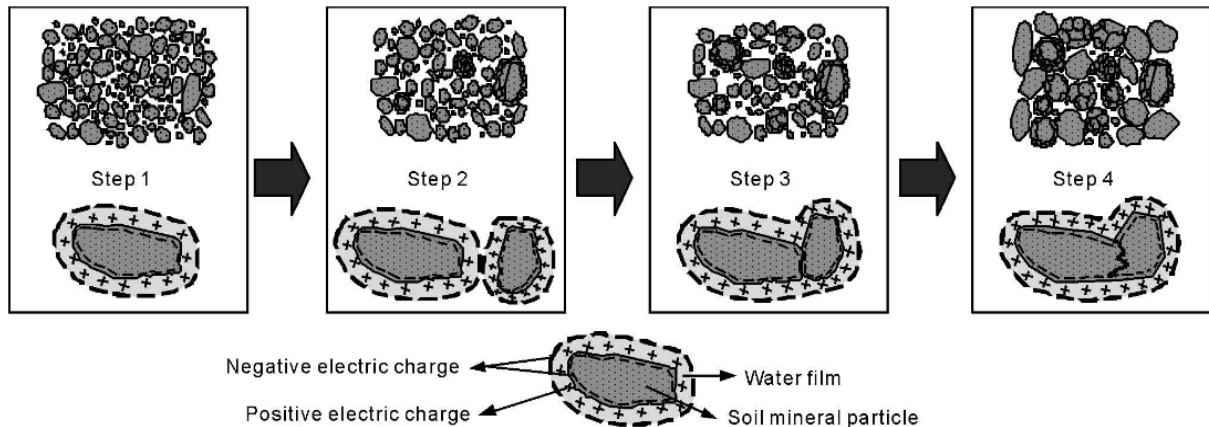
2.13 Freeze and thaw cycles

Soils in cold climate regions can be subject to freeze and thaw (FT), where temperatures fluctuate above and below 0°C (Zhang et al., 2016b, Cheng et al., 2016). (Zhang et al., 2016b) adds that cold climate ground conditions may experience over 100 FT cycles in the span of a year. The changes in the soil properties due to FT cycles, can lead to engineering challenges concerning shear strength, bearing capacity of foundations, capillary water pressure and changes in soil plasticity and collapsibility. In that regard, (Cheng et al., 2016) note that foundations subject to FT cycles can experience significant structural damages, which can lead to frost heave and uneven stresses within the soil, compromising the stability of the soil.

Freezing is a weathering process, that can be more severe than common physical weathering, due to the large volume change ($\Delta V \sim +9\%$) when water transforms into ice. In their work, (Ferrick and Gatto, 2005) note that more ice will form in soils with high water content, where the higher expansion forces, increase the separation of interparticle bonds. In soils with lower water content, ice crystals have enough space to expand inside the pores, thus the particle bonds are not compromised.

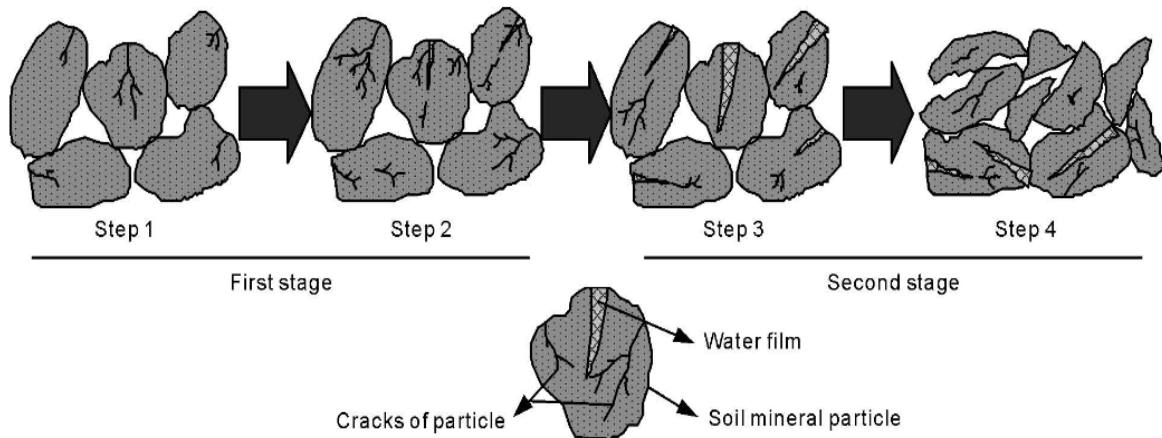
Fragmentation of particles due to freezing only occur in relatively coarse soil, whereas clay particles do not experience fracturing due to a large amount of bound water within the soil, that will not freeze. However, (Zhang et al., 2016b) state that clay particles are prone to aggregation due to the diffuse double layer, which causes an increase of the interparticle forces and enable larger amounts of adsorbed water within the clay. FT cycles can enhance the capacity for bonding between minerals due to increased formation of associations between particle

surfaces and the sorption of oxides on the particle surface. The process of aggregation in clay is illustrated in the schema presented below.



Figur 23. Show the process of aggregation in fine particles. Illustration from (Zhang et al., 2016b)

(Zhang et al., 2016b) note that early work by Poltev (1967), suggested that the frost weathering process of soil particles could be divided into two phases. In the first stage, the phase transformation of water in the soil cause surface cracks in the particles, due to tension. Pore water freezes to ice and expand the volume, which transform microcracks into macrocracks. In the second stage, the water film expands and further fragmentation of primary minerals occur. The illustration presented below, show this weathering process.



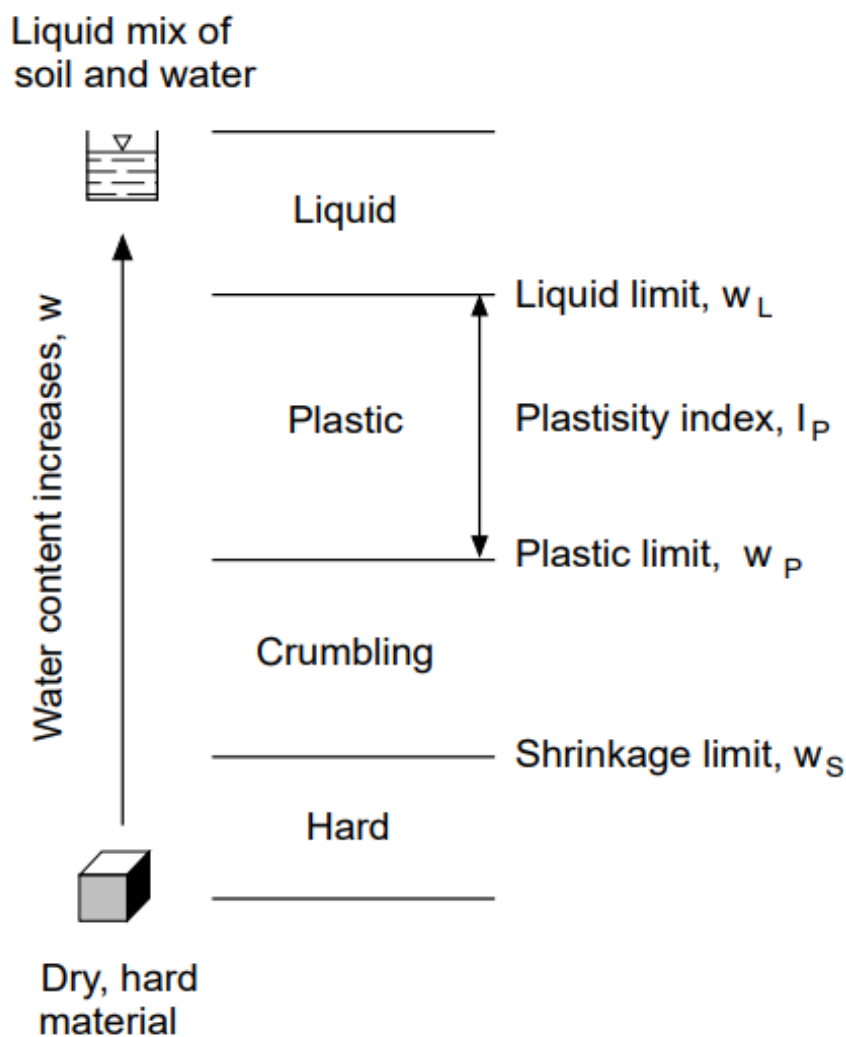
Figur 24. Show the fracturing process in coarse particles due to frost. Illustration from (Zhang et al., 2016b).

2.14 Plasticity of cohesive soils

The plasticity of a soil can be defined as its ability to sustain deformation without cracking or fracture, where plastic deformation of a soil means that the rearranging of particles is irreversible (K:R, 2004). The plasticity of a given soil will be influenced by the share of clay minerals in the soil. This is due to adsorption of

water between the clay mineral layers, where the adsorbed water give the soil its plastic characteristics. Hence, soils with no clay minerals, will not have plastic characteristics, no matter the share of fines.

Natural clays can depending on their natural water content (W), be hard (dry), firm or crumbling, plastic or liquid (Atterberg, 1913). According to (Sandven et al., 2012), the water content of the sample in transition from one state to another, are called consistency limits or Atterberg limits. The liquid limit (w_L) is defined as the water content at which the behavior of a clayey soil changes from plastic to liquid state. The plastic limit (w_P) represents the lowest water content at which the clayey soil is plastic in the remoulded state, and the shrinkage limit (w_S) defines the water content at which the volumetric change of the sample during drying, is zero. The illustration below show the different consistency states as a function of water content in remoulded fine grained soils.



Figur 25. Show consistency changes as a function of water content in cohesive soil. Illustration from (Sandven et al., 2017).

The plasticity index (I_p) and liquidity index (I_L) are calculated as:

$$I_p = w_L - w_p \quad \text{Eq. 2.14.1}$$

$$I_L = \frac{w - w_p}{w_L - w_p} \quad \text{Eq. 2.14.2}$$

A measured I_L greater than 1, indicate a sensitive soil and might together with other factors such as low salinity (<0,5%) of pore water and very low remould-ed undrained shear strength (<0,5 kPa), indicate clays that will display a quick behaviour if disturbed. Different classification intervals of I_p for different regions might be applied, but for Norwegian clays, the values listed in the table below are used.

Tabell 9. Lists classification and range of plasticity index in Norwegian clays. Data adapted from (Sandven et al., 2017).

Classification	I_p
Low plasticity	< 10
Medium plasticity	10-20
High plasticity	> 20

The activity (α_c) of a clay, provides a measure on the clays ability to retain water and can be calculated as:

$$\alpha_c = \frac{I_p}{d < 0,002 \text{ mm} [\%]} \quad \text{Eq. 2.14.3}$$

2.15 Anisotropy

In natural soil deposits, the horizontal stress is rarely equal to the vertical stress, hence the stress is often anisotropic, where (Muir Wood et al., 2001) note that the particles of soils which experience different level of stress in different directions, will have an anisotropic arrangement and anisotropic magnitude of the forces acting in the particle contacts. (Chen et al., 1988) adds that the average orientation of the grains and interparticle forces, determine the anisotropic behaviour of the material and provides it with a memory of the soils previous states. They further note that, anisotropy in granular materials can be induced by strain or it may exist before straining, where direction of shear relative to direction of the particles deposition, govern the behaviour during shear.

In clays, (Fauskerud et al., 2012) note that the undrained shear strength (S_u) is dependent on the direction of the strain in relation to the orientation of the clays stress and particles, in situ. The evaluation of anisotropy in saturated clays is important when assessing slope stability, due to the fact that available undrained shear resistance in the critical sliding surface is dependent on the direction of the occurring strain, where low plasticity clays with brittle properties, generally display higher anisotropy than high plasticity clays.

The coefficient of lateral earthpressure at rest (K'_o), is defined as the ratio (σ'_y / σ'_x) between effective horizontal stress (σ'_x) and the vertical effective stress (σ'_y). K'_o is according to (Holtz et al., 1981), dependent on the density of overlying layers and the soils stress history, but will given constant density, be constant with depth in one and the same layer. K'_o for friction materials in a horizontal layer can be calculated as:

$$K'_o = 1 - \sin \varphi' \quad \text{Eq. 2.15.1}$$

And for fine grained soils in a horizontal layer, as:

$$K'_o = (1 - \sin \varphi') \sqrt{OCR}^{\sin \varphi'} \quad \text{Eq. 2.15.2}$$

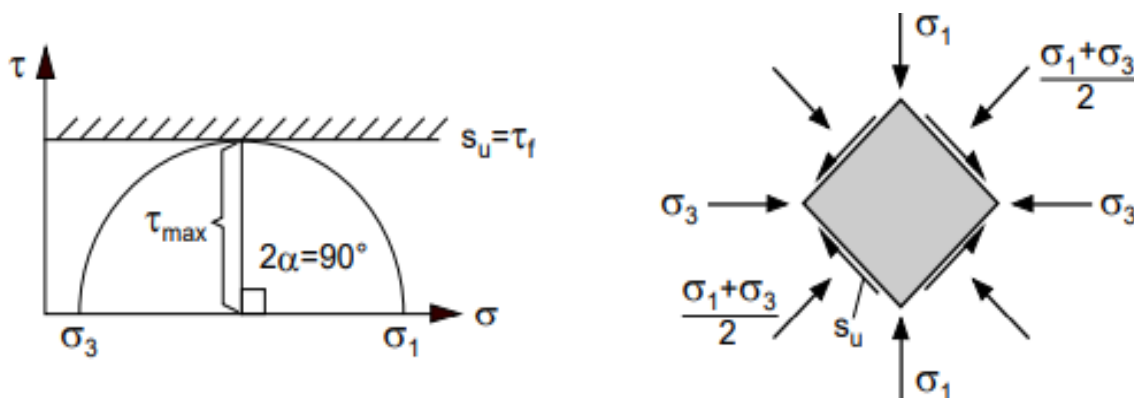
K'_o normally range between 0.4-0.6 in granular materials, 0.4-0.5 for NC clays and up to 3 or more for heavily OC sediments such as dry crust.

2.16 Shear strength

The shear strength defined as the internal frictional resistance of a soil to shearing forces, is a very important parameter for geotechnical engineering and is required to determine bearing capacity of soils, slope stability and the stability of geotechnical structures. For clays and fine silts in a short term perspective, the shear strength is considered on a total stress (σ) basis by the undrained shear strength. The undrained shear strength (S_u) is the strength when sheared at constant volume and is dependent on the confining stress and thus, S_u is not a fundamental soil parameter. (Emdal et al., 2009) note that S_u is constant, independent of the mean stress level and defined by the maximum shear stress (τ_{max}), which is equal to the shear stress at failure (τ_f) :

$$\tau_{max} = \frac{\sigma_1 - \sigma_3}{2} = \tau_f = S_u \quad \text{Eq. 2.16.1}$$

S_u , is constant and in the Tresca failure criteria, equal to the radius of the Mohr circle or half of the deviatoric stress (Eq. 2.16.1). The Tresca failure criteria is illustrated to the left below.



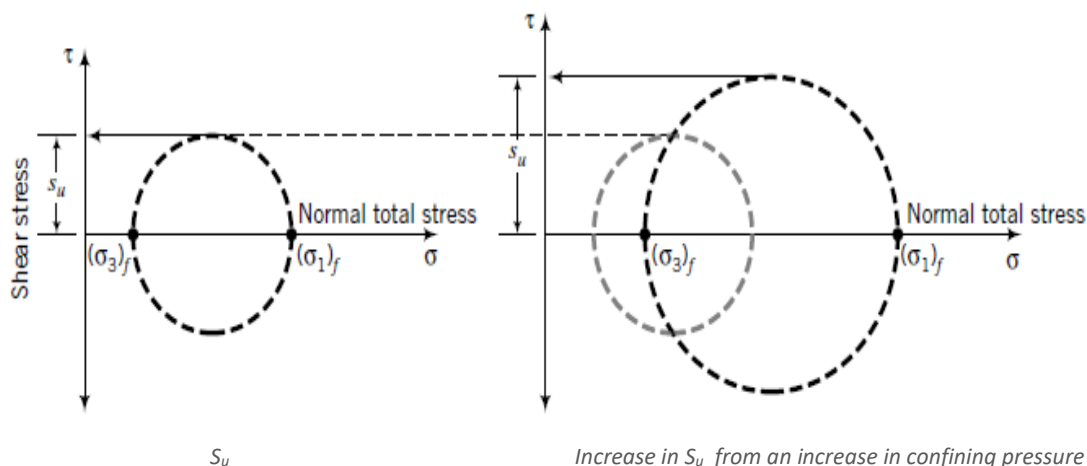
Figur 26. Illustrate the Tresca failure criterion for undrained shear strength and the equilibrium conditions.. Illustration from (Emdal et al., 2009)

The maximum applicable shear stress under undrained conditions, is theoretically determined by the existing effective stress level in NC clays or σ'_c in OC clays, before sampling. The maximum in situ shear stress can hence be expressed as:

$$\tau_{max} = \frac{1}{2} \cdot (1 - K'_o) \cdot (\sigma'_{vo} + a) \quad \text{Eq. 2.16.2}$$

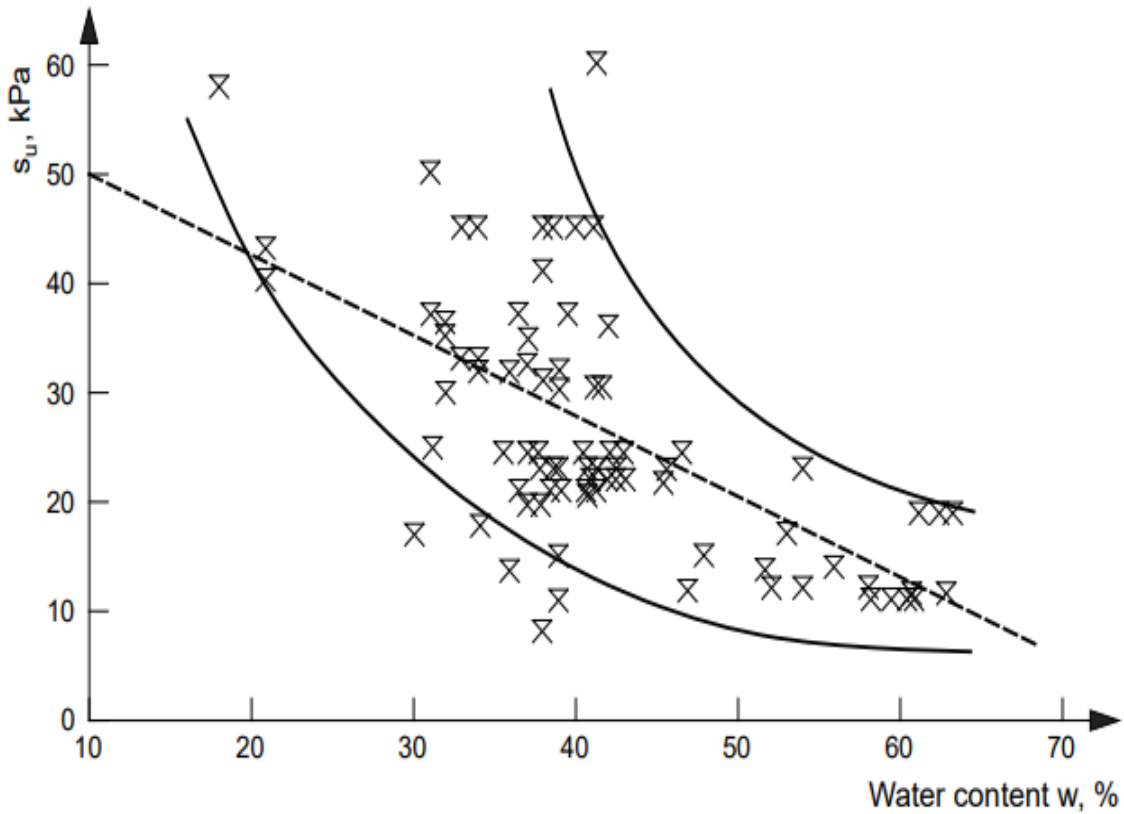
Where a is the attraction, φ is the friction angle of the soil and σ'_{vo} is the effective overburden stress.

In their work, (Holtz et al., 1981) note that the magnitude of S_u under undrained loading is governed by the initial void ratio (e) and water content (W). An increase in confining pressure during undrained shear, will lead to a decrease in e and a larger Δu . This causes an expansion of total stress (σ) in Mohr's circle, where S_u increases, as can be seen in the illustration presented below.



Figur 27. Show effect of increased confining pressure on undrained shear strength. Illustration from (Holtz et al., 1981).

It is stated by (Sandven et al., 2012) that S_u of clay is strongly affected by water content (W) in the soil, where increasing W is correlated with decreasing S_u . The plot below show this correlation in Norwegian clays.



Figur 28. Show correlation between undrained shear strength and water content in Norwegian clays. Illustration from (Sandven et al., 2017).

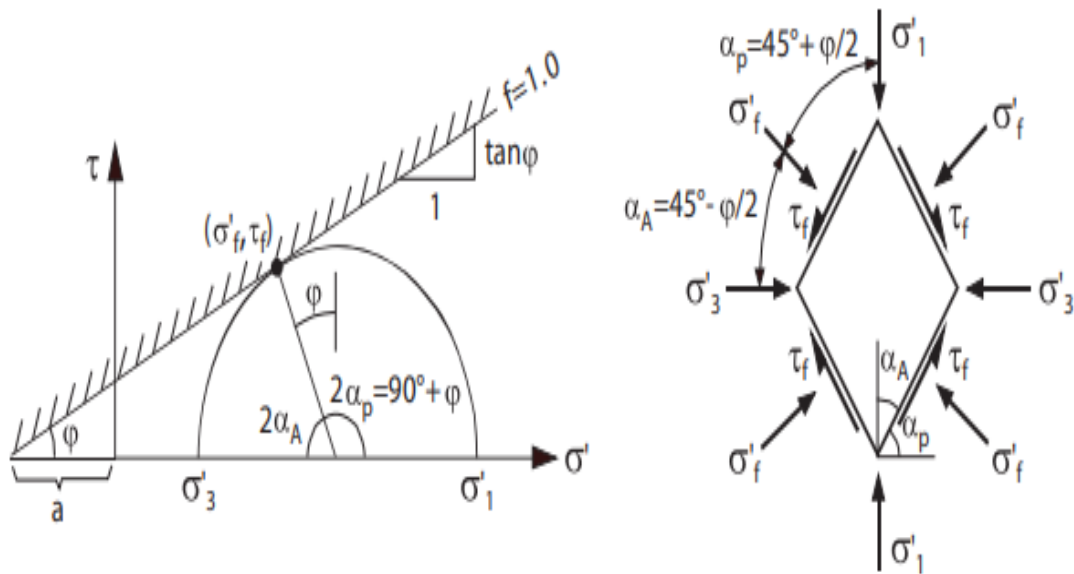
According to (Sandven et al., 2012), free water and air in the soil pores cannot take shear when a load or force is applied, thus only the soil skeleton will take the resulting shear stress. For this reason, the internal shear resistance in granular soils, is governed by the effective normal stress (σ'), which in a saturated soil, is expressed as:

$$\sigma' = \sigma - u \tag{Eq. 2.16.3}$$

where σ is the total stress and u the pore pressure.

Effective shear strength of soil is commonly expressed with the Mohr Columb failure criteria. As noted by (Mitchell and Soga, 2005), the shear strength is plotted as a function of the principal effective stresses on the failure plane or as the maximum shear stress versus the average of major and minor effective stresses at failure. In their work, (Sandven et al., 2017), note that the attraction (a) can be regarded as an isotropic pre-stress similar to suction in the soil or a

product between the friction and level of stress. The Mohr Coulomb failure criterion for effective stress, where major and minor principal effective stresses acting on a plane are noted respectively as σ'_1 and σ'_3 . The failure criterion is illustrated to the left below.



Figur 29. Illustrate the Mohr columb failure criterion for effective shear strength and the equilibrium conditions. Illustration from (Emdal et al., 2009)

According to (Mitchell and Soga, 2005), the strength of soil is defined as the stress state at failure. The strength can, when excluding cohesion or chemical cementation between grains, be expressed as an approximated linear relationship with stress through the major (σ'_{1f}) and minor (σ'_{3f}) principal effective stresses at failure and the friction angle (φ') of the material, in the following equations:

$$\tau_f = \sigma'_f \cdot \tan (\varphi') \text{ or } (\sigma'_{1f} + \sigma'_{3f}) = (\sigma'_{1f} - \sigma'_{3f}) \cdot \sin (\varphi') \quad \text{Eq. 2.16.4}$$

For cemented soils, the effective strength can be expressed as (Budhu, 2008):

$$\tau_f = c' + \sigma'_f \cdot \tan (\varphi') \quad \text{Eq. 2.16.5}$$

Where c' is the apparent cohesion in the cemented soil. (Knappett and Craig, 2012) note that cohesion include the effects of inter-molecular forces (c_o), which have a minor contribution to the shear strength of the soil, soil tension (c_t) due to capillary suction, and cementation (c_{cm}) from chemically bonding between particles. The c_o is usually neglected due to minor impact and c_t should generally not be included in geotechnical design due to potential loss of capillary effect

when soil is saturated or dried up. The contribution from c_{cm} , should be used with caution due to the very small shear strain at which this shear strength is mobilized. Within most geotechnical systems, the mobilized shear strain is larger than that required to mobilize the shear strength due to cementation. Cohesion c is the apparent shear strength at zero normal effective stress, where:

$$c = c_o + c_t + c_{cm} \quad \text{Eq. 2.16.6}$$

The effects of dilation during shear on the effective strength can be expressed as (Holtz et al., 1981):

$$\tau_f = \sigma'_f \cdot \tan(\varphi' \pm \psi) \quad \text{Eq. 2.16.7}$$

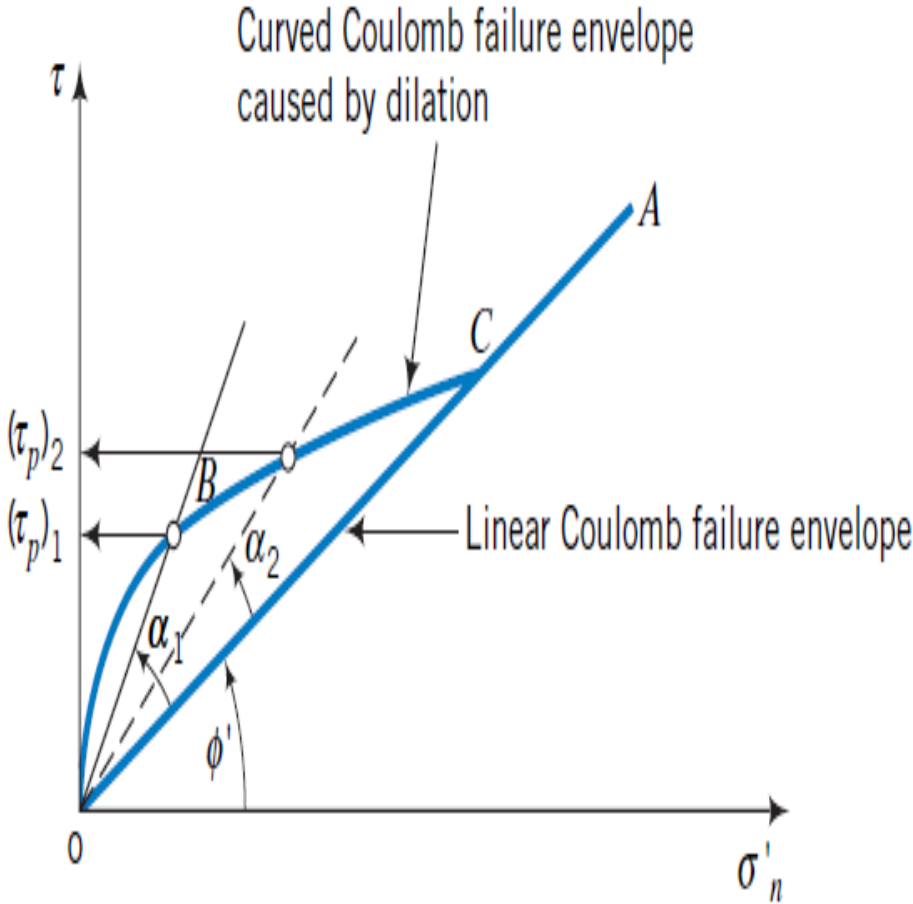
Where σ'_f is the normal effective stress and ψ is the dilation angle, which is a measure of the change in volumetric strain with respect to the change in shear strain. Negative values of ψ , indicate volumetric compression (contraction), while positive values of ψ , indicate volumetric expansion (dilation).

The stress state in a soil at continuous shear and constant shear stress, normal effective stress ratio and volume, is defined as the critical state (cs). Where φ'_{cs} is the friction angle at critical state and a fundamental soil parameter, whereas the friction angle at peak shear stress (φ'_p) in dilating soils, depend on the capacity of the soil to dilate, thus it is not a fundamental soil parameter. When the rate of dilation reaches its highest value, it creates the peak failure condition (φ'_p) at peak dilation (ψ_p), which can be expressed as:

$$\varphi'_p = \varphi'_{cs} + \psi_p \quad \text{Eq. 2.16.8}$$

It is noted by (Budhu, 2008), that dilation is suppressed at higher pressures due to crushing, where the dilation will equal zero when the soil has reached critical state during shear. The effect of dilation, is increased shear strength and a curving of Coulomb's failure envelope. Stress states located on the peak strength envelope (φ'_p), can lead to sudden collapse of the material. States below (φ'_{cs}) represent a stable state (safe design) and a ductile failure mode, whereas states on the critical state failure envelop (φ'_{cs}) are considered at failure or critical state.

The different states are presented in the Mohr columb criteria below.



Figur 30. Show effects of dilation on the Columb's failure envelope and the different soil states . Illustration from (Budhu, 2008).

For further deformation after ϕ'_{cs} , platy clay particles will align along the failure plane (shear band), where the shear resistance decreases until it reaches its residual shear strength (ϕ'_r). The shearing displacement required to cause a reduction in friction angle from ϕ'_{cs} to ϕ'_r , will vary with soil type, normal stress on the shear plane, and shear conditions (Mitchell and Soga, 2005). In the case of effective stress analyses (drained), it is noted by (Budhu, 2008) that the values for ϕ'_{cs} are constant, regardless of the soils initial condition and the magnitude of σ'_N , whereas ϕ'_p will depend on effective normal stress (σ'_N).

The degree of dilation that is derived from shear tests, may not be mobilized by the soil during construction load, indicating that ϕ'_p is not reliable in geotechnical design. The shear strength parameter ϕ'_{cs} should be used in design, unless

experience dictates otherwise. In the table below some typical ranges for effective strength parameters for different soils are listed.

Tabell 10. Lists range of friction angle for different soils. Data adapted from (Budhu, 2008).

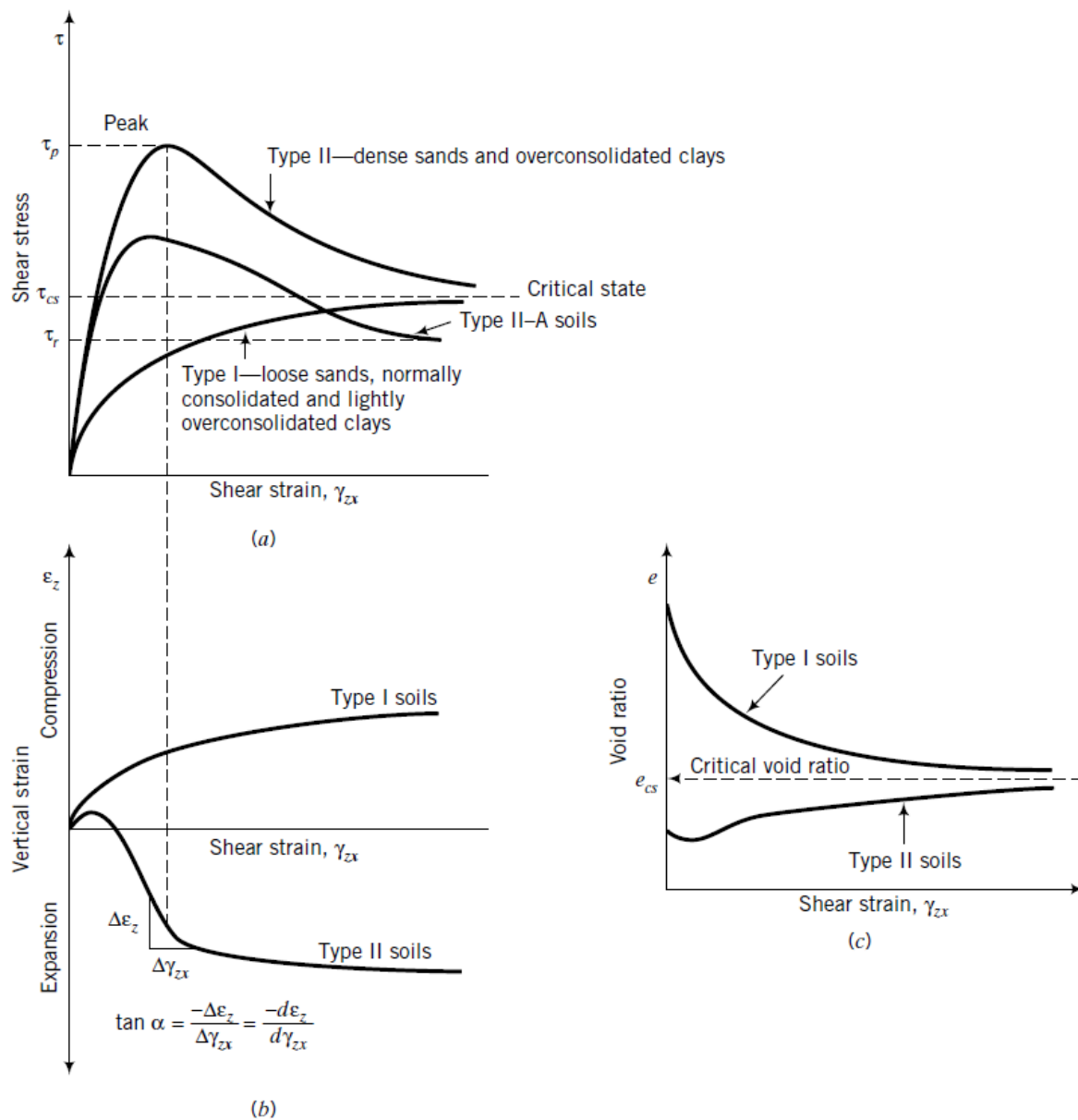
Soil type	ϕ'_{cs}	ϕ'_p	ϕ'_r
Gravel	30-35	35-50	
Sand/gravel/fine soil mixture	28-33	30-40	
Sand	27-37	32-60	
Silt or silty sand	24-32	27-35	
Clays	15-30	20-30	5-15

2.17 Stress-strain and soil states

For safe geotechnical design adapted to the problem in hand, identification of shear and volumetric strains are important for the evaluation of deformation properties in a given soil. The Tresca and Mohr-columb failure criteria do not take into account or adress the shear strains required to initiate failure, nor the initial stresses, initial void ratio (e_0) or OCR. (Holtz et al., 1981) state that the void ratio is the single most significant parameter, affecting shear strength of sands, where the lower the void ratio in drained triaxial shear, the higher the shear strength.

In their work, (Mitchell and Soga, 2005, Holtz et al., 1981) note that the internal friction between soil particles as well as internal constraints of particles from volumetric change due to stress, are the basic contributions to the strength of a given soil. (Mitchell and Soga, 2005) adds that following a large shear induced volume change, the soil will at a given effective confining stress, acheive a unique void ratio which is independent of the initial state. At that stage, the interlocking of particles will be gone in dense soils, the structure of loose soils will have collapsed, and the soil is fully destructured and have reached its shear strength at critical state. In work by (Holtz et al., 1981), it is noted that loose sands, NC and lightly OC clays ($OCR \leq 2$) here noted as (I), show strain-hardening at gradual increase of shear stress (τ) with increasing shear strain, until the critical state shear stress (τ_{cs}), is reached. These soils tend to contract during drained shear until reaching a constant void ratio at critical state (e_{cs}). Dense sands and higly OC clays ($OCR > 2$) here noted as (II), display a rapid increase in τ , where peak shear

(τ_{peak}) is reached at low strain, followed by decreasing τ with increasing shear strain (strain-softening) until reaching τ_{cs} . These soils tend to initially contract due to particle arrangement under shear and then dilate, increasing the void ratio until reaching the same e_{cs} as the type I soil. In some OC and sensitive clays here noted as (II-A), the particles orient themselves parallel to the direction of the shear band, resulting in the final shear stress dropping below τ_{cs} and stabilize on a level of residual shear stress (τ_r). The τ_{cs} and e_{cs} will depend on σ' , where increasing σ' result in increased τ_{cs} and lower e_{cs} . The plots below show the response to shear for the suggested type I, II, II-A and III soils.



Figur 31. Show the response of different types of soils to shear. Illustration from (Holtz et al., 1981)

The strain-softening response in the type II soils are according to (Budhu, 2008), due to localized failure zones (shear bands), which develop just before τ_{peak} is reached and then turn into loosened soil pockets that have reached τ_{cs} . The soil between the shear bands is denser soil that gradually loosen with the continuation of shear. These bands are subject to intense shear, while the soil above and below the band, behave as rigid bodies, where increased permeability in the band could if in presence of water, induce a flow through the bands and trigger flow slides in slopes. The development of shear bands, depend according to (Budhu, 2008) on the boundary conditions, soil homogeneity, grain size, uniformity of loads and initial density.

2.18 Triaxial shear test

When designing a geotechnical structure, both undrained and drained testing conditions can be considered, depending on which one is more critical. For an excavated slope or road cut, the longterm or drained condition is more critical, whereas for embankments, the short-term or undrained condition is more critical.

The triaxial test is conducted on a cylindrical soil sample, where an increase in axial and radial stresses can be controlled. The flow of water in and out of the sample can be controlled accurately, enabling both drained and undrained conditions. It is noted by (Knappett and Craig, 2012), that the porewater pressure (u) in the sample can be recorded, enabling the determination of the effective stress in the sample. Further, it is important to adapt the test to the different stress situations for the situation in hand, where drained or undrained tests can be conducted in extension ($\sigma'_3 > \sigma'_1$) i.e radially compressed or compression (σ'_1

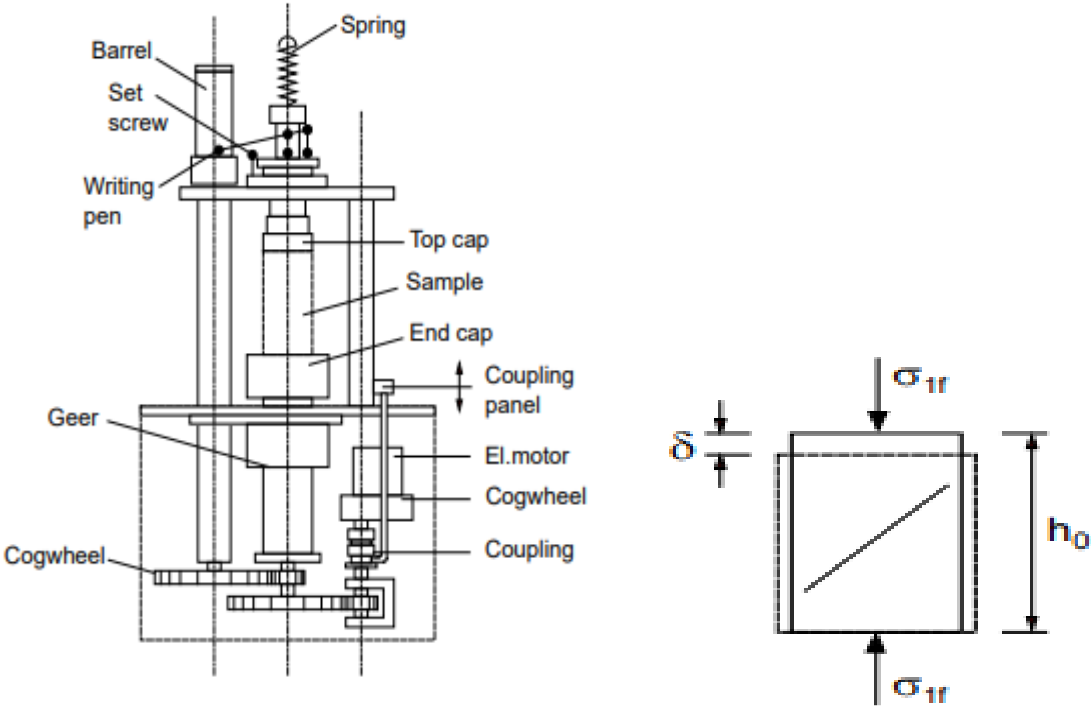
$> \sigma'_3$) i.e vertical compressed. The tests further need to be conducted according to the vertical and horizontal effective stresses that the soil actually experiences in situ. This is achieved through drained consolidation of the sample either to an isotropic ($K'_o=1$) or anisotropic effective stress ($1 > K_o > 1$) consolidation is reached. The drained or undrained shearing of the sample initiates after drained consolidation is reached. The most common triaxial tests, which can be conducted in compression (active) or in extension (passive), are listed below:

- Isotropically consolidated drained/undrained → CID/CIU
- Anisotropically consolidated drained/undrained → CAD/CAD

The stress, strain and pore pressure data collected during the shearing test is plotted as stress paths and stress-strain curves, which in the case of drained tests are used to derive the friction angle ϕ'_{cs} / ϕ'_p , the effective Young's modulus E' , shear modulus G , attraction a and cohesion c . From undrained tests both undrained S_u and ϕ'_{cs} can be derived. The stress paths and stress-strain curves can further be used to determine the drained volumetric response and undrained porepressure response of the soil during shear as well as identifying strain-hardening or strain-softening behaviour of the soil when subjected to applied stress.

2.19 Unconfined compression test

Unconfined compressive strength (UCS) stands for the maximum axial compressive stress that a specimen can bear under zero confining stress. Due to the stress being applied along the longitudinal axis, the test is also known as uniaxial compression test (UCT). The test is according to (Sandven et al., 2017) conducted by axially loading a cylindrical or prismatic test sample until failure. The axial stress in the sample (σ_1) at a certain compression, is calculated as the ratio between the axial failure load and the corresponding sample area at the actual deformation. Lateral stresses are not applied on the sample, i.e. $\sigma_3 = 0$. The loading is assumed undrained in cohesive soils.



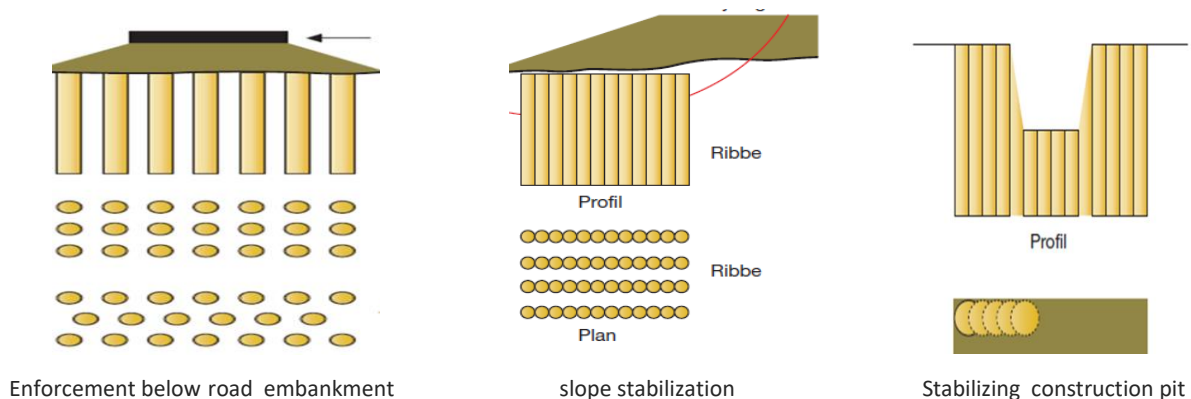
Figur 32. Show sketch of the unconfined compression test rig and stress conditions acting upon the sample during uniaxial shear. Illustration from (Sandven et al., 2017).

2.20 Soil enhancement with binders

In different parts of the world, it is often the case that the mechanical soil properties required to build on a property, are not satisfactory. Roads and railways are subject to settlements in soft or loose soils, while dikes, dunes and slopes can experience a reduction or loss of sufficient stability. Coastlines and rivers are exposed to erosion and earthquakes can cause liquefaction in loose saturated sediments, damaging structures. In cases such as those mentioned above, ground improvement by stabilization or strengthening of the soil are often used.

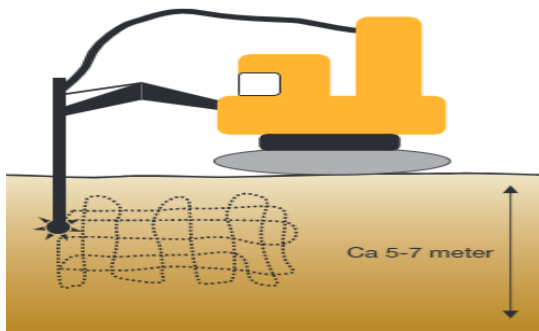
The geotechnical applications described in this chapter, are today conducted by traditional grouting and mixing methods with cement and lime based binders, among others. MICP can potentially be suitable for these applications, but might be limited to applications where the stabilization is not restricted to geometric forms such as the creation of stabilized columns during deep soil mixing (DSM) or for soil improvement at large depths.

When the soil subject to improvement is of shallow depth, techniques such as compaction, nailing, pilesheeting or mass soil mixing (MSM) can be applied, DSM can be applied on larger depth (0-25m). MSM and DSM mixes dry cement or wet mortar under high injection pressure depending on soil saturation, where MSM mixes in a pattern that covers the entire soil mass with a 5-8 m depth limit, whereas DSM creates columns of stabilized soil, which can be in the form of single columns in different patterns or overlapping as ribwalls, as can be seen in illustration below.



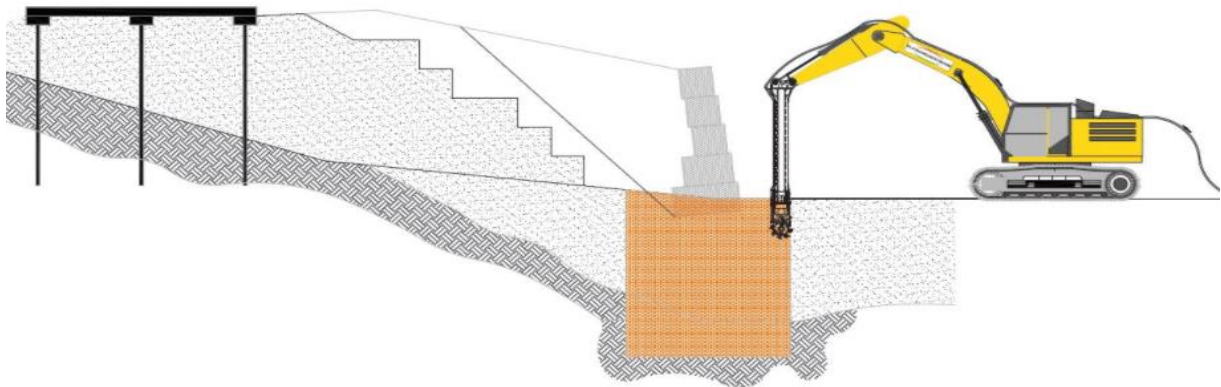
Figur 33. Show different applications for DSM columns. Illustration from (Covicorp, 2020).

The illustration below show an example of mixing pattern applied with MSM in the field.



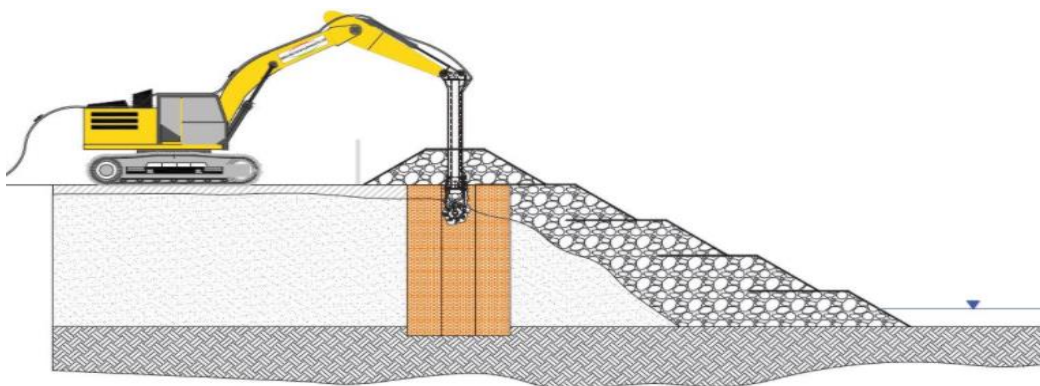
Figur 34. Show example of mixing pattern with MSM. Illustration from (Covicorp, 2020).

Illustration below shows MSM applied to stabilize or reinforce soil below earth retaining walls.



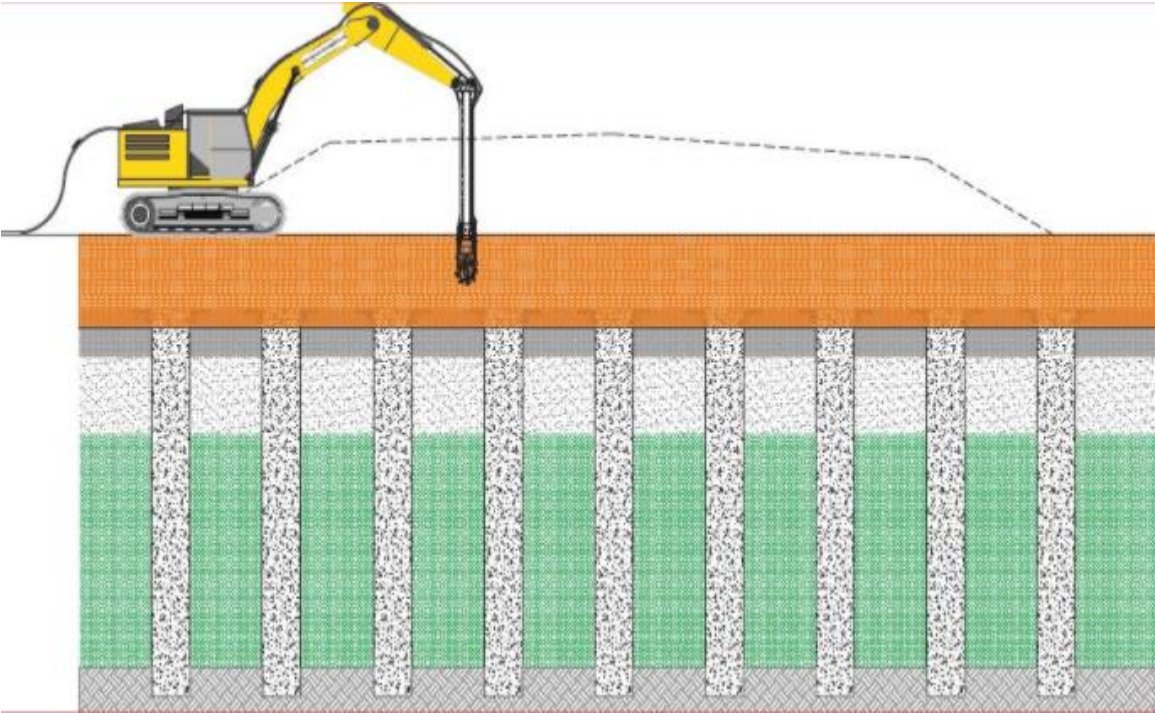
Figur 35. Show stabilizing ground under planned retaining wall with MSM. Illustration from (Covicorp, 2020).

Illustration below shows MSM/DSM used in flood protection schemes to control ground water migration by reducing the permeability. It is also applicable for dike restorations, erosion containment of river banks, reservoirs and coastal areas among others.



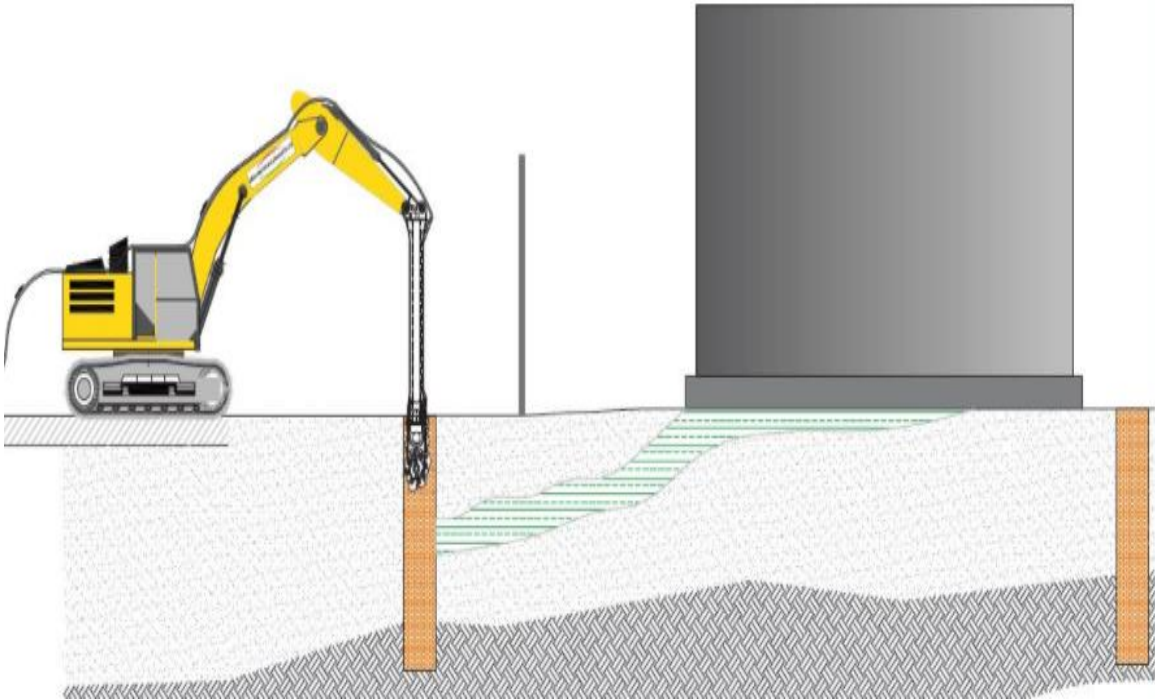
Figur 36. Shows MSM/DSM used to reduce permeability under flood protective constructions. Illustration from (Covicorp, 2020).

The illustration below show application of MSM above cemented columns to strengthen base layer below road embankment.



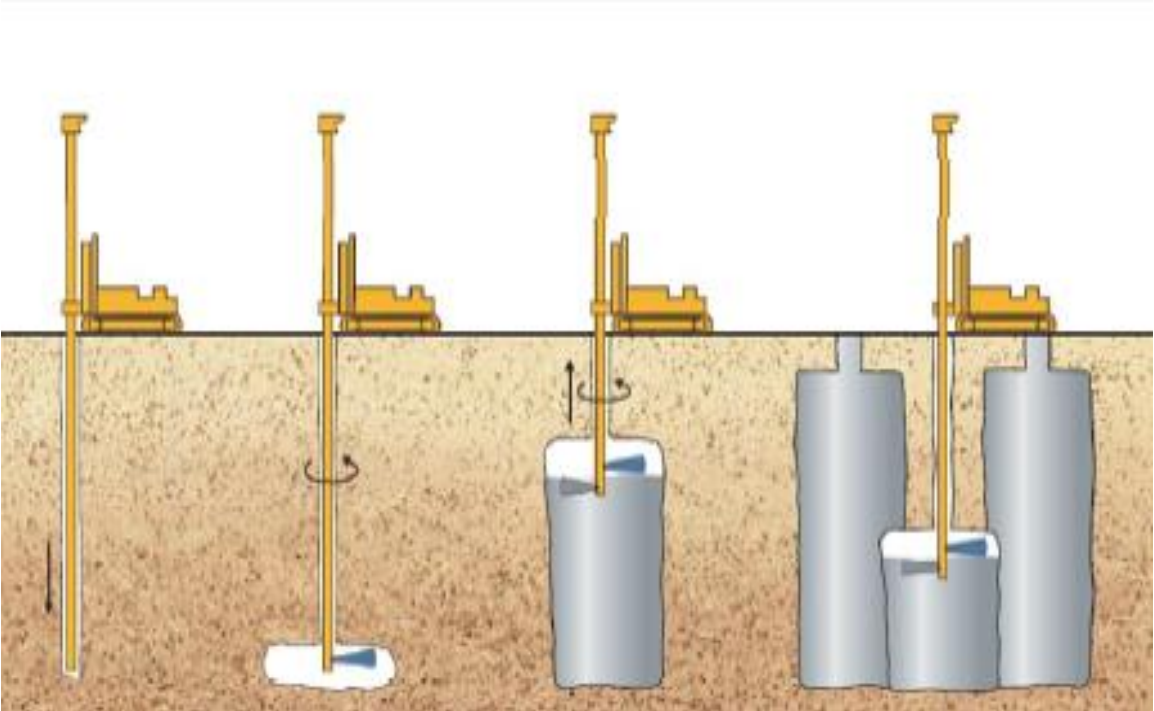
Figur 38. Show MSM applied over cemented columns to strengthen the base layer below a road embankment. Illustration from (Covicorp, 2020).

Illustration below shows MSM/DSM applied in cutting off flow from contaminated soils and sludge in situ. Low permeability cut off walls can also be applied to reduce ground water migration.



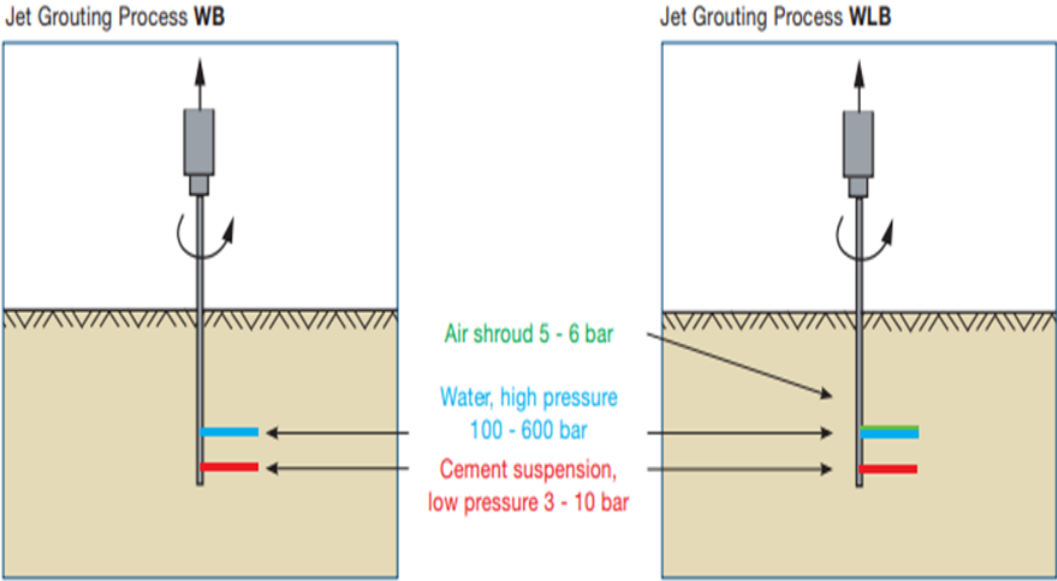
Figur 39. Show DSM used to cut off contaminated flows. Illustrations from (Covicorp, 2020).

The illustration below show jet grouting, where cement slurry is injected under very high pressure and rotational speed, creating cemented soil columns.



Figur 40. Show principle for jet grouting. Illustration from (Van Passen et al., 2010)

For cohesive soils, up to 600 bar of injection pressure (water) is used during jet grouting, as can be seen in the illustration presented below.



Figur 41. Shows applied pressures during jet grouting in cohesive soils. Illustration from (grouting, 2021).

Microbiologically induced calcite precipitation (MICP) is a method for ground improvement that can help achieve a reduction in use of cement products, where precipitated CaCO_3 act as a binder that cement the particle contacts and reduces the voids in MICP-treated soil. MICP can be used as a geotechnical application to:

- Increase shear strength and stiffness in soil
- Reduce porosity and permeability in soils
- Increase resistance to liquefaction in loose and saturated soils

During production of cement, both the combustion of fossil fuels for operating the rotary ovens and the chemical process of converting limestone to lime, generate CO_2 , where (Naeimi and Haddad, 2018) note that 1.3 tons of CO_2 is generated per ton of produced cement. Cement is an integral part in most of the existing grouting and mixing methods, where (Andrew, 2019) note that the cement industry is assumed to contribute to as much as 8% of global CO_2 emissions. To achieve the goals of reductions in CO_2 emissions set in the Paris agreement, the construction industry needs to get access to new and more sustainable methods that contribute to reaching this goal. The following disadvantages of ground improvement with cement and lime products, are incentives for the development of MICP as viable and more sustainable alternative method for ground improvement:

- High carbon footprint
- Limited impact radius from injection (mixing) point.
- High injection pressure which is intrusive to the soil
- Expensive
- Require heavy machinery
- Noise pollution
- Introduces chemicals to the soil and groundwater system.

3. Microbiologically induced calcite precipitation (MICP)

3.1 Bacteria in soils

It is noted by (Ingham, 2021), that bacteria are one-celled organisms, generally $1 \mu\text{m}$ wide and somewhat longer in length, whereas (Mitchell and Santamarina, 2005a) note that they have a cell diameter in the range of $0.5\text{--}3 \mu\text{m}$, and spores

that can be as small as 0.2 μm . They are abundant in soils, where a teaspoon of productive soil, can contain 10^8 - 10^9 bacteria.

Bacteria are the dominant microorganisms in soils and exist from the soil surface and down to larger depths in the ground. Some bacteria have the ability to develop spores, which enables them to endure adverse environmental changes. They can be nearly round, rodlike or spiral in shape (Mitchell and Santamarina, 2005b, Ingham, 2021). They can according to (Mitchell and Santamarina, 2005a) endure pH in the range 2-10, freshwater of varying hardness, very saline water, pressures > 100 bars, temperatures from frozen to above boiling and they can reproduce on an exponential scale under ideal conditions.

Bacteria are particularly concentrated in the narrow region (rhizosphere) next to and in the roots, where (Ingham, 2021) note that some bacteria produce substances that bind soil particles into small aggregates, which improve water infiltration and the ability of a soil to retain water. (Mitchell and Santamarina, 2005a) note that nutrients are required by microorganisms for cellular carbon and minerals as well as energy, where (Ingham, 2021) state that competition for nutrients between bacterial species in the soil, increase when easily metabolized substrates are present. The table presented below lists common nutrients for soil bacteria.

Tabell 11. Lists common nutrients for bacterial growth. Data adapted from (Mitchell and Santamarina, 2005b).

Elements needed to form molecules in the cell	Cellular carbon: CO_2 , HCO_3^- Organic compounds* Minerals: N, P, K, Mg, S, Fe, Ca, Mn, Zn, Cu, Co, Mo
Energy needed to sustain life	Organic compounds* Inorganic compounds* Sunlight
Growth conducive factors	Amino acids, vitamins, etc
<i>Organic and inorganic compounds* O, NO_3^-, NO_2^-, N_2O, SO_4^{2-}, CO_2, Fe^{3+}</i>	

3.2 Bacterial transport within the soil

In their work, (Ng et al., 2012) note that soil microbes move through the soil via the pore throats located between soil particles, either by self-propelled

movement or by passive diffusion, where bacteria 0.3-2 μm in width can move freely within sandy soil with particle size 0.05-2.0 mm, while an increased share of fine particles in a soil, would limit or block the bacteria's movement within the soil. (Schijven et al., 2017) add that bacteria can shelter inside pores in the range 0,2-6 μm depending on the bacterias size, whereas porethroats equal to, or smaller than the bacteria, will restrict their movement.

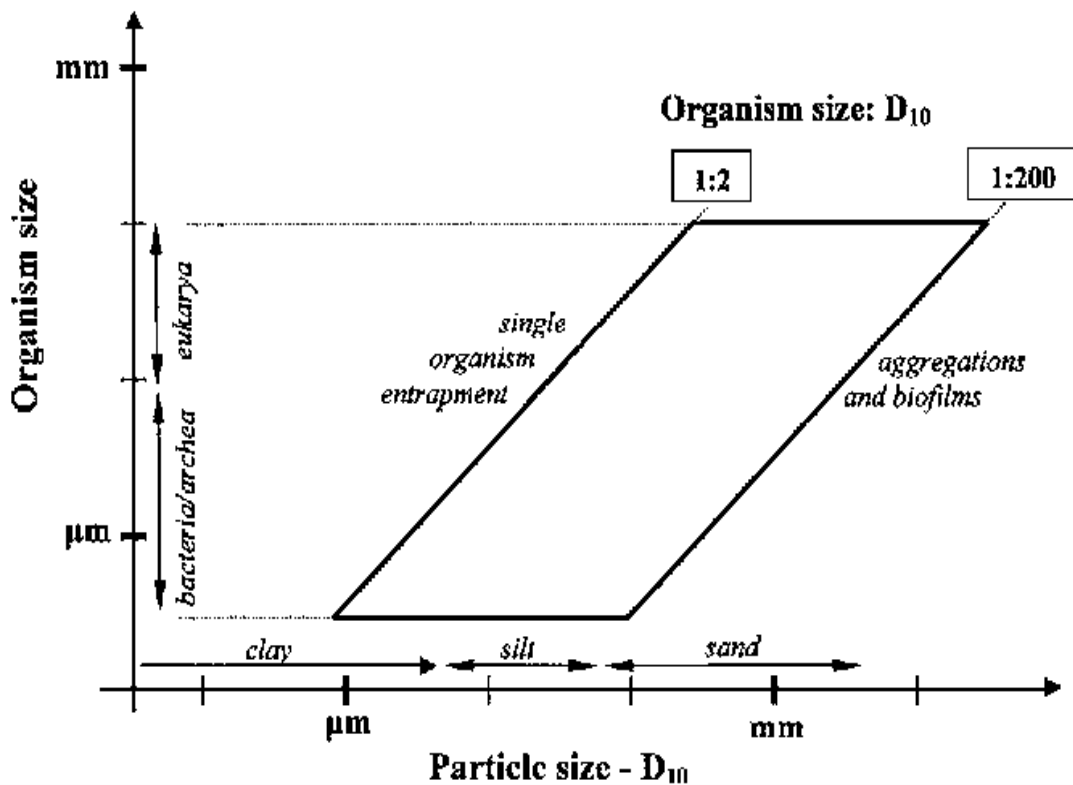
(Bitton and Harvey, 1992) state that in fine grain sediments, both sorption and straining can result in significant removal or transport of unattached bacteria as they are transported down gradient, where straining occur when average cell diameter is greater than 5% of average particle size. (Schijven et al., 2017) note that attractive forces exerted by particle surfaces, can reduce the bacterias ability to move within the soil.

The transport and survival of microorganisms in the rhizosphere, is influenced by the vertical flow or percolation, which is enhanced by flow channels created by plant roots and worms. However, (Schijven et al., 2017) note that high degree of density in a soil, will limit the microbial movement with percolating water. Saturated soil enables bacteria to be transported over much greater distances than under unsaturated conditions, where (Lamka et al., 1980, Zyman and Sorber, 1988) found that bacterial transport through soil is accelerated by heavy (≥ 12.3 cm/day) rainfall. (Schijven et al., 2017) note that attractive forces exerted by particle surfaces on the bacteria, can reduce the bacterias ability to move within the soil, while percolating fresh water from rain fall reduce the ionic strength in the pore water, which contribute to bacterial transport by reducing the attractive forces (Zyman and Sorber, 1988).

According to (Schijven et al., 2017), the macropores have more influence on the transport of bacteria in soil than the soil texture. In work by (Yang and van Elsas, 2018), it is noted that increased water content increases the bacterial cell motility (movement through fluid), where pores filled with water, have greater connectivity with eachother than air filled pores, due to the discontinuous liquid phase. It is further noted that bacterial movement between pores much larger than the bacteria itself, would still impaire motility if unsaturated.

3.3 Geometric compatibility

In work by (Mitchell and Santamarina, 2005b), a relationship of compatibility between d_{10} particle size of the soil and size of organisms, was integrated into a diagram, where very fine or very coarse soils do not fall within geometric compatibility for ureolytic bacteria (0,5-3 μm). The compatibility diagram is presented below.

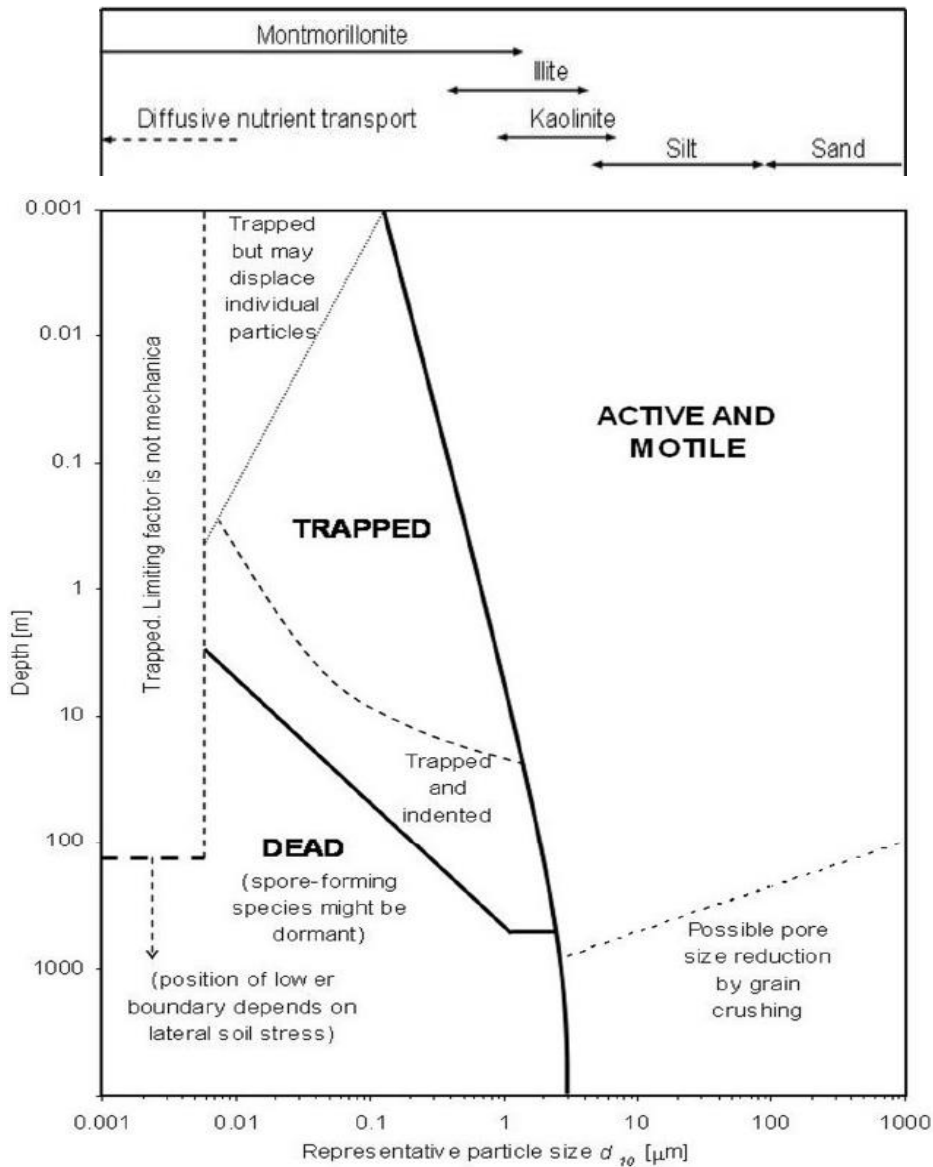


Figur 42. Shows compatibility for effective particle size (d_{10}) in relation to size of organism. The bounded region in the diagram represent the range of geometric compatibility between pore size and bacteria size. Illustration from (Mitchell and Santamarina, 2005b)

In work by (Lin, 2016), it is noted that habitable pores and pore throats are found in coarse soils, and in some clayey soils at shallow depth, where particle size in silts and sands correlate with the size pores and pore-throats, whereas pores in clayey soils can be several times larger than the particles and still be relatively enclosed. The lack of habitable pore space and limited mobility between pores, lead to a decline in microbial density with decreasing particle size.

The bacteria in the soil are according to (Rebata-Landa, 2007), "active and motile" when pore and pore throats are large enough to allow cells moving through the pore network and find sufficient space for growth and metabolic activity, while "trapped" when pore throats are too small for the bacteria to

migrate and “dead” when confining pressure due to depth in the soil profile, exceeds the resistance of the cell structure. However, spore forming bacteria can be dormant in this region. The diagram below illustrate the relationship between effective particle size (d_{10}), soil depth and state of bacteria, where maximum d_{10} for mobility at 5-20 m depth is less than $2 \mu\text{m}$.



Figur 43. Show limitation boundaries in terms of effective particle size (d_{10}) and depth. Illustration from (Lin, 2016).

3.4 Driving factors for MICP

There are according to (Chaparro-Acuña et al., 2018), two types of biomineralization:

- Biologically controlled mineralization (BCM)
- Biologically induced mineralization (BIM)

In BCM, minerals are usually deposited within organic matrices in living cells, enabling organisms to exert control over the nucleation and growth of minerals, whereas in BIM the microorganisms secrete one or more metabolic products that react with the ions or compounds in the environment, followed by a deposition of the mineral as a metabolic by-product. According to (Bindu J, 2017), biomineralization in soil, most commonly occur as:

- Ureolysis (hydrolysis of urea)
- Denitrification
- Iron reduction
- Sulphate reduction

The method of MICP was adopted from BIM, a biomineralization process occurring in the natural environment, where urease enzyme producing soil bacteria through ureolysis degrade urea and precipitate calcium carbonate (CaCO_3). Ureolysis predominates in most of the reaction environments, as the increase in pH caused by the by-products of the reaction, inhibits other competitive reactions. The MICP process is according to (Zehner et al., 2020) driven and controlled mainly by the following factors:

- Availability of nucleation sites
- pH and temperature
- Concentration of dissolved inorganic carbon and free calcium ions
- Geometric compatibility of bacteria
- Availability of urea and oxygen

The properties of the CaCO_3 crystals precipitated during MICP, are dependent on:

- Soil permeability and residence time of injected cementation solution
- Rate of ureolysis, concentration of ions at supersaturation and precipitation rate

According to (Hsu et al., 2017) ureolytic bacteria can be divided into two groups based on their urease response to ammonium:

- Bacteria with a repressed response to ammonium
- Bacteria which do not have a repressive response to ammonium

For the ureolytic bacteria chosen as a causative agent for the MICP process, the following factors are important:

- Cost effective and exponential growth

- High urease capacity *sustained under*:
 - *conditions with limited dissolved oxygen*
 - *presence of ammonium*
 - *both low and high temperatures as well as high pH*
- Robust and negatively charged cell surface
- Geometric compatibility
- non-pathogenic and have no transferable elements

3.5 Ureolytic bacteria

Studies on MICP focused on potential geotechnical applications, have used different ureolytic bacteria as causative agents. The table below lists some of the

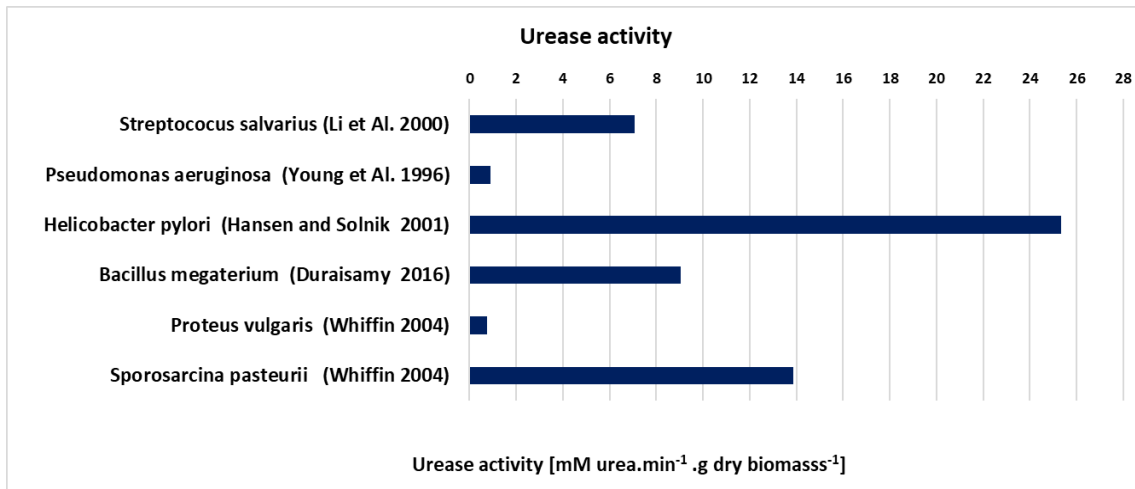
bacteria strains studied for different applications.

Tabell 12. Listsintended geotechnical applications for different bacteria used in previous studies. Data adapted from (Choi et al., 2020a).

Bacteria	Geotech. application	Referances
<i>S.pasteurii</i>	Soil stabilization Settlement reduction	Choi et Al. 2017, Dejong et Al. 2006, Al Quabany and Soga, 2013, Zhao et Al. 2014, Choi et Al. 2016, van Passen et Al. 2009.
<i>Bascillus megaterium</i>	Soil stabilization Settlement reduction	Li et Al. 2018
<i>Bascillus sp. VS1</i>	Permeability reduction	Chu et Al. 2013
<i>B.sphaericus</i>	Permeability reduction	Cheng et Al. 2014, Cheng et Al. 2013.
<i>Bascillus megaterium</i>	Permeability reduction	Smith et Al. 2017, Soon et Al. 2013.
<i>S.pasteurii</i>	Erosion control	Meyer et Al. 2013, Malaki et Al. 2016, Salifu et Al. 2016.
<i>S.pasteurii</i>	Liquefaction protection	Burbank et Al. 2013.

In a review of previous studies, (Rahman et al., 2020a) found that *S. pasteurii*, which is moderately alkaliphilic, non-pathogenic and have highly active urease enzymes, was the most widely used ureolytic bacteria in studies on MICP.

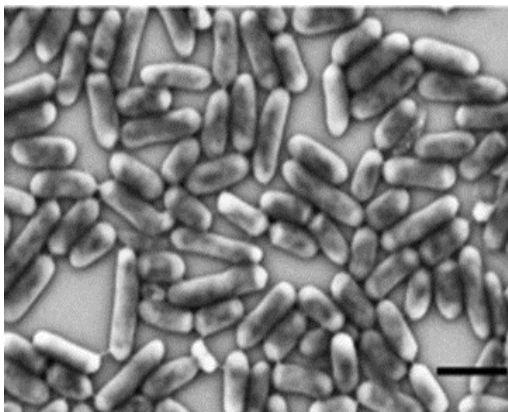
The urease activity for different ureolytic bacteria was investigated in work by (Duraismy, 2016), where *Helicobacter pylori* was found to have the highest urease activity followed by that of *S. pasteurii*. However, *Helicobacter pylori*, *Proteus vulgaris* and *Pseudomonas aeruginosa* can cause stomach infections. The results of the comparison study are presented in the graph below.



Figur 44. Show measured urease activity for different ureolytic bacteria. Data adapted from (Duraismy, 2016)

In their work, (Oliveira et al., 2015) compared *S. pasteurii* and *I. insulsalsae* as agents for MICP in sandy soils, where *I.insulsalsae* was found to be more effective than *S. pasteurii* in precipitating CaCO_3 .

S. pasteurii are according to (Asgharzadeh et al., 2016), 0,5-1,2 μm in diameter and 1,3-4 μm long soil-borne facultative anaerobes, which make them able to use other electron acceptors in the absence of oxygen (O_2). They utilize ammonium to enable substrates to cross the cell membrane into the cell, while urea is used as their source for nitrogen and carbon. In the SEM image presented below, the physical appearance of the bacteria can be observed.



Figur 45. Show Scanning Electron Microscopy (SEM) image of *S.pasteurii* bacteria. Image from (Ma et al., 2020b).

In their work, (Wiffin, 2004, Hsu et al., 2017) note that *S. pasteurii* is considered to be among the most robust and stable ureolytic bacteria, due to its capacity to survive extreme environmental conditions, where (Ma et al., 2020b) observed that it remained in good physical shape, despite being surrounded by CaCO_3 crystals during precipitation. The other bacteria (*B. subtilis*) used in the study, did not tolerate the harsh conditions and was damaged and lysed (cell death). (Hammad et al., 2013) found that the urease activity of *S. pasteurii* showed stability and consistency, where its capacity to precipitate larger amounts of CaCO_3 , is due to its ability to secrete large amounts of urease enzyme, which works as a catalyst and accelerator for the ureolysis (Bhadur et al., 2016).

3.6 Biochemical reactions

3.6.1 Ureolysis and precipitation

Ureolysis is according to (Van Paassen, 2009a), the most thermodynamically favored mechanism of bio-mineralization with the highest CaCO_3 conversion rate, compared to aerobic oxidation, denitrification and sulfate reduction. Hence, ureolysis is the most widely used bio-mechanism within MICP. Bacteria used for the purpose of MICP need to have the capacity to produce urease enzyme, such that ureolysis can initiate, where urea ($\text{CO}(\text{NH}_2)_2$) is decomposed into ammonia (NH_3) and carbon dioxide (CO_2) in the following reaction (Choi et al., 2020a):



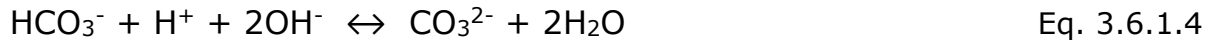
When NH_3 is dissolved in water (H_2O), ammonium (NH_4^+) and hydroxide (OH^-) ions are produced and pH rises, in the following reaction:



The released ammonium is highly soluble and will remain in the immediate surroundings such as soil and groundwater. The ammonia (NH_3) is unstable and can be released as a gas. The dissolved CO_2 produces bicarbonate (HCO_3^-) and hydrogen ions (H^+) in the following reaction:



As a result of the increased pH, HCO_3^- react with OH^- to form negatively charged carbonate ions (CO_3^{2-}) in the following reaction:



Calcium carbonate (CaCO_3) is precipitated when the concentration of calcium ions (Ca^{2+}) and CO_3^{2-} is greater than the solubility product (K_{sp}) i.e at supersaturation and pH exceeds 8,3:

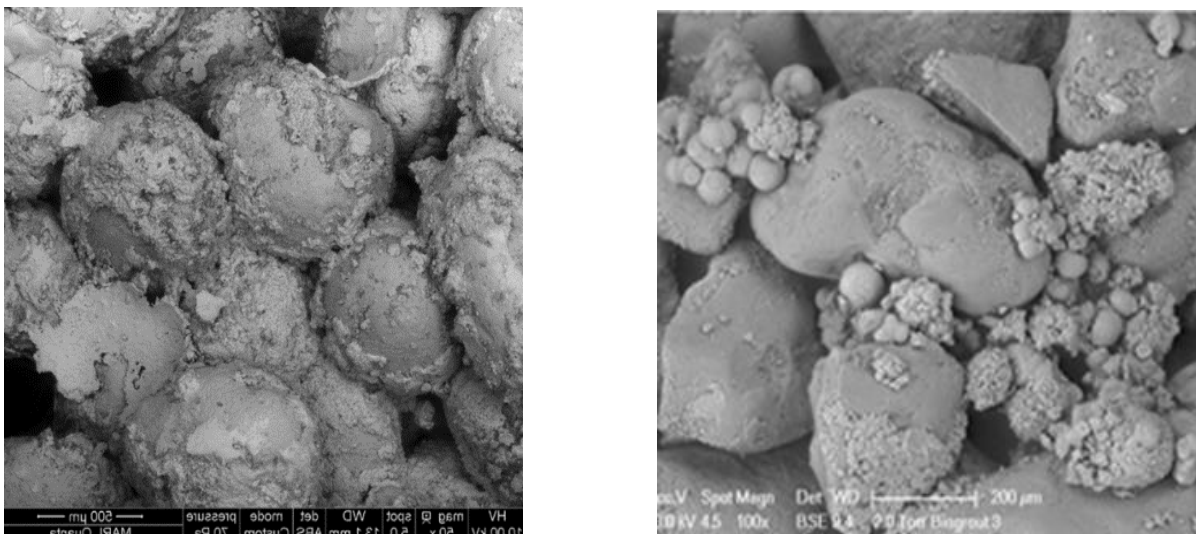


The precipitation rate increases up to $\text{pH} \sim 9$, where the precipitation rate again is reduced when pH approaches neutral. However, the final pH of the solution will depend on the reaction rates and substrate concentrations.

Calcium ions are bound to the external cell surface because of the negatively charged functional groups in the cell wall. The CaCO_3 formation occurs in the cell surface, once supersaturation is reached.



Successive CaCO_3 layers (stratification) are developed on the external cell surface. This limits the nutrient and oxygen transfer and the cells will finally be encapsulated by CaCO_3 crystals, provoking cellular degradation (lysis). In the images below, precipitated calcite (CaCO_3) is shown on the grain surfaces and particle contacts in a sand.



Figur 46. Show SEM image of percipitated CaCO_3 on and in between sand particles. Image from at left side from (Choi et al., 2020a) and image at right from (Cheng et al., 2017)

3.6.2 CO₂ in ureolysis

One of the incentives for MICP as an alternative method for ground improvements is the reduction in use of cement and lime based binders, where the production of these are associated with large emissions of CO₂. Ureolysis utilizes inorganic carbon such as CO₂ in the bio-chemical process.

Urea is according to (Okuyay et al., 2016) a compound containing nitrogen found in urine of mammals and is widely used in fertilizers. During the degradation of urea (ureolysis), CO₂ and NH₄⁺ are produced. Dissolved NH₄⁺ increases the pH, causing the CO₂ in the air to dissolve in water and to then be converted into HCO₃⁻ and then CO₃²⁻. In environments where unsaturated calcium concentrations and ureolytic bacteria are present, the microorganisms will serve as a catalyst of the reaction of CO₃²⁻ with Ca²⁺ ions to form CaCO₃. There are two possible CO₂ sources for the precipitation of CaCO₃ in MICP:

- CO₂ dissolution present in the air or from dissolved minerals
- CO₂ produced during ureolysis and respiration

For CO₂ produced during ureolysis to be sustainable, the amount of CO₂ produced by bacterial metabolism, have to not exceed the bacterial capability to sequester CO₂ through MICP.

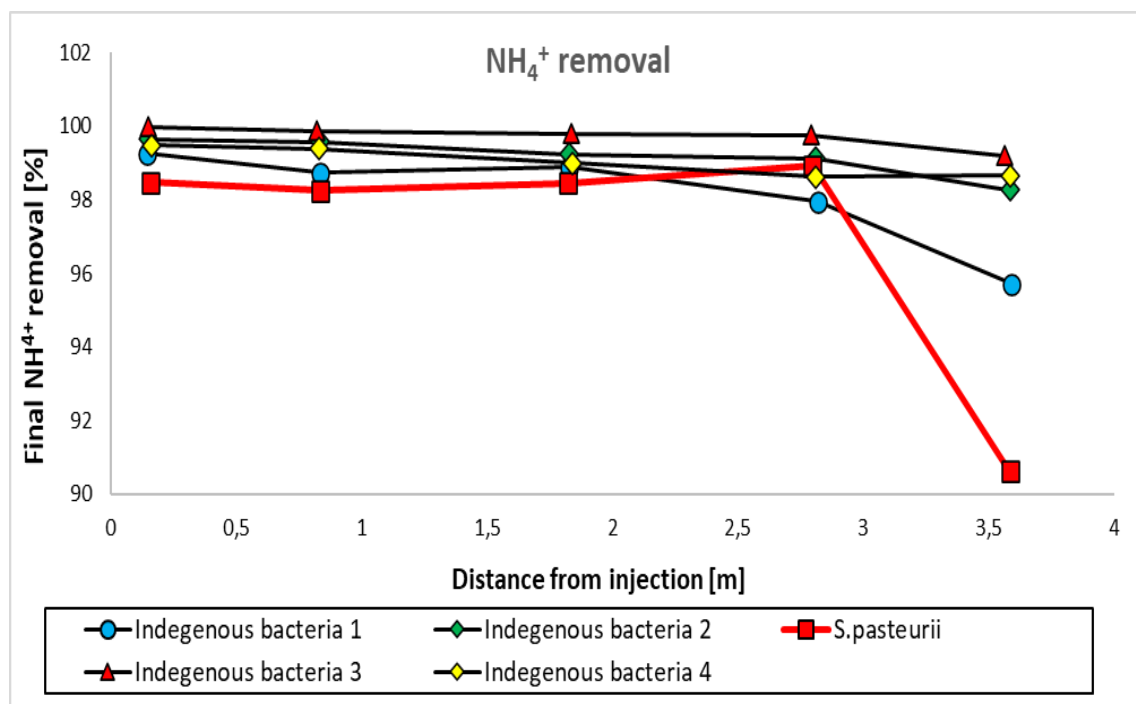
3.6.3 Ammonium as a byproduct

As part of the ureolysis in MICP, NH₄⁺ is released as a by-product. The other form of ammonia that is released during this process is the unionised form of ammonia (NH₃), which is volatile and can be released as a foul smelling gas and considered toxic at long-term exposure (Cheng et al., 2019). In their work, (Lee et al., 2019a) note that high concentrations of NH₄⁺ in surface waters, decreases the pH, stimulate growth of toxic algae, decrease amount of dissolved oxygen, produce toxins and contribute to bacterial growth. This can threaten fish, flora and fauna, where infiltration of NH₄⁺ into the groundwater, could pollute the drinking water, where high concentrations of NH₄⁺, is linked to health risks.

Removal of aqueous NH₄⁺ in the treated soil during MICP have to be addressed for MICP to be viable as an alternative method for ground improvement. The NH₄⁺ can be extracted from the ground through rinsing with high ionic and high pH solutions, whereas NH₃ need to be addressed by somehow suppressing the

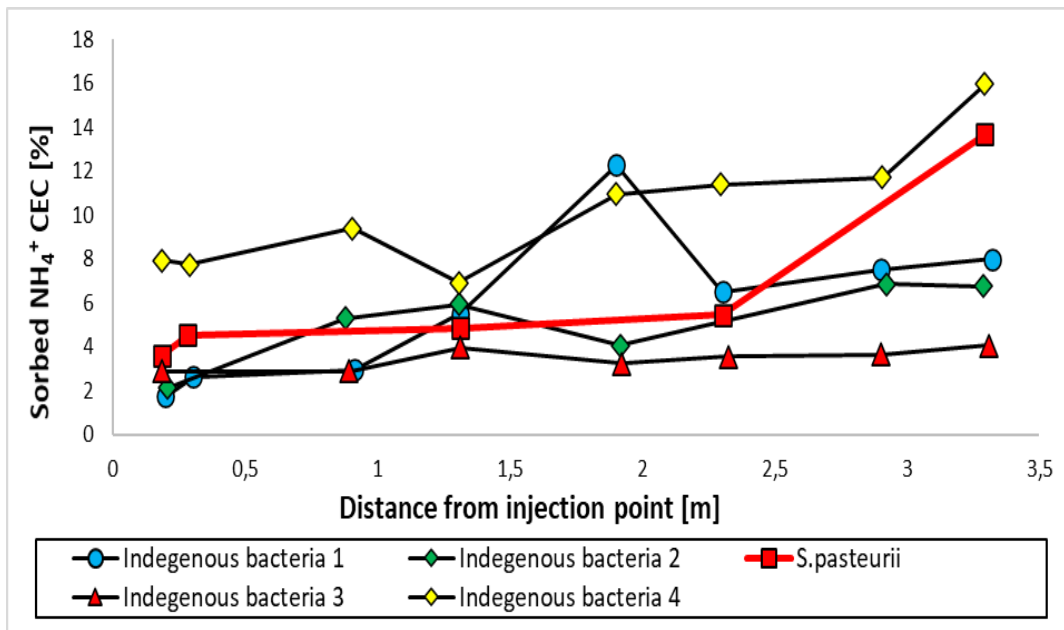
release. Few studies have been conducted on removal of NH_4^+ in MICP-treated soils, where most have been on lab-scaled samples and focused on the amount of produced NH_4^+ as an indication of urease activity. However, (Van der Star et al., 2011) successfully removed almost all NH_4^+ from a 1000 m^3 MICP-treated area of sand and coarse gravel. The injection and extraction wells utilized during treatment to create an artificial gradient through the target area, were also used in the extraction of the NH_4^+ by increasing the extraction flow rate, post-treatment. The extraction was continued until electrical conductivity and concentrations of NH_4^+ , returned to pre-treatment values.

In their work, (Lee et al., 2019b) removed NH_4^+ from five 3,7 m long (0,2m x 0,2m) MICP-treated sand columns with 525 L of a high pH and high ionic strength rinse solution, where reduction in concentrations of aqueous NH_4^+ in the columns, was controlled over time (24 hours). After rinsing and a 12 hour residence period, all distances from injection point achieved more than 95,7% NH_4^+ removal, with the exception of the most distal location in the column treated with *S. Pasteurii* (90.6%). At distances less than 2.82 m, high (> 98.0%) degree of removal was observed for all columns. The results are presented in the plot below.



Figur 47. Show final NH_4^+ removal as a function of distance from injection point. Data adapted from (Lee et al., 2019b)

However, the study showed that there was residual sorbed NH_4^+ in the rinsed MICP-treated soil, where concentration of sorbed NH_4^+ increased with distance from injection point. The results are presented in the plot below.



Figur 48. Show sorbed NH_4^+ remaining after rinsing of MICP-treated soil. Data adapted from (Lee et al., 2019b).

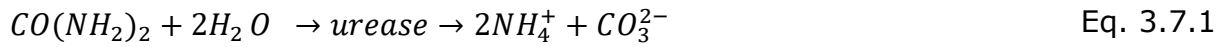
The study concludes that rinsing of NH_4^+ from MICP-treated soil with high pH and high ionic strength rinse solution, where measured shearwave velocity (v_s) indicated no adverse effects on the cementation during rinsing, could be viable in the field. However, the remaining aqueous NH_4^+ and sorbed NH_4^+ indicate a need for further studies.

3.7 Urease activity

The level of urease activity is related to the end product which is precipitation of CaCO_3 . For MICP to be viable as a method for ground improvement, it is necessary to identify the factors that affect the urease activity, so that regulation of these factors can be utilized to steer the process towards the desired outcome, which for example could be amount or pattern of precipitation. The affecting factors are further important for evaluating the suitability of MICP in different kind of soils and ground conditions.

The urease capacity of the ureolytic bacteria is of great significance, given that ureolysis is the core part of the MICP process. Ureolytic bacteria utilized in MICP, should be able to sustain high urease activity over time, including under conditions with limited access to dissolved oxygen as well as under a broad range of

temperature and pH. As noted by (Van Paassen, 2009a), ureolysis is an irreversible reaction, where urea reacts with water and forms ammonium and carbonate in the following reaction:



At neutral pH, HCO_3^- is more abundant than CO_3^{2-} , which increases the pH to obtain charge equilibrium. The rise of pH causes NH_4^+ to dissociate into NH_3 until equilibrium is reached between NH_4^+/NH_3 and HCO_3^-/CO_3^{2-} , normally at pH ~ 9.

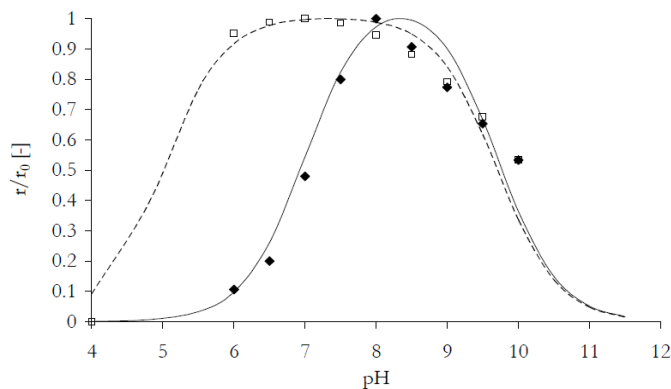
It is noted by (Stocks-Fischer et al., 1999) that the rate of ureolysis among others factors, will depend on the concentration of urea. When urea is almost depleted, the rate decline and this can according to Michaelis-Menten kinetics be expressed as:

$$\frac{r_h}{r_{h0}} = \frac{C_{urea}}{K_{m,urea} + C_{urea}} \quad \text{Eq. 3.7.2}$$

Where r_{h0} is the actual rate, r_h the maximum rate, C_{urea} is the urea concentration and $K_{m,urea}$ is the half saturation constant, representing the concentration at which the rate is reduced by 50%. (Stocks-Fischer et al., 1999) found the optimum rate of ureolysis at $pH_{opt} = 8,5$. At values below and above pH_{opt} , the urease activity decreases, forming a bell shaped inhibition curve, described as:

$$\frac{r_b}{r_{h0}} = \frac{1 + 2 \cdot 10^{0,5(pH_{LL} - pH_{UL})}}{1 + 10^{(pH_{opt} - pH_{UL})} + 10^{(pH_{opt} - pH_{LL})}} \quad \text{Eq. 3.7.3}$$

Where r_{h0} is the rate of ureolysis at pH_{opt} and pH_{LL} and pH_{UL} are the lower and upper limits at which the rate is reduced by 50%. The effect of pH on the normalised urease activity is presented in the plot below.



Figur 49. Shows the effect of pH on the normalised urease activity. Data from Stocks-Fischer et Al. 1999 (■) and Whiffin 2004 (□). Illustration from (Van Paassen, 2009a)

In work by (Whiffin, 2004) it is noted that the concentration of Ca^{2+} affect the urease activity, where low concentrations of CaCl_2 up to 50 mM had no significant effect on the urease activity, whereas concentrations $> 0,5 \text{ M}$, resulted in decreasing urease activity. This inhibitory effect of CaCl_2 can be approximated using the following expression:

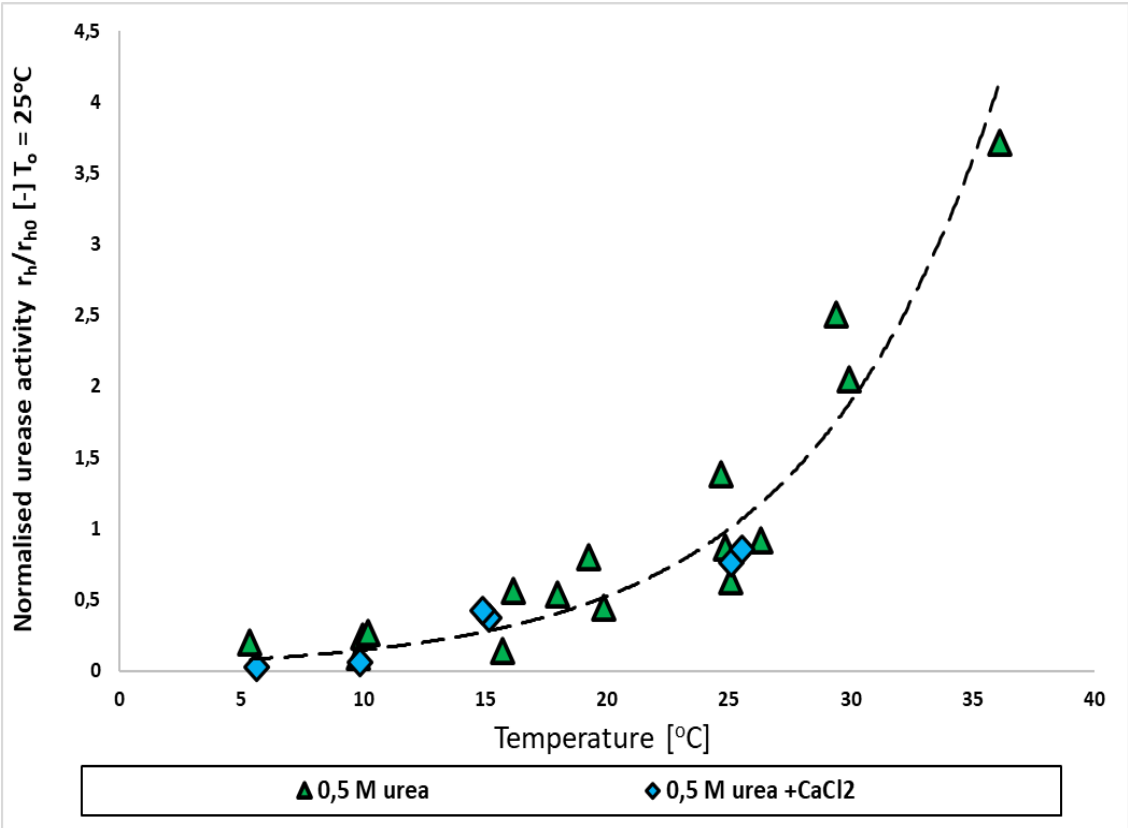
$$\frac{r_h}{r_{h0}} = e^{-C_{Ca} / K_{i,Ca}} \tag{Eq.3.7.4}$$

Where C_{Ca} is the concentration of Ca^{2+} and the coefficient $K_{i,Ca}$, is the concentration at which the urease activity is reduced to 37% of its initial value.

It is further noted by (Whiffin, 2004), that temperature have a significant effect on the rate of ureolysis, where no urease activity was registered below 5°C , while a 10°C rise in temperatures within the range of $5\text{-}35^\circ\text{C}$, increase the urease activity with a factor of Q_{10} and can be expressed as:

$$\frac{r_h}{r_{h0}} = \exp \left[(T - T_o) \frac{\ln Q_{10}}{10} \right] \tag{Eq. 3.7.5}$$

In the plot below, the effect of temperature on normalised urease activity (r_h/r_{h0}) using different cementation solutions is presented.



Figur 50. Show normalised urease activity as a funtion of temperature for different cementation solutions. Data adapted from (Whiffin, 2004).

According to (Whiffin, 2004), the urease activity will eventually decrease and finally decay due to cell lysis, which can occur at depletion of nutrients or due to encapsulation of the bacteria during precipitation of CaCO₃ crystals. The effect of progressive cell lysis on the urease activity, assuming exponential decay, can be expressed as:

$$\frac{r_h}{r_{h0}} = \exp\left[-\frac{t}{t_d}\right] \quad \text{Eq. 3.7.6}$$

where t_d is the exponential time constant, at which the urease activity has been reduced by a factor e to about 63% of its initial value.

According to (Whiffin, 2004), the cell lysis is slow (weeks) at temperatures around 10°C, where increased concentrations of salt, toxic compounds or increased temperature will accelerate the lysis and reduce the capacity for ureolysis. Under such conditions, bacteria tend to excrete their enzymes, which will degrade faster outside of the cell than inside. The encapsulation of the bacteria during the precipitation process, causes further decay of the urease activity, which if assuming exponential decay, can be expressed as:

$$\frac{r_h}{r_{h0}} = \exp\left[-\frac{S_{CaCO_3}}{S_d}\right] \quad \text{Eq. 3.7.7}$$

where S_d is the characteristic decay concentration of precipitated CaCO₃ at which the urease activity has been reduced by a factor e , to about 63% of its initial value.

3.8 Factors affecting the urease activity

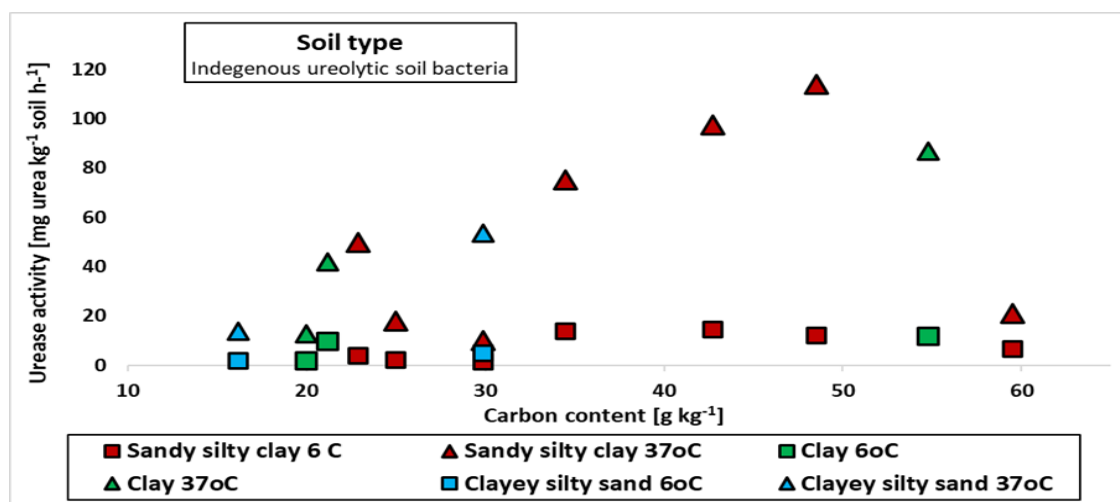
3.8.1 Soil properties

Physical and chemical properties vary between different types of soils and for MICP to be well adapted to the target soil, investigating the effect of the different properties on the urease activity, is important. In work by (Vahed et al., 2011), it is noted that the rate of naturally occurring ureolysis in the soil, depends on factors such as soil type, organic matter, water content, temperature, salinity and pH, where some factors reduce the rate and others accelerate the rate.

In their work, (Gillman et al., 1995) investigated unbuffered urease activity of indigenous bacteria in clay, clayey silty sand and sandy silty clay at 6°C and at

37°C, where the results show that urease activity did occur at 6°C in all the soils, but was lower at 6°C than at 37°C. The ratio (37°C /6°C) between urease activity at 37°C and 6°C for a given soil was found to be in the range 3,1-12,4. Results further show increasing urease activity with increasing carbon content at 37°C but not at 6°C, where the sandy silty clay obtained higher urease activity than the other soils at 37°C, but not at 6 °C.

The urease activity was low at 6°C, where variation in level of urease activity between the soils was minimal and where 34% of the urea was still not hydrolyzed at end of experiment. This could suggest that temperature is the reason for slower ureolysis at 6°C and not depletion of urea. Results for urease activity as a function of carbon content in the soil, is presented in the plot below.



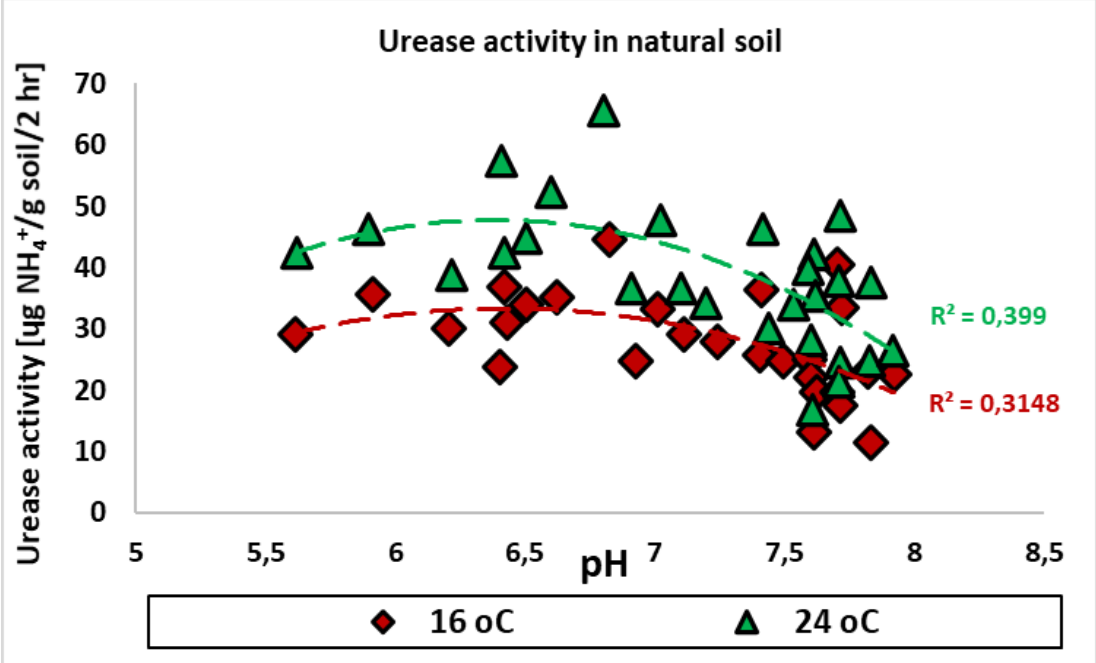
Figur 51. Show urease activity for different soils as a funtion of carbon content in the soil. Data adapted from (Gillman et al., 1995).

In their work, (Vahed et al., 2011) evaluated the influence of physical and chemical properties on the urease activity in soils at 16°C and 24°C. The results show a strong positive correlation between nitrogen in the soil and urease activity, moderate correlation for clay content or cation exchange capacity and urease activity, while weaker correlations between silt or sand content and urease activity. The derived correlation factors, are presented in the table below.

Tabell 13. Lists degree of correlation between urease activity in indegenous soil bacteria and different soil properties at 16°C and 24°C. Data adapted from (Vahed et al., 2011)

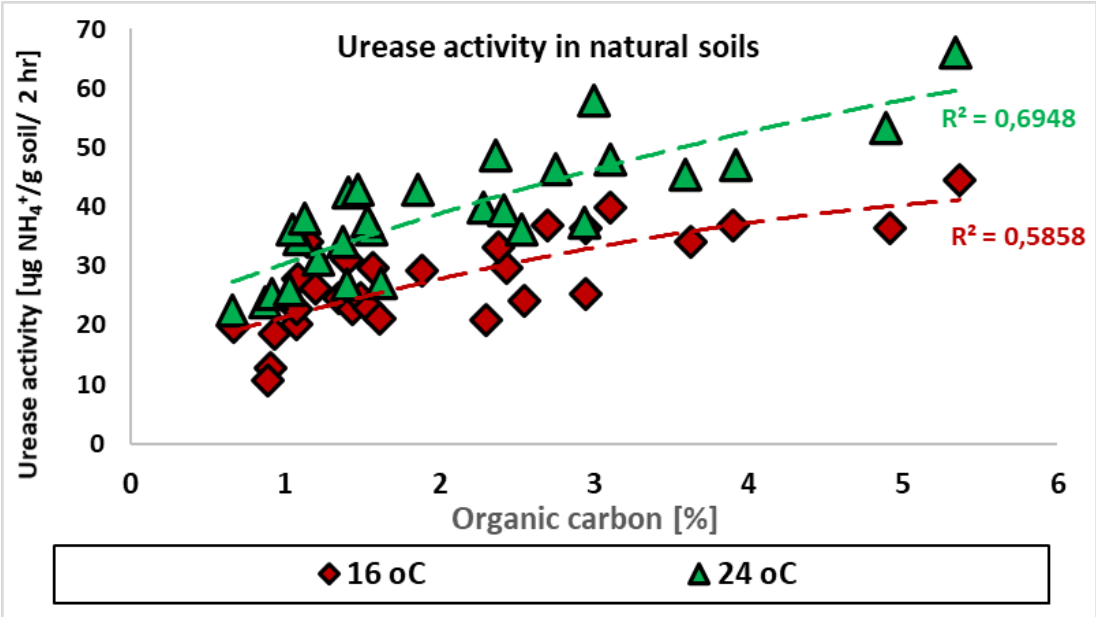
Soil properties	Correlation coefficient at 24 °C	Correlation coefficient at 16°C
Clay particles	0,44	0,47
Silt particles	0,08	0,13
Sand particles	0,19	0,18
Total nitrogen	0,82	0,74
Cation exchange	0,30	0,35

The study by (Vahed et al., 2011), further found moderate correlation between pH and urease activity, where increasing temperature increased the urease activity and optimal pH was observed at around pH 7. The results are presented in the plot below.



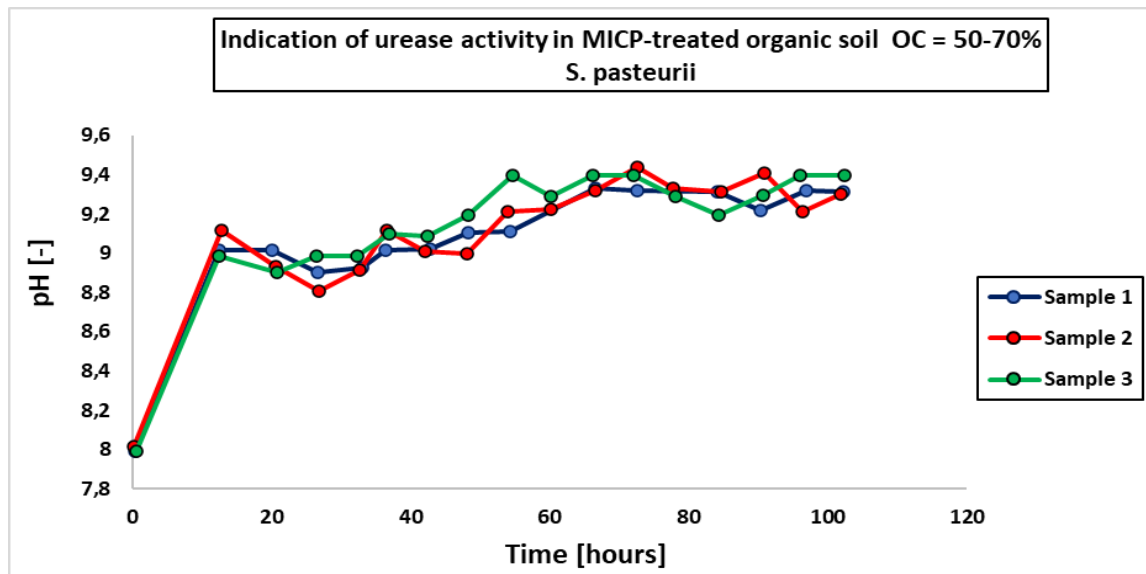
Figur 52. Show urease activity at different temperatures as a function of pH in natural soils. Data adapted from (Vahed et al., 2011)

A moderate to strong correlation between organic content in the soil and urease activity, was further observed by (Vahed et al., 2011). The results are presented in the plot below.



Figur 53. Show urease activity at different temperatures as a function of organic content in natural soils. Data adapted from (Vahed et al., 2011)

In their study, (Sidik et al., 2014) used *S. pasteurii* for MICP treatment of organic soil classified as peat, which contained approximately 15% fines, 60% organic materials and with liquid limit (L_L) of 125%. To investigate if ureolysis was occurring in the soil, the pH in the samples were monitored over time, where pH reached around 9.3 after 12 hours, where the rise in pH was suggested to indicate urease activity in treated samples. This was later confirmed by precipitated CaCO_3 in the samples. The results are presented in the plot below.

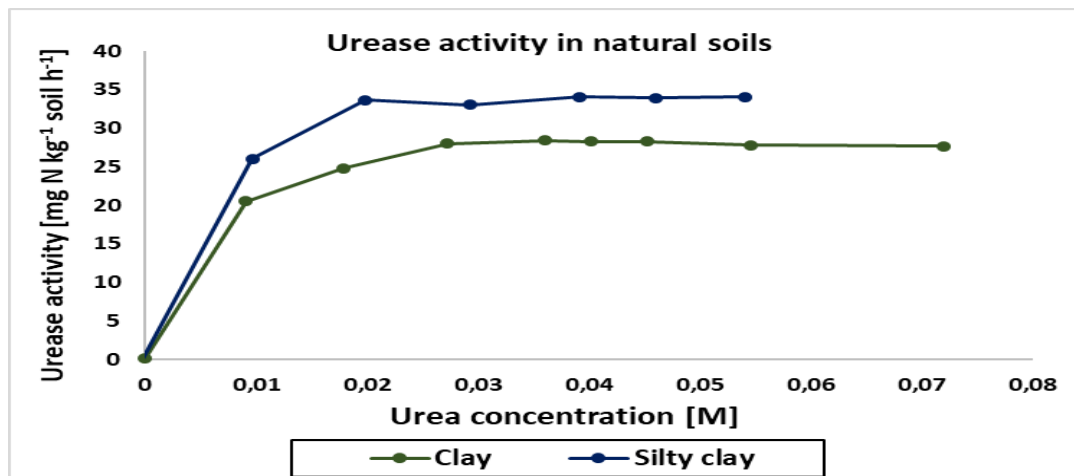


Figur 54. Show rise in pH in MICP-treated organic soil as an indication of urease activity. Data adapted from (Sidik et al., 2014).

The results showed that the amount of CaCO_3 in the organic soil was less than that of MICP-treated sands in other studies. The difference in precipitation for organic soil and sand, is suggested to be due to soluble organic ligands and other organic matter that have an inhibitory effect on nucleation of crystals. This is suggested to be due to induced dissolution or impairment of the crystal growth, when organic matter is adsorbed to the CaCO_3 surface.

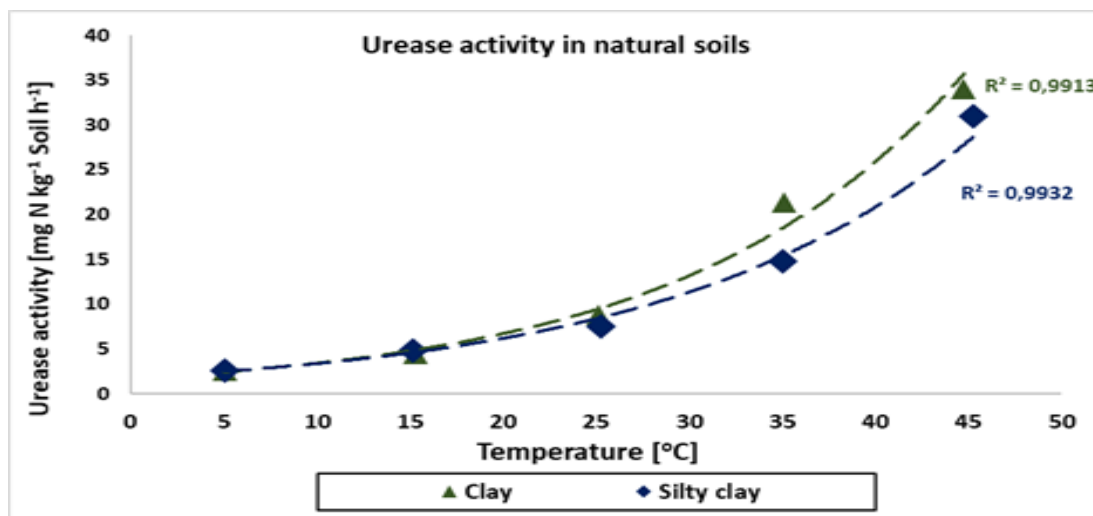
In their work, (O'Toole and Morgan, 1984) suggest that variations in organic content, texture and cation exchange capacity will have an impact on the urease capacity. In their work, (Moyo et al., 1989) measured the urease activity as a function of concentration of urea in a clay (63,6% silt, 6,4% sand) and a silty clay (76,1% silt, 3,2% sand) with similar carbon content, where the clay had higher pH (7,1) than the silty clay (5,5). The results show a rapid initial increase in urease activity in the range 0-0,02 M urea and where the urease activity is

stagnant when the concentration id further increased from 0,02 to 0,06 M. The results are presented in the plot below.



Figur 55. Show urease activity as a function of urea concentration. Data adapted from (Moyo et al., 1989)

The results further show an exponential increase in urease activity when temperature is increased from 5°C and upwards to 50 °C. The measured urease activity as a function of temperature is presented below.



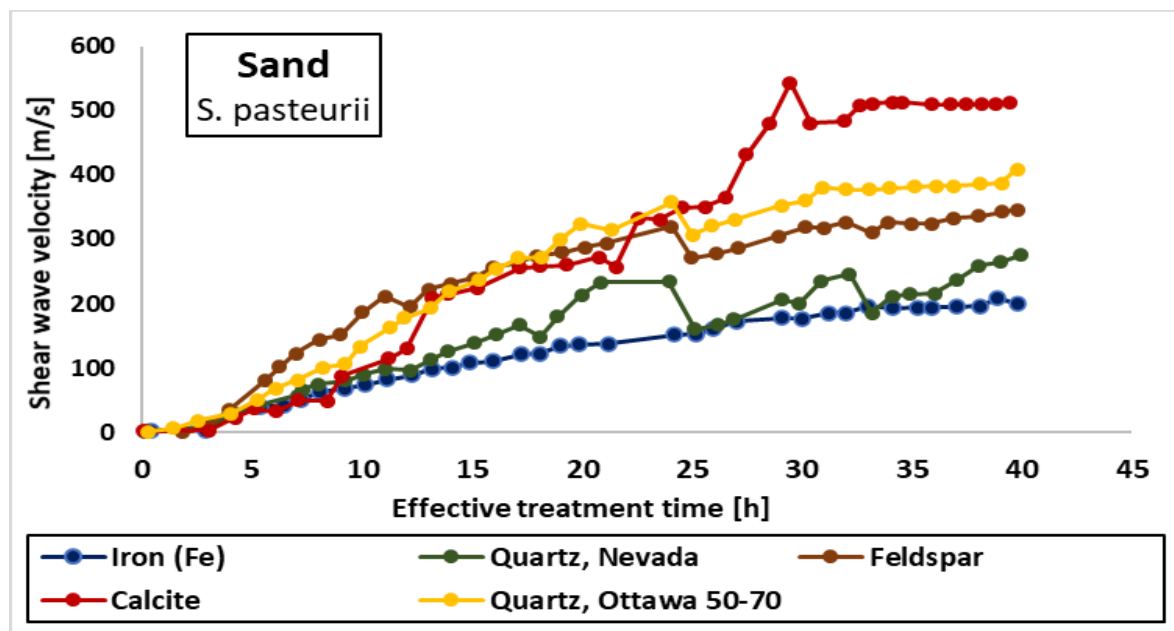
Figur 56. Show urease activity as a function of temperature. Data adapted from (Moyo et al., 1989)

Work by (Makboul and Ottow, 1979) investigated the specific effect of clay minerals on the half urease saturation constant (K_m), where montmorillonite (3:1) and kaolinite (2:1), enhanced the K_m value of urease considerably more than illite (3:1).

The effect of adding 2.5, 5.0 and 7.5% kaolin clay to a poorly sorted ($d_{50}=0,3$ mm) sand before MICP-treatment with *S.pasteurii*, was investigated by (Sun et al., 2019c). They found that the added clay overall seemed to have an inhibitory

effect on the urease activity, where all parameters besides varying pH due to the added clay was kept constant and urease activity decreased with increasing share of clay. Al_2O_3 and FeCl_3 was then added separately, where both decreased the urease activity, while FeCl_3 decreased the urease activity significantly more than Al_2O_3 .

The effect of minerals on precipitation by *S. pasteurii* in MICP-treated sands differentiated as rich in quartz, calcite, feldspar and iron oxide was investigated by (Montoya, 2012). The cemented samples were measured for their shear wave velocity, where the mineral composition of the different sands was found to have significant effect on the precipitation rate. Sand rich in calcite (CaCO_3) showed the fastest precipitation rate, whereas the sand rich in Iron (Fe) obtained the lowest rate. The results are presented in the plot below.



Figur 57. Show the increase in density due to precipitation over time, in sands with a variation in dominating minerals. Data adapted from (Montoya, 2012)

3.8.2 Anoxic conditions

For geotechnical applications of MICP, it will often be the case that the target soil is located below the groundwater table. Evaluation of the effect of limited or no dissolved oxygen on urease activity and cell growth, is of great relevance when considering viability of MICP-treatment in soil below the watertable. Cultivation and growth of bacteria are normally conducted in the presence of oxygen. However, for further growth and sustained urease activity over time in the subsurface below the watertable, anoxic growth, urease production and ureolysis must be feasible.

Aerobic bacteria need free or dissolved oxygen and use O_2 as the electron acceptor, whereas facultative anaerobic bacteria such as *S. pasteurii*, can survive in the absence of oxygen (anoxic conditions) using compounds besides O_2 as electron acceptors. This suggests that facultative anaerobic bacteria are more robust and more suited to survive in environments with little or no presence of oxygen. However, the ureolysis requires available oxygen to sustain the urease activity over time.

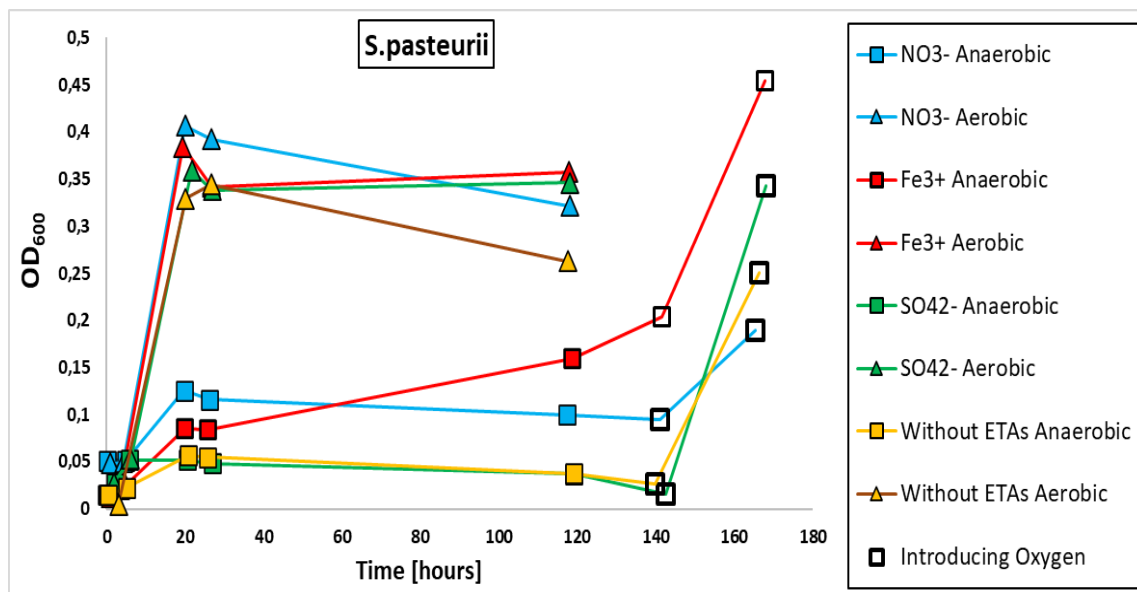
Once a soil is saturated, the availability of oxygen is according to (Inglett et al., 2005), reduced due to the displacement of oxygen in the pore space. When the limited oxygen present in the pore water is consumed, oxygen can only be supplied to the microorganisms in the saturated zone through diffusion from the nearest aerobic zone. This process is a relatively slow process under saturated soil conditions, causing the microbial biomass to decrease and the microbially induced reactions to decline, where some reactions may be replaced by new ones. Under such conditions, bacteria must use other compounds besides O_2 as electron acceptors. Bacteria capable of utilizing the electron acceptor with the next-highest thermodynamic potential, will under these conditions dominate. The use of electron terminal acceptors (ETA) occur in the order of NO_3^- , Mn^{4+} , Fe^{3+} , SO_4^{2-} and then CO_2 .

In their work, (Hamdan et al., 2011) note that since *S. pasteurii* uses aerobic respiration during ureolysis, ureolysis is severely limited when the oxygen levels are low, such as in subsurface aqueous environments. (Jain and Arnepalli, 2019) reported on limited urease activity and minimal amounts of precipitation from *S. pasteurii* under anoxic conditions, where the minor precipitation was attributed to urease enzymes produced during aerobic cell growth. (Teng et al., 2020, DeJong et al., 2010) stated that *S. pasteurii* can survive in an anaerobic environment, but the capacity to produce urease in the absence of oxygen, is time limited. By contrast, (Tobler et al., 2011, Mortensen et al., 2011b, Mitchell et al., 2019) found that the urease activity of *S. pasteurii* was not negatively affected by anoxic conditions, where (Mitchell et al., 2019) perceived the rise in pH to above 9, as an indication for urease activity. However, (Jain and Arnepalli, 2019) state that rise in pH during anoxic conditions could also be due to break-down of complex proteins during the stationary growth phase, whereas (Martin et al., 2012) suggest that findings indicating urease activity under anoxic conditions for

S. pasteurii is due to urease enzyme already being present in the cells of aerobically grown bacteria. (Mitchell et al., 2019) adds that to sustain the urease activity over time, addition of suitable electron acceptors might be required.

In their work, (Martin et al., 2012) found that *S. pasteurii* was not capable of anaerobic growth, which was suggested to be due to lack of de novo synthesis (new production) of urease under anoxic conditions, causing a decline of ureolysis over time, while (Whiffin, 2004) found that *S. pasteurii* can be grown under conditions with reduced oxygen levels. However, the growth was slow and extended periods of reduced availability of oxygen, lead to 25% reduction in urease activity.

In their study, (Mitchell et al., 2019) investigated the cell growth of *S.pasteurii* under oxic and anoxic conditions. The results indicate a low capacity for cell growth under anoxic conditions in the short term and no capacity over time. Cell growth or bacterial density (OD_{600}) under anoxic conditions was lower than that under oxic conditions, regardless of added ETAs. However, the growth was low and did not sustain over time, but did increase when oxygen (O_2) was allowed to enter the system. There was no cell growth with NO_3^- , SO_4^{2-} and Fe^{3+} as ETAs. This suggests that further cell growth in the sub-surface post-injection, requires the bacteria to be resuscitated by stimulation through cyclic injections of oxygenated fluids. The plot presented below show growth evolution by bacterial density (OD_{600}) over time.



Figur 58. Show bacterial density as optical density at 600 nm (OD_{600}) of *S.pasteurii* under aerobic and anaerobic conditions, as a function of time. Data adapted from (Mitchell et al., 2019).

A study by (Chen et al., 2012) sought to develop a continuous oxygen releasing material, which can be introduced to the sub-surface. They used a mixture of gypsum, calcium peroxide (CaO_2), sand and water, which showed high initial oxygen retention and slowly declining oxygen release rate. The observed optimal ratio of the components in the mixture, is listed in the table presented below.

Tabell 14. Lists compounds by ratio for proposed oxygen releasing mixture. Data adapted from (Chen et al., 2012)

Compound	Ratio by weight
Gypsum	1
Calcium peroxide (CaCO_2)	0,5
Sand	0,14
Water	0,75

3.8.3 Cell growth

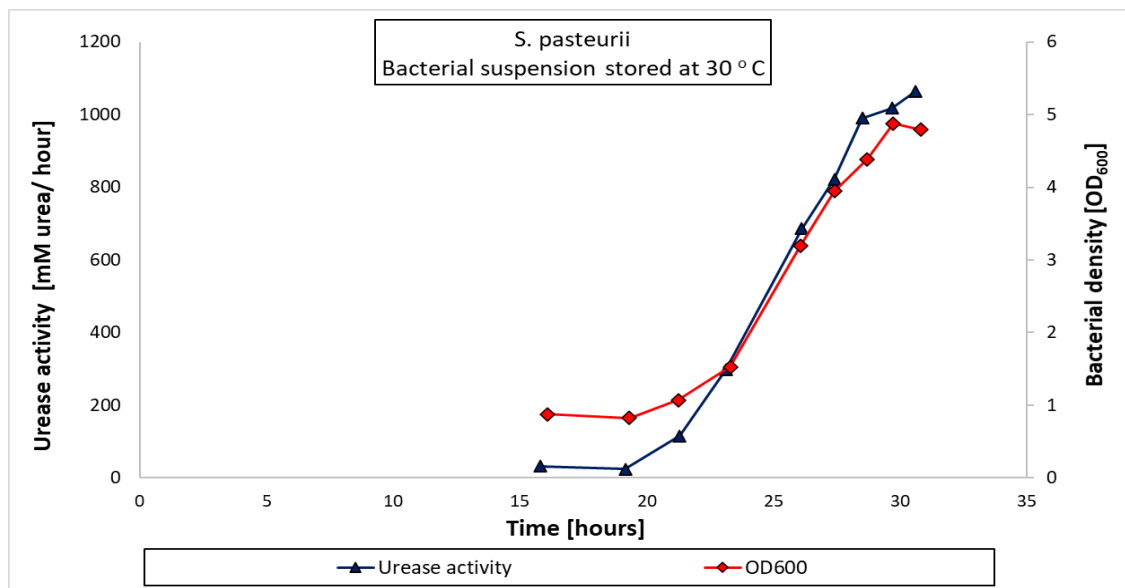
For an ureolytic bacteria to be viable as a causative agent in the MICP process, it should have a healthy and robust cell surface with a high negative charge, have capacity for exponential growth and high capacity for urease enzyme production as well as a capacity for efficient conversion of urea through ureolysis. In their work (Van Paassen, 2009a), note that a variation in the composition of nutrients and temperature, will yield different levels of urease activity and cell growth, where optimal growth yield is achieved when batch cultivations are stored at late exponential or early stationary growth state.

(Van Paassen, 2009a) adds that limited access to oxygen during cultivation can reduce the growth, where (Whiffin, 2004) found that increased levels of oxygen during cultivation, increased cell growth and generated normal cell physiology (rod-shaped, non-motile). On the contrary, reduced oxygen levels reduced growth, altered the physiology of bacteria (shorter, highly motile) and reduced the urease activity.

(El Mountassir et al., 2018, Soon et al., 2014) reported that increased amount of urea enzyme in solution, increases the urease activity, which in turn increases the rate of ureolysis, where (Okwadha and Li, 2010, Teng et al., 2020) reported on increased rate of ureolysis with increasing bacterial concentration. However, (Teng et al., 2020) found that the increased urease activity with increasing bacterial concentration was just initially and hence temporarily, where (Whiffin, 2004) found no correlation between bacterial concentration and urease activity. (Teng et al., 2020) conclude that high bacterial concentration is a limiting factor

for sustained urease activity. (Okwadha and Li, 2010) adds that bacterial concentration showed greater influence on the rate of ureolysis than initial concentrations of urea.

In work by (Van Paassen, 2009b, Nayanthara et al., 2019), it is noted that *S. pasteurii* follows a typical growth curve with initial exponential growth and then a stationary phase. The growth curve and corresponding urease activity for *S. pasteurii* at 30°C conducted in work by (Van Paassen, 2009a), can be observed in the plot presented below.

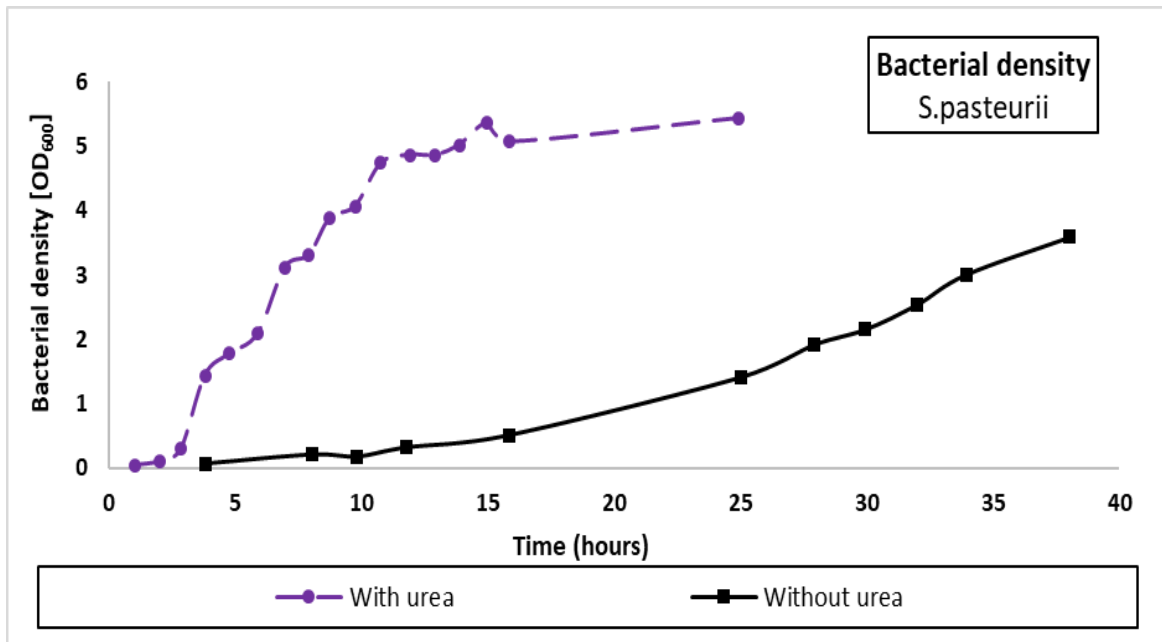


Figur 59. Show bacterial density and corresponding urease activity for *S.pasteurii* at 30°C . Data adapted from (Van Paassen, 2009a).

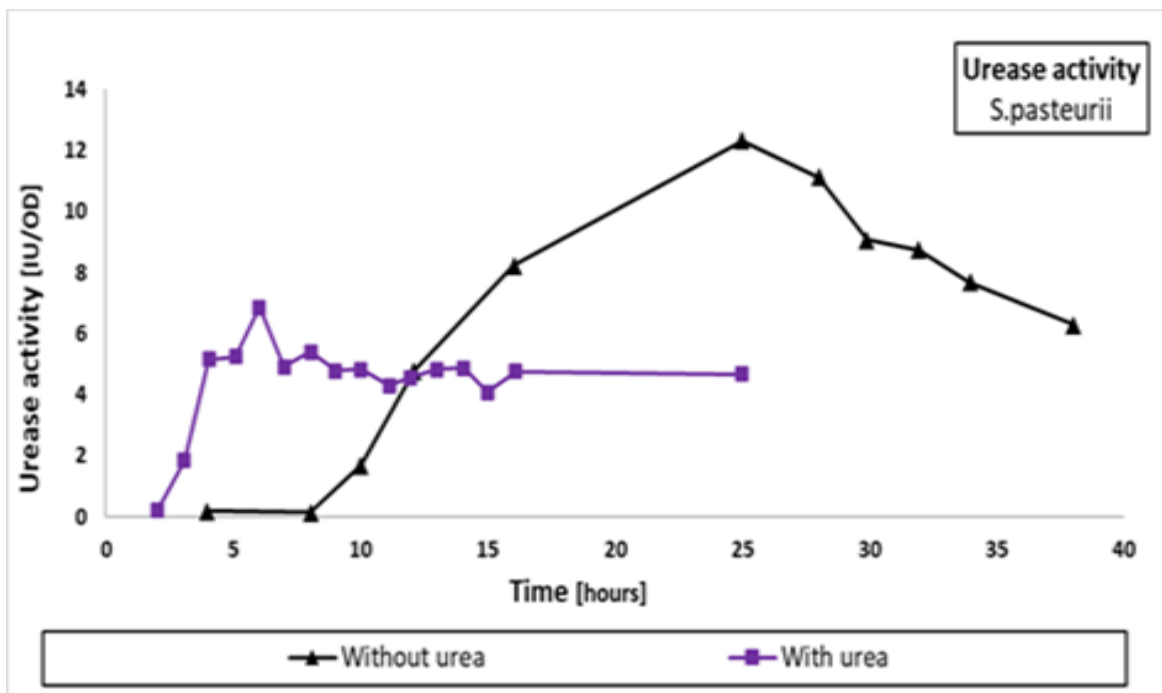
Work by (Stocks-Fischer et al., 1999, Li et al., 2012) suggests that the bacteria cell wall, serve as nucleation site for precipitation, where a robust cell wall will enable the bacteria to better withstand the weight of the precipitated crystals, thus delaying lysis due to encapsulation.

Early studies by (Wiley and Stokes, 1962), found optimal growth for *S. pasteurii* occurring at pH 9.25, whereas the bacteria stopped growing when pH exceeded 10.0. In their work (Ma et Al.,2020) found that for *S. pasteurii* grown in the presence of urea, pH rised from 7.4 to 9.4 in 5 hours and generated much higher growth, more robust physiology and higher negative cell charge, compared to *S. Pasteurii* grown without urea, where pH stagnated at 7.7 throughout the growth phase. However, the urease activity was much lower for *S. pasteurii* grown with urea, than for that grown without. However, it displayed a much faster initiation

of the urease activity than for that grown without urea. The results for the cell growth (OD_{600}) and urease activity are presented in the plot below.



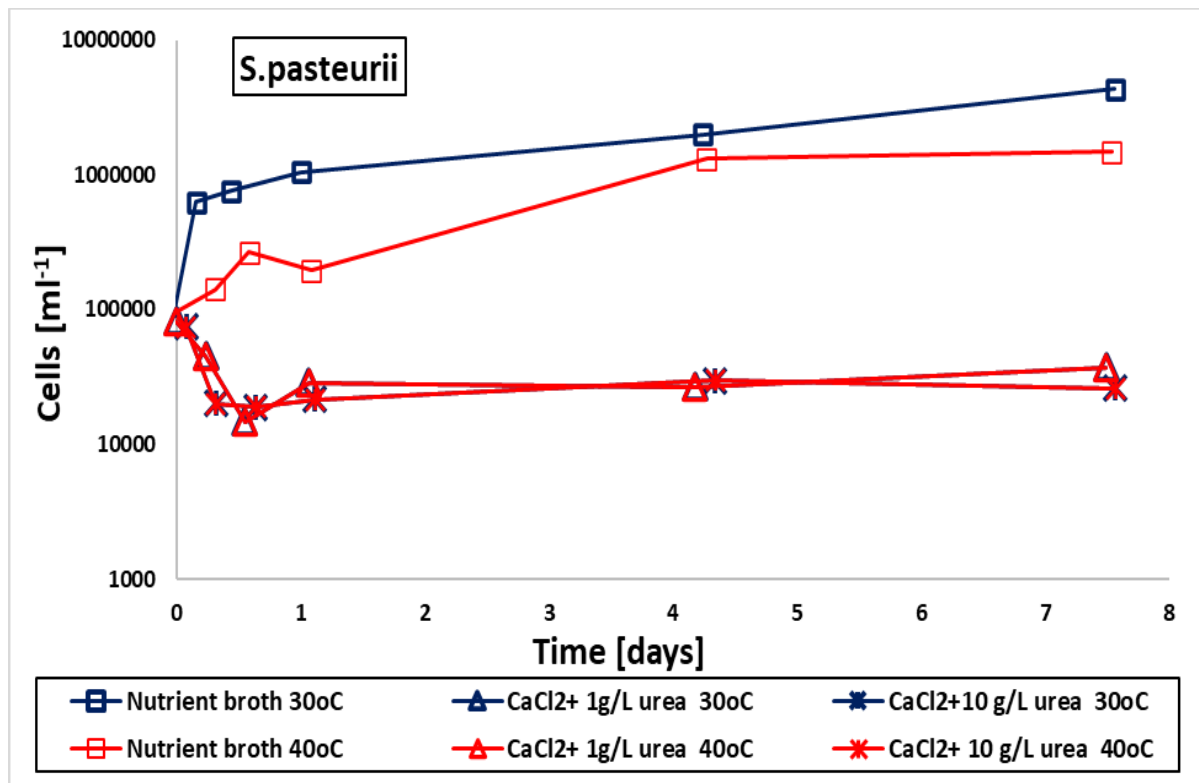
Figur 60. Show bacterial concentration as a function of time for *S. pasteurii*, grown with and without urea. Data adapted from (Ma et al., 2020b)



Figur 61. Show urease activity as a function of time for *S. pasteurii*, grown with and without urea. Data adapted from (Ma et al., 2020a)

The effect of temperature and inoculation (growth) solutions on the growth of *S. pasteurii* was investigated by (Verba et al., 2016), where highest growth was achieved in nutrient broth (ATCC medium) at 30°C. Both cultures inoculated in

the nutrient broth, achieved significant higher growth than those in solution of (1 and 10 g/L) CaCl_2 /urea. The results are presented in the plot below.



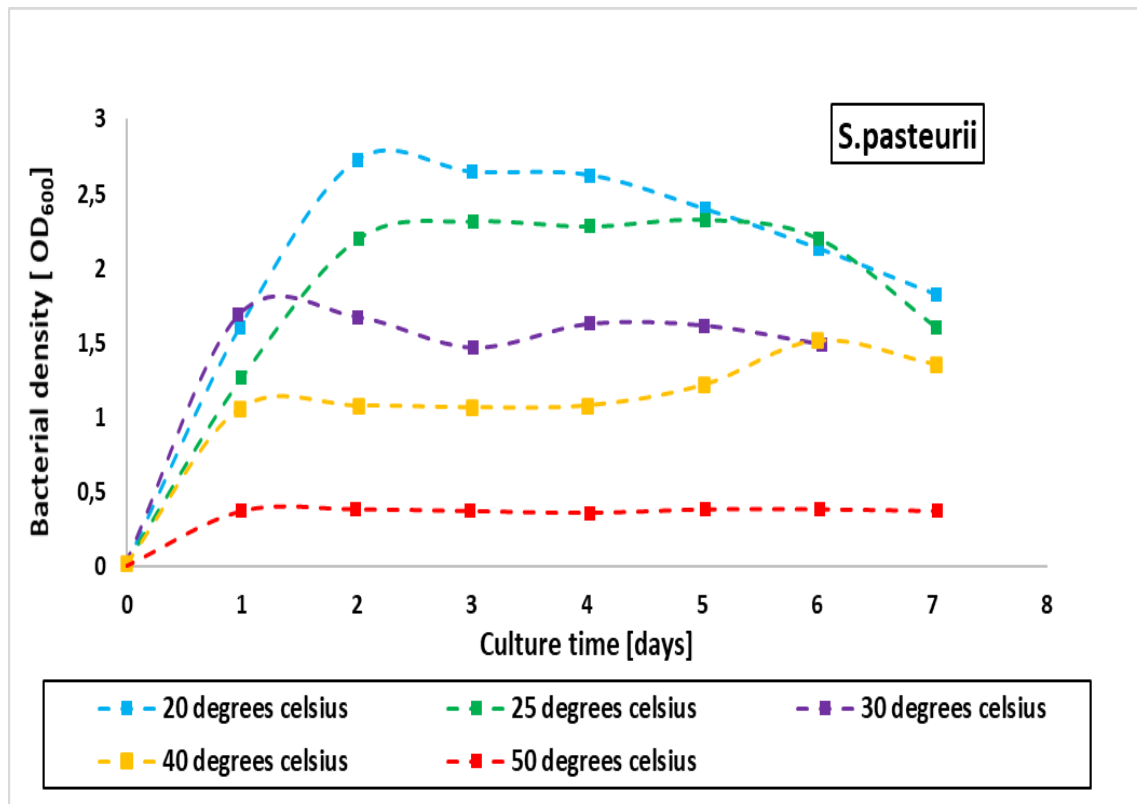
Figur 62. Show effect of temperature and inoculation solution on growth of *S. pasteurii*. Data adapted from (Verba et al., 2016)

Nutrients used in growth medium, can be expensive and for MICP to be a viable application for ground improvement on an industrial scale, cost effective growth procedures need to be developed. (Griffiths, 1986) notes that for scale-up of cell culture, the overall product cost and labour component decreases with scale up, whereas the cost of cultivation medium increases proportionally.

In work by (Whiffin, 2004), an economically viable growth medium for large scale production of *S. pasteurii*, was developed. Expensive components of the cultivation medium were replaced with food-grade protein sources and acetate, which reduced the cost by 95% and sustained high urease activity in the suspension.

The microbial growth is according to (Ng et al. 2012), generally less sensitive to temperature changes in the range 20–30°C, where (Nayanthara et Al. 2019) found the bacterial growth to be more stable and comparatively higher at 20–25°C, whereas it decreased to almost zero at 50°C. The study found that *S. pasteurii* displayed an initial exponential growth up to a maximum and then a

stationary phase followed by a gradual fall, for growth in the range 20-40°C. The results for effect of temperature on bacterial density over time, are presented in the plot below.



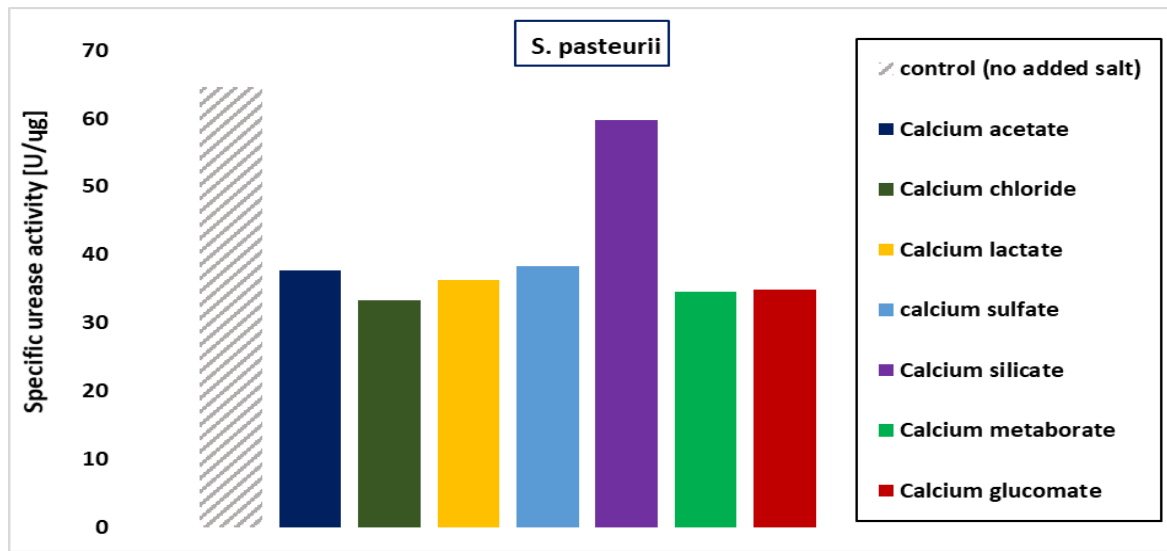
Figur 63. Show bacterial density as a function of time for cultivation under different temperatures. Adapted with data from (Nayanthara et al., 2019).

3.8.4 Cementation solution

The cementation solution most widely used in MICP applications is CaCl₂/urea at varying concentrations. CaCl₂ buffer the pH and provides a supply of calcium ions, while urea increases the pH when it is degraded by the urease enzyme and converted into ammonium during ureolysis. The urease activity is a core component of the MICP process and it is important to investigate how the components in the injected cementation solution affects the ureolytic activity.

In their work, (Gorospe et al., 2013) note that urease enzymes, are sensitive to environmental stresses, where specific conditions promote optimal urease activity up until a limit is reached, where exceeding this limit causes the enzyme performance to decline. (Tang et al., 2020) state that the concentration and proportion of cementation solution have a significant influence on the urease activity, where (Hammes et al., 2003) found that adding 30 mM Ca²⁺ to solution of urea enzyme, increased the urease activity by 10 times.

Work by (Gorospe et al., 2013), investigated the effect of different salts on the urease activity of *S. pasteurii* urease enzyme, where salts (50 mM) were added to 1 mL enzyme reaction mixture, leaving one crude urease enzyme reaction mixture without added salt, as a control sample. The different salts, all decreased the urease activity, where the lower decrease with calcium silicate relative to the other salts, is suggested to be due to low solubility in water. The results are presented in the diagram below.



Figur 64. Show effect of different salts on the urease activity of the *S. pasteurii* urease. Data adapted from (Gorospe et al., 2013).

3.8.5 pH

It is noted in work by (Tang et al., 2020), that the pH value can affect urease activity through the metabolism of ureolytic bacteria, where (Stocks-Fischer et al., 1999) found that pH causes significant changes in the bacterial metabolism, hence it will govern the ability to decompose urea. Ammonium generated during ureolysis will increase the pH of the medium, while the carbon dioxide from ureolysis and microbial respiration, slows or counteract the rapid increase in pH (Ng et al., 2012a, Soon et al., 2014).

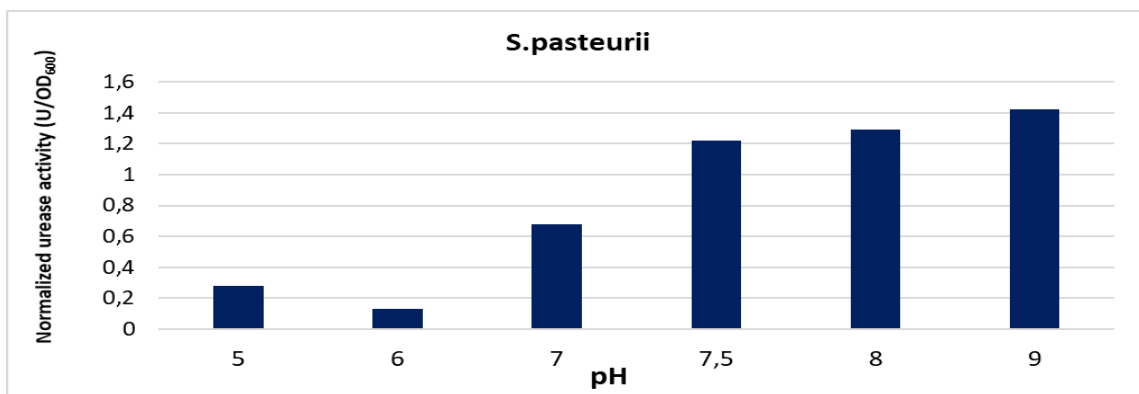
According to (Van Paassen, 2009a), the pH rises rapidly until critical supersaturation is reached and precipitation is initiated, where (Stocks-Fischer et al., 1999) reported optimal pH of *S. pasteurii* at 8, while (Whiffin et al., 2007) observed optimal pH for *S. pasteurii* between 7 and 8, whereas (Kim et al., 2018) suggested an optimal pH around 7. (Stocks-Fischer et al., 1999) adds that after precipitation, the pH drops to about neutral where it stays until all substrat-

es are depleted. In the table below, some results from previous studies on optimum pH range for *S.pasteurii*, are listed.

Tabell 15. Lists previous findings of optimal pH range for *S.pasteurii*. Data adapted from (Crowley et al., 2019)

pH _{opt}	9	8	9,3	9,1	8,7-9,5	8	6-8	7-9
S.pasteurii	(Feng and Montoya, 2016)	(Stocks-Fischer et al., 1999)	(Ferris et al., 2004)	(Fujita et al., 2004)	(Dupraz et al., 2009)	(Arunachalam et al., 2010)	(Van Elsas and Penido, 1982)	(Khan, 2011)

In their work, (Kim et Al. 2018) found that *S. Pasteurii* was more sensitive to a change in pH than *S. saprophyticus*, where the precipitation of *S. pasteurii* was reduced with up to 60% by varying the pH. (Nayanthara et al., 2019) observed the highest urease activity at pH 9, where a high and distinct increase in urease activity was observed for increasing pH from 6 to 7,5, and a smaller increase from pH 7,5 to 9,0. The results are in line with findings of (Stocks-Fischer et al., 1999), which showed a drastic increase in urease activity for *S. pasteurii* between pH 6 and 8 and then a gradual decline above 8. The results from (Nayanthara et al., 2019) are presented in the graph below.

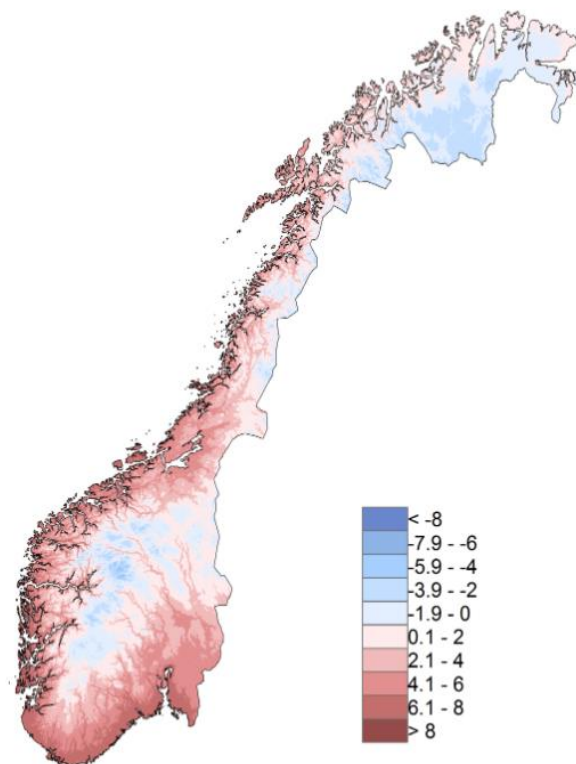


Figur 65. Show normalized urease activity under varying values of pH. Data adapted from (Nayanthara et al., 2019)

3.8.6 Temperature

The capacity to initiate and sustain urease activity and consequently precipitation under a broad range of temperatures, is one of the core requirements for the viability of MICP as a method for ground improvement. For viability in cold climate ground conditions, the ureolytic capacity under low temperatures are of particular importance.

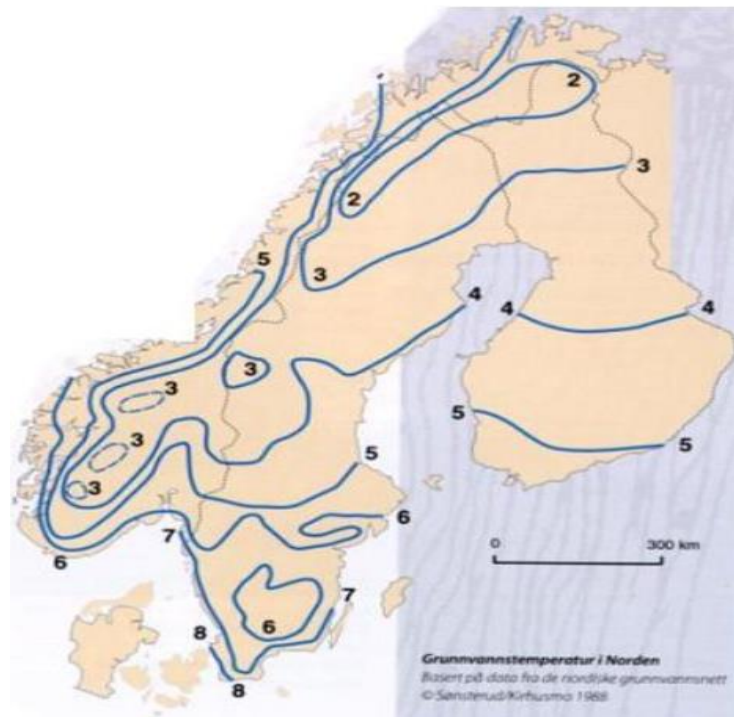
Ground temperatures will according to (SENER, 2021), be dependent on air and ground surface temperatures, heat flow from the interior of the earth and the soils thermal properties. The ground temperature is further affected by snow cover, vegetation and other climatic factors. The surface temperature will fluctuate daily and annually, while the ground temperature would normally be 1-2 °C higher than the annual average air temperature at a given location, with some dependency on number of snowcover days on the ground in cold climate regions. In Norway the annual average temperature varies depending on the region, with +6 °C in the coastal areas in west and -4 °C in the mountainous areas and the inland in the north. The graphic presented below, show variations in annual average temperature in Norway by region.



Figur 66. Show regional average annual (1985-2014) temperatures in Norway. Illustration from (2021).

The yearly average temperature of the groundwater in Norway, ranges according to (NVE, 2021) between +1°C in the northern parts and +6°C in the coastlines of western and southern Norway. Measurements show a latency in the groundwater temperature in respect to the air temperature, where the lowest temperature is registered in the summer months, while the highest temperatures are measured in the winter months. A rule of thumb has been that the groundwater tempe-

perature is equal to the yearly average air temperature for a given region. However, the type of soil, depth of the unsaturated zone, depth of snow cover, frost and vegetation, can have an influence on temperature of the groundwater. The map presented below show groundwater temperature in the nordic countries.

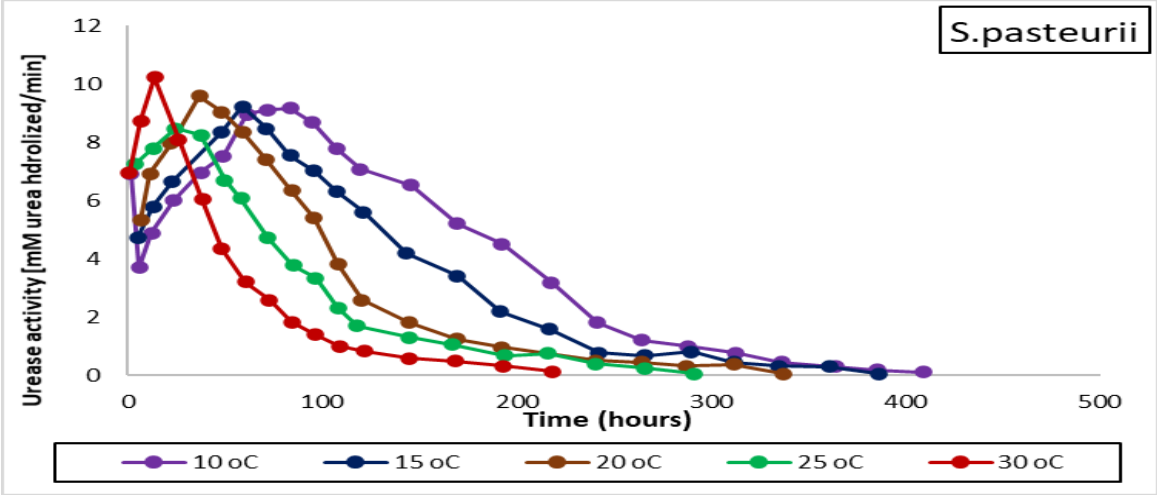


Figur 67. Show groundwater temperatures in the nordic countries. Illustration from (NVE, 2021).

Soil temperatures in parts of the globe that do not have cold climate, have a peak temperature range of 10-30°C with an average of 10-16°C, 3-4 m below ground surface. According to (Cheng et al., 2016), the temperature can affect the urease activity, rate of ureolysis and precipitation rate, where (Nayanthara et al., 2019) note that ureolysis is a temperature dependent enzymatic reaction.

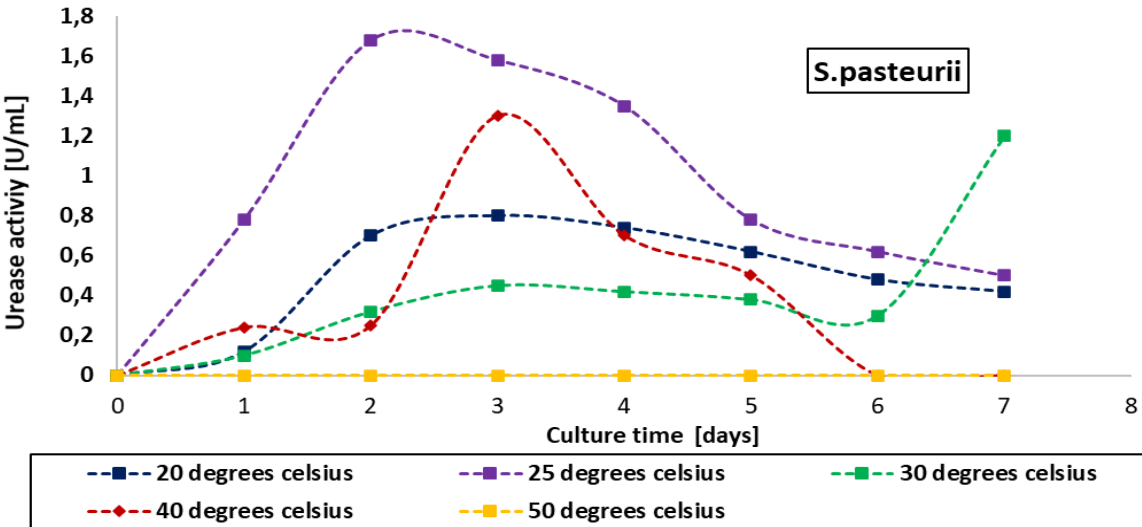
Work by (Cacchio et al., 2003), reported on slow initiation of ureolysis at low temperatures and a faster initiation with increasing temperature, while (Ng et al., 2012b) reported on marginally higher rate of ureolysis at 30°C compared to 20°C, where the urease activity was less sensitive to changes in the range 20-30°C. (Gillman et al., 1995) reported on a nearly 18 times increase in rate of ureolysis when temperature was increased from 5 to 20 °C, whereas increase in temperature above 30°C, did not further increase the rate. (Wiffin, 2004) observed a high urease activity for *S. pasteurii* in the range of 30–70°C, while (Sahrawat, 1984) reported on increasing urease activity from 10°C to 60°C and ceasing at 100°C, where optimal activity was registred at 60°C.

As part of their study, (Peng and Liu, 2019b) investigated the effect of temperature on the urease activity of *S. pasteurii*. The results show increased peak activity and initial rate with increased temperature, and faster rate of decrease in activity after peak i.e shorter duration with increased temperature. The results are presented in the plot below.



Figur 68. Show urease activity as a funtion of time for different temperatures. Data adapted from (Peng and Liu, 2019a).

In their work, (Nayanthara et al., 2019) investigated the effect of temperature on urease activity over time for *S. pasteurii*, where the highest rate of increase in urease activity upon initiation and highest peak activity was observed at 25° C, whereas almost no activity was observed at 50°C. An unstable and short duration, but high peak activity was observed at 40°C .The graph presented below show the results from the study.



Figur 69. Show urease activity as a function of time for different curing temperatures. Data adapted from (Nayanthara et al., 2019)

3.9 Cell surface charge

The magnitude of negative cell charge in a ureolytic bacteria affects the suitability of the cell surface as a nucleation site for precipitation, where (Ma et al., 2020b) state that an increase in negative surface charge is favorable for binding positively charged calcium ions (Ca^{2+}) or magnesium ions (Mg^{2+}). According to (Williams et al., 2017), the cell surface charge can be approximated by the zeta potential. The zeta potential is a measure of the electrokinetic potential of the discontinuous phase in a colloidal dispersion, where (Ma et al., 2020b) note that $\text{mV} > 30$ indicate good stability, and the higher the value (positive or negative), the more stable the potential.

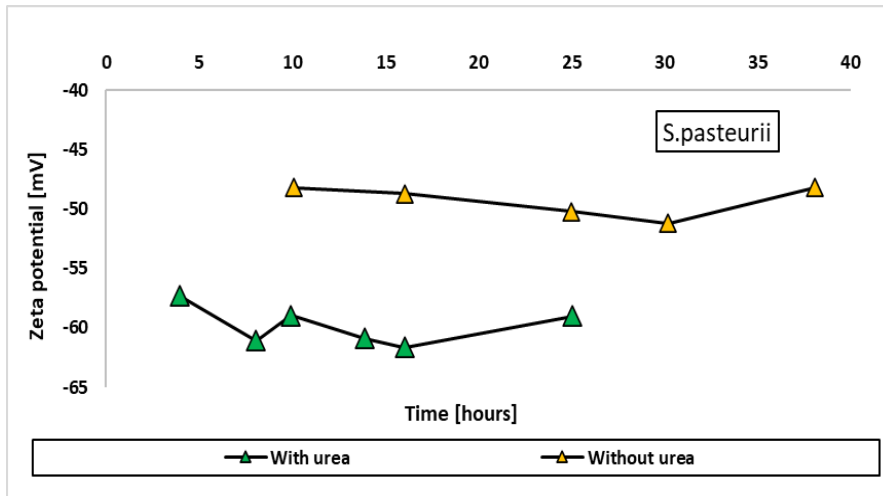
In their study, (Williams et al., 2017) measured the zeta potential of the *S. pasteurii* cell during exposure to different stressors such as heat, lack of nutrients, high pH, and autoclaving. They found that the cells negative surface charge was sustained over time during exposure to the different stressors. They further investigated the zeta potential at varying levels of urease activity, where negative zeta potential was observed at all levels of activity. The highest negative potential was registered for the two cultures with highest urease activity, but there was no observable correlation between negative potential and level of urease activity, for levels of activity below those. The results are presented in the diagram below.



Figur 70. Show measured zeta potential for *S. pasteurii*. Data adapted from (Williams et al., 2017)

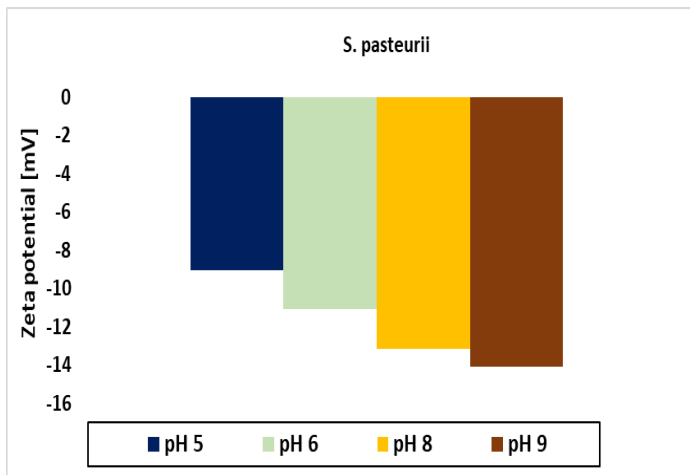
In their study, (Ma et al., 2020b) found the highest (-67mV) negative zeta potential for *S. pasteurii*, when they compared with the zeta potential of *S. aureus* (-26mV), *B. subtilis* (-40,8mV) and the non-mineralizing bacteria *E. coli* (-28mV). They further observed that adding urea to *S. pasteurii* culture during

cultivation, increased the negative cell charge of the bacteria, compared to *S. pasteurii* cultivated without added urea. The graph presented below show the measured zeta potential over time for the two cultures of *S. pasteurii*.



Figur 71. Show zeta potential as a function of time for *S. pasteurii* cultivated with and without urea. Data adapted from (Ma et al., 2020b).

In work by (Keykha et al., 2017), an increased negative zeta potential for *S. pasteurii* with increasing pH, was observed. The results are presented in the diagram below.



Figur 72. Show measured zeta potential for *S. pasteurii*. Data adapted from (Keykha et al., 2017)

3.10 Cementation

3.10.1 Precipitation of CaCO₃

Precipitation of CaCO₃ is the end product of the MICP process, where rate and duration of precipitation as well as type of output mineral will affect how the cementation is realized through amount, crystal size and pattern of CaCO₃, thus

affecting the objective of the MICP application. For this reason, it is important to investigate the mechanisms that affect or govern the precipitation.

In work by (Al-Thawadi and Cord-Ruwisch, 2012), it is noted that biomineralization by ureolysis occur when the concentration of Ca^{2+} and CO_3^{2-} exceed the solubility product (K_{sp}) i.e when supersaturation of solution is reached. Increasing supersaturation index (SI), increases the possibility for precipitation of CaCO_3 . SI of a solution in the context of CaCO_3 is defined as:

$$SI = \frac{[\text{Ca}^{2+}][\text{CO}_3^{2-}]}{K_{sp}} \quad \text{Eq. 3.10.1.1}$$

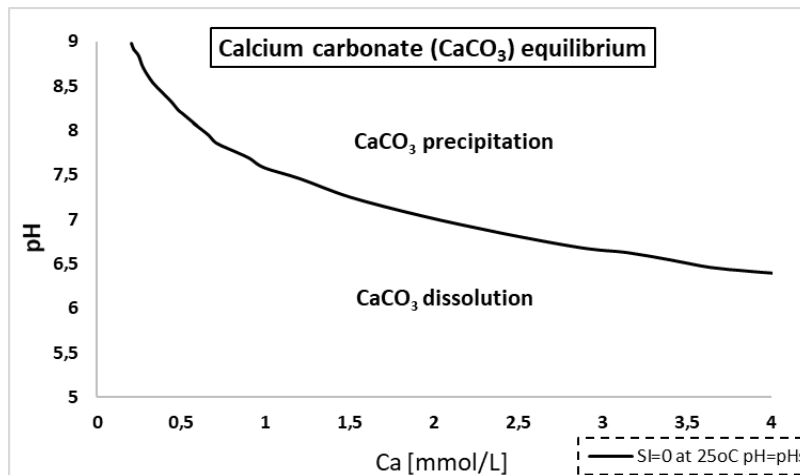
(Ferris et al., 2004) state that *S. pasteurii* precipitation of CaCO_3 crystals, occur through three steps:

Stage 1 → Solution approaches supersaturation, driven by increasing pH

Stage 2 → Nucleation at the point of critical saturation (precipitation initiates)

Stage 3 → Spontaneous crystal growth on the stable nuclei (cell surface)

In work by (Stocks-Fischer et al., 1999), it is noted that the pH at equilibrium or at supersaturation, is higher for water with lower calcium content such as soft water and lower for hard water. The equilibrium between precipitation and dissolution at 25°C, is presented below.



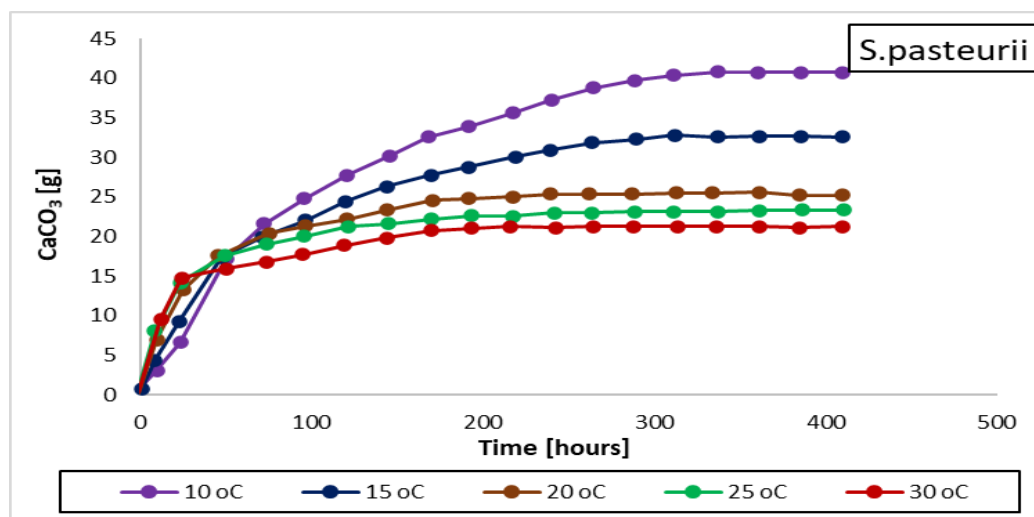
Figur 73. Show equilibrium between precipitation and dissolution for CaCO_3 at 25°C. Data adapted from (De Moel et al., 2013)

The saturation of solution is according to (El Mountassir et al., 2018), strongly influenced by the pH of the solution, where adding hydrochloric acid into the injected solution can delay precipitation by reducing the pH to 6,5. They further note that urease activity tend to favor a highly alkaline environment and since

CaCO₃ solubility decreases with increasing pH, precipitation is likely to increase with increasing pH.

In their work, (Nemati and Voordouw, 2003, Hammad et al., 2013) note that the ureolytic activity affect the precipitation, where (Hammad et al., 2013) reported on increased precipitation rate with increasing urease activity and (Nemati and Voordouw, 2003) on increased amount of CaCO₃ precipitated with increasing concentration of urease enzyme. On the contrary, (Konstantinou et al., 2021) found that the precipitation of *S. pasteurii* decreased with increasing level of urease activity and vice versa, where the lower precipitation at high urease activity is suggested to be due to uneven distribution of CaCO₃ in the sample. The density of bacteria could through the amount of generated urease enzyme, also affect the urease activity, where (Stocks-Fischer et al., 1999) found that bacterial densities exceeding 10⁸ cells/ml, reduced the precipitation.

In their research (Kim et Al. 2018), found that the optimum temperature for precipitation for both *S. pasteurii* and *S. saprophyticus* was 30°C, and lowest at 50°C. However, the precipitated amount of CaCO₃ from *S. saprophyticus* was greater than that of *S. pasteurii* under all variations of pH, temperature and curing time. In their work, (Peng and Liu, 2019a) demonstrated precipitation from *S. pasteurii* in the range 10-30°C, where amount of precipitated CaCO₃ declined with increasing temperature. The results are presented in the plot below.



Figur 74. Show precipitated CaCO₃ as a function of time for different temperatures. Data adapted from (Peng and Liu, 2019a).

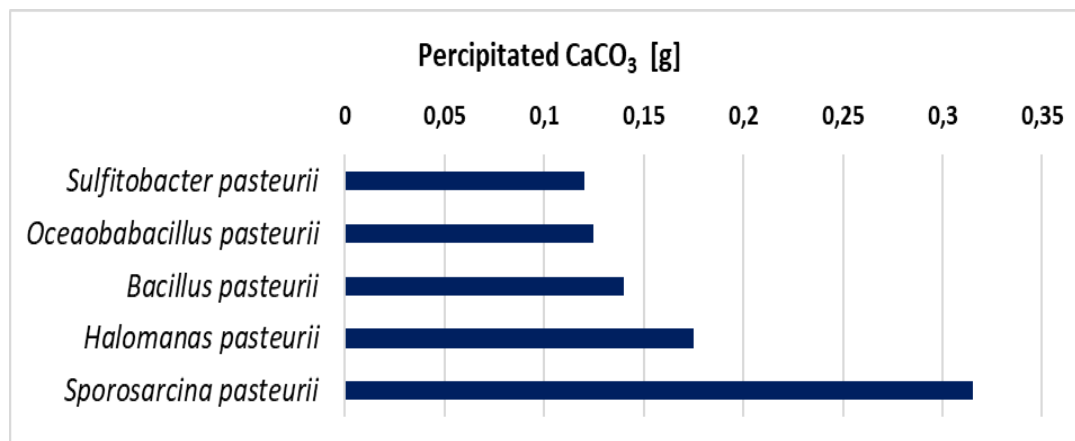
In their work, (Cheng et al., 2016) found that using 0,4 M cementation solution (urea/CaCl₂) generated the largest amount of precipitated CaCO₃, while (Nemati

et al., 2005), found that increasing the CaCl_2 share from 0,045 to 0,27 M produced higher amounts of CaCO_3 , whereas (Shahrokhi-Shahraki et al., 2015) achieved highest unconfined compression strength (UCS) with a concentration over 0,5 M and a higher share of urea than CaCl_2 .

In work by (Van Paassen, 2009b), it is noted that the urease activity is affected by the reduction of pore size due to precipitation. Reduced flow through the soil cause stagnant areas, which at constant flow rate increases linear flow velocity, thus reducing the residence time of the substrates within the soil volume and hence the urease activity per soil volume.

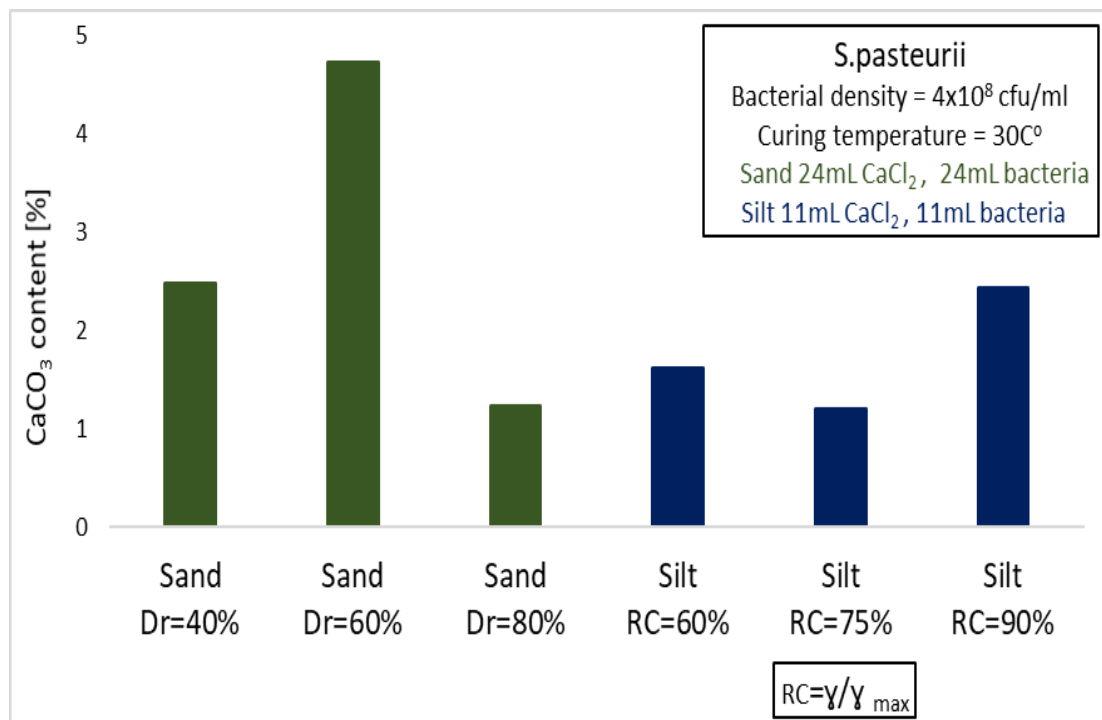
Work by (Oliveira et al., 2015), found that the *I. insulsalsae* bacteria generated more precipitated CaCO_3 than *S.pasteurii*. In their work, (Zhang et al., 2016a) found that the *Bacillus* species which *S.pasteurii* is part of, displayed the most effective (rate of conversion) precipitation, with a calcium precipitation activity (CPA) of 94,8%, while (Liu et al., 2019) found that *S. pasteurii* in artificial soil provided a higher CPA than in natural soil, probably due to competition for nutrients from indigenous bacteria in the natural soil.

In a comparison study by (Hsu et al., 2017) with a monoculture of *S. pasteurii* and a co-culture of *S. pasteurii* and *B. subtilus*, both cultures reached the same rate of precipitation at the end of the experiment. However, *S. pasteurii* displayed a faster initial rate of precipitation. In a study on stabilizing beachsand, (Nayanthara et al., 2019) found that *S. pasteurii* precipitated significantly more CaCO_3 at 25 °C in a moderately alkaline environment, compared to the other ureolytic bacteria included in the study. The results are presented in the graph below.



Figur 75. Show comparison of amounts of precipitated CaCO_3 for different ureolytic bacteria. Adapted with data from (Nayanthara et al., 2019).

Through MICP-treatment with *S. pasteurii* in silt and sand, (Kim et al., 2014) found that that the amounts of CaCO_3 generated in the sand samples, were about two times more than those for silt samples. The larger voids in the sand is suggested to be the reason for greater degree of precipitation in sand, compared to silt. They conclude that void ratio and pore size have a significant effect on microbial cementation in soils. The results are presented in the graph below.

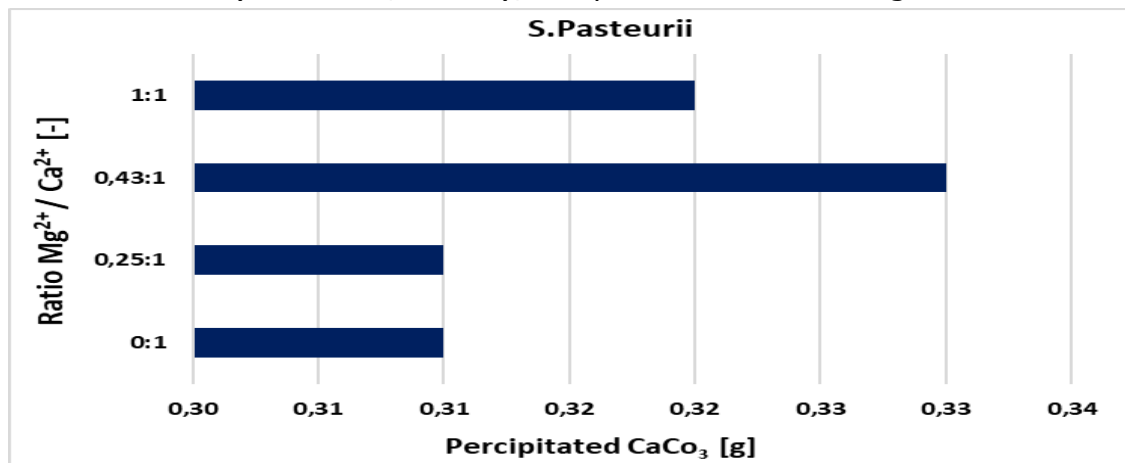


Figur 76. Show precipitation of *S. pasteurii* in sand and silt at different densities. Data adapted from (Kim et al., 2014).

Soil or groundwater can in some cases have high concentrations of magnesium ions (Mg^{2+}), which in the same way as calcium ions (Ca^{2+}), can be part of the biochemical reactions resulting in precipitation. Studies on the effect of Mg^{2+} ions on the precipitation are important for evaluation of suitability of MICP in different ground conditions.

In their work, (Sun et al., 2019a) found that Mg^{2+} generated less precipitation than Ca^{2+} , under similar conditions. Increments in share of Mg^{2+} did not significantly affect the quantity of CaCO_3 precipitated, whereas the crystal morphology was far more sensitive to the increased share of Mg^{2+} . (Nayanthara et al., 2019) integrated both Ca^{2+} and Mg^{2+} in ratios from 0-1 in the cementation solution in sand. The study found that optimal ratio $\text{Mg}^{2+}/\text{Ca}^{2+}$ was 0,5:1. The crystal morphology was adversely affected by high shares of Mg^{2+} which is in line with findings of (Sun et al., 2019a).

The results of (Sun et al., 2019a), are presented in the diagram below.



Figur 77. Show precipitation of $CaCO_3$ as a function of Mg^{2+} concentration. Adapted from (Nayanthara et al., 2019).

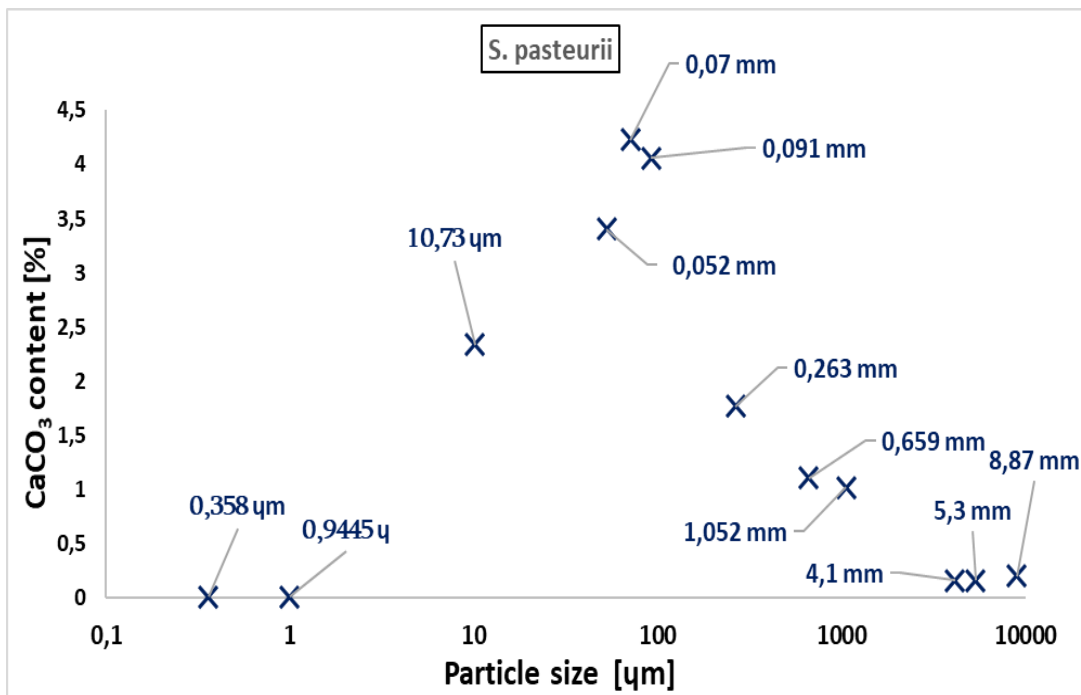
3.10.2 Effect of grain size distribution

The distribution of particle size affect the number of particle contacts per soil volume, porosity and hydraulic conductivity of a given soil. These properties would in turn affect the flow and distribution of bacterial suspension and cementation solution and consequently the spatial distribution of precipitated $CaCO_3$ within the treated area. For these reasons, it is important to investigate the effect of particle size and distribution on the cementation, so that knowledge of these effects can be integrated into the evaluation of MICPs suitability in a given soil as well as to adapt strategies for treatment in different type of soils.

In their work, (Mortensen et al., 2011a) note that effective cementation by MICP is reliant on a grain size distribution or pore size distribution that provide sufficient flow within the soil. In soils with higher permeability and connected pores, the injected solutions are dispersed more evenly and provide a better spatial distribution of $CaCO_3$. For MICP-treated (*S. pasteurii*) fine sand (0,075-0,015 mm), fine to medium sand (0,15-0,3 mm) and medium sand (0,3-0,6 mm), (Yang et al., 2020) found that increasing particle size increased the distribution of precipitated $CaCO_3$.

In work by (Mortensen et al., 2011a), it is noted that for soils at a constant porosity, dense well graded soils will have a higher number of particle contacts per volume, compared to loose poorly graded coarse soil. They observed a higher precipitation rate in coarse well graded sand, compared to fine uniform and loose sand. The higher number of contact points in well compacted and well graded soils, are suggested to be favorable for achieving improved strength and stiffness with MICP.

(Rebata-Landa, 2007) conducted MICP-treatment (*S.pasteurii*) in 11 different soils including kaolin clay, silt, fine sand, medium sand and among others, coarse sand. The study found that particle sizes between 10 and 100 μm , achieve the most effective cementation, where poor cementation in the very fine particles, is suggested to be due to bacterial activity and metabolism being reduced in small voids. Coarse silt and fine sand achieved high degree of cementation, whereas the degree of cementation declined for increasing particle size above fine sand. The results are presented in the plot below.

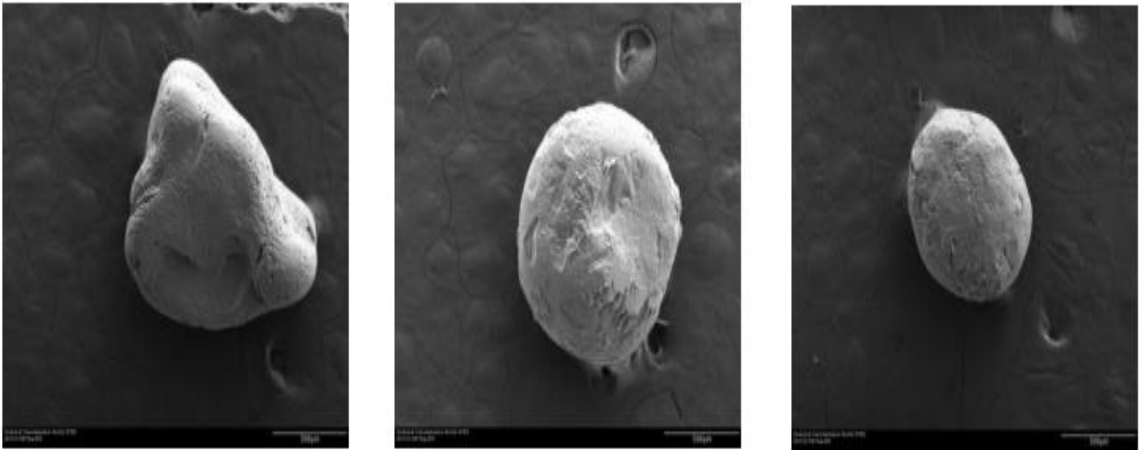


Figur 78. Show cementation as a function of particle size in different soils. Data adapted from (Rebata-Landa, 2007)

3.10.3 Effect of grain shape and surface texture

The variation in shape and size can affect the number of contactpoints between particles in a soil and thus the effectiveness of the cementation and consequently the achieved improvement of strength and stiffness, during MICP treatment. (Alshibli and Alsaleh, 2003) note that shape, surface roughness, and size distribution have a significant influence on the strength and deformation properties of granular materials. Considering that there are more contact points per soil volume in sand with fine round particles, compared to sand with coarse round particles, (Ismail et al., 2002) suggests that the efficiency of the cementation bond is higher in the fine rounded particles. (Alshibli and Alsaleh, 2003) adds that sands with a predominance of angular particles, have greater internal

friction than those consisting mainly of rounded particles, where ϕ increases with increasing angularity of particles, and decreases with increasing effective particle size (d_{10}). In their work, (Nafisi et al., 2018) MICP-treated (*S. pasteurii*) different sands with same particle size, but with a variation in shapes as shown in the images presented below.



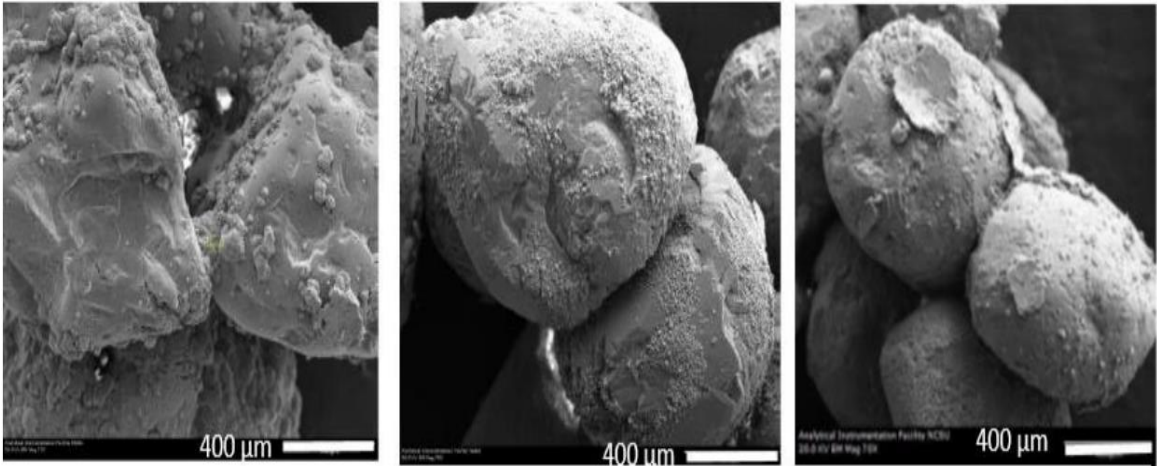
coarse angular

coarse round

fine round

Figur 79. Show SEM images of grain size and shape used in the study. Image from (Nafisi et al., 2018).

The results showed that the interparticle cementation was more effective in the angular coarse particles, compared to round coarse particles. Both interparticle cementation and increasing surface roughness contributed to improved shear strength in coarse angular particles, whereas only surface roughness contributed in round coarse particles. In the images below the precipitated calcite (CaCO_3) for each shape, is presented.



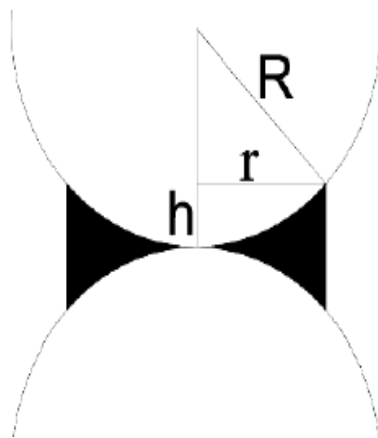
coarse angular

coarse round

fine round

Figur 80. Show SEM images of cementation on and between grains post-treatment. Image from (Nafisi et al., 2018)

In their work, (Nafisi et al., 2018) applied numerical modelling of particle shapes and conducted numerical triaxial tests to investigate the bonding effect of grains in MICP. The results showed that degree of improvement in shear strength due to biocementation, is affected by the particle shape, where particle angularity and particularly the parallel bond radius (R) of the cementation bond, determine the degree of increase in shear strength post-cementation. The larger the radius (R), the greater the strength of the bond. A parallel bond is shown in the illustration presented below.



Figur 81. Show the principle of paralell bond in particle to particle cementation, Illustration from (Nafisi et al., 2018).

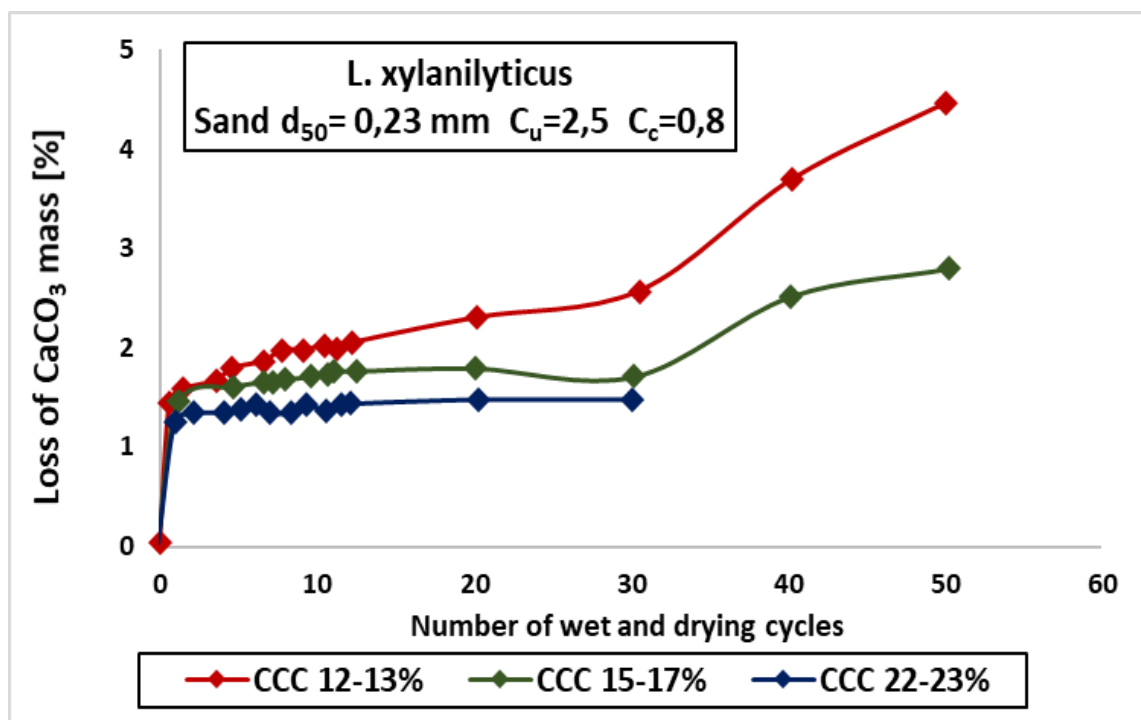
3.10.4 Calcium carbonate crystals

Depending on the conditions at supersaturation, different mineral types (polymorphs) of both stable and metastable CaCO_3 and varying morphology, can be precipitated. The CaCO_3 binder is the main component that enables the alteration or improvement of the soil properties in MICP-treated soil. The crystals size, shape and strength, needs to be suitable for the objective of the geotechnical design as well as provide adequate resistance to environmental factors that can cause corrosion or erosion of the CaCO_3 mass. It is for this reason important to investigate the factors affecting these aspects, so that the treatment approach in situ, can be adapted to achieve and sustain the desired outcome.

It is noted by (DeJong et al., 2009), that the precipitated CaCO_3 need to be stable and have a realistic design life, where the long-term compatibility of the precipitated CaCO_3 with the in situ conditions, is critical. Calcium carbonate (CaCO_3) crystals will according to (Bindu J, 2017), dissolve very slowly, either when continuously flushed by buffered acidic groundwater or as a result of acidifying processes in the pores. (DeJong et al., 2009) note that ground

conditions where pre-existing and stable CaCO_3 can be observed, could be an indication of suitable environment for the durability of the binder. The life span of precipitated CaCO_3 , is estimated to be more than 50 years.

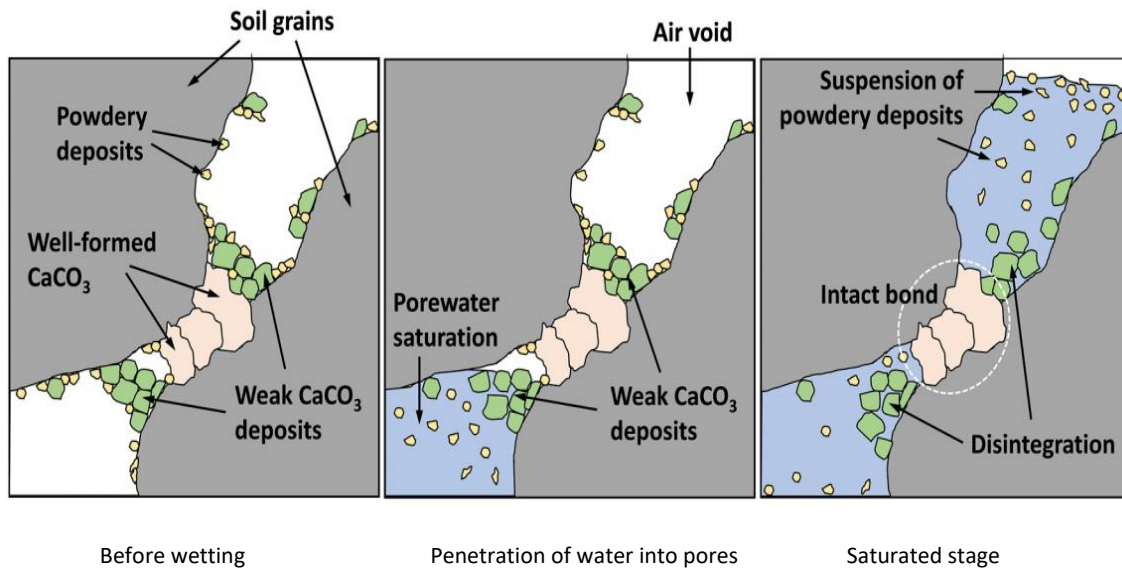
Precipitated CaCO_3 in the unsaturated zone of regions with frequent rainfall, will experience a high number of wetting and drying (WD) cycles. (Gowthaman et al., 2021) investigated the effect of up to 50 WD cycles on loss of CaCO_3 mass under cyclic WD exposure in MICP-treated poorly graded sand. The results show that loss of mass due to WD cycles, induced greater erosion in samples with the lowest calcium carbonate concentration (CCC), where initial cycles and cycles above the 30th cycle, had the greatest loss of mass per WD cycle.



Figur 82. Show loss of mass (CaCO_3) as a function of number of WD cycles, for MICP-treated poorly graded sand with different CCC. Data adapted from (Gowthaman et al., 2021).

In their work, (Gowthaman et al., 2021) note that CaCO_3 is initially induced as non-crystalline and then during growth, transformed into crystals in the aqueous media. However, where depletion of resources or presence of organic content in the reaction system occur, the initial non-crystalline precipitates tend to stabilize on particle surfaces as powdery deposits of CaCO_3 before transforming to crystalline structure. Such secondary formations of CaCO_3 which are precipitated on locations beside the particle contacts, can accumulate in aggregated clusters, individual clusters or powdery deposits. During rainfall, percolating water will surround the CaCO_3 material, leading to the powdery deposits and their

accumulations to fall into suspension, which leads to the erosion of CaCO_3 mass. The process is illustrated in the schematic presented below.



Figur 83. Show the process of erosion of CaCO_3 mass during wetting. Illustration from (Gowthaman et al., 2021).

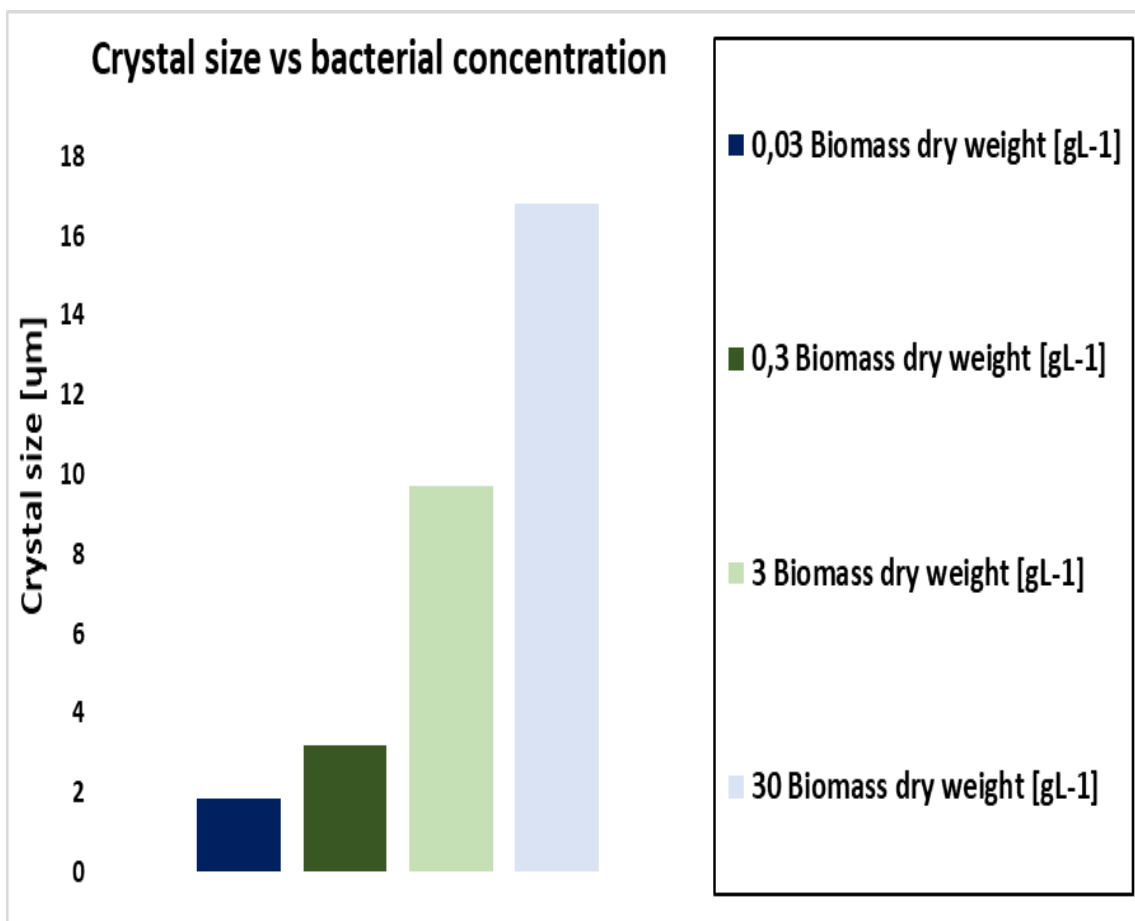
Work by (Gowthaman et al., 2020), investigated the effect of acidic rain on the durability of precipitated CaCO_3 binder in MICP-treated poorly graded sand, by measuring the corrosion of CaCO_3 during exposure. They found that the corrosion rate of CaCO_3 , depend on the intensity of the acidic rain and the level of pH. However, the loss of shear strength due to corrosion of CaCO_3 is governed by CCC, meaning that for same degree of corrosion, the higher the CCC the lower the loss of mass and shear strength.

In their work, (Tang et al., 2020) note that due to different extracellular polymeric substances (EPS) on the cell surface, output mineral and morphology will vary with bacterial strain, where (Cheng et al., 2007) note that cell size, size of urease enzyme, interaction between organic and inorganic substances at the cell surface and electrostatic surface charge affect the morphology of crystal formation.

Calcium carbonate can crystallize as *calcite*, *vaterite* or *aragonite* (Zehner et al., 2020, Tang et al., 2020), where (Zehner et al., 2020) state that calcite is the most common polymorph, due to its low solubility. (Paassen, 2009) found that the output mineral mainly depend on the rate of the ureolysis, where high rates generated spherical vaterite and lower rates generated calcite. (Tang et al., 2020, Cheng et al., 2007) state that the higher the concentration (CO_3^{2-} , Ca^{2+})

at supersaturation in solution, the faster the precipitation and the smaller the crystals, and vice versa. Whiffin (2004) found that at $\text{pH} < 8$, the concentration of CO_3^{2-} was lower, resulting in a lower precipitation rate and larger crystals.

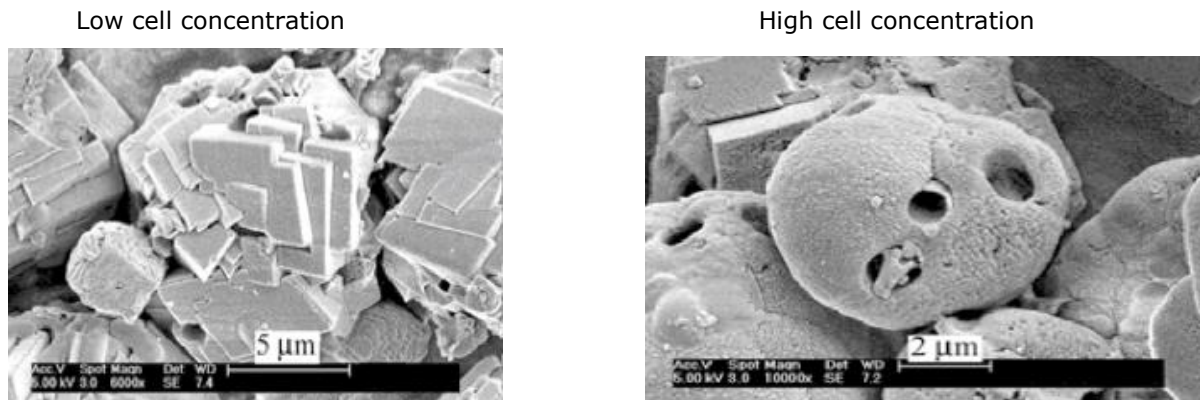
In work by (Tang et al., 2020), it is noted that bacterial concentration have a significant effect on the concentration of supersaturation. In their work, (Xu et al., 2017) found that increasing concentrations of Ca^{2+} , increased the crystal size and altered the morphology, while bacterial concentration was found to be more related to the development of surface structure. (Al-Thawadi and Cord-Ruwisch, 2012) observed increasing size of precipitated crystals with increasing bacterial concentration for all samples, where bacterial concentration was increased ten fold for each sample. The results are presented in the diagram below.



Figur 84. Show CaCO_3 crystal size as a function of biomass (bacterial density). Data adapted from (Al-Thawadi and Cord-Ruwisch, 2012)

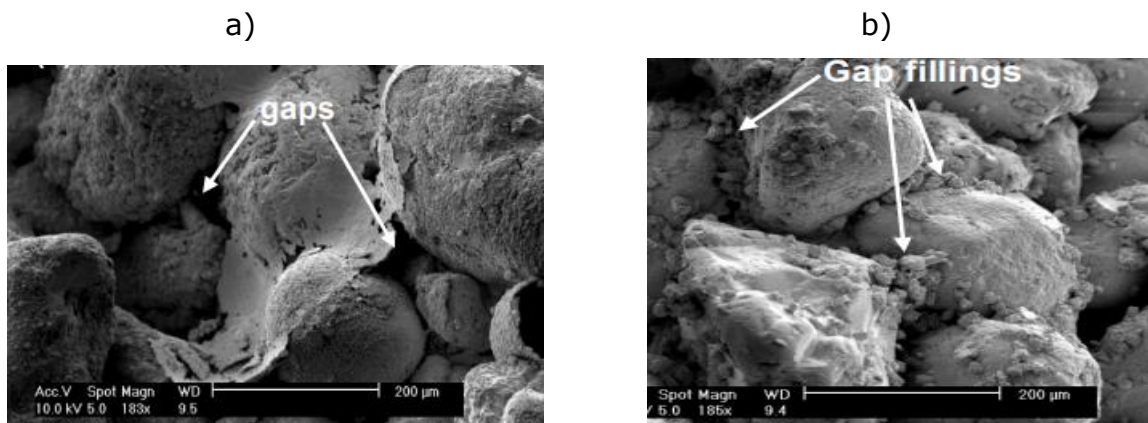
(Cheng et al., 2007) notes that when bacterial concentration is low, the nucleation sites on the cell surface where crystals are precipitated, are far apart and do not interfere with each other, leading to formation of cubic crystals,

whereas high cell concentration cause cells to flocculate, leading to formation of spherical crystal.



Figur 85. Show cubic (left) CaCO_3 crystal formation at low cell concentration and spherical (right) at high concentrations. Image from (Cheng et al., 2007)

In work by (Cheng et al., 2016), MICP-treatment (*S. pasteurii*) of sand under high urease activity at 50°C, formed small (2-5 µm) crystals forming thin coating layers (t=5 µm) over the sand particles, whereas lower urease activity at 4°C and 20°C, formed large (20-50 µm) clusters of crystals, where the gaps between the sand grains were almost completely filled with crystals. Precipitated CaCO_3 for high (a) and low (b) urease activity are shown in the images presented below.

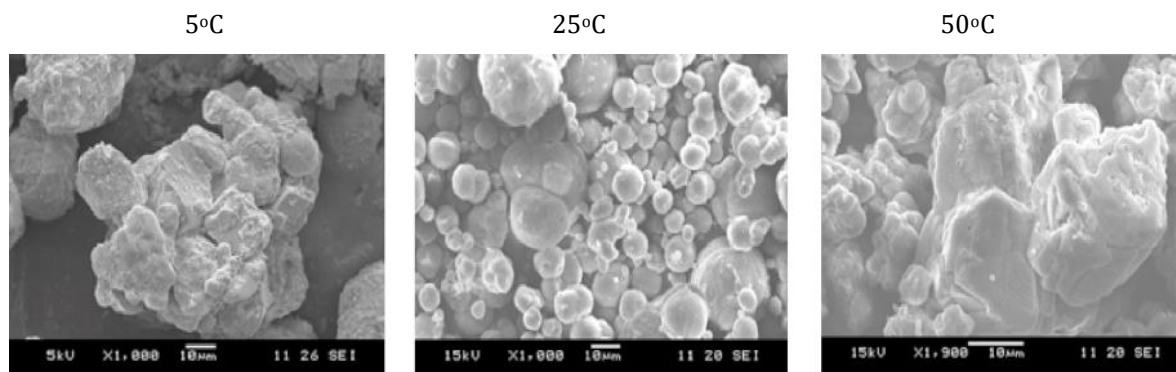


Figur 86. Shows a) weak CaCO_3 coating from high urease activity and effective CaCO_3 bridging of the grains from low urease activity. Image from (Cheng et al., 2016).

The crystals generated at low urease activity generated effective particle bonding and increased shear strength, whereas crystals generated at high urease activity did not contribute to increased shear strength. (Cheng et al., 2016) suggest that the competition between the crystal growth and crystal nucleation is the cause of the difference in crystal formation. High number of cells result in an abundance in nucleation sites (cell surfaces), where the supplied cementation solution is used for nucleation of new CaCO_3 crystals rather than growth of existing crystals.

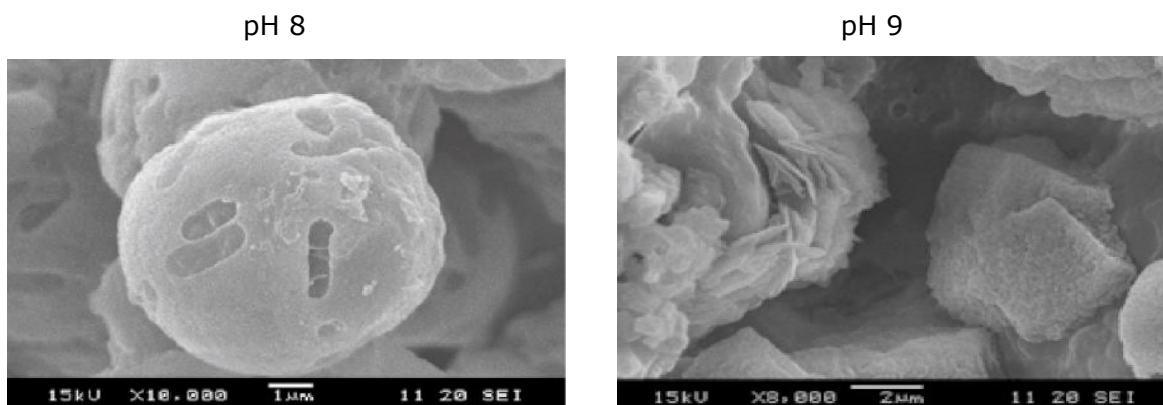
This leads to an abundance of small crystals forming dense crystal layers, given a continuous supply of cementation solution. In contrast, with low number of cells, the nucleation sites are limited and the supply of cementation solution is used in further growth of the already precipitated crystals.

(Kralj et al., 1994) found that change in temperature of inorganic salt solutions such as CaCl_2 , affected the precipitation rate. (Jianyun, 2005) reported that CaCO_3 precipitated by *S. pasteurii*, was mainly calcite with amorphous, aggregated and poorly crystallized material at 5 °C, uniformly distributed well-spherical crystallized calcite at 25 °C and crystallized calcite and vaterite with spherical, square, and spindle appearance with poor stability at 50 °C. They concluded that 25°C was most favorable for precipitation of high quality crystals. The results are shown in the images presented below.



Figur 87. Show morohology of precipitated CaCO_3 by *S. pasteurii* at different temperatures. Images from (Jianyun, 2005)

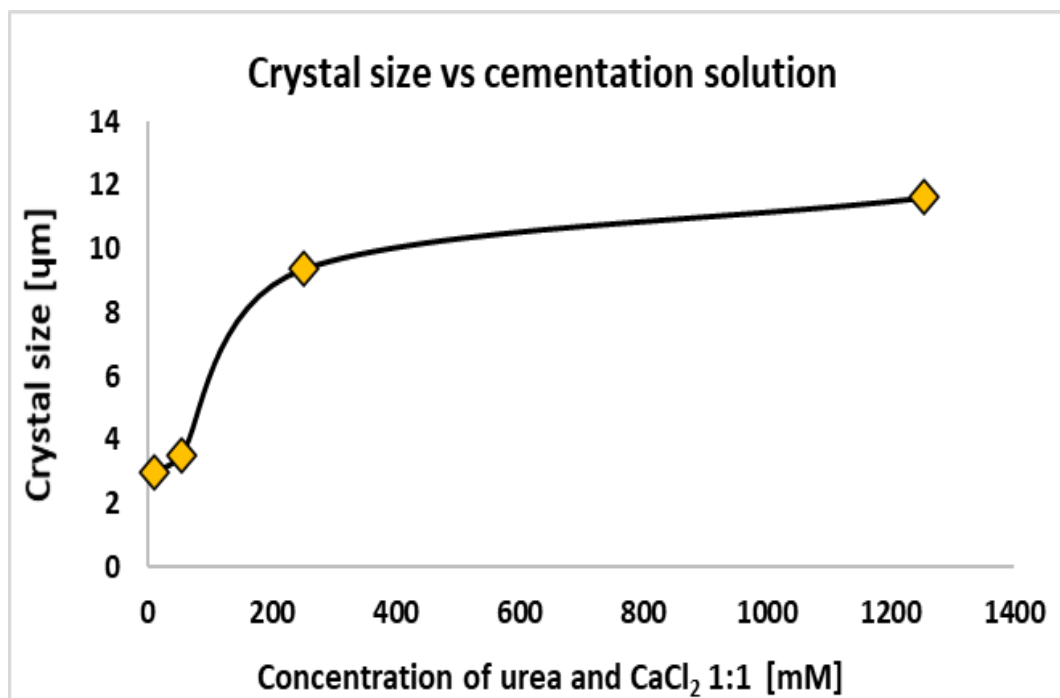
(Cheng et al., 2007) found that CaCO_3 precipitated by *S. pasteruii* at pH 8 and 9, both generated calcite. XRD analysis showed that at pH 8.0, the shape was spherical, whereas at pH 9 the crystals were cubical. The morphology for pH 8 and pH 9 is presented in the images below.



Figur 88. Show morohology of CaCO_3 precipitated by *S. pasteurii* under different pH. Images from (Tang et al., 2020)

In work by (Wang et al., 2019), it is noted that the size of the crystals formed from MICP, are highly dependent on the time interval between injections of cementation solution. They found that the average size of CaCO_3 crystals was significantly higher at 23–25 h injection interval, compared to the shorter injection intervals.

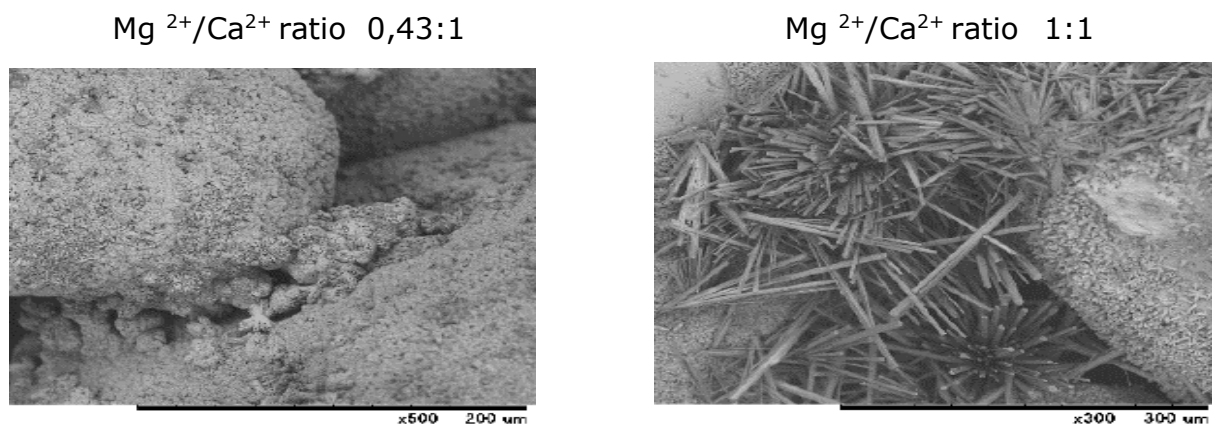
In their work, (Al-Thawadi and Cord-Ruwisch, 2012) reported on a high increase in crystal size when concentration of cementation solution ($\text{CaCl}_2/\text{urea}$) was raised from 55 mM to 258 mM and a much lower increase in crystal size when concentration was further increased from 258 mM to 1255 mM. The results are presented in the plot below.



Figur 89. Show crystal growth or size, as a function of cementation solution. Data adapted from (Al-Thawadi and Cord-Ruwisch, 2012)

In most areas of Norway the groundwater is soft but in the northern parts of the country and central areas around Oslo, the rock surface contain calcium and in these regions the groundwater can be hard and rich in Ca^{2+} . (Aamodt and Dahl, 2016) state that Norway has lower concentrations of magnesium in the groundwater than many other european countries which have metamorph and eruptive rockbeds in the sub-surface. Regions with sedimentary rock, which are more soluble and magnesium rich, would have more magnesium (Mg^{2+}) in the groundwater.

In their work, (Nayanthara et al., 2019) investigated how concentration of Mg^{2+} , affect the morphology of $CaCO_3$ crystals precipitated by *S. pasteurii*. They found that increasing the Mg^{2+}/Ca^{2+} ratio from 0.43 to 1, drastically changed the crystal morphology of the precipitated $CaCO_3$. The particles were slightly covered by small crystals while the pore voids were completely occupied by needle shaped long crystals, some as long as 100–200 μm . These displayed a lower cementing ability and lower resistance to compressive forces, compared to the rhombohedral or spherical crystals accumulated together at the grain contacts. The resulting morphology is shown in the images presented below.



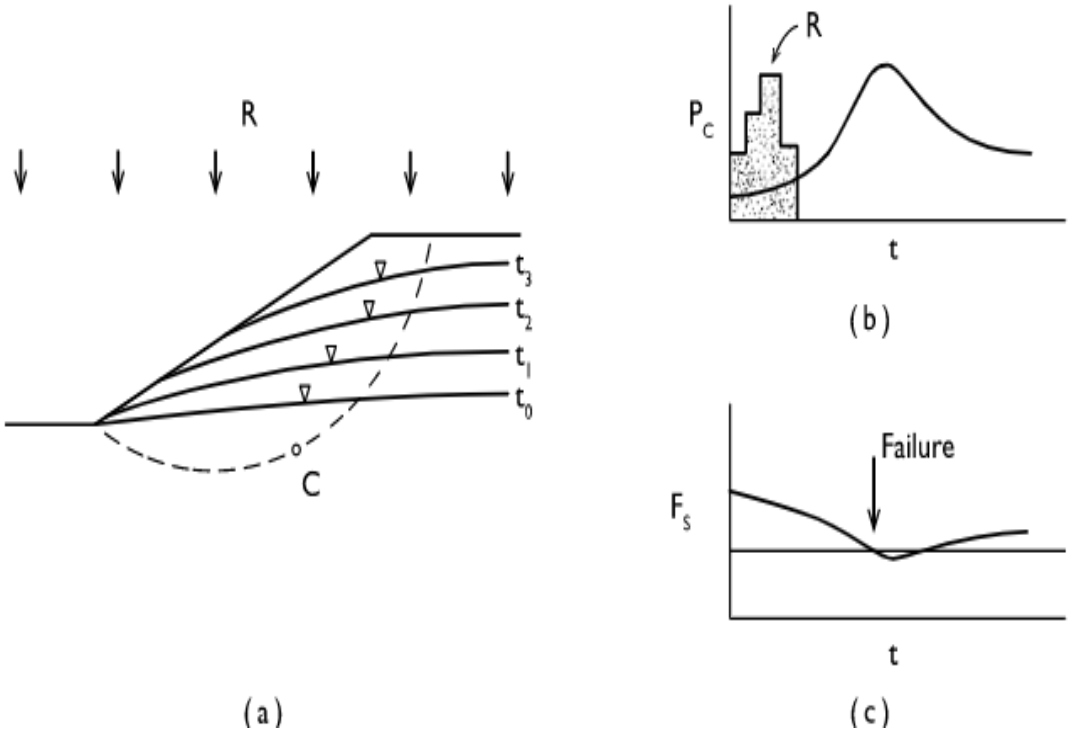
Figur 90. Show SEM images of the morphology of percipitated $CaCO_3$ crystals at different ratios of Mg^{2+} and Ca^{2+} . Image from (Nayanthara et al., 2019).

3.10.5 Residual permeability post treatment

For some applications of MICP, such as cut off walls or other applications intended to reduce waterflow, a reduction of porosity and permeability is desirable. For other applications such as geotechnical design where rise of porepressure due to lack of drainage, residual permeability post-treatment is critical. For MICP to be a viable method for ground improvement, the reduction of permeability during treatment must be controllable, so that sufficient residual permeability while acheiving desired improvement in strength and stiffness, can be acheived.

Stratified soil deposits can contain distinct or diffuse layers with different degree of permeability. Permeable layers within layers of lower permeability will act as drainage paths, while draining layers on top of low permeability layers will limit the elevation of the phreatic line or water table in inclined terrain. Elevated phreatic line or watertable will reduce the effective strength of the soil that is submerged.

For the use of MICP to stabilize or enhance soil properties in slopes, it is important that existing draining layers within the slope obtain residual permeability post-treatment. If a slope already have a low safety factor close to 1 (failure), an increase in the waterpressure could likely cause the slope to fail. The illustration below illustrate the effect on slope stability due to a rising phreatic line caused by intensive rainfall (R), where the principle also is valid for significant reduction of permeability in draining layers within the slope. As the phreatic line (t) in the slope (a) starts to rise (t_0), the porepressure P_c (b) rises at point C on the critical slip surface and with the watertable further rising (t_1-t_3), the resisting shear force at point C and along the slip surface are reduced, thus reducing (c) the factor of safety (F_s) until the the driving forces exceed the resisting shear along the slip surface, causing the slope to fail.



Figur 91. Show effect of rising phreatic line in a slope. Illustration from (borders, 2021)

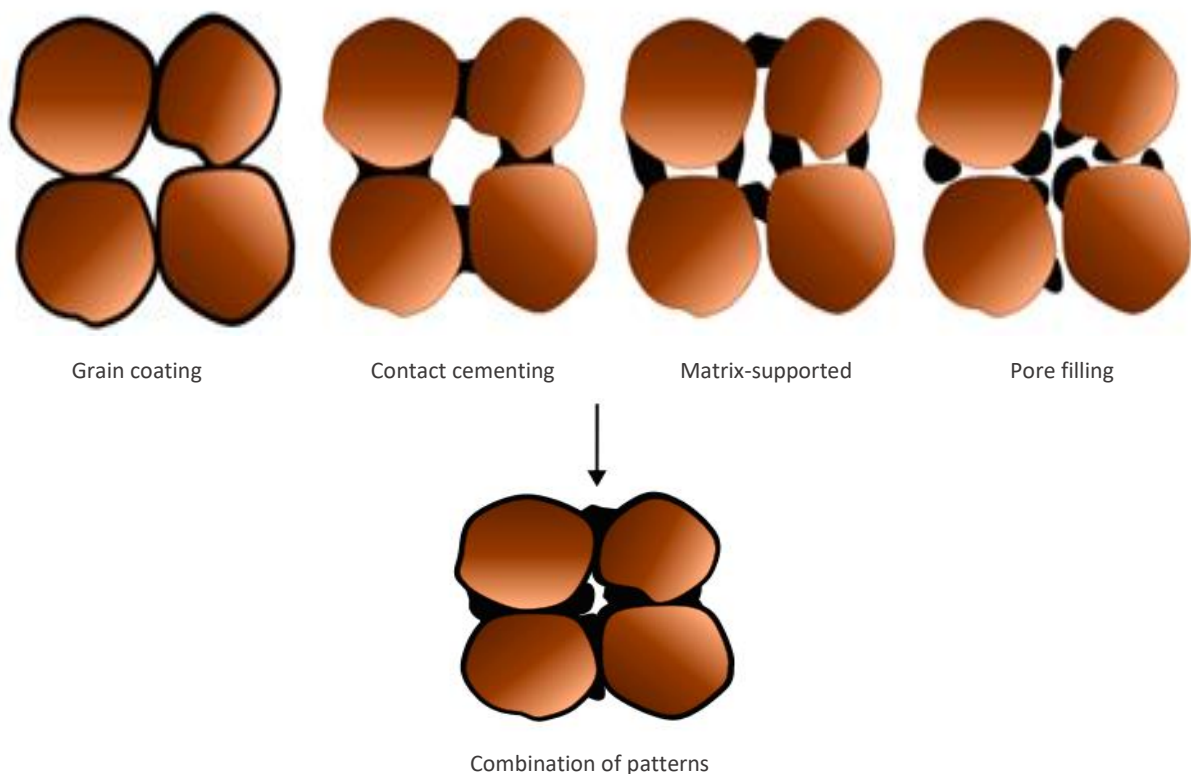
3.10.6 Cementation patterns

In work by (Cheng et al., 2016, Al Qabany et al., 2012, Nayanthara et al., 2019), it is noted that the precipitation pattern influence the flow properties of porous media, where (Al Qabany et al., 2012) adds that the cementation pattern also affect the stress transfer between the cemented particle contacts.

According to (Rong and Qian, 2012), the following cementation patterns can be generated during precipitation:

- *Grain coating*, where the crystals grow on grain surfaces and encapsulate them.
- *Contact cementing*, where crystals can be precipitated at or near contact points of particles.
- *Matrix support*, where crystals grow into the void spaces from particle surfaces, bridging the particles.
- *Pore filling* (clogging), where crystals fill the pore voids without bridging the particles, hence reducing the porosity or permeability of the soil.

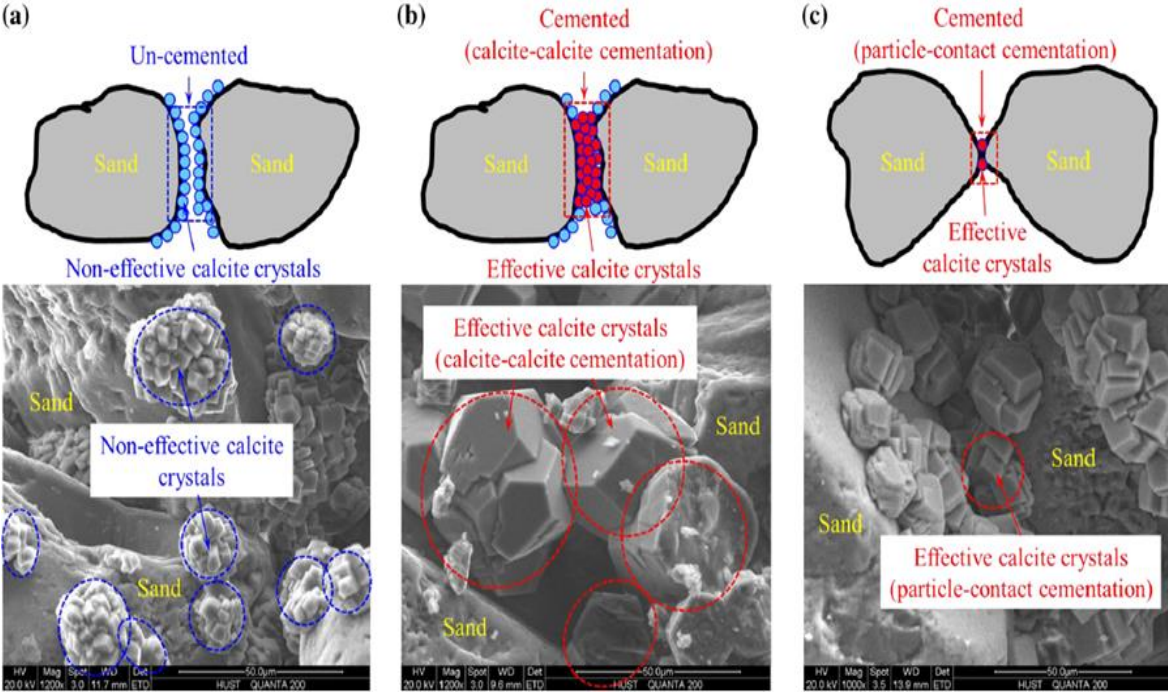
The illustration presented below show the different cementation patterns described above.



Figur 92. Show individual patterns and a combination of cementation patterns. Illustration from (Nayanthara et al., 2019).

Particle cementation by CaCO_3 can according to (Cui et al., 2017a), be classified as either effective or non-effective crystals. Cementation between particle contacts contribute to particle bonding and are considered effective, whereas

cementation on particle surfaces do not contribute to particle bonding and is considered non-effective. It is suggested, that one can further classify effective cementation into particle-contact cementation and calcite-calcite (crystal-crystal) cementation. The illustrations and images presented below show how cementation in the context of actual strength enhancement, is differentiated.



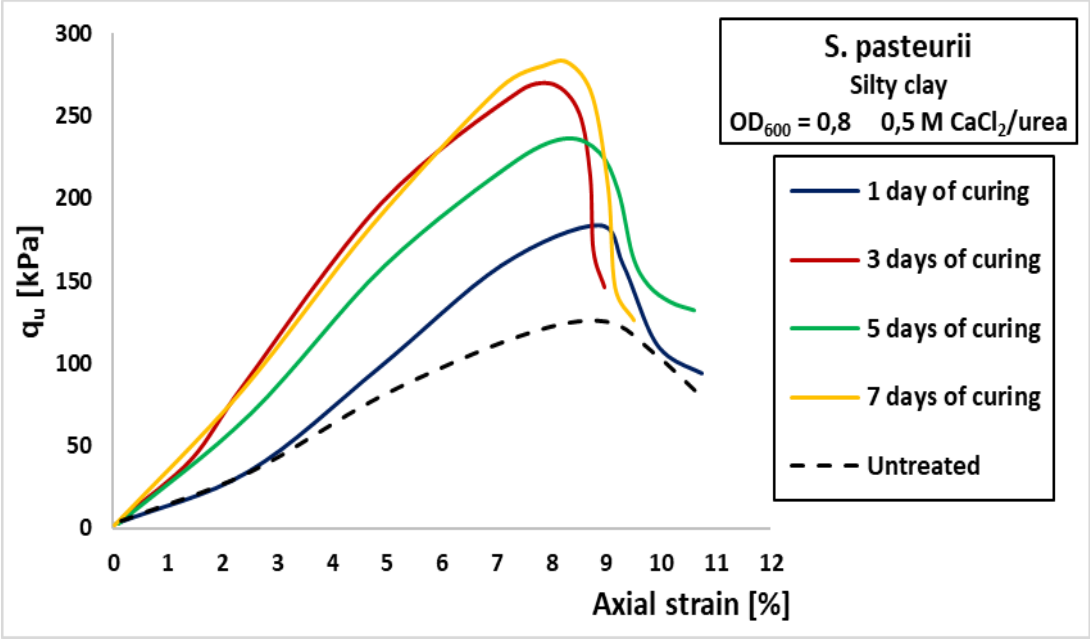
Figur 93. Show classification of calcite (CaCO₃) crystals. Images from (Cui et al., 2017a).

The crystals are according to (Cui et al., 2017a), precipitated in cluster form, where the size of the cluster increases with increasing number of injection cycles of cementation solution, where some of the non-effective crystals would be transformed into effective calcite crystals in the span of the cyclic injections. At lower cementation levels, the effective crystals are mainly precipitated as particle-contact cementation, while at increased cementation level, effective crystals are precipitated as calcite-calcite cementation.

3.11 Curing time

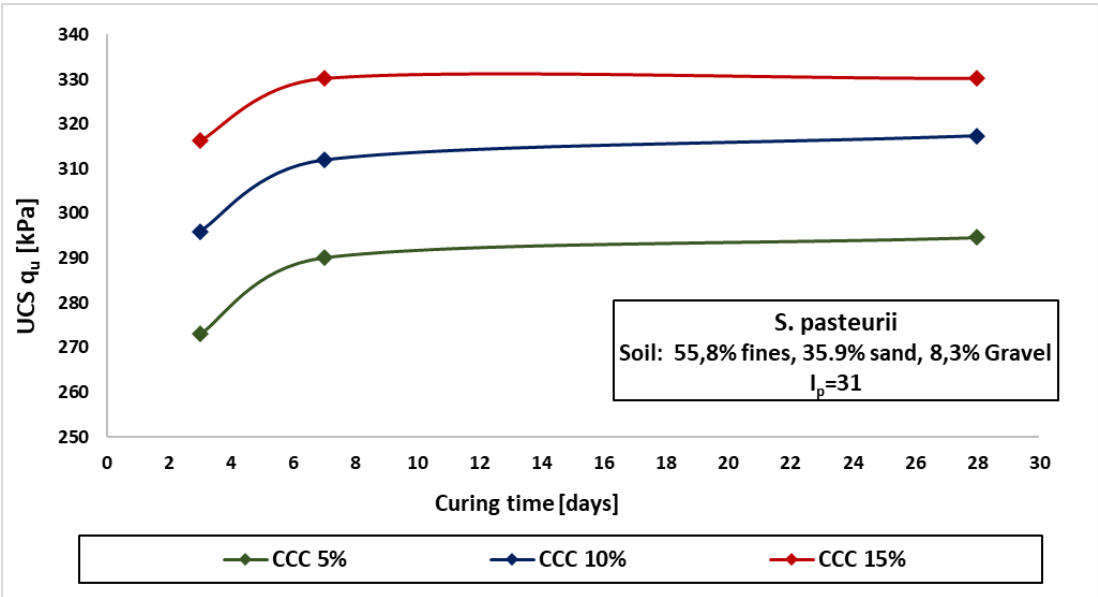
The effect of curing time on achieved shear strength from precipitated CaCO₃ can be important, when determining the time span for post-treatment quality control where achieved shear strength is to be controlled up against the set design criteria. In their work, (Teng et al., 2020) used manual mixing during MICP-treatment of high plasticity silty clay (68,7 % silt) with *S. pasteurii*. They found that UCS increase with increasing curing time, except for sample at 5 days of curing, which could indicate a lower urease activity in this particular sample, where all

samples had the same initial parameters during preparation. The results are presented in the plot below.



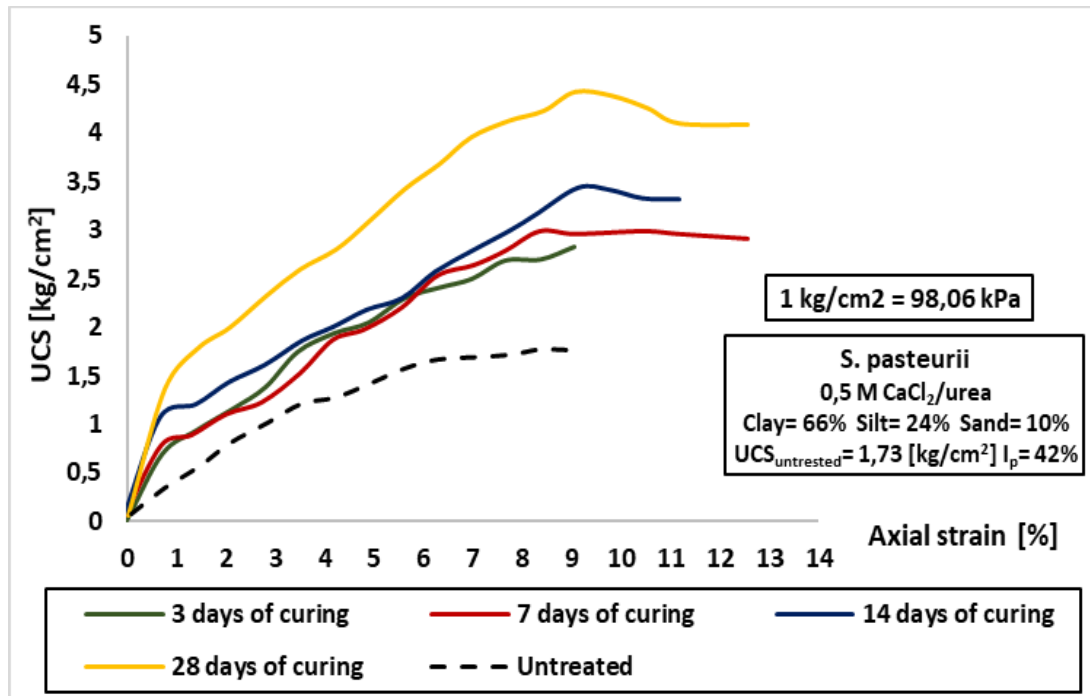
Figur 94. Show UCS for increasing curing time for MICP-treated silty clay. Data adapted from (Teng et al., 2020)

(Oyediran and Ayeni, 2020) found that MICP-treated fine grained soil followed the same rate of initial strengthening (3-7 days) for different levels of CCC, where the increase in UCS from 7-28 days was negligible. However, the initial UCS increased with increasing (CCC). The results are presented in the plot below.



Figur 95. Show UCS as a function of curing time for MICP-treated fine grained soil with different CCC. Data adapted from

(Godavarthi Rajani, 2020) found that MICP-treated high plasticity clay achieved a higher increment in increase of UCS from 14-28 days of curing, compared to increment in increase of UCS from 3 to 14 days. The results are presented in the plot below.



Figur 96. Show UCS as a function of curing time for MICP-treated high plasticity clay. Data adapted from (Godavarthi Rajani, 2020)

3.12 In situ application of MICP

3.12.1 Injection strategies

The way bacterial suspension and cementation solution is introduced to the sub-surface during MICP, affect the achieved spatial distribution in the target area. The injected solutions need to cover the targeted area and depth for the following precipitation of CaCO_3 and consequently the desired alteration of the soils properties, to be adequately distributed. This is one of the most important components for the viability of MICP as a method for ground improvement and have in past studies proven to be a challenge.

The literature describes several treatment strategies for improvement of soils by MICP. Work by (Whiffin et al., 2007) developed the two-phase injection method, where an injection of bacterial culture is followed by an injection of cementation solution. This method has been widely used in later studies on MICP in soils and was later modified in work by (Cheng and Cord-Ruwisch, 2012), where a

retention period after the injection of bacteria and before injecting the cementation solution, was applied. (Van Paassen, 2009a, Van der Star et al., 2011) used injection/extraction wells in a grid pattern, where the injected solutions are transported through the target area by an induced hydraulic gradient created by the extraction wells on the opposite side. (DeJong et al., 2009) suggested applying this method to inject bacterial suspension in one direction and cementation solution and nutrients in the reversed direction. (Harkes et al., 2010b) introduced a multi-phased procedure, where bacterial suspension is injected first, then a fixation solution (to attach bacteria) is injected followed by injection of cementation solution.

In their work. (Cheng et al., 2014) demonstrated that surface percolation in coarse and highly permeable soils, where bacterial suspension and cementation solution are alternately trickled on the soil surface, achieved cementation exceeding 2m in depth from the surface. (Zhao et al., 2014) used mechanically mixing of bacteria and cementation into sand during an experiment in the lab, while (Gomez et al., 2018) used stimulation of existing ureolytic bacteria in the sub-surface, where nutrients and cementation solution is injected to stimulate growth and precipitation.

In work by (Cheng et al., 2019), a low pH one-phase integrated solution (bacteria+urea/CaCl₂) was developed. This approach requires only one injection and show promising potential for solving known practical problems with MICP such as release of NH₃ and poor spatial distribution of CaCO₃. This method was first explored by (Stocks-Fischer et al., 1999) on sand columns using a higher pH, which lead to an instant and rapid precipitation of CaCO₃ in the solution before injection, causing the solution to clog.

Due to the ability to control flow, saturation, pressure and hydraulic gradient, the injection method is a preferred method, but it has a disadvantage in the uneven distribution of precipitated CaCO₃ in the soil mass. In research conducted by (Whiffin et al., 2007), the two-phase injection method was used to treat a 5 m long sandy soil column, where both bacteria culture and cementation solution was injected alternately from top to bottom, where the vertical flow of the reactants was regulated by a pump. The study found that CaCO₃ was precipitated throughout the column, but the distribution was not uniform along the column length i.e declining concentration of CaCO₃ with distance from injection point.

When bacteria are injected through the pore space of the soil, they are according to work by (Ginn et al., 2001), likely to be filtered through the sand with a long-linear reduction of microbe concentration along the injection path i.e lower concentrations of bacteria will end up in locations further from the injection point.

As noted by (Cheng et al., 2014), the reaction of cementation solution with bacteria during penetration of the soil, leads to less reagent moving further into the soil. This is due to localized cementation around the injection points, where further supply of cementation solution eventually leads to plugging of the pores in the area near the injection point. (Harkes et al., 2010b) proposed a solution to improve this problem, by applying a slower flow rate in the injected bacterial solution, while (Whiffin et al., 2007) suggested that the flow rate of the cementation solution should be increased to reach further into the soil. Later, (Al Qabany et al., 2012) suggested a retention period before injecting the cementation solution to allow for the bacteria, to be transported further into the soil and reach a firm attachment on and in between the grains.

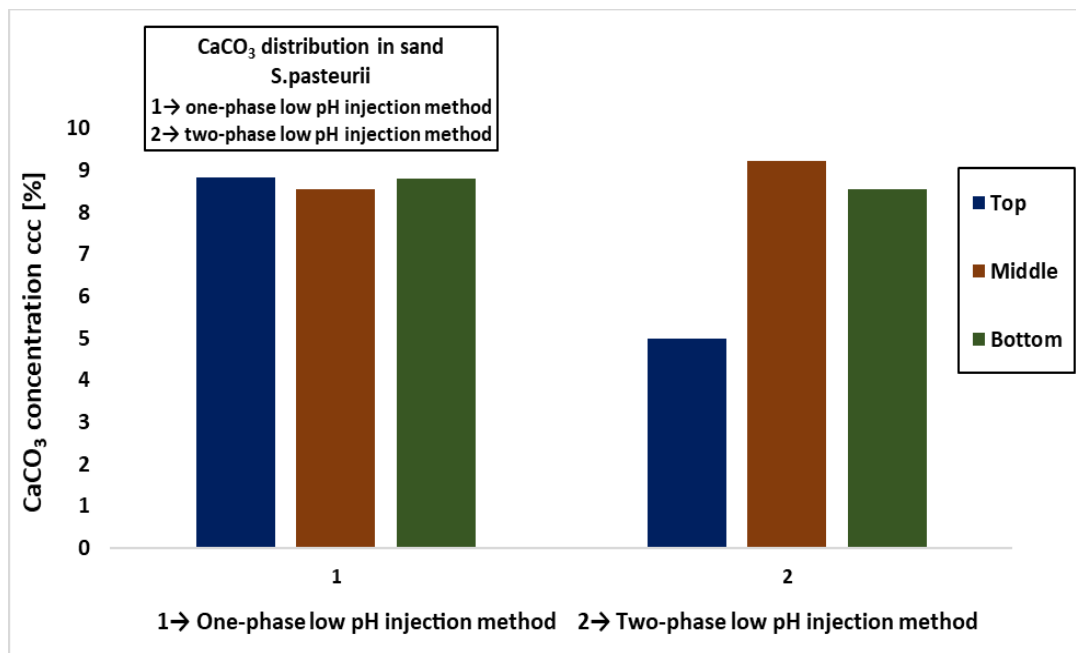
The surface percolation method described by (Cheng et al., 2014) found that the approach is suitable for porous granular materials with high permeability such as coarse sands and gravels, where cementation in the MICP-treated coarse soil was achieved down to more than 2m of depth. However, in fine sand ($d < 0,3$ mm), the slow infiltration rate (0.25–4.8 cm/min) limited cementation to 1m depth. In their work (Zhao et al., 2014) found that 83% of the CaCO_3 precipitated in the treated sand using manual mixing was homogeneously distributed throughout the sand columns used in the study. Despite solving the problem with uneven distribution, (Zhao et al., 2014) note that the method is still considered the least favorable of the methods, due to disturbance of the stress level in the soil during the mixing.

The one-phase low pH injection method proposed and demonstrated in work by (Cheng et al., 2019), uses bacteria and cementation solution ($\text{CaCl}_2/\text{urea}$) integrated in one injection, which provide a controllable lag period (35 min.) due to low pH, before precipitation of CaCO_3 is initiated. The lag time can, theoretically be prolonged by increasing the acidic buffer capacity of the integrated solution. The use of injection and extraction wells in a grid pattern applied by (Van Paassen, 2009a), could according to (DeJong et al., 2009) be applied to inject

bacteria in one direction and nutrients and cementation solution in the opposite direction. Due to the reduction in concentration with distance from injection point and delayed precipitation, the reversed injection could provide an even distribution along the flow path and could significantly reduce issues with clogging.

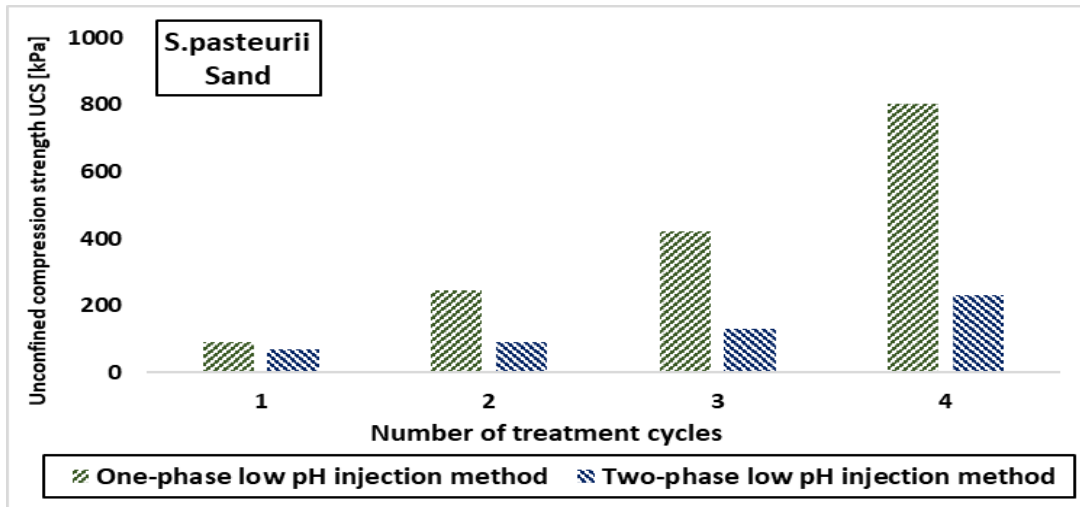
(Cheng et al., 2019) note that the urea driven urolysis, produces toxic ammonium, which is highly soluble in water and remain in the soil as aqueous NH_4^+ and must be extracted from the ground post-treatment. However, the unionised form of ammonia (NH_3), is volatile and can be released as a gas which have a foul smell and is toxic under long-term exposure. Increased pH, increases the concentration of NH_3 present in the water, thus more NH_3 gas is released. However, the low pH in the one-phase solution proposed by (Cheng et al., 2019), renders most of the NH_3 generated during the MICP process, as ionised form of NH_4^+ , which significantly reduces the production of NH_3 during treatment.

In their work, (Cui et al., 2021) compared the two-phase injection method and the one-phase method by using the low pH solution proposed by (Cheng et al., 2019). The one-phase method, achieved more uniform distribution of CaCO_3 through top, middle and bottom of sample, compared to the two-phase method. The results are presented in the diagram below.



Figur 97. Show concentration and distribution of CaCO_3 for one- and two-phase injection methods. Data adapted from (Cheng et al., 2019).

The one-phase method, achieved significant higher UCS, compared to the two-phase method. The results are presented in the diagram below.



Figur 98. Show achieved UCS for one- and two-phase injection methods. Data adapted from (Cheng et al., 2019).

(Minto et al., 2019), found through numerical fluid flow modelling (OpenFOAM) that an increased reaction period between treatment cycles, result in more precipitation of CaCO_3 and higher efficiency. However, the increased efficiency of urea conversion, required longer (duration) treatment cycles. A reduction in the concentration of urea/ CaCl_2 , increased the efficiency but decreased amount of precipitated CaCO_3 .

3.12.2 Liquid flow and bacteria retention

During injection of bacterial suspension to the sub-surface, the distribution of bacteria in the soil will according to (Van Paassen, 2009b, Cheng et al., 2016), be affected by the soil porosity and flow conditions, where only a fraction of the bacteria is adsorbed to the grain surface or is attached to the pore walls. (Cheng et al., 2016) adds that the retention of bacteria inside the target area is crucial, where weak attachment could lead to the bacteria being flushed away or detached by the following injection of cementation solution. This would cause uneven distribution of precipitated CaCO_3 crystals.

Due to attractive forces, high salinity fluids such as CaCl_2 causes the bacteria to attach to the soil particles, whereas low salinity fluids such as rainwater will reduce the attraction. (Cheng et al., 2016) simulated heavy rainfall by water flushing samples during MICP-treatment of sand. The flushing caused significant decrease in the efficiency of urea conversion down to less than 5% and consequently a very low precipitation ($\text{CCC} < 0,3\%$), whereas the control sample

achieved 10 times more precipitation, where the reason for the poor results in flushed is suggested to be due to washing out of bacteria and substrate during flushing.

In work by (Van Paassen, 2009b), it is noted that increased flow velocity due to narrowing of flowpaths from precipitation, shorten the residence time of substrates within the flow path. This reduces the urease activity per soil volume, where (El Mountassir et al., 2018) add that the increased velocity within the channels where precipitation still have not occurred, make it difficult for the bacteria to attach itself.

(Minto et al., 2016) suggested that flow velocity can be used to control where bacteria attach within the soil, where constant pressure rather than constant flow rate or sequentially decreasing the flow rate for consecutive injection cycles, may enable distribution of bacteria over a larger area. (Van Paassen, 2009b) used flow velocity at 0,4/m/hr in a large scale MICP-treatment of fine sand, where no precipitation of CaCO_3 within a 100 mm radius around the injection point, could be observed. This is suggested to be an indication that velocity can be used to control location of precipitation, even in granular and porous soils.

In their work, (Ng et al., 2012a) note that high salinity solution drives flocculation, which supports the adsorption of bacteria and retention in sand. They suggest that low salinity solutions such as fresh water, can be effective in increasing the impact radius and spatial distribution, due to low ionic and adsorption strength.

In work by (Harkes et al., 2010a), it was found that injection of undiluted bacteria suspension, followed by one time pore volume of sample with 50 mM high salinity (CaCl_2) fixation fluid, which was then followed by cementation solution ($\text{CaCl}_2/\text{urea}$), retained almost all bacteria suspension in the sand. The fixation fluid, caused the bacteria to flocculate, fixing them to particle surfaces, resulting in an increase of precipitation around these assemblages of bacteria. The study suggested that the use of high salinity fluids can increase adsorption and flocculation, while low salinity fluids can increase transport and remobilization of adsorbed bacteria to improve the distribution. It is noted by (Cuthbert et al., 2013), that to achieve adequate retention of bacteria in a desired area, 200 mM CaCl_2 and 400 mM urea needs to be mixed with the bacterial suspension

before injection. However, this approach would most likely cause immediate precipitation and clogging around the injection point.

3.13 Scaled up MICP experiments

Large scale MICP in gravel:

Two 48 inch steel gas pipelines with a length of 600 and 900 are to be placed in the ground across the river Waal. (Van der Star et al., 2011) note that Horizontal Directional Drilling (HDD) is a method for trenchless and steerable installation of underground pipelines, which provides minimal disturbance to the surrounding ground and can be applied both in rocks and porous soils. After drilling, the stability of the bore hole is maintained by a viscous and high density drilling fluid, that stabilize the bore hole during the initial drilling and the reaming phase. However, due to the tendency of coarse gravel to collapse during drilling, MICP using *S. paterii* is investigated as a potential solution for stabilizing the ground along the river banks, before drilling is conducted.

Due to fewer contactpoints in coarse gravel, the achieved effect of biocementation was unclear, so laboratory tests were conducted before large scale application. 18 kg of gravel was treated with initial injection of bacterial suspension, then fixation solution of 50 mM CaCl_2 and finally 5 and 9 injection cycles of 1 M cementation solution ($\text{CaCl}_2/\text{urea}$). In the test with 9 cycles of $\text{CaCl}_2/\text{urea}$, a second bacterial suspension was injected after the first cycles, whereas in the test with five cycles, the gravel was mixed with 1.5 kg coarse sand. Precipitated CaCO_3 post-treatment was mainly located within the pore voids, where CaCO_3 had sedimented by gravity onto the gravel particles. The results are shown in the images presented below.



Figur 99. Show cementation for varying treatment strategies in coarse gravel. Images from (Van der Star et al., 2011)

To test the suitability of cemented gravel under drilling using the same bacteria and cementation solutions, two 3 m³ containers were filled with gravel and treated. One was filled with a uniform medium-grained gravel (d₅₀=10 mm) and the other with the same gravel, mixed with coarse gravel (d₅₀=40 mm) and cobble stones up to d= 300 mm. The procedure and results are shown in the images presented below.

Drilling through cemented mass



Drilled pathway for pipe



Figur 100. Shows drilling through cemented mass (left) and drilled pathway (right). Images from (Van der Star et al., 2011)

1000 m³ of ground was MICP-treated at two different locations along the river Waal, with a single injection of bacteria solution with *S. pasteurii* followed by a single injection of cementation solution. Injection and extraction wells were installed in a grid pattern above the projected pathway of the pipeline, where the extraction wells are used to create an artificial and directed gradient as well as to extract NH⁴⁺ post-treatment. The set up is shown in the images presented below.

Injection and extraction wells in a grid pattern

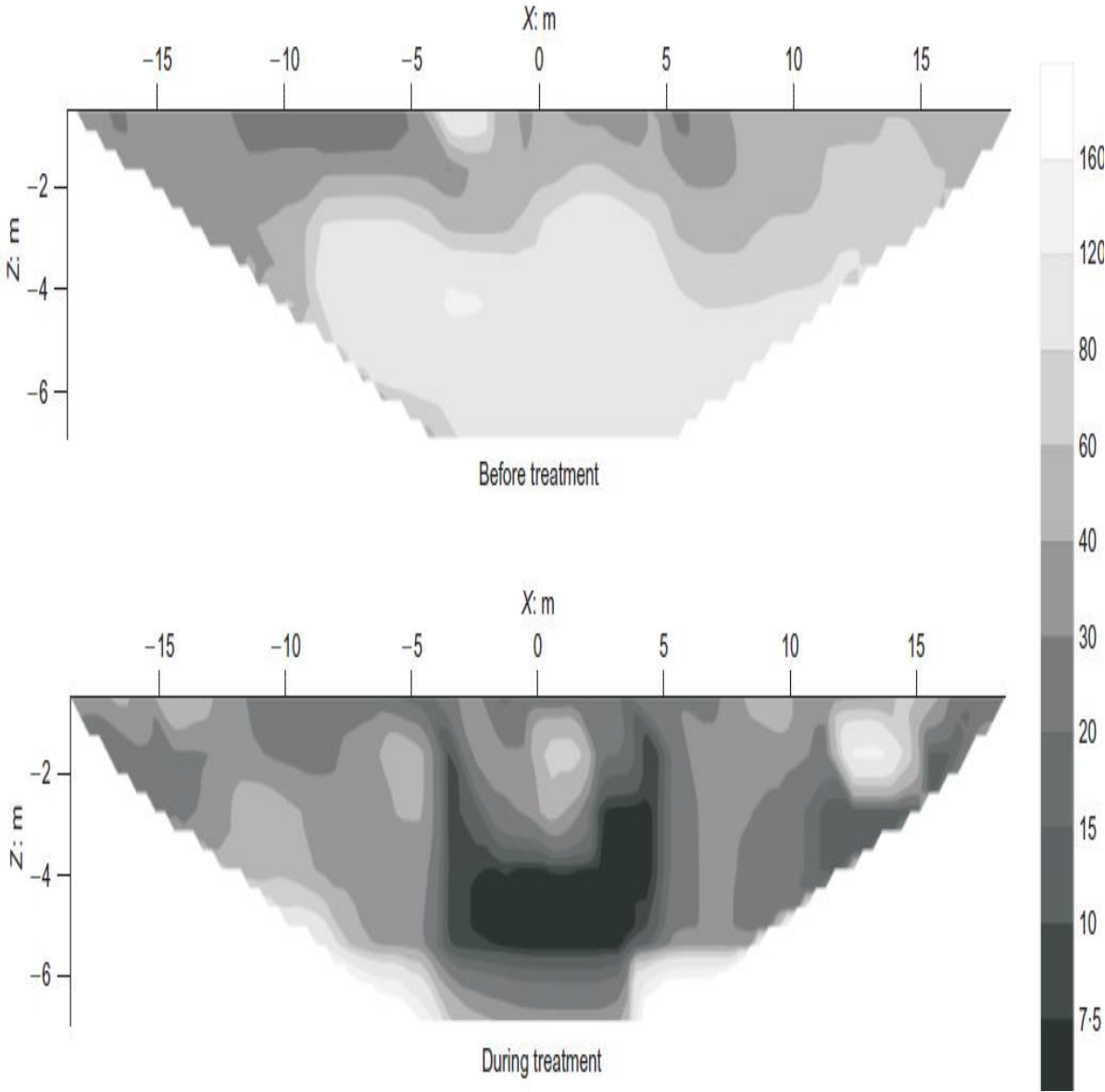


MICP-treated sand and gravel



Figur 101. Show grid of injection wells on top of projected pathway for pipeline (left) and stabilized gravel (right). Images from (Van der Star et al., 2011) (left) and (DeJong et al., 2014) (right)..

The resistivity maps below show the extent of change in the soil profile during MICP-treatment.



Figur 102. Resistivity mapping for soil profile before and after MICP-treatment. Illustration from (DeJong et al., 2014) (Deltares).

The MICP-treatment of loose gravel was found to be a suitable and risk-reducing measure when drilling in masses, where high permeability hinders fluids to form a stabilizing cover in the borhole. The installation of the gas pipeline across the river was concluded to be successful.

Large scale MICP in sand:

In a large scale experiment conducted by (Paassen, 2009), 100m³ of Itterbeck fine sand was built in a 8 m x 5.6 m x 2.5 m concrete box structure, while a

bioreactor was built on site to manage 5m³ nutrient broth. In the image below, three injection wells are placed to the left in the picture, while three extraction wells used to create an artificial gradient through the sand mass, are placed to the right in the picture.



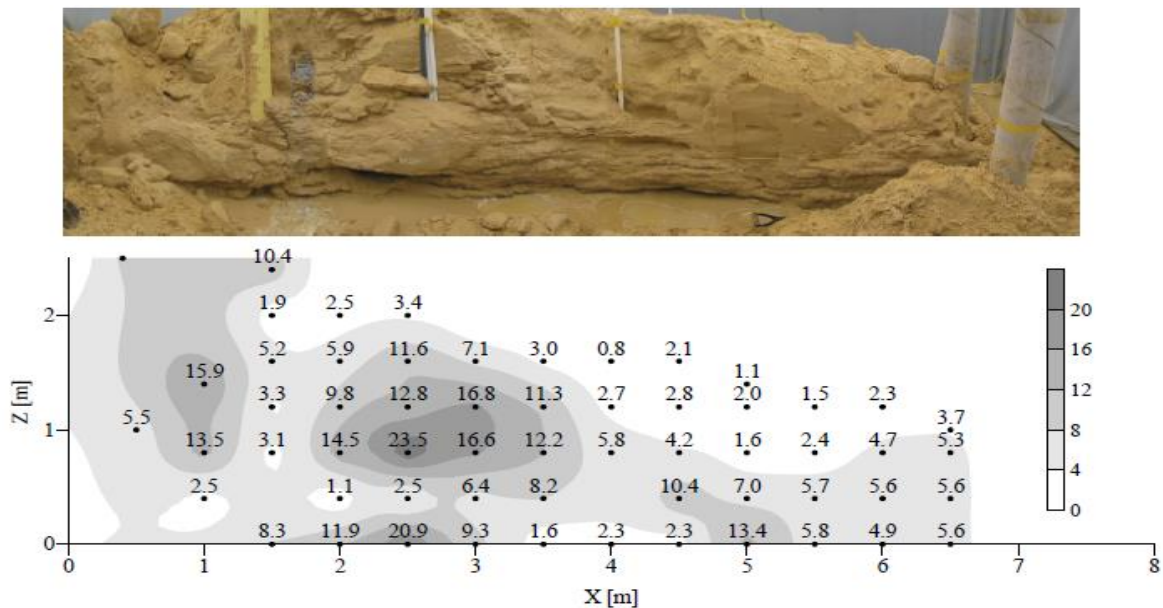
Figur 103. Show setup for larger scale MICP experiment in sand. Image from (Paassen, 2009)

First bacterial suspension was injected, then 100m³ cementation solution (1M urea/CaCl₂) was injected sequentially in 10 cycles (over 12 days), where 80% of the urea was hydrolysed after 12 days. The fluid was injected through the three injection wells and transported through the sand over the length (5m) of the box towards the three extraction wells. The treated sand was rinsed with water and excavated. As can be seen on the excavated body in the picture below, cementation along the flow lines were reasonably homogeneous, while perpendicular to the flow lines, CaCO₃ content varied significantly. Further, as can be observed to the left in the picture below, the cemented patterns close to the extraction points are clearly related to the flow paths through the sand body. The cemented mass, seen in the image below was estimated to 40m³.



Figur 104. Show the exposed cemented sand body. Image from (Paassen, 2009)

A vertical cross-section made along the centre flow line, showed that below the cemented phreatic surface, lenses varying between 0,8-24% of dry weight CaCO_3 content was formed.



Figur 105. Show CaCO_3 concentration and distribution along the longitudinal centre line of cemented mass. Injection well at 1.5 m and extraction well at 6.5 m.. Plot and image from (Paassen, 2009).

The study showed that the injection method is feasible, both as single point injection in an other smaller experiment (1 m^3) or over a horizontal distance using screens of injection and extraction wells. The CaCO_3 content was not as homogeneously distributed as desired. It is suggested that the cementation in the sand mass was limited by the induced flow field, where the distribution of bacteria varied over the distance and between different flow paths.

3.14 Challenges with upscaling

For the MICP method to be viable as a alternative method for ground improvement adapted in the industry, it needs to:

- Provide a uniform distribution of CaCO_3 binder in the target area
- CaCO_3 binder need to be resistant to erosion and corrosion, where the service life of binder should be equal to or close to that of cement and lime based binders.
- Be applicable in stratified soils with layers of different permeability, pore size distribution and grain size distribution

- Be applicable under conditions with limited dissolved oxygen and under a broad range of ground temperatures
- Provide means for the control of crystal morphology, crystal size and cementation pattern
- Provide method for obtaining residual permeability, while increasing the strength and stiffness of the treated soil
- Provide a method for reducing NH_3 and removal of aqueous and adsorbed NH_4^+

Controlled experiments can never fully simulate in situ conditions, where a high number of combinations of variables affecting the MICP process, can be expected. In that regard, (DeJong et al., 2009) note that most soils are heterogenous, where variation in particle size and mineralogy, can affect the distribution of injected solutions and consequently the distribution of precipitated CaCO_3 .

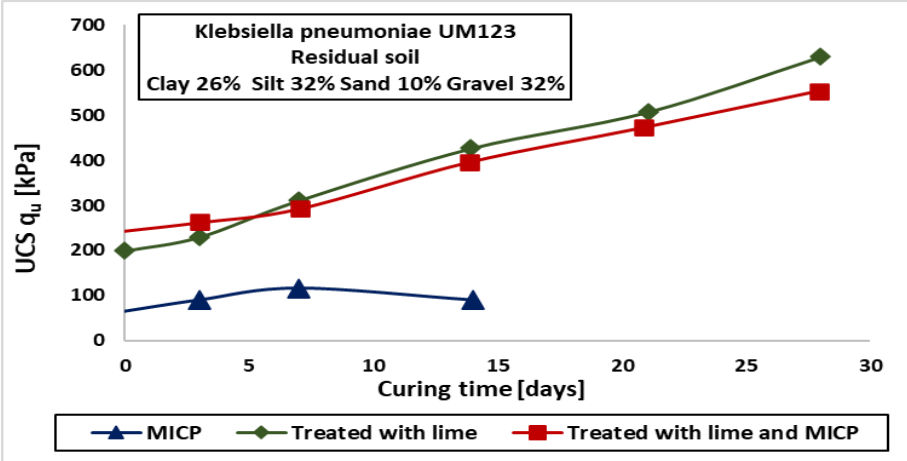
It is further noted by (DeJong et al., 2009), that the achieved improvement of strength will vary with the number of particle contacts in the designated soil, where stratification in the soil could lead to variations in strength and other properties sought to be enhanced with MICP. The soil mineralogy may affect precipitation, where some minerals may provide more favorable nucleation sites than others, whereas existing native bacteria can affect the urease activity and consequent precipitation due to competition for nutrients. Groundwater rich in calcium can enhance precipitation, while groundwater with higher levels of organic matter can have an inhibitory effect on precipitation, whereas groundwater in coastal areas may be affected by salt water intrusion.

As noted by (Ginn et al., 2001), filtration of cells in injected bacterial suspension results in a reduction of microbe concentration along the injection path, where (DeJong et al., 2009) adds that the gradient of reduction generally will correspond to a gradient in reaction and cementation rate. The degree and form of cementation determine the achieved strength and stiffness in the treated soil,

where the degree of cementation at given spot, is determined by bacterial density and their access to cementation solution. Achieving a uniform cementation throughout the soil is crucial for predictability and design purposes. This challenge has to be properly addressed for MICP to be a viable option for ground improvement, while treatment below the watertable would require further clarification on capacity for growth and ureolysis under anoxic conditions or solutions for supplying oxygen to the sub-surface during treatment.

3.15 Comparison of methods

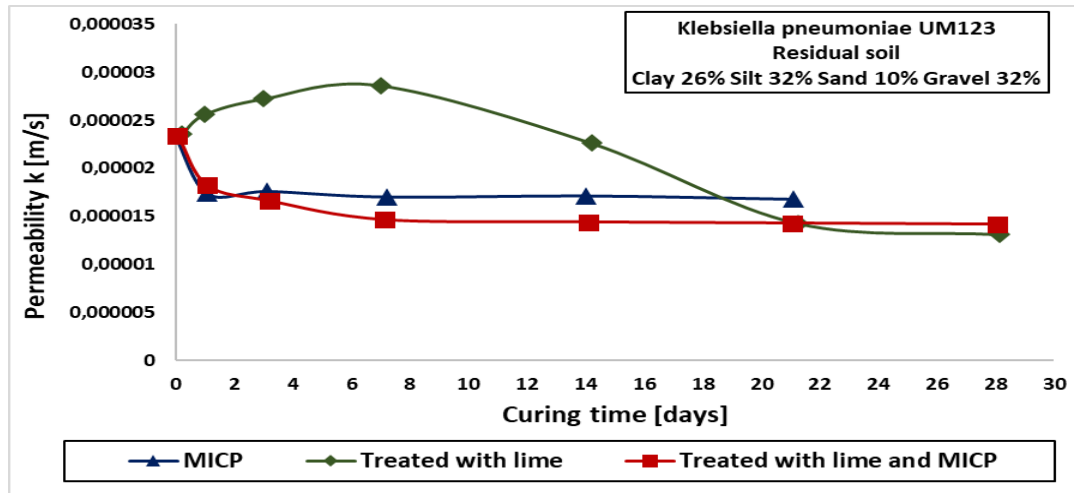
The competitiveness of MICP in respect to methods utilizing cement and lime products will have an effect on whether MICP will be adopted as a method for ground improvement in the industry. (Umar et al., 2019) compared MICP-treatment with lime treatment in residual soil with both fines and coarse gravel particles. The sample treated with only MICP, achieved lower UCS than sample treated with lime and sample treated with MICP and lime. The samples treated with lime increased the UCS significantly over time, whereas the sample treated with only MICP, lost shear strength over time. The results are presented in the plot below.



Figur 106. Show UCS as a function of curing time for samples treated with lime and samples treated by MICP. Data adapted from (Umar et al., 2019)

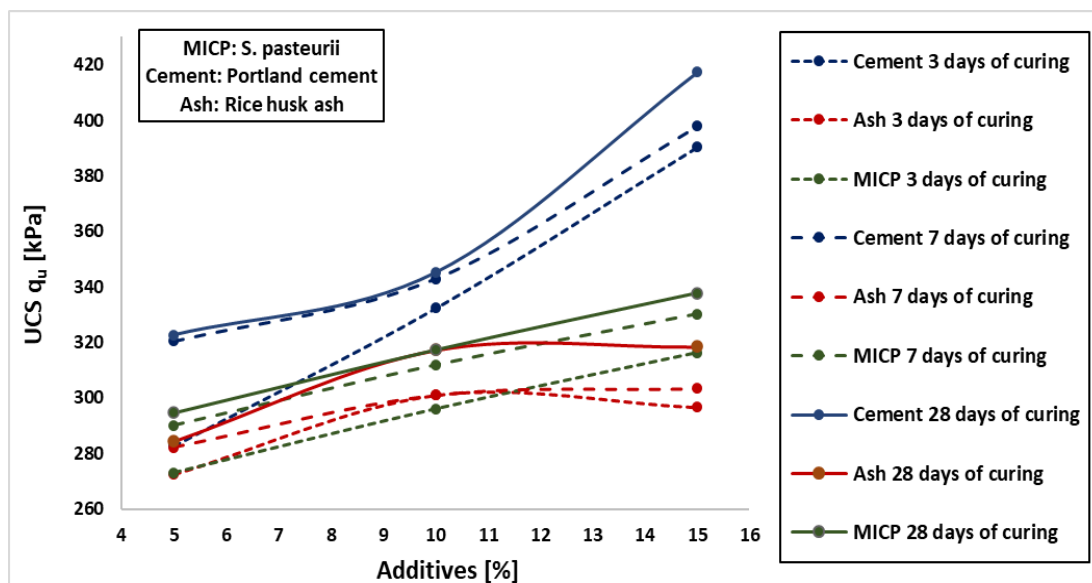
In their work, (Umar et al., 2019) further observed that the permeability of the MICP-treated soil and soil treated with both lime and MICP, is rapidly reduced within the first day, where the MICP-treated soil remain at that level of hydraulic conductivity, whereas soil treated with both lime and MICP, stabilizes at a lower level. The sample treated with lime increases its hydraulic conductivity for the first 7 days, where it then starts to decline and stabilizes at about the same level

as sample treated with both lime and MICP. The results are presented in the plot below.



Figur 107. Show hydraulic conductivity as a function of curing time for samples treated with lime and samples treated with MICP. Data adapted from (Umar et al., 2019)

(Oyediran and Ayeni, 2020) compared the use of Portland cement (OPC), Ash (RHA) and MICP in highly plastic weathered soil consisting of 55,8% fines, 35,9 % sand and 8,3% gravel. The results show increased UCS with increasing curing time for all samples. However, the results show higher UCS for samples treated with cement compared to samples treated with MICP and ash. The rate of increase in UCS, is similar for samples treated with cement and samples treated with MICP in the range 5-10% in additives, whereas the rate of increase is significantly higher for samples treated with cement when percentage additives, is increased from 10 to 15%. The results are presented in the plot below.



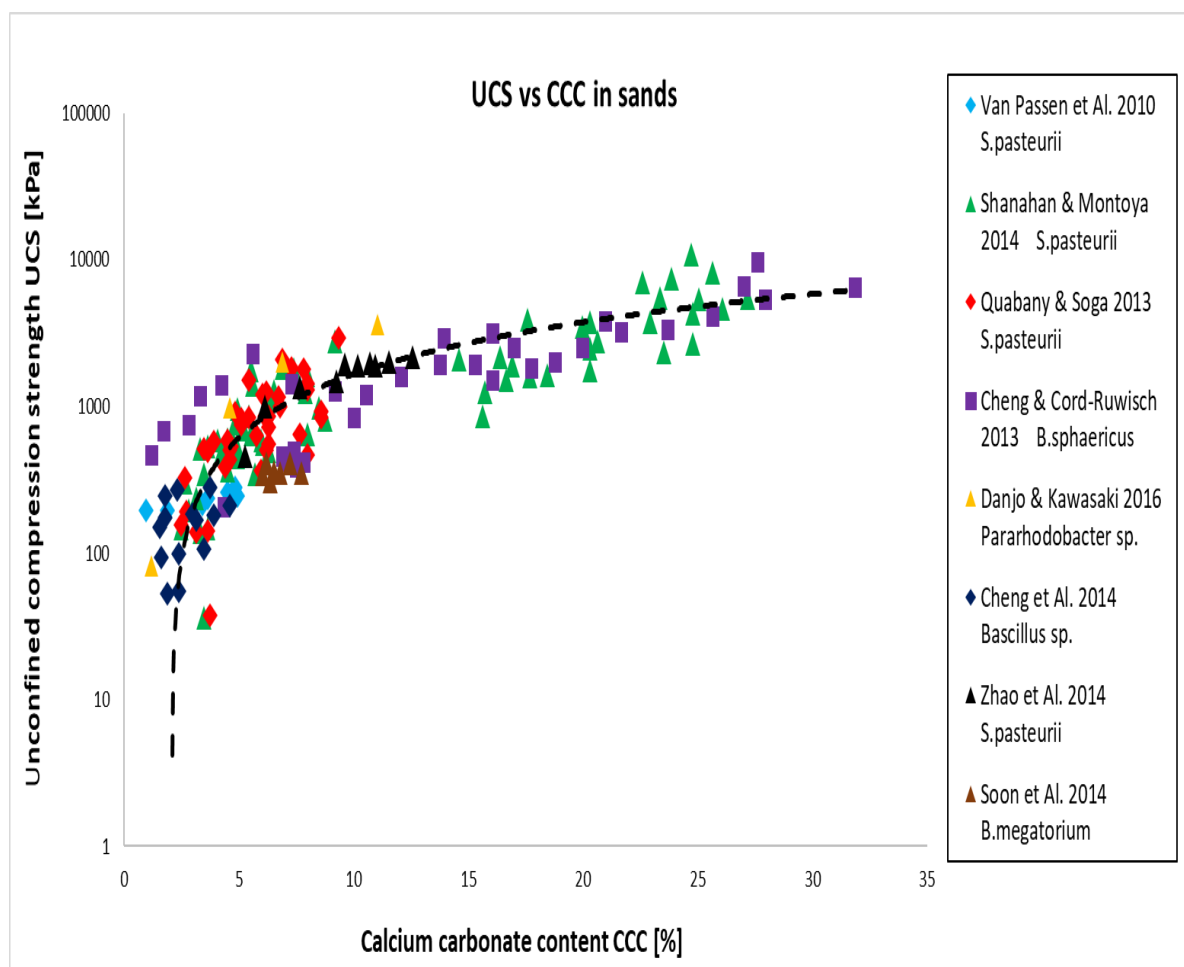
Figur 108. Show comparison of achieved UCS between treatment with MICP, ash and cement in soil as a function of percentage additives for different curing times. Data adapted from (Oyediran and Ayeni, 2020)

4. Improvement of engineering properties

4.1 Granular soils

4.1.1 Unconfined compression strength

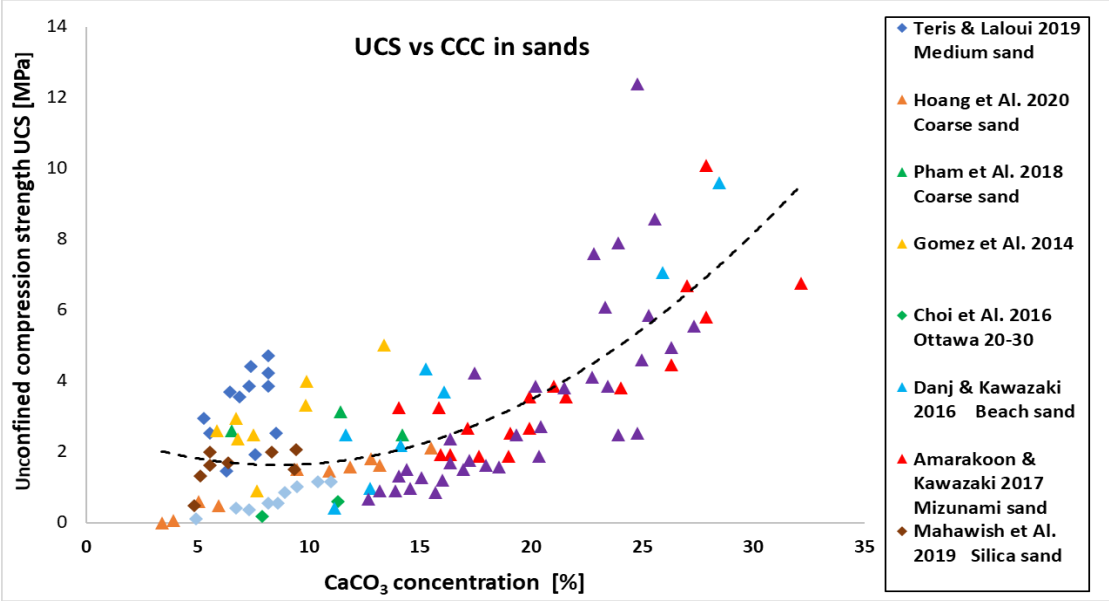
Through a review of several studies on MICP in sands, (Choi et al., 2020a) found a positive correlation between calcium carbonate concentration (CCC) and UCS noted in kiloPascal as [kPa]. Some studies reported higher effect on UCS from lower urease activity and others from higher urease activity. The compiled results for UCS as a function of CCC in MICP-treated sands with different ureolytic bacteria, are presented below.



Figur 109. Show achieved UCS as a function of CCC in sands, compiled from different studies. Data adapted from (Choi et al., 2020a).

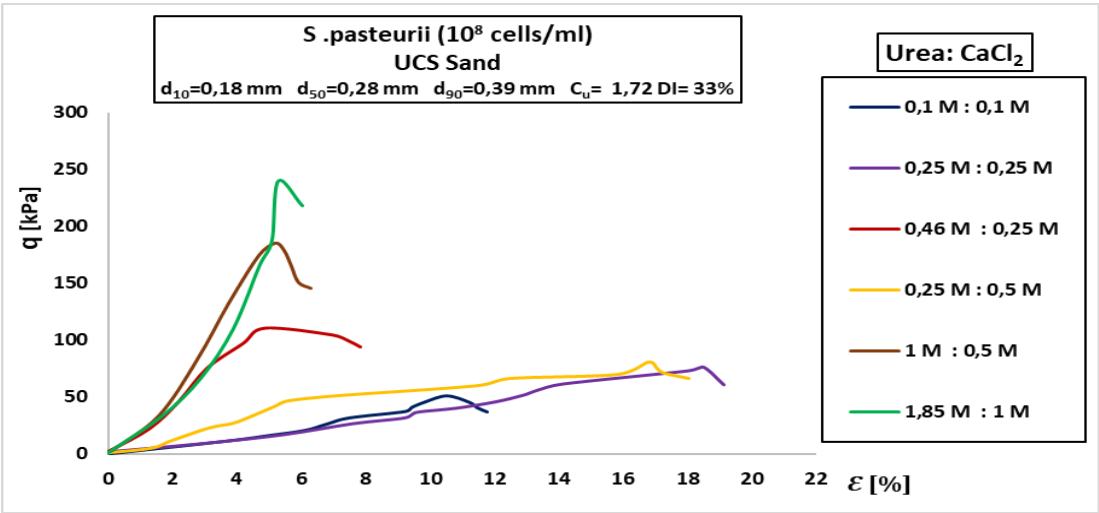
Through a review of several studies on MICP in sands, (Rahman et al., 2020a) found that measured UCS for MICP-treated samples ranges from 0.03 to 14.5 MPa with CCC in the range 0.6 to 32.0%. The UCS is found to increase exponentially with increasing CCC. However, high variability in this trend is observed

at CCC less than 5%. The compiled results for UCS as a function of CCC in MICP-treated sands with different ureolytic bacteria, are presented below.



Figur 110. Show acheived UCS as a function of CCC in sands, compiled from different studies. Data adapted from (Rahman et al., 2020a).

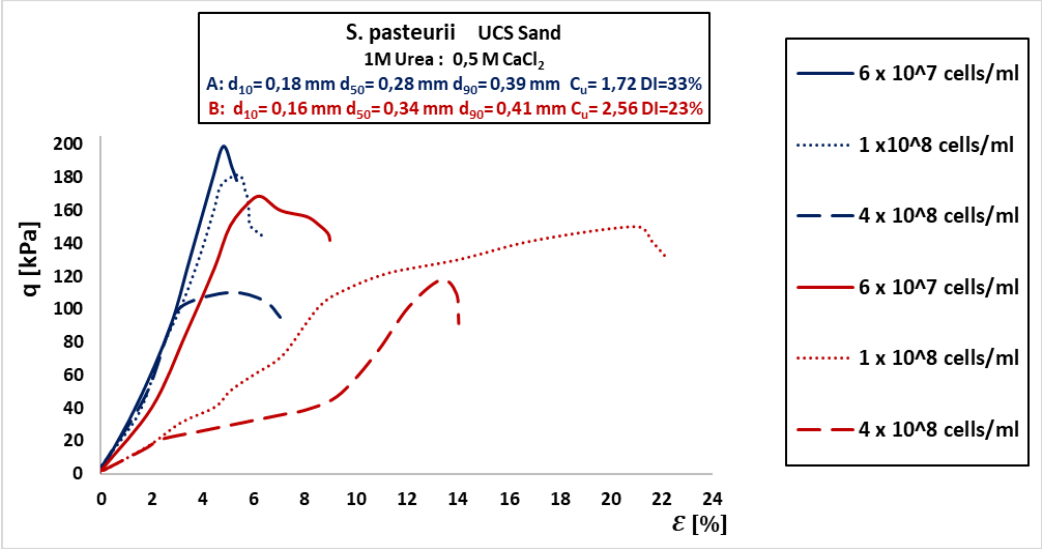
Work by (Shahrokhi-Shahraki et al., 2015) investigated the effect of cementation solution (Urea/CaCl₂) on UCS in MICP-treated medium sand, using *S. pasteurii*. The results show an increase in brittleness and peak and critical shear strength with increased concentrations, where increased share of urea had greater impact than share of CaCl₂. The results are presented in the plot below.



Figur 111. Shows acheived UCS in MICP-treated medium sand for different concentrations of cementation solutions. Data adapted from (Shahrokhi-Shahraki et al., 2015).

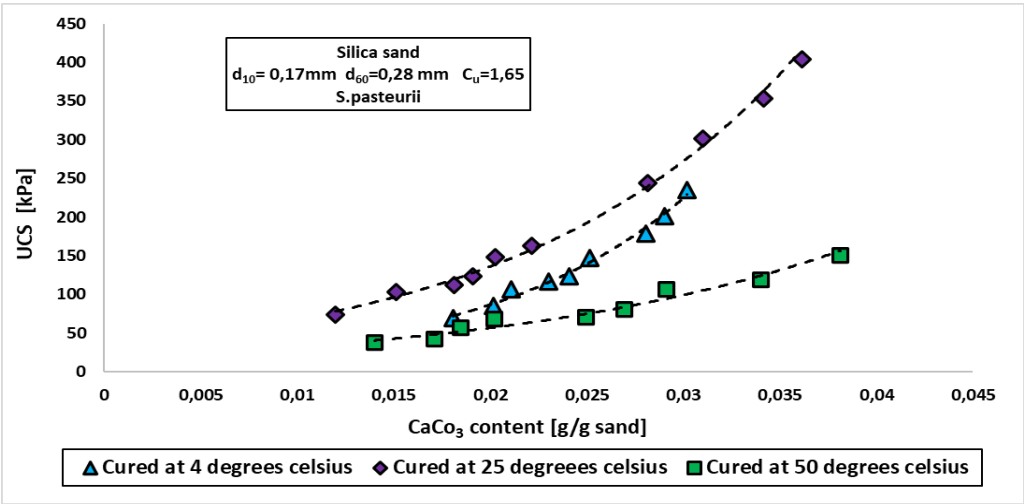
(Shahrokhi-Shahraki et al., 2015) further investigated the effect of bacterial concentration (cells/ml) on the shear strength in MICP-treated medium sands, using *S. pasteurii*. The results show that for same concentration of cementation

solution (urea/CaCl₂), increased bacterial concentration resulted in decreased shear strength and brittleness, where the moderately finer and more uniform sand (A), consistently achieved higher peak shear strength. The results are presented in the plot below.



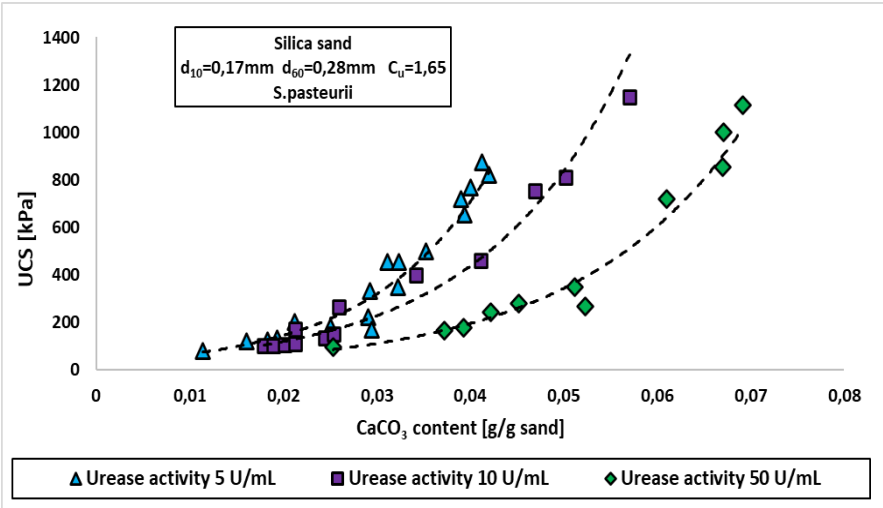
Figur 112. Show achieved UCS in two MICP-treated medium sands with different bacterial concentrations, with *S. pasteurii*. Data adapted from (Shahrokhi-Shahraki et al., 2015)

Work by (Cheng et al., 2016), found that UCS in MICP-treated sand using *S. pasteurii* increased exponentially with increase in CaCO₃ content at 4°C and 25°C and a more moderate increase at 50°C. However, the improvement in UCS per amount of CaCO₃, was much higher at 25°C and 4°C compared to at 50°C, where the crystals were numerous but small, forming a sheet cover over the particles and not contributing to effective particle bonding. The results are presented in the plot below.



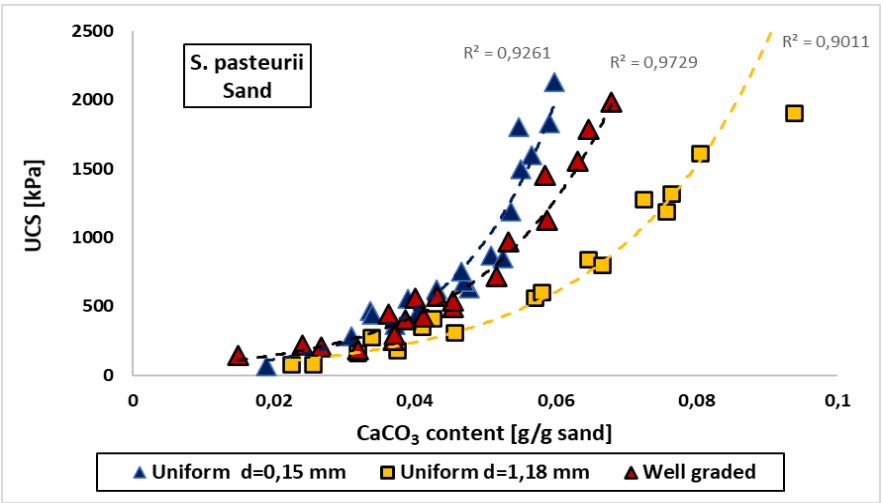
Figur 113. Show achieved UCS as a function of CaCO₃ content for different temperatures in MICP-treated sand. Data adapted from (Cheng et al., 2016).

The work by (Cheng et al., 2016) further showed an exponential increase in UCS in MICP-treated sand with increasing amount of precipitated CaCO_3 , for all measured urease activities. The achieved UCS per amount CaCO_3 was greater for the lowest urease activity (5 U/mL), suggesting that precipitation which generate more effective bonding, occur at lower levels of urease activity. The results are presented in the plot below.



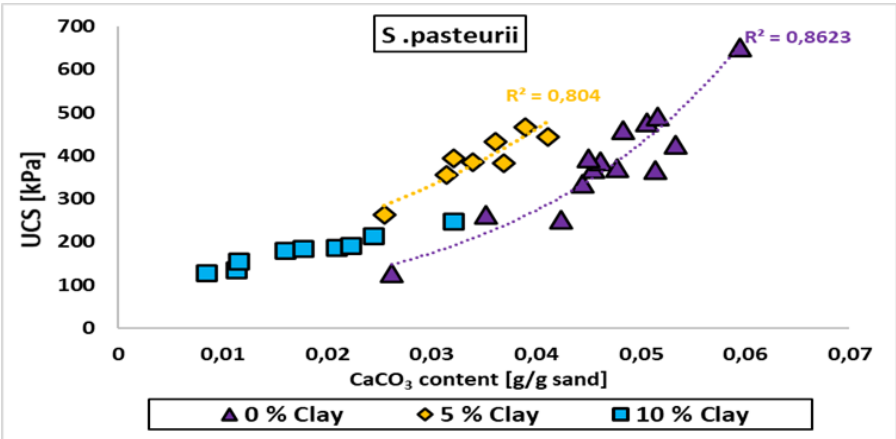
Figur 114. Show acheived UCS as a function of CaCO_3 content for different levels of urease activity. Data adapted from (Cheng et al., 2016).

In their work, (Cheng et al., 2016) further found an exponential increase in UCS with increasing amount of precipitated CaCO_3 for uniform fine, uniform medium and well graded MICP-treated sand. However, significantly lower UCS per amount of CaCO_3 for the coarser uniform sand than the fine uniform sand, was observed. The well graded sand displayed similar effectiveness of cementation as the fine uniform sand. The results are presented in the plot below.



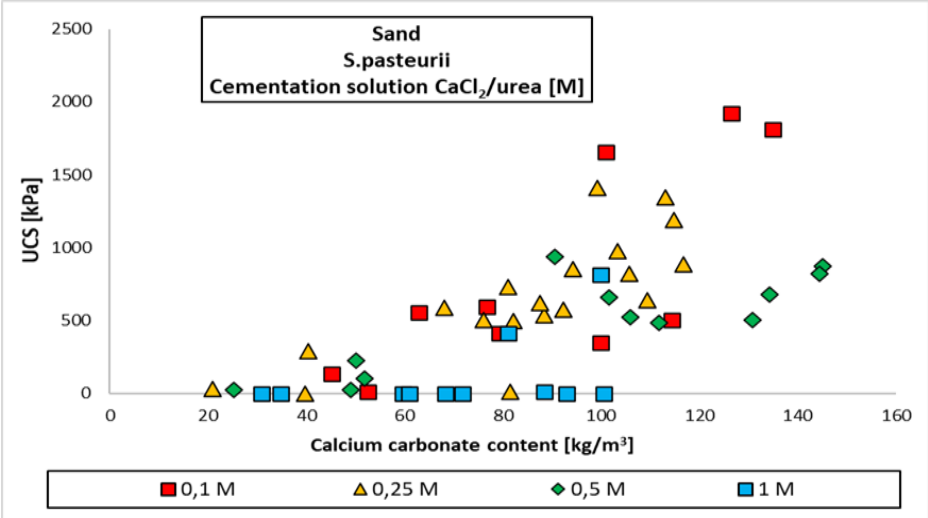
Figur 115. Show acheived UCS as a function of CaCO_3 content for differently graded MICP-treated sands. Data adapted from (Cheng et al., 2016)

Work by (Cheng and Shahin, 2015), used manually mixing in MICP treatment of sand and clayey sand (5%, 10% clay), where bacterial (*S.pasteurii*) solution was manually mixed into sample, followed by low (100 kPa) pressure injection of cementation solution. The results show a decrease in UCS with increasing share of clay and increased UCS with increasing CaCO_3 content in sample. The results are presented in the plot below.



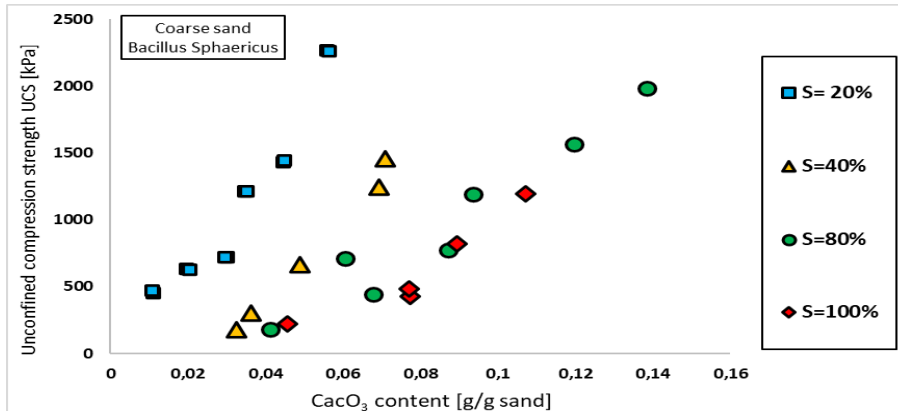
Figur 116. Show acheived UCS as a function of CaCO_3 content for MICP-treated sand with different share of clay. Data adapted from (Cheng and Shahin, 2015)

In their work, (QABANY and Soga, 2014) found that for MICP-treated sand using *S. pasteurii*, very low concentrations of CaCl_2 /urea acheived the highest UCS. Samples treated with 0.1 M, displayed highest degree of homogeneity and higher UCS than the samples treated with 0,25 M. Samples treated with 0,25 M acheived higher UCS than samples treated with 0,5 M and 1 M, where several of the samples treated with 1M solution, were highly inhomogenous with almost no compressive strength. The results are presented in the plot below.



Figur 117. Show acheived UCS in MICP-treated sand as a function of CaCO_3 content for different concentrations of cementation solution. Data adapted from (QABANY and Soga, 2014)

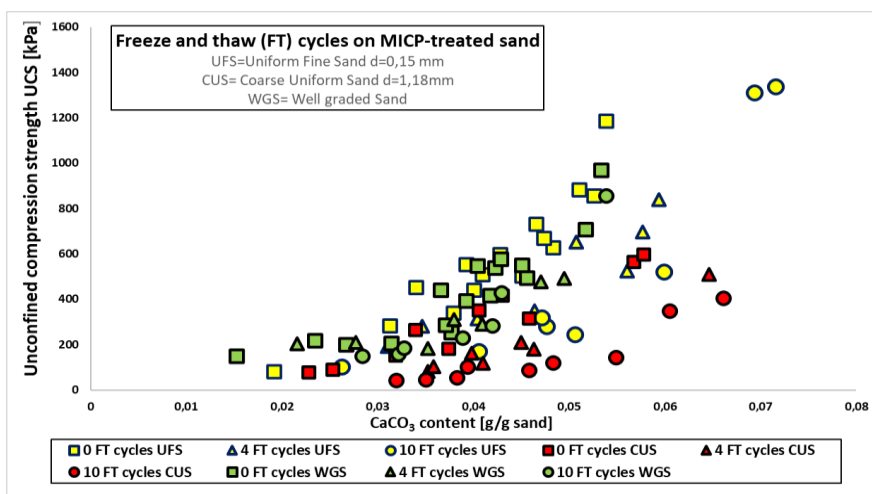
Work by (Cheng et al., 2013), investigated the achieved UCS in MICP-treated coarse sand with varying degree of saturation (S). The results show increasing UCS with increasing CaCO_3 content and for the same amount of CaCO_3 , UCS increase with reduced saturation. However, saturation above 80% was found to have little impact on UCS in the coarse sand. The results are presented in the plot below.



Figur 118. Show achieved UCS as a function of CaCO_3 content for varying degree of saturation in MICP-treated coarse sand. Data adapted from (Cheng et al., 2013)

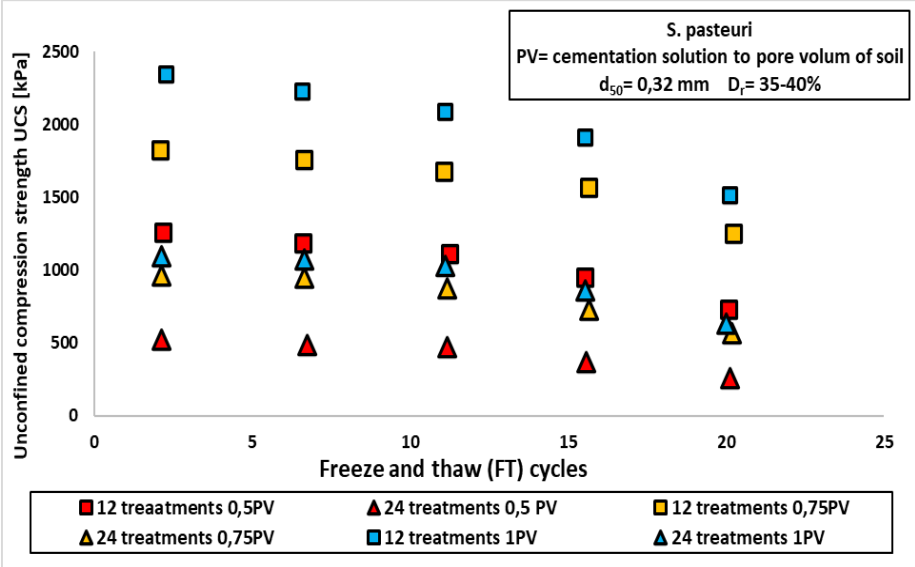
4.1.2 Durability under cyclic freeze and thaw

In work by (Cheng et al., 2016), the effect of grain size distribution on durability of MICP-treated sand under freeze and thaw (FT) cycles, was investigated. The results show that an increase in the number of FT cycles is associated with a decrease in UCS for both uniform fine and coarse sand, whereas FT cycles had a minor impact on the well graded sand. However, the fine uniform sand with lower porosity showed more durability, compared to the coarse sand with higher porosity.



Figur 119. Show UCS as a function of CaCO_3 content for MICP-treated uniform and well graded sands during FT cycles. Data adapted from (Cheng et al., 2016).

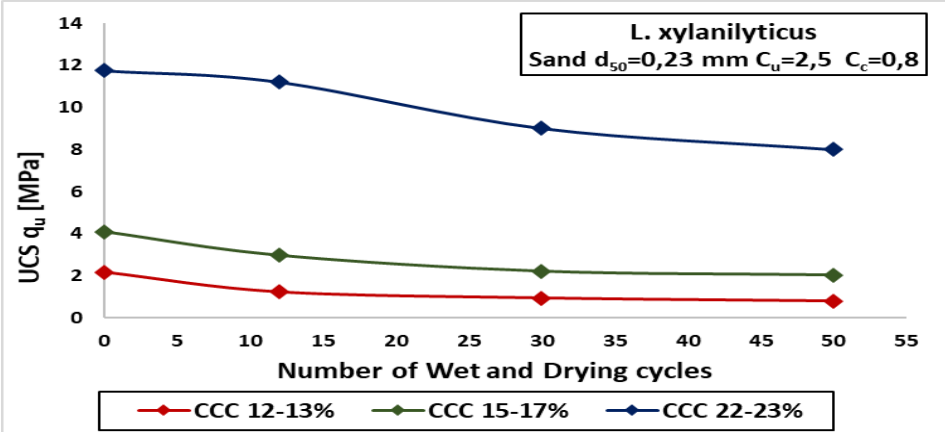
In their work, (Sharma et al., 2021) found decreasing UCS with increasing number of FT cycles, where the reduction in UCS was less than 5% and 10% after respectively 5 and 10 FT cycles in all samples. The results were valid, irrespective of amount of cementation solution per injection (treatment) and number of injections. The results are presented in the plot below.



Figur 120. Show UCS as a function of FT cycles with varying number of treatment cycles of cementation solution in MICP-treated sand. Data adapted from (Sharma et al., 2021)

4.1.3 Durability under wetting and drying cycles

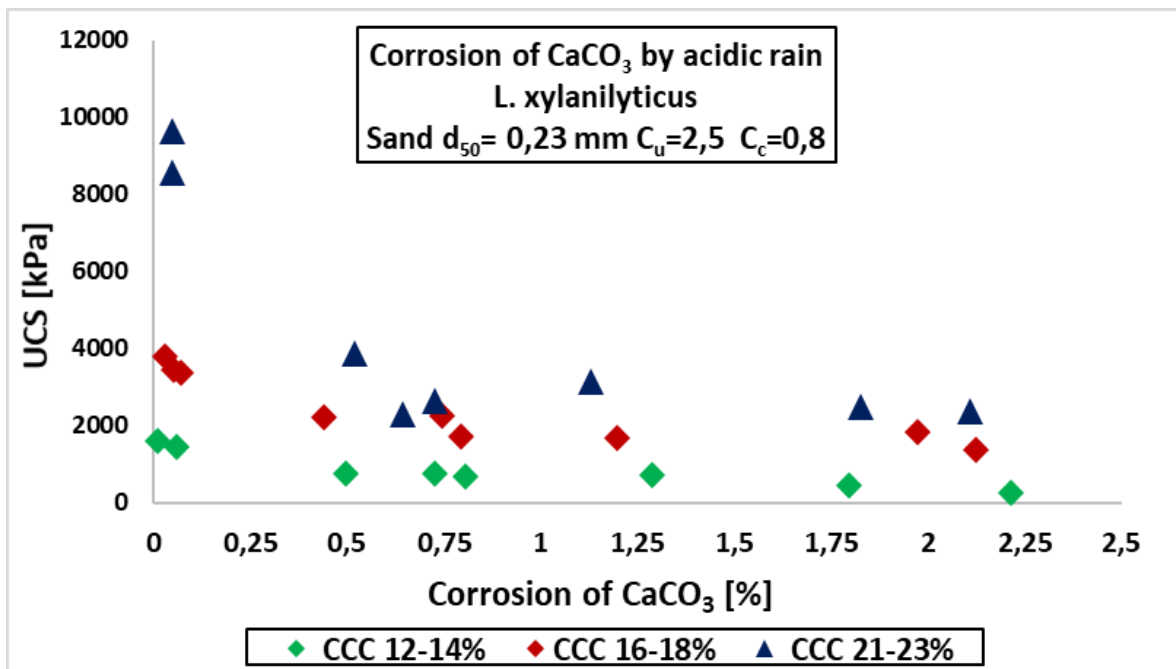
Precipitated CaCO₃ in the unsaturated zone of regions with frequent rainfall, will experience a high number of wetting and drying (WD) cycles. (Gowthaman et al., 2021) investigated the effect of up to 50 WD cycles on the UCS in MICP-treated poorly graded sand. The results show 63,33 % reduction in UCS for samples with 12-13% CCC, 50.43% reduction in UCS for samples with 15-17% CCC and 32% % reduction for samples with 22-23% CCC, in the course of 50 WD cycles.



Figur 121. Show reduction in UCS as a function of number of WD cycles for MICP-treated poorly graded sand with different CCC. Data adapted from (Gowthaman et al., 2021).

4.1.4 Durability under acidic rain exposure

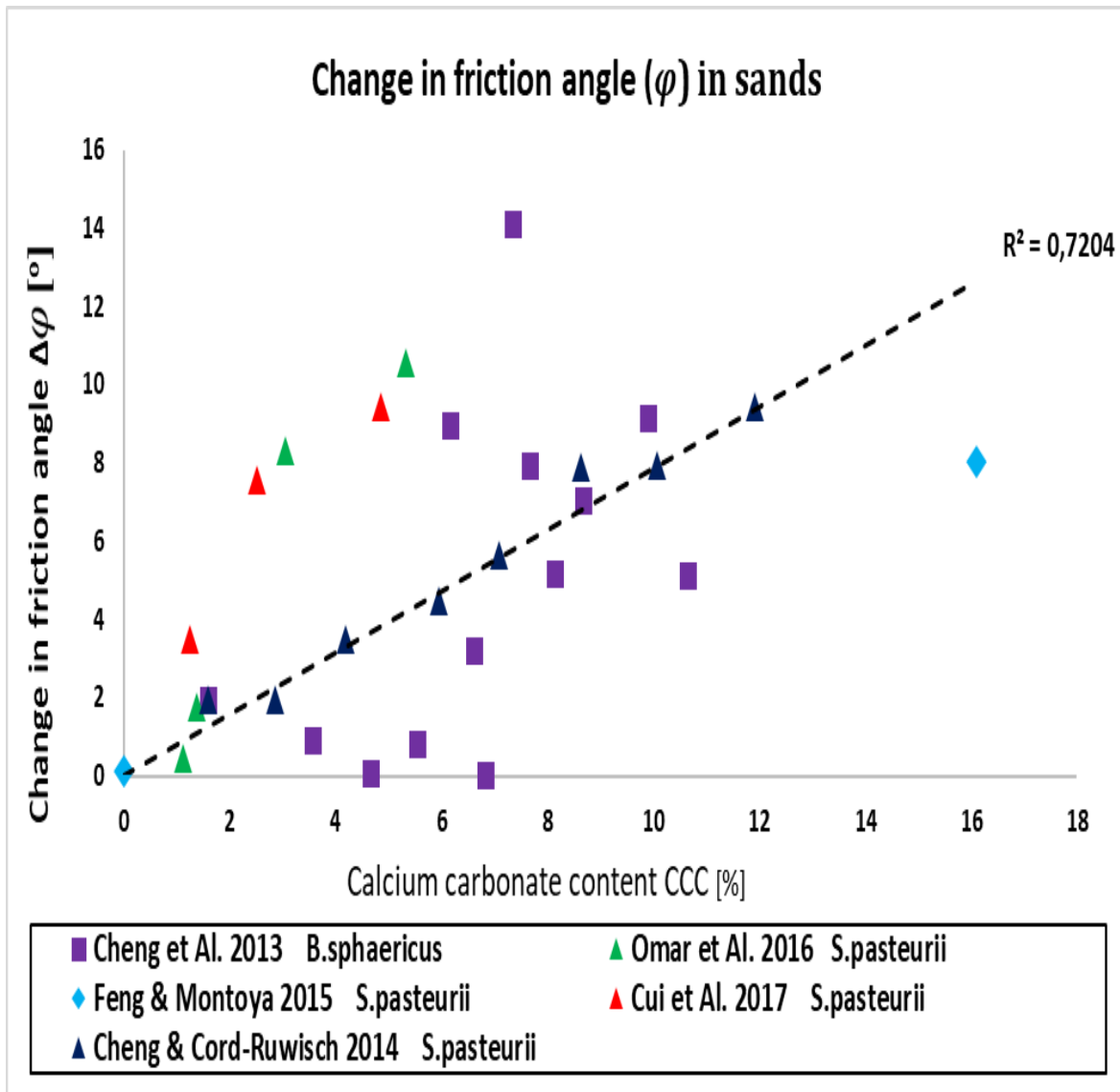
In their work, (Gowthaman et al., 2020) investigated the effect of acidic rain (AR) on the durability of precipitated CaCO_3 binder in MICP-treated poorly graded sand, by measuring the corrosion of CaCO_3 during exposure. They simulated acidic exposure by cyclic injections of solution made by adding nitric acid (HNO_3) and sulfuric acid (H_2SO_4) to deionized distilled water, where the pH level was adjusted. The results suggest that the corrosion rate of CaCO_3 depend on the intensity of the acidic rain and the level of pH. However, the loss of UCS due to corrosion of CaCO_3 was found to be governed by CCC, meaning that for same degree of corrosion, the higher the CCC the lower the loss of mass and UCS. The results are presented in the plot below.



Figur 122. Show UCS as a function of corrosion of CaCO_3 in MICP-treated sand with different CCC, due to acidic flushing. Data adapted from (Gowthaman et al., 2020).

4.1.5 Triaxial shear strength and volumetric response

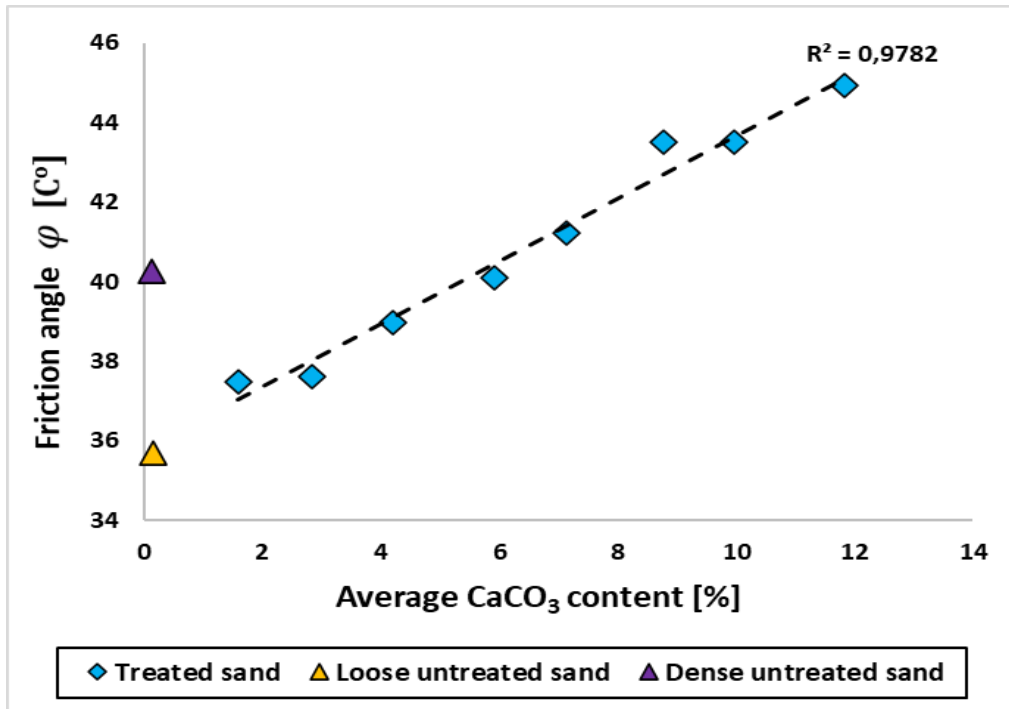
Through a review of several studies on MICP in sands, (Choi et al., 2020a) found that shear strength of cemented soils in general increase with increasing CCC, which is suggested to be an indication of an increase in the angle of internal friction, with increasing CCC. The plot presented below show change in friction angle (φ) from untreated to treated state as a function of CCC, compiled from different studies.



Figur 123. Show change in friction angle as a function of CCC in MICP-treated sands, compiled from different studies. Data adapted from (Choi et al., 2020a)

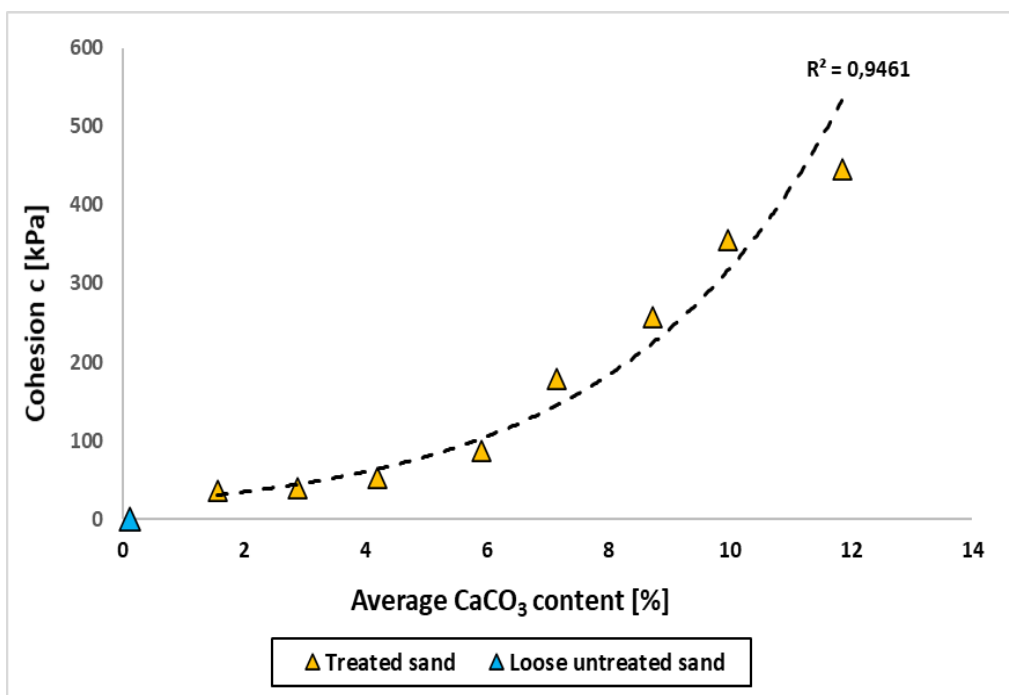
(Cui et al., 2017b) reported on an approximate linear relation between increased φ and increasing CCC in MICP-treated sand ($d = 0,5-1$ mm). However, similar φ measured in untreated dense sand and sand with CCC of 6%, indicate that deg-

ree of compaction before treatment could possibly affect the acheived strength post-treatment. Measured ϕ post-treatment are presented in the plot below.



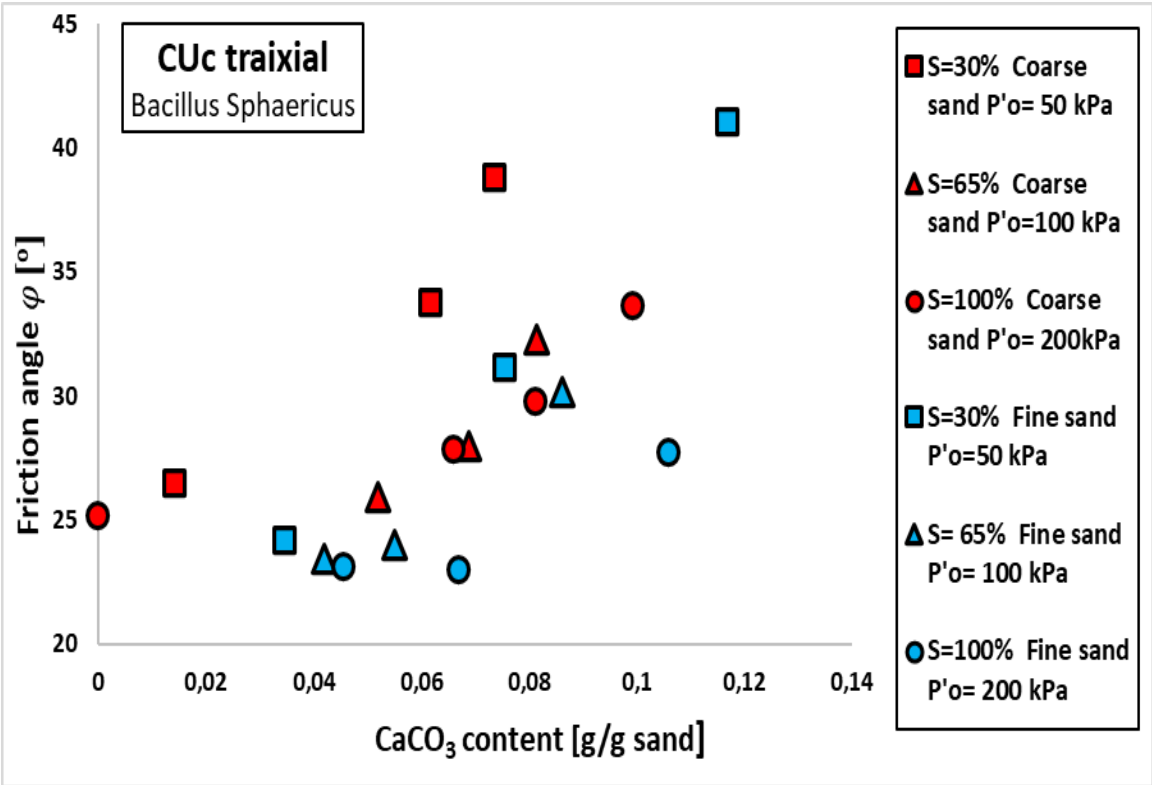
Figur 124. Show measured friction angle as a function of CCC in MICP-treated sand with different degree of compaction. Data adapted from (Cui et al., 2017a).

(Cui et al., 2017b) note that the increase in cohesion (c) showed an approximate exponential relation to increasing CCC. Measured c post-treatment is presented in the plot below.



Figur 125. Show measured cohesion as a function of CCC in MICP-treated sand with different degree of compaction. Data adapted from (Cui et al., 2017a).

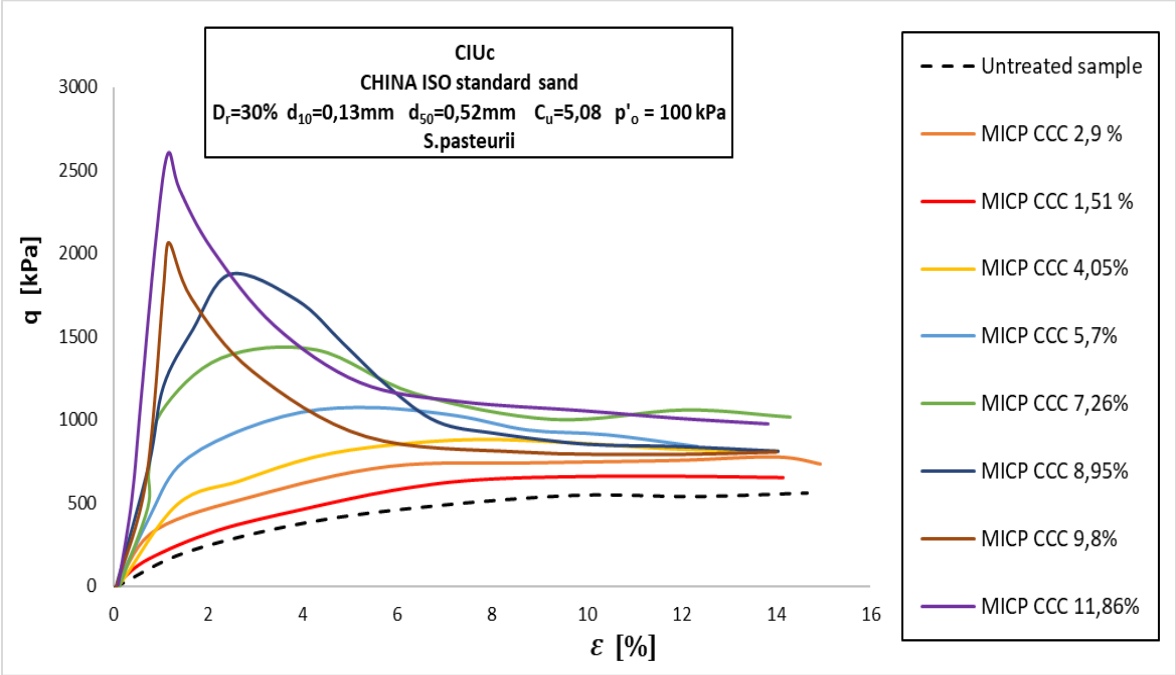
Work by (Cheng et al., 2013) investigated change in friction angle and cohesion for MICP-treated (*Bacillus Sphaericus*) fine and coarse sand with varying degree of saturation (S). The results show that both c and φ increase with increasing CCC at all degrees of saturation, for both fine and coarse sand. However, under the same saturation condition, the coarse sand achieve a higher φ , compared to the fine sand at similar CCC. The fine sand at similar CCC showed significantly higher values of c than the coarse sand. This is assumed to be due to a higher number of particle contacts in the fine sand. Further, it was found that samples with lower degree of saturation achieved higher shear strength than those with higher degree of saturation. The results for achieved friction angle post-treatment are presented in the plot below.



Figur 126. Show change in friction angle as a function of CaCO₃ content in MICP-treated sands with varying grading and degree of saturation. Data adapted from (Cheng et al., 2013).

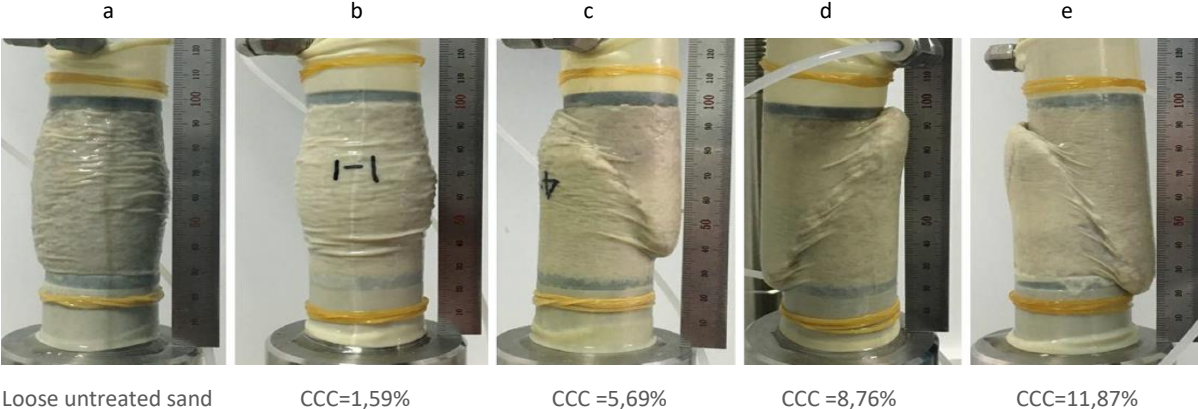
In a review on MICP, (Rahman, et al., 2020) note that the behaviour of MICP-treated soils, generally is affected by the initial relative density (D_r), initial confinement pressure (p'_o) and CCC. The study by (Cui et al., 2017b), conducted undrained triaxial tests (CIUc) on MICP-treated sand with the same initial D_r and P'_o for all tests, seeking to isolate the significance of CCC. The results show that the brittleness at low strains increases with increasing CCC for $CCC > 3\%$ and

that peak as well as critical shear strength increases with increasing CCC. The plot presented below show results for undrained shear strength post-treatment.



Figur 127. Show undrained shear strength for MICP-treated sand with different CCC. Data adapted from (Cui et al., 2017a).

(Montoya and DeJong, 2015) suggested that there is a transition from barreling failure at low cementation, towards a more defined shear zone in material with increasing CCC. (Cui et al., 2017a) found that for samples at same p'_o (100 kPa), a barreling failure mode was observed for samples with low (b) or no (a) CCC. They suggest that this could indicate that a low degree of cementation, do not alter the failure behaviour. It is further observed that in samples with a higher degree of cementation (c-e), an increasingly more distinct and defined shear plane develop with increasing CCC, as can be seen in the images presented below.

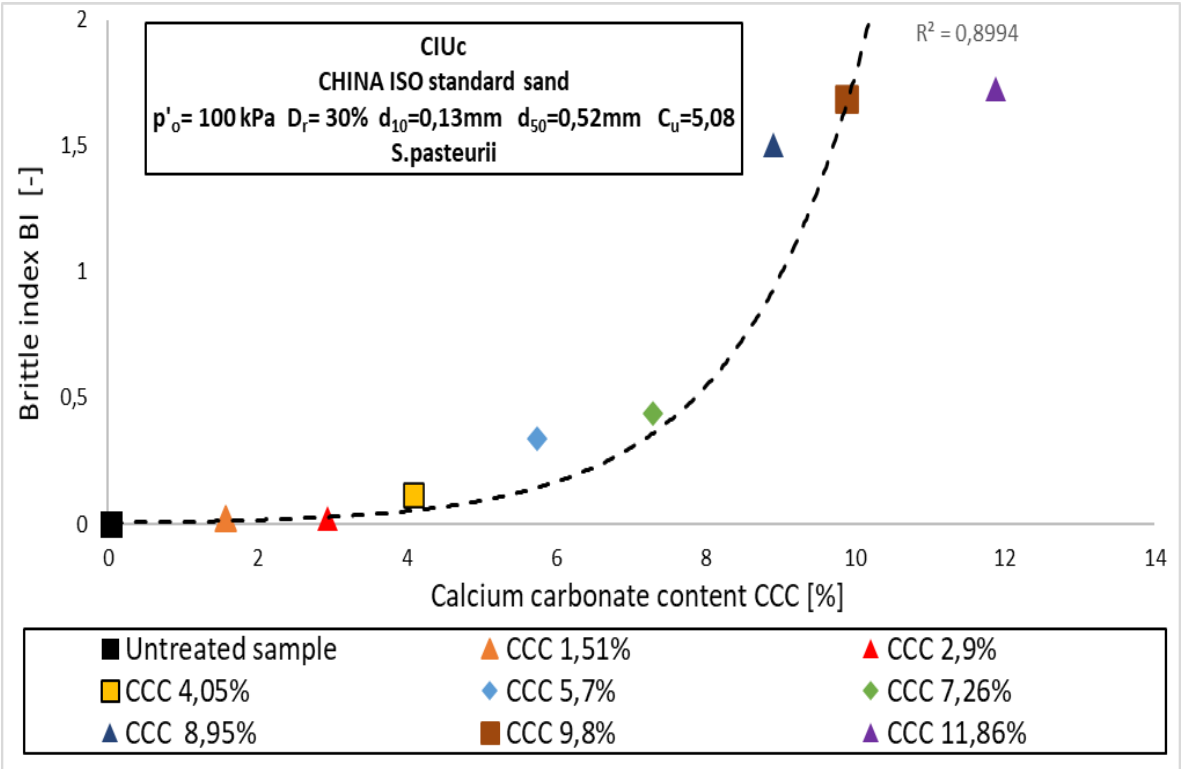


Figur 128. Show undrained failure modes under triaxial shear in MICP-treated sand with different CCC. Image from (Cui et al., 2017a)

The brittle stress-strain response was further evaluated by (Cui et al., 2017a), using the brittleness index (BI) proposed by (Consoli et al., 1998). The BI can be expressed as:

$$BI = \frac{q_{peak}}{q_{res}} - 1 \tag{Eq. 4.1.5.1}$$

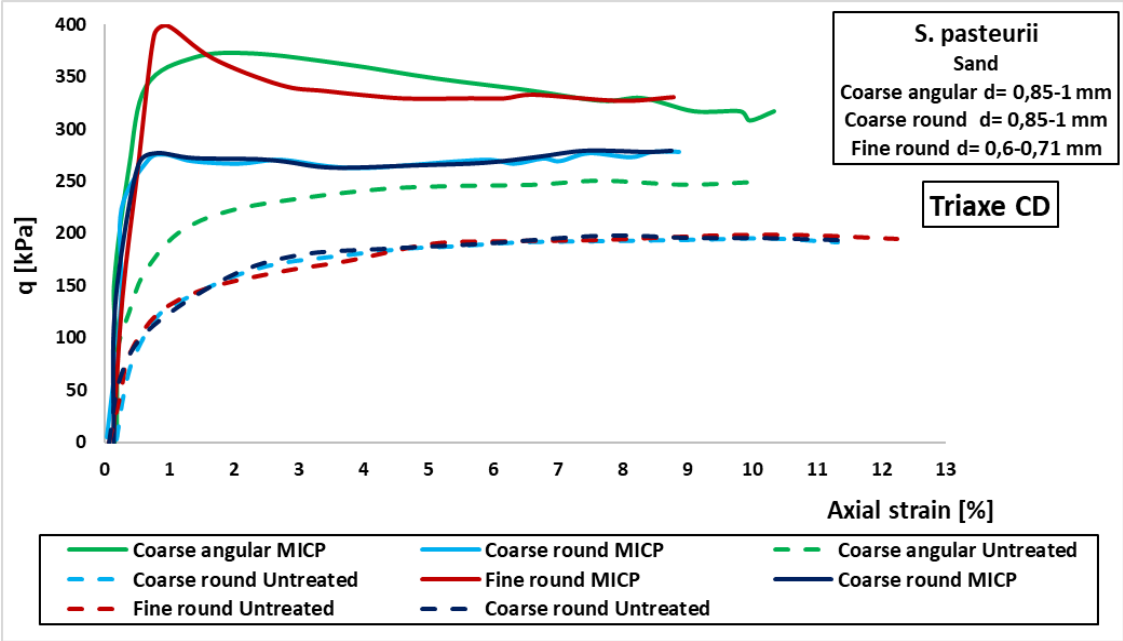
The BI-CCC plot presented below, show an approximate exponential increase in BI with increasing CCC.



Figur 129. Show brittleness index as a function of CCC in MICP-treated sand with different CCC. Data adapted from (Cui et al., 2017a).

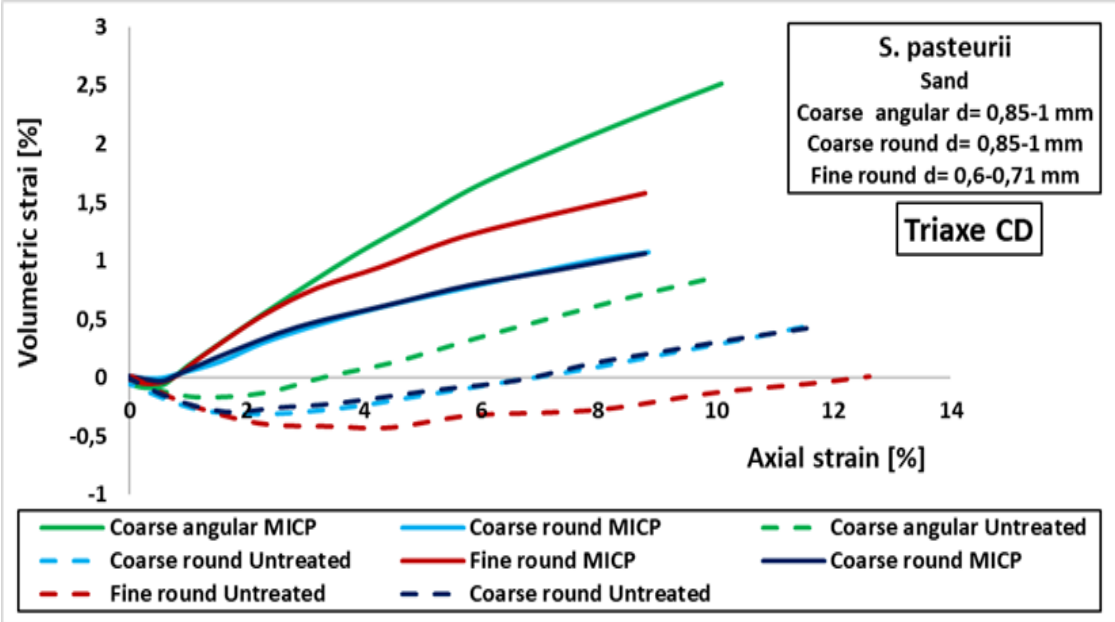
In a study by (Nafisi et al., 2018) a set of drained triaxial tests were conducted on MICP-treated (*S. pasteurii*) sands with same particle size but varying shape. The sands were characterized as particles of coarse angular, coarse round and fine round. The results show a higher increment in shear strength for the coarse angular ($\Delta q_{dev} = 50\%$), than in the coarse round ($\Delta q_{dev} = 35\%$) as well as more pronounced change in volumetric response post-treatment for the coarse angular than in the coarse round. However, the fine sand achieved the highest increment in peak shear strength and most pronounced change in volumetric response of the three. The MICP treatment increased the brittleness and dilatancy and reduced contraction at low strain in all samples, but induced a more pronounced

strain-softening at low strain for the fine round sand. This could suggest a higher degree of particle cementation in the fine sand. The results for drained shear strength are presented in the plot below.



Figur 130. Show drained shear strength and strain response for MICP-treated sand with different particle shape. Data adapted from (Nafisi et al., 2018)

The results for drained volumetric response are presented in the plot below.



Figur 131. Show drained volumetric response for MICP-treated sand with different particle shape. Data adapted from(Nafisi et al., 2018)

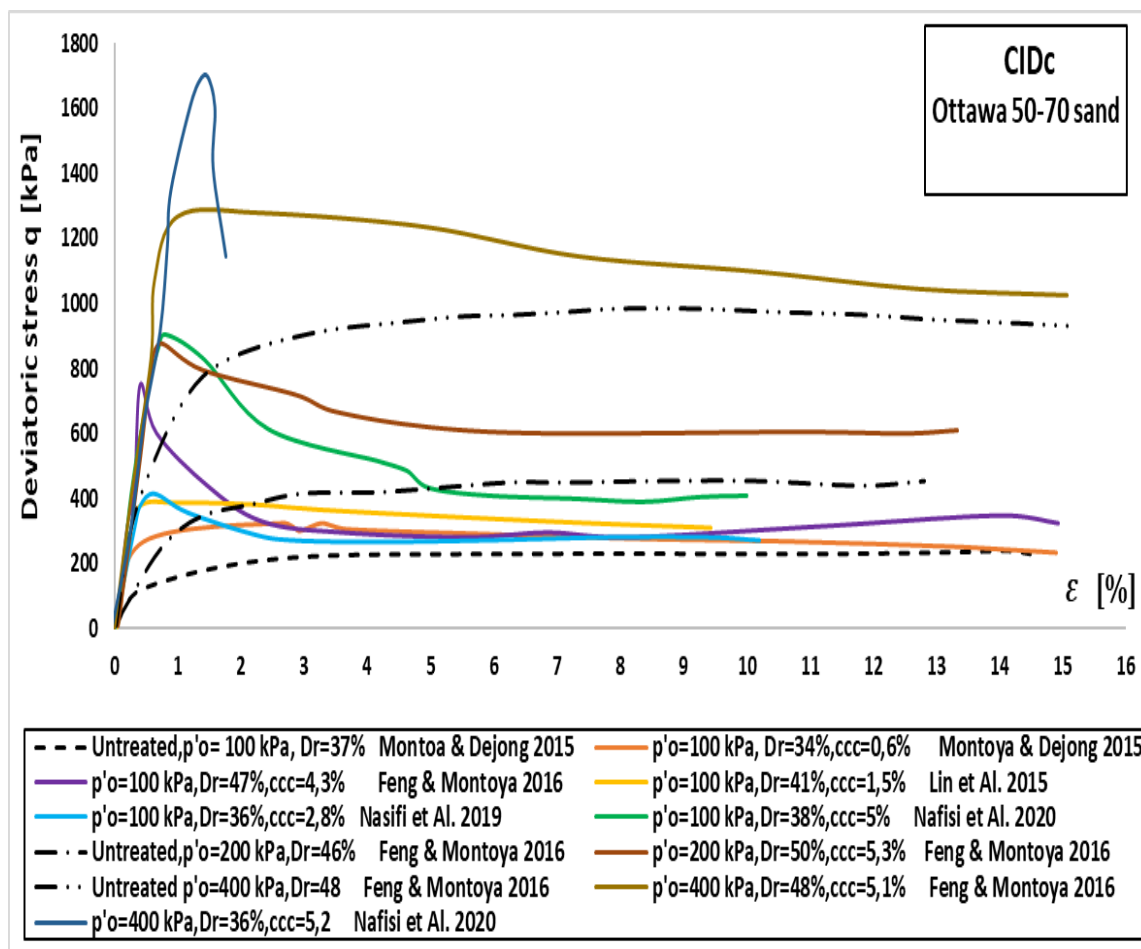
A selection of data from drained triaxial tests on MICP-treated sand compiled from the litterature, was compared by (Rahman et al., 2020a). Two distinct soil types Ottawa 50-70 and 20-30 sands were selected to eliminate the influence of

grain size in the comparison. The grain size distribution for the sands in the selected studies are listed in the table below.

Tabell 16. Lists gradation for the Ottawa sands. Data adapted from (Covicorp, 2020)

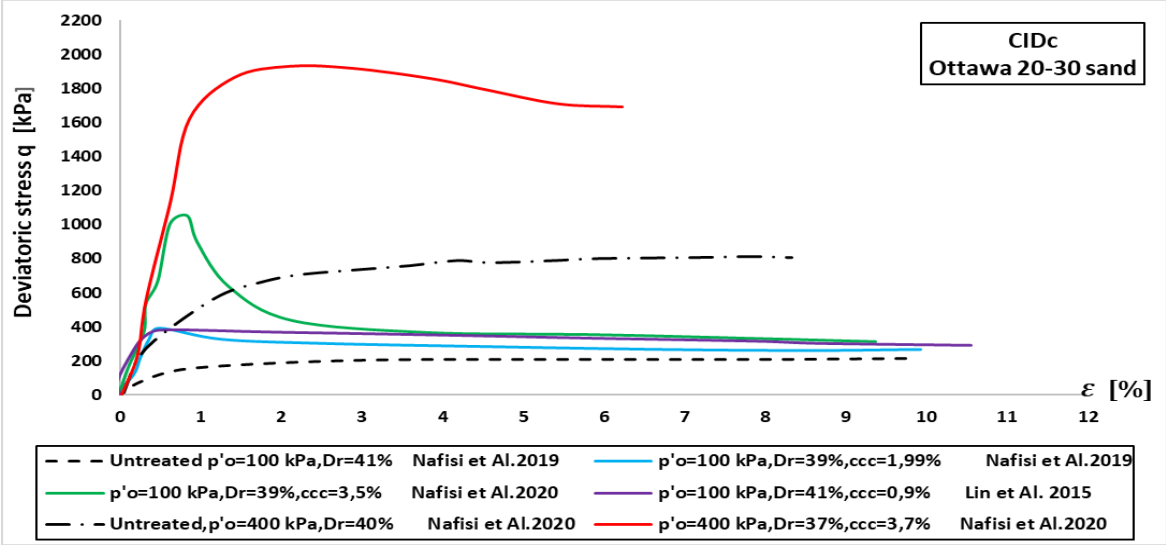
Grading	0,8 mm	0,71 mm	0,6 mm	0,5 mm	0,425 mm
20-30	0,6%	57,8%	39,5%	1,9%	0,1%
Grading	0,3 mm	0,25 mm	0,212 mm	0,15 mm	
50-70	1,1%	55,1%	40,6%	3,2%	

The 50-70 and 20-30 sands both show increasing peak shear strength and brittleness at low strains with increasing CCC, when comparison is made among samples with similar p'_o and D_r . The results showing drained shear strength and stress-strain response for Ottawa 50-70 sand are presented below.



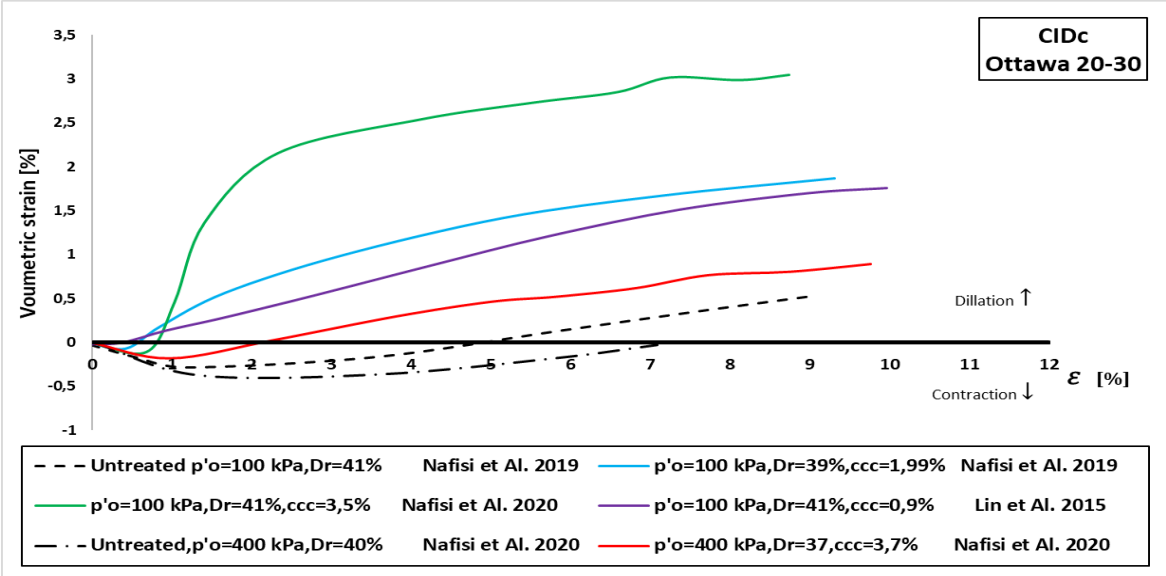
Figur 132. Show drained shear strength and strain response for MICP-treated 50-70 Ottawa sand at different confining pressure and CCC, compiled from different studies. Data adapted from (Rahman et al., 2020a).

The results showing drained shear strength and stress-strain response for Ottawa 20-30 sand, are presented below.



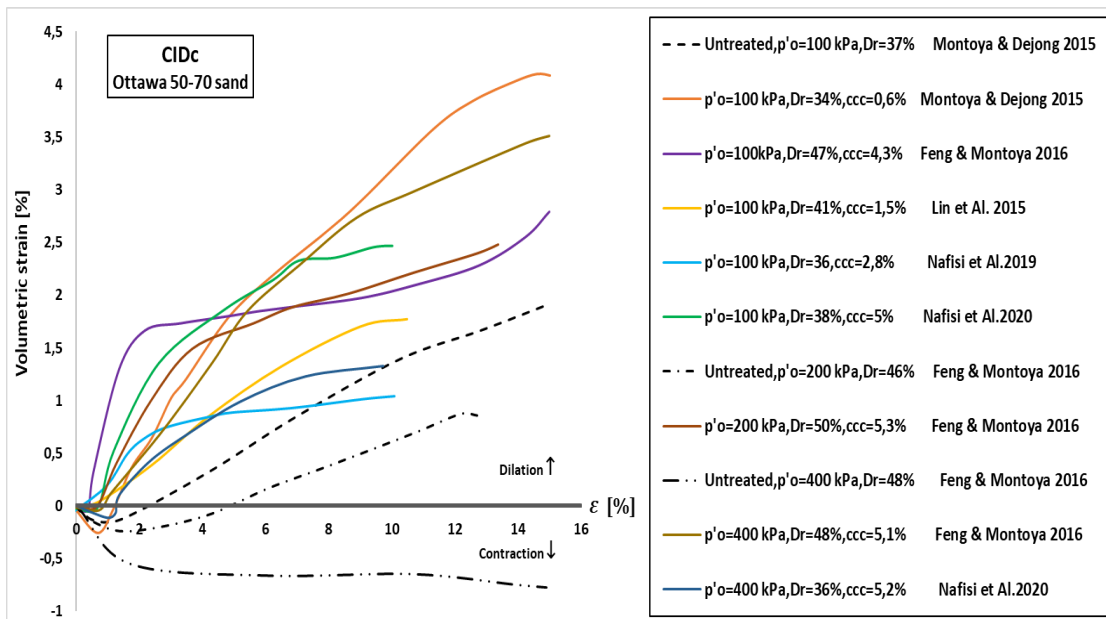
Figur 133. Show drained shear strength and strain response for MICP-treated 20-30 Ottawa sand at different confining pressure and CCC, compiled from different studies. Data adapted from (Rahman et al., 2020a).

For both the 50-70 and 20-30 sand, the volumetric strain response was found to be more dilative for treated samples compared to the untreated ones at similar p'_o . The treated samples display less contraction at small strains followed by an increase in dilation at larger strains, compared to the untreated samples. The results show an increase in dilityancy with increasing CCC. The drained volumetric response for Ottawa 20-30 sands, are presented below.



Figur 134. Show drained volumetric response for MICP-treated 20-30 Ottawa sand at different confining pressure and CCC, compiled from different studies. Data adapted from (Rahman et al., 2020a).

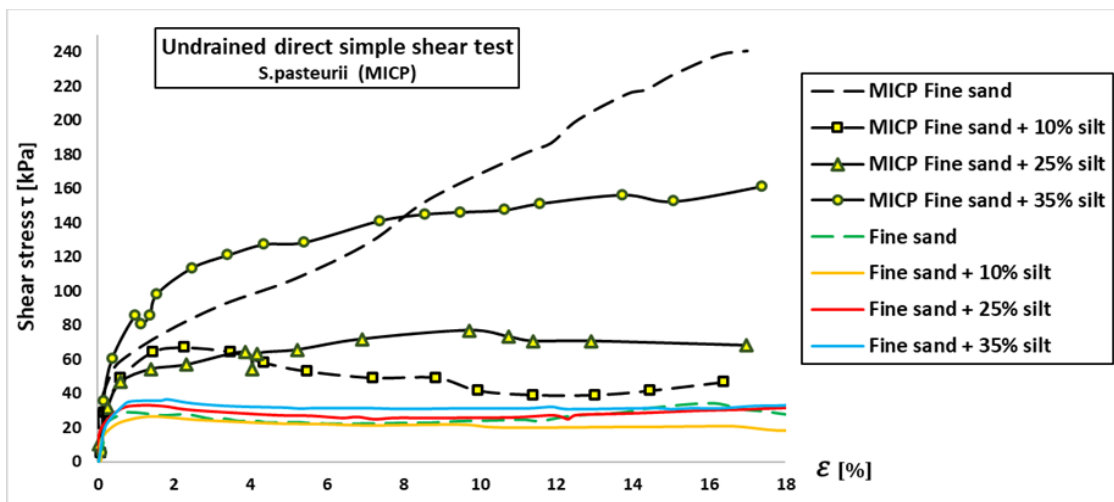
The drained volumetric response for Ottawa 50-70 sands are presented below.



Figur 135. Show drained volumetric response for MICP-treated 50-70 Ottawa sand at different confining pressure and CCC, compiled from different studies. Data adapted from (Rahman et al., 2020a).

4.1.6 Direct shear in silty sand

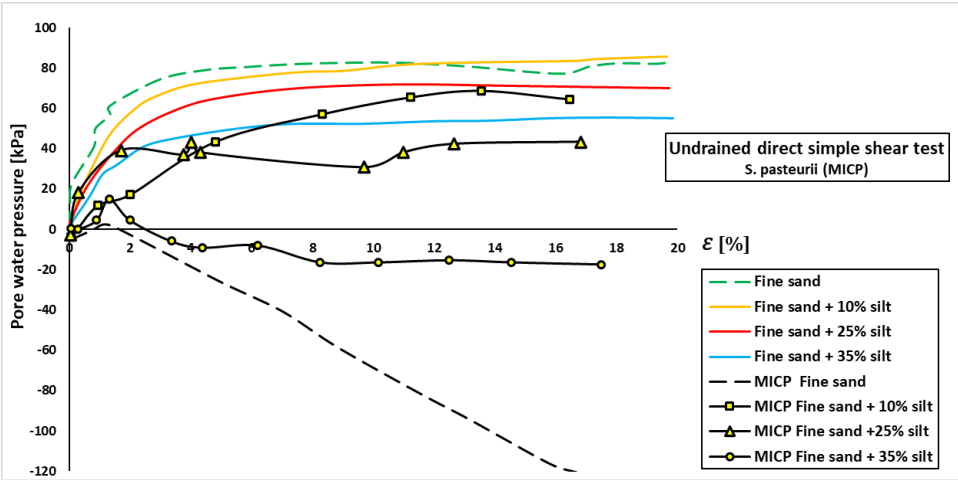
In work by (Zamani and Montoya, 2015), the effect of silt content (10, 25, 35%) in MICP-treated (*S. pasteurii*) fine sand was investigated in the context of increasing resistance to liquefaction. The results show increased shear strength with increasing share of silt under undrained direct shear. The results are presented in the plot below.



Figur 136. Show undrained shear strength and strain response in MICP-treated sand with different degree of silt content. Data adapted from (Zamani and Montoya, 2015)

The study by (Zamani and Montoya, 2015) found that excess pore pressure decreased with increasing share of silt under undrained shear in the MICP-

treated silty sand. The MICP-treated pure sand and MICP-treated sand with 35% silt, generated negative pore pressures. The results are presented in the plot below.

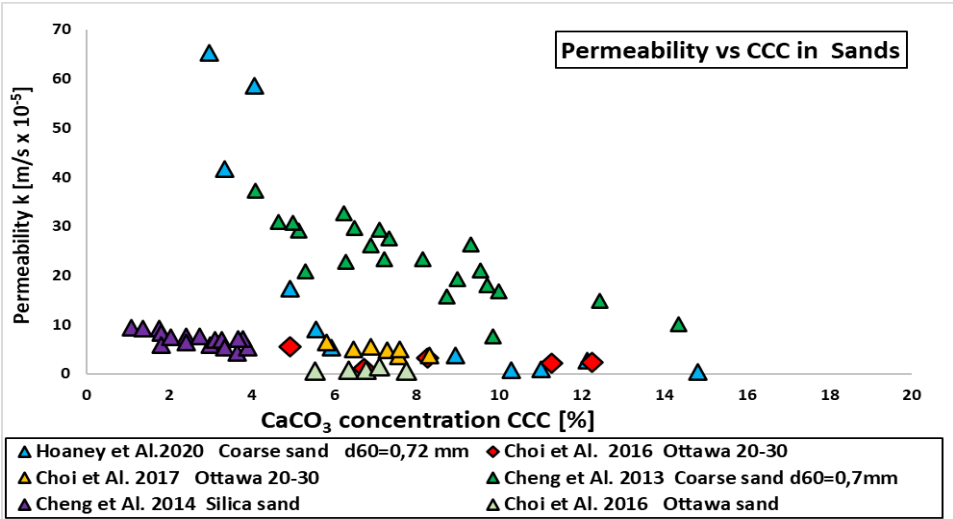


Figur 137. Show undrained porepressure response for MICP-treated sand with different degree of silt content. Data adapted from (Zamani and Montoya, 2015).

The study further showed that MICP-treated silty sand with silt contents up to 35% and tested to shear wave velocities ranging from 400–500 m/s, show improved resistance to liquefaction.

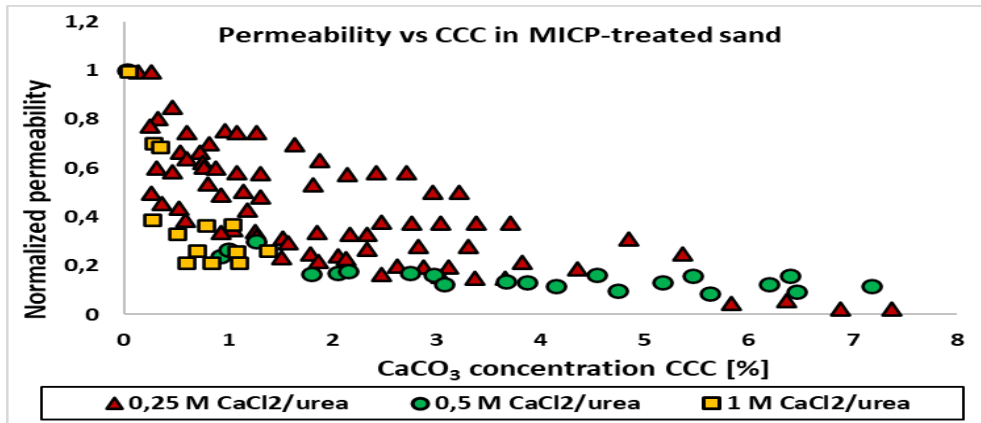
4.1.7 Reduction of permeability

Through a review of several studies on MICP in sands, (Rahman et al., 2020a) found that acheived permeability in MICP-treated soils ranged from 0.01×10^{-5} to 66×10^{-5} m/s with CCC ranging from 2-14.8%. The permeability in the MICP-treated sands, tends to decrease with higher increment in coarse sands compared to finer sand. The plot presented below show the results from the study.



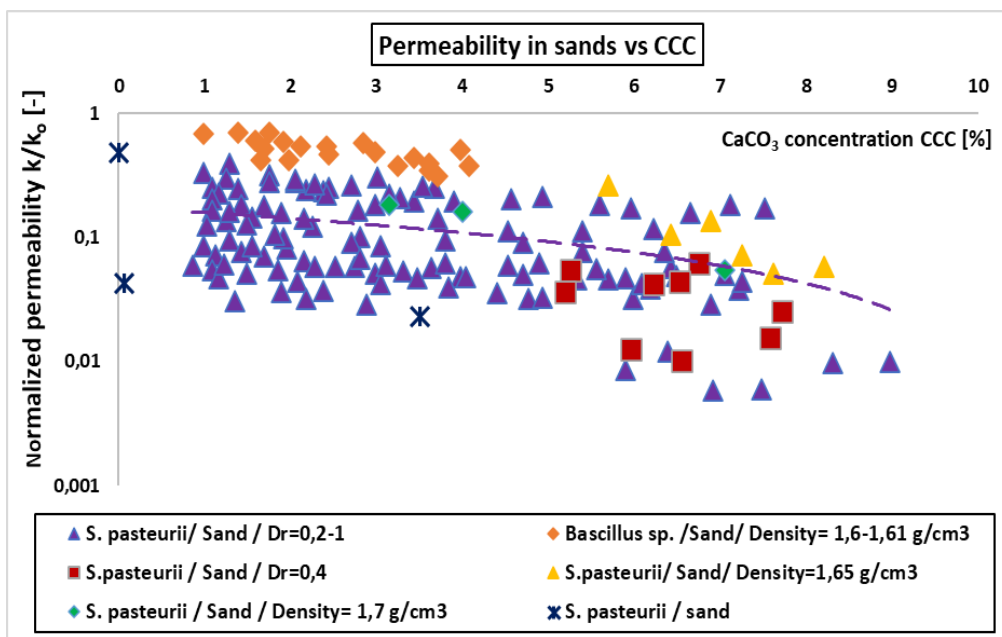
Figur 138. Show permeability post-treatment as a function of CCC in different MICP-treated sands. Data adapted from(Rahman et al., 2020b)

In their work, (QABANY and Soga, 2014) found that 1 M (mol/L) cementation solution ($\text{CaCl}_2/\text{urea}$) reduced permeability in MICP-treated sand with 30%, where the major part of the reduction was reached at initial precipitation of CaCO_3 , whereas low (0,25 M) concentration resulted in a slower decrease in permeability. The results are presented in the plot below.



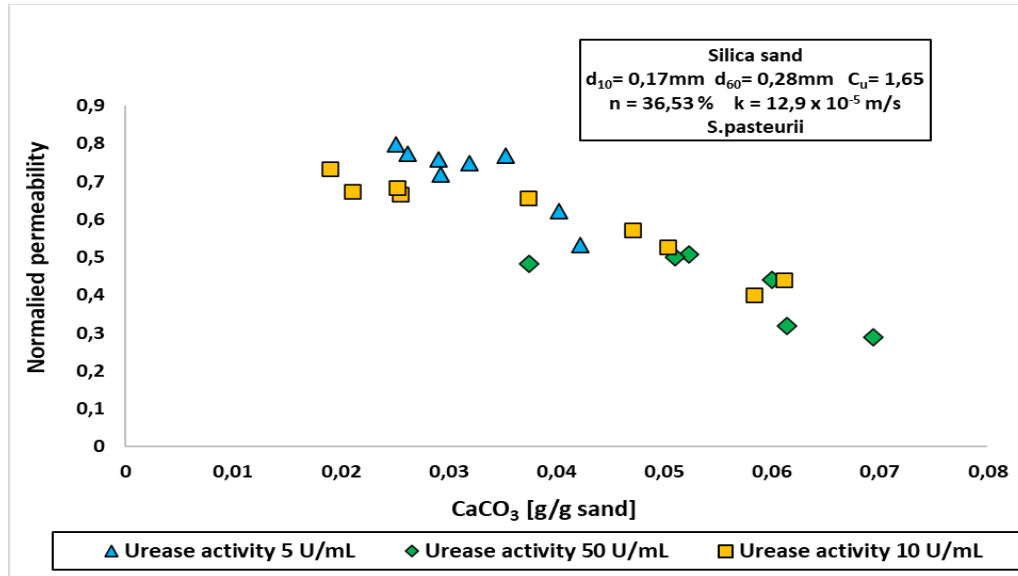
Figur 139. Show normalized permeability post-treatment as a function of CCC for different concentration of cementation solution ($\text{CaCl}_2/\text{urea}$) in MICP-treated sand. Data adapted from (QABANY and Soga, 2014).

In a review on several studies on MICP, (Choi et al., 2020a) found that the reduction of permeability in the MICP-treated sands was mainly governed by CCC, whereas the level of urease activity had a minor impact. They further found that CCC around 10 %, was needed to reduce the permeability by two orders of magnitude. The compiled results are presented below.



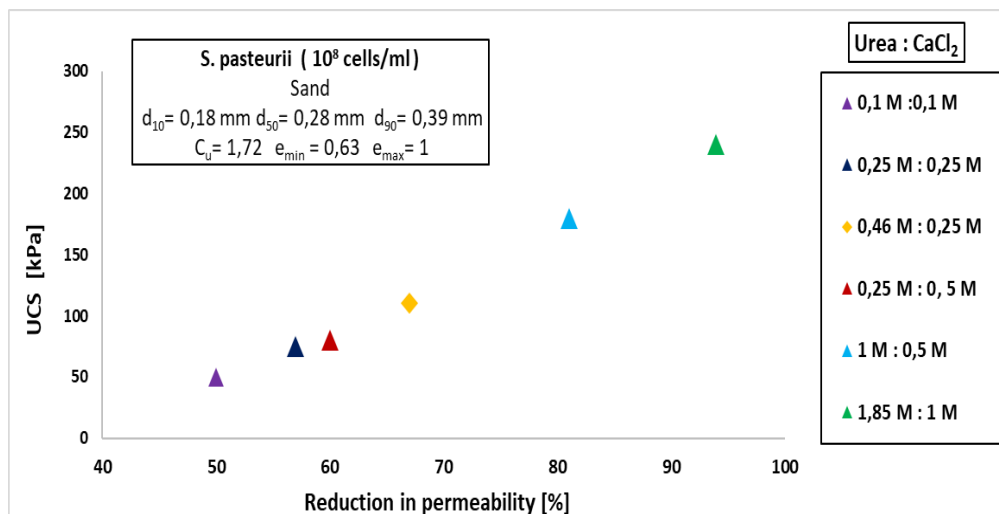
Figur 140. Show normalized permeability post-treatment as a function of CCC in MICP-treated sands with varying relative density. Data adapted from (Choi et al., 2020b)

Work by (Cheng et al., 2016), found increased reduction in permeability of MICP-treated sand with increasing amount of precipitated CaCO_3 , where the highest urease activity provided the largest decrease. The results are presented in the plot below.



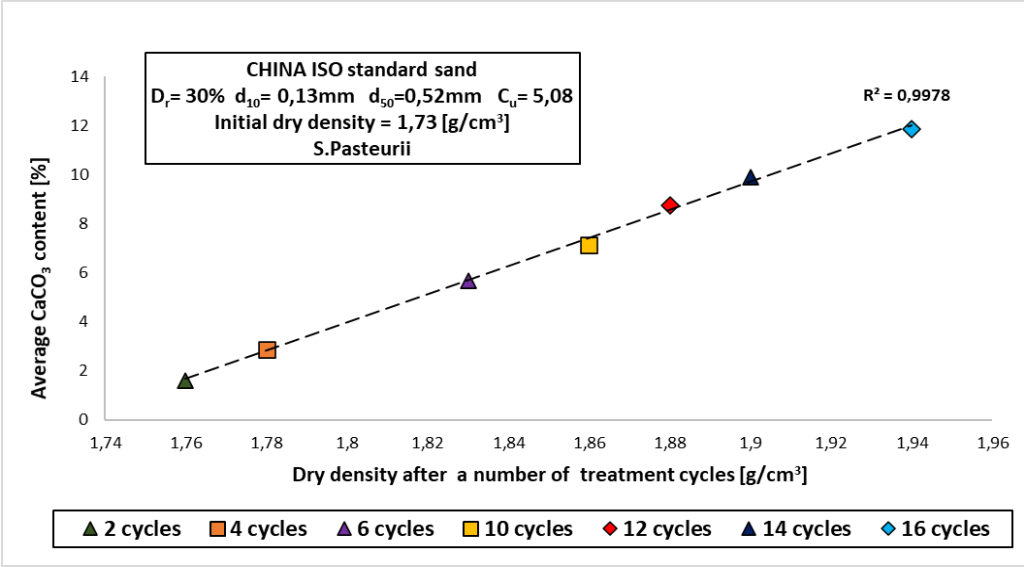
Figur 141. Show normalized permeability post-treatment as a function of CaCO_3 content for different levels of urease activity in MICP-treated sand. Data adapted from (Cheng et al., 2016)

Work by (Shahrokhi-Shahraki et al., 2015) investigated the reduction in permeability in MICP-treated medium sand. The results show that for most samples, increased concentrations [M] of Urea/ CaCl_2 , led to higher degree of reduction in permeability and increasing UCS. The permeability coefficient was reduced by less than one order of magnitude, so the drainage capacity of the MICP-treated sand was not significantly affected. The results further indicate that concentration of urea have a greater impact on the precipitation, than CaCl_2 .



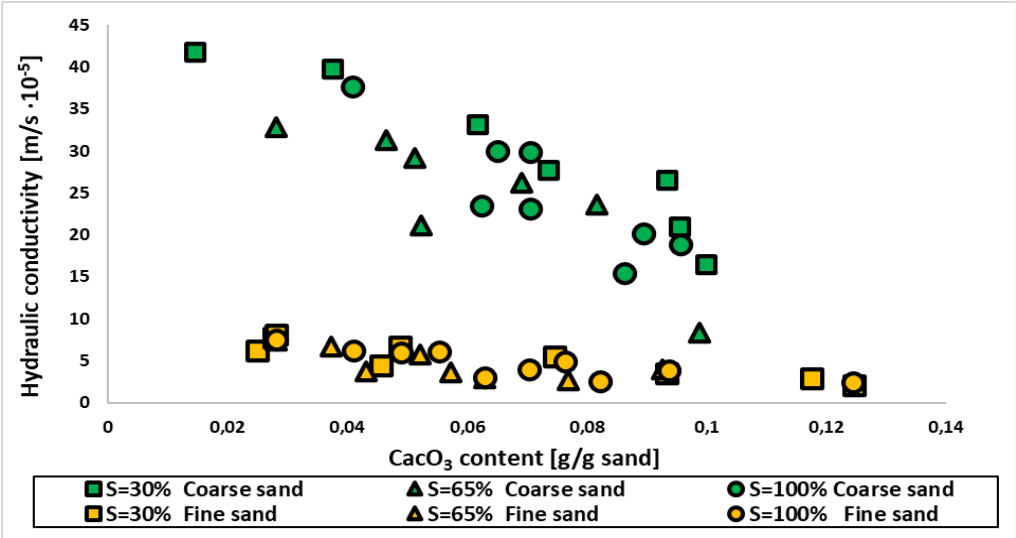
Figur 142. Show UCS as a function of reduction in permeability in MICP-treated sand for different concentrations of cementation solution. Data adapted from (Shahrokhi-Shahraki et al., 2015).

In their work, (Cui et al., 2017a) observed a linear relationship between increasing number of treatment cycles (urea/CaCl₂) and an increase in dry density, in MICP-treated sand. The plot presented below show the results.



Figur 143. Show acheived dry density as a function of CaCO₃ for increasing number of treatment cycles in MICP-treated sand. Data adapted from (Cui et al., 2017a).

In work by (Cheng et al., 2013), the permeability for MICP-treated fine and coarse sand with saturation (S) at 30, 65 and 80% were determined. The results show smaller range in reduction of permeability in respect to varying degree of CaCO₃ content in the fine sand, whereas the coarse sand show a larger range. However, all samples acheived an increased reduction in permeability with increasing CaCO₃ content. They suggest that the results indicate that lower saturation is preferable for MICP, as it enabled improved mechanical behavior while maintaining relatively high residual permeability.



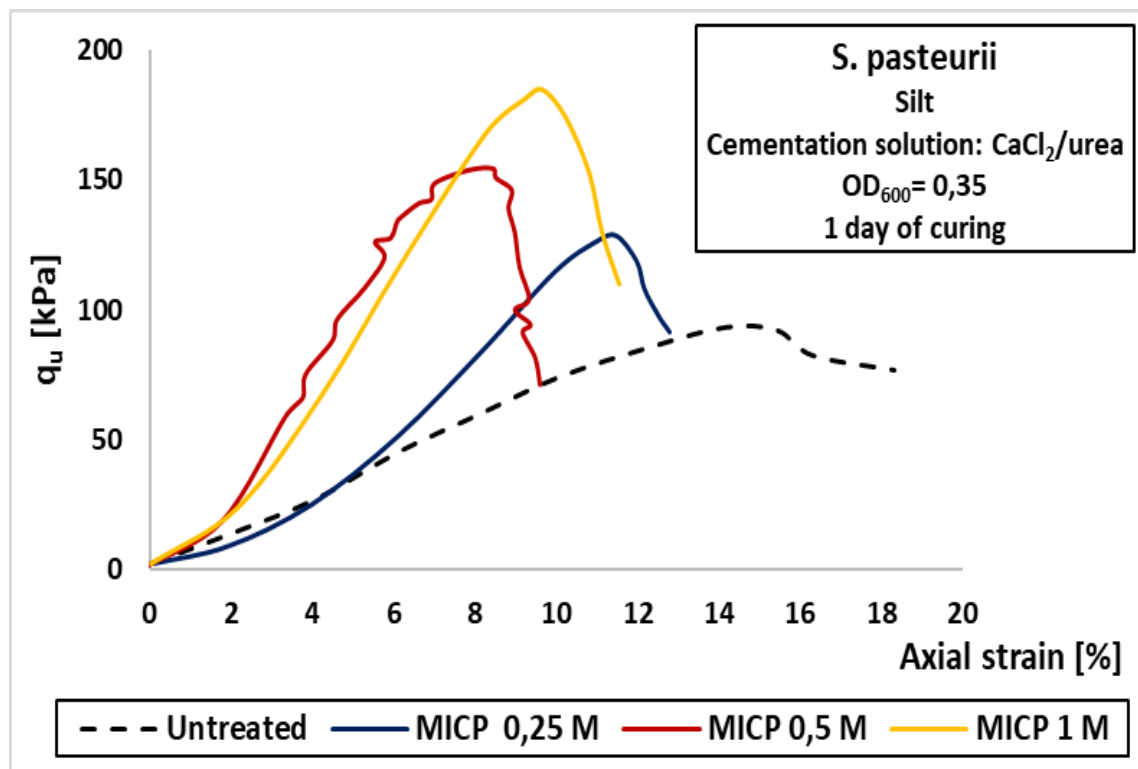
Figur 144. Show permeability post-treatment as a function of CaCO₃ content for different levels of saturation and different grading in MICP-treated sand. Data adapted from (Cheng et al., 2013)

4.2 Cohesive soils

4.2.1 Unconfined compression strength UCS

In work by (Bing, 2015), it is noted that the calcium in the cementation solution ($\text{CaCl}_2/\text{urea}$), may lead to reduced increments of shear strength in MICP-treated clayey soils. This is suggested to be due to Ca^{2+} increasing the electrolyte concentration in the pore water, thus reducing the thickness of the diffuse double layer around clay particles. This causes the clay particles to flocculate rather than disperse, which enables a higher share of free pore water, compared to adsorbed water.

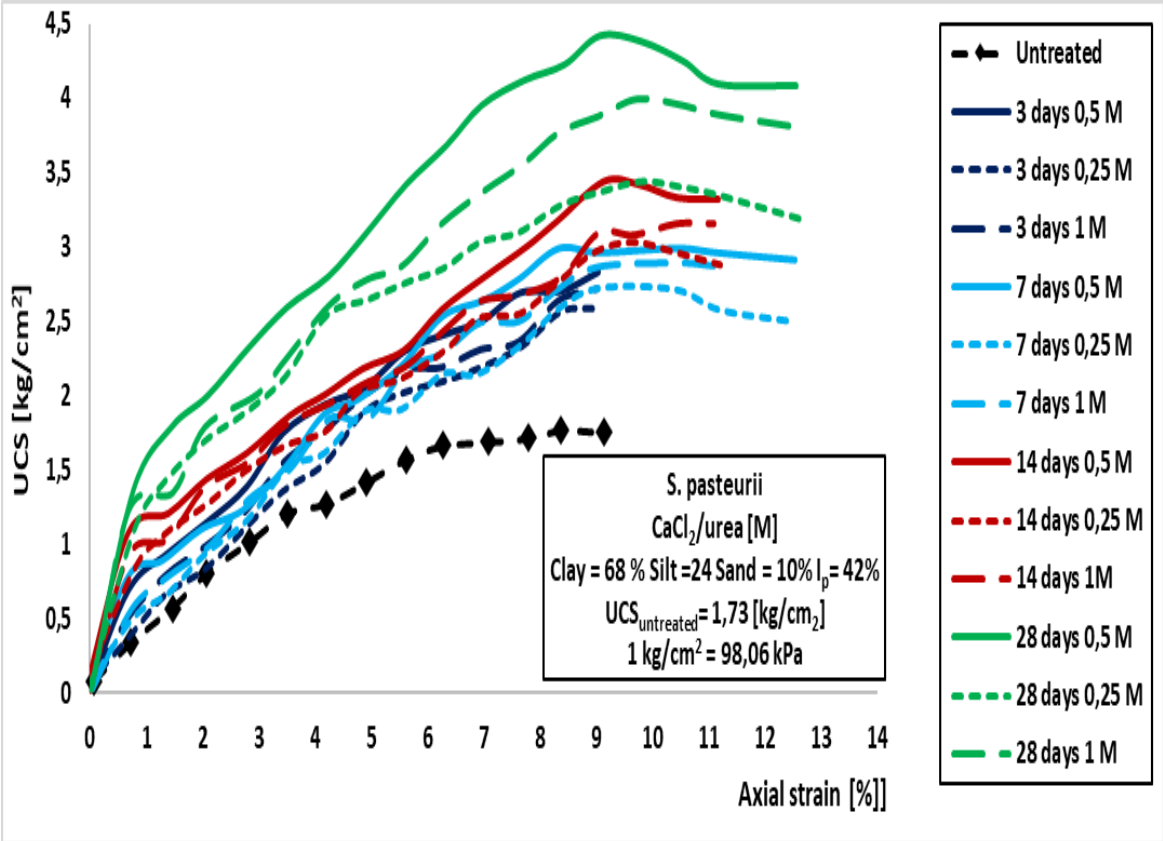
In their work, (Teng et al., 2020) used manual mixing for MICP-treatment with *S. pasteurii* in silty clay (68,7 % silt) with high plasticity and low pH. They found that UCS increased bacterial concentration was increased from 0.35 OD_{600} to 0.8 OD_{600} . However, a decrease in UCS was observed when the bacterial concentration was further increased to 1.45 OD_{600} . Further, the UCS increased with increasing concentration [M] of urea/ CaCl_2 . The results are presented in the plot below.



Figur 145. Show UCS in MICP-treated silty clay for different concentrations of cementation solution ($\text{CaCl}_2/\text{urea}$). Data adapted from (Teng et al., 2020)

The work of (Godavarthi Rajani, 2020), investigated the effect of concentration [M] of cementation solution ($\text{CaCl}_2/\text{urea}$) and curing time on achieved UCS for

MICP-treated (*S. pasteurii*) high plasticity clay. The results show that all treated samples irrespective of concentration and curing time, achieved increased UCS post-treatment, where 0,5 M was found to be the most favorable concentration. A higher increment in increased UCS was observed from 14 to 28 days of curing than from 3 to 14 days. Due to flocculation of particles during treatment, the share of silt sized particles increased post-treatment, while share of clay sized particles declined. The results are presented in the plot below.



Figur 146. Show UCS in MICP-treated high plasticity clay for different concentration of cementation solution and curing time. Data adapted from (Godavarthi Rajani, 2020)

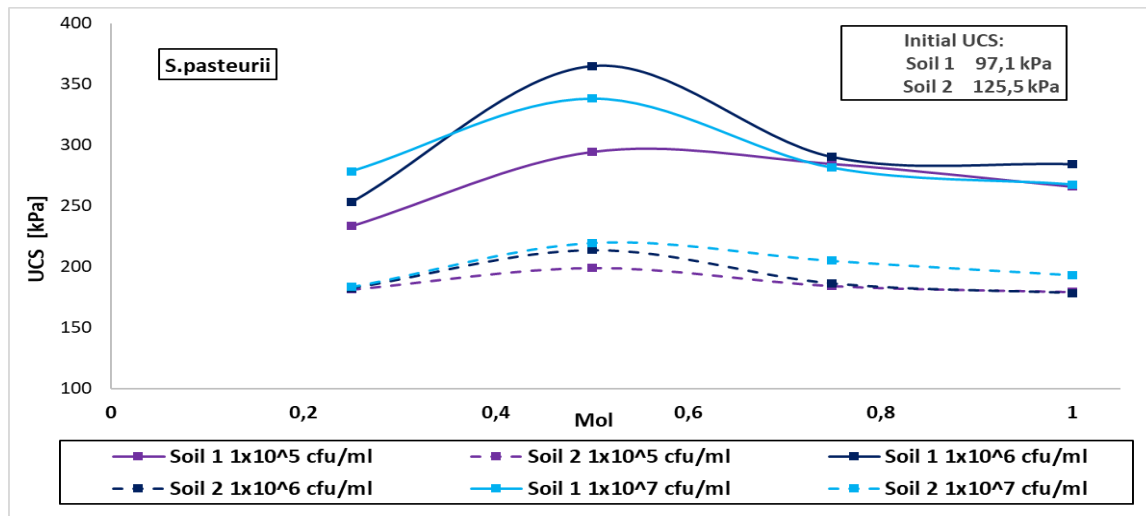
(Sharma and Ramkrishnan, 2016) used *S. pasteurii* for MICP-treatment by manually mixing of two fine grained soils, cured at 24°C for 7 days. The properties of the untreated soils are listed in the table below.

Tabell 17. Lists soil properties of samples in the study. Data adapted from (Sharma and Ramkrishnan, 2016)

Soil	Sand [%]	Silt + Clay [%]	I _p [%]
1	46,4	53,6	28,5
2	17,7	82,3	33,2

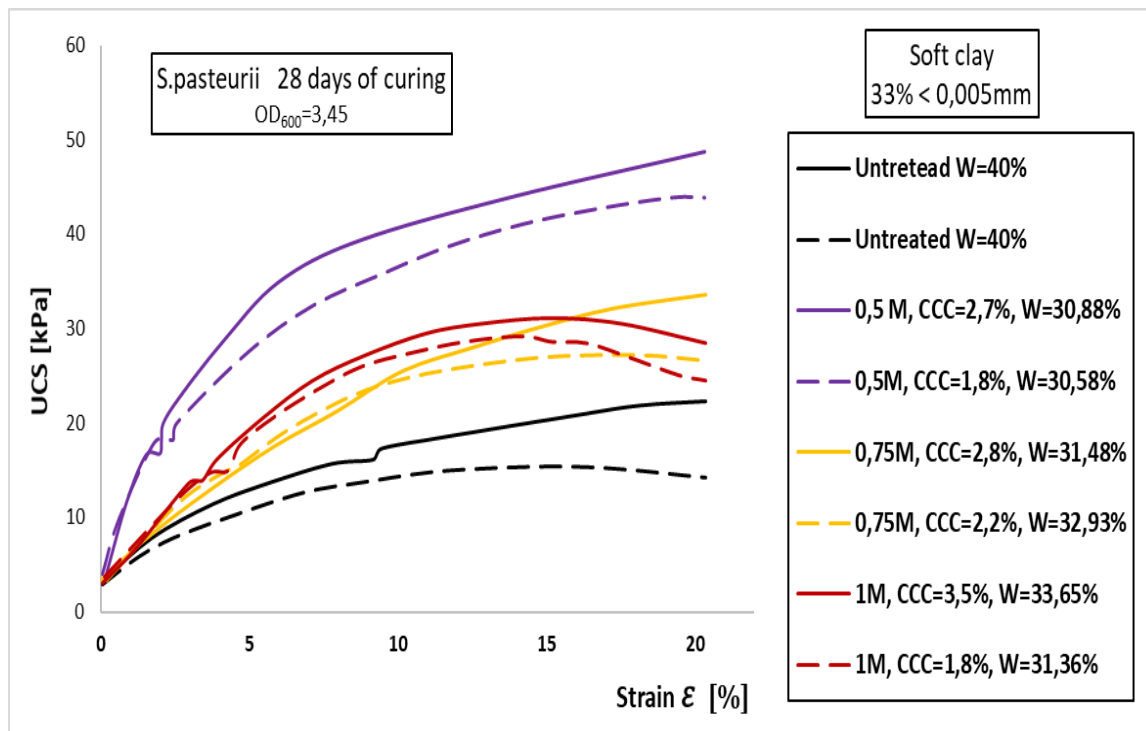
The results show increased UCS with increasing curing time, where the highest increment in UCS from untreated to treated state, was achieved in soil 1 with bacterial density of 1x10⁶ cfu/ml and 0,5 M cementation solution (CaCl₂/urea).

Soil 2 with the highest share of fines, achieved a significantly lower increment in shear strength from untreated to treated state. The results are presented in the plot below.



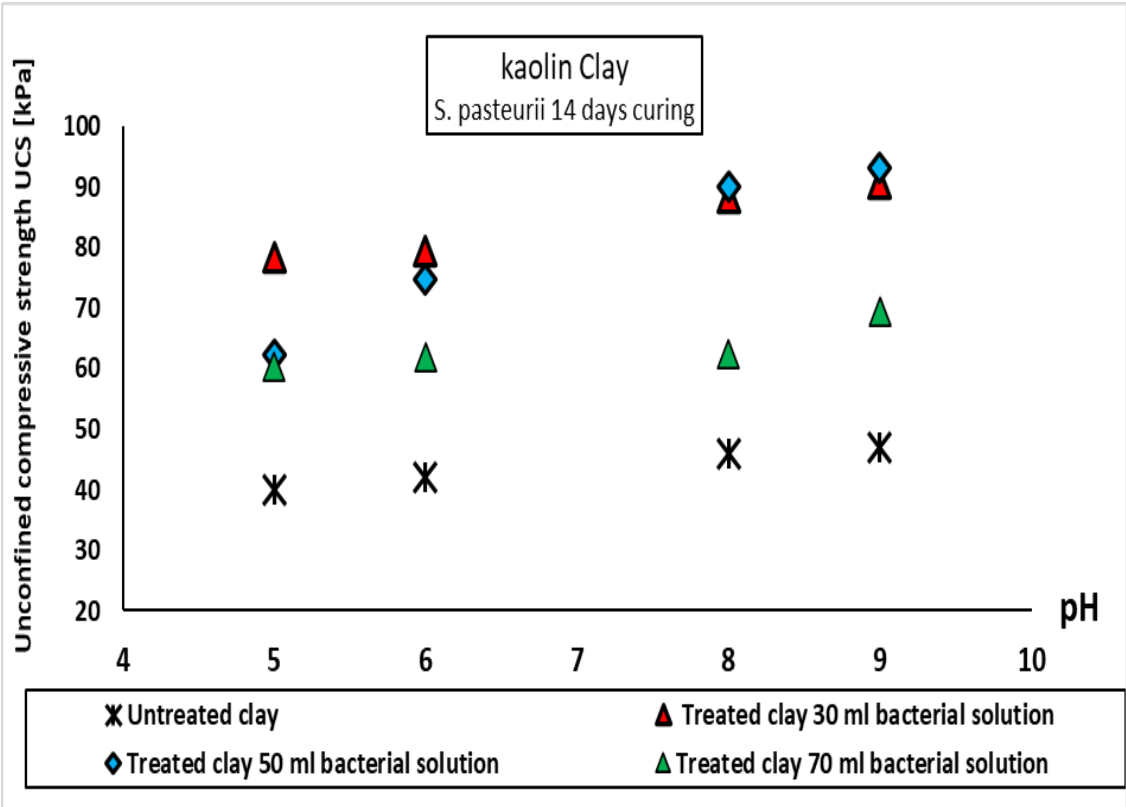
Figur 147. Show achieved UCS as a function of concentration of cementation solution ($\text{CaCl}_2/\text{urea}$) for the MICP-treated fine grained soil with varying degree of fines and sand. Data adapted from (Sharma and Ramkrishnan, 2016).

Work by (Xiao et al., 2020), used manually mixing with *S. pasteurii* for MICP-treatment of soft clay cured for 28 days at 24°C. The results show increased UCS with increasing CCC, where initial UCS increased up to 242% and initial water-content was reduced up to 23 %. The results are presented in the plot below.



Figur 148. Show achieved UCS and degree of reduction in water content for different concentrations of cementation solution ($\text{CaCl}_2/\text{urea}$) in MICP-treated soft clay. Data adapted from (Xiao et al., 2020).

(Keykha et al., 2017) investigated achieved UCS in MICP-treated kaolin clay (50% clay, 50% silt) using *S. pasteurii*. The study used three different amounts of bacterial solutions (30 ml, 50ml, 70 ml) and a constant concentration of cementation solution ($\text{CaCl}_2/\text{urea}$). The results show that both untreated and treated samples increase their UCS with increasing pH. However the largest increments are observed for 30 and 50 ml bacterial solution, where optimal parameters for increasing UCS in the clay, were found to be 50 ml at pH 9 and 40°C. The results are presented in the plot below.

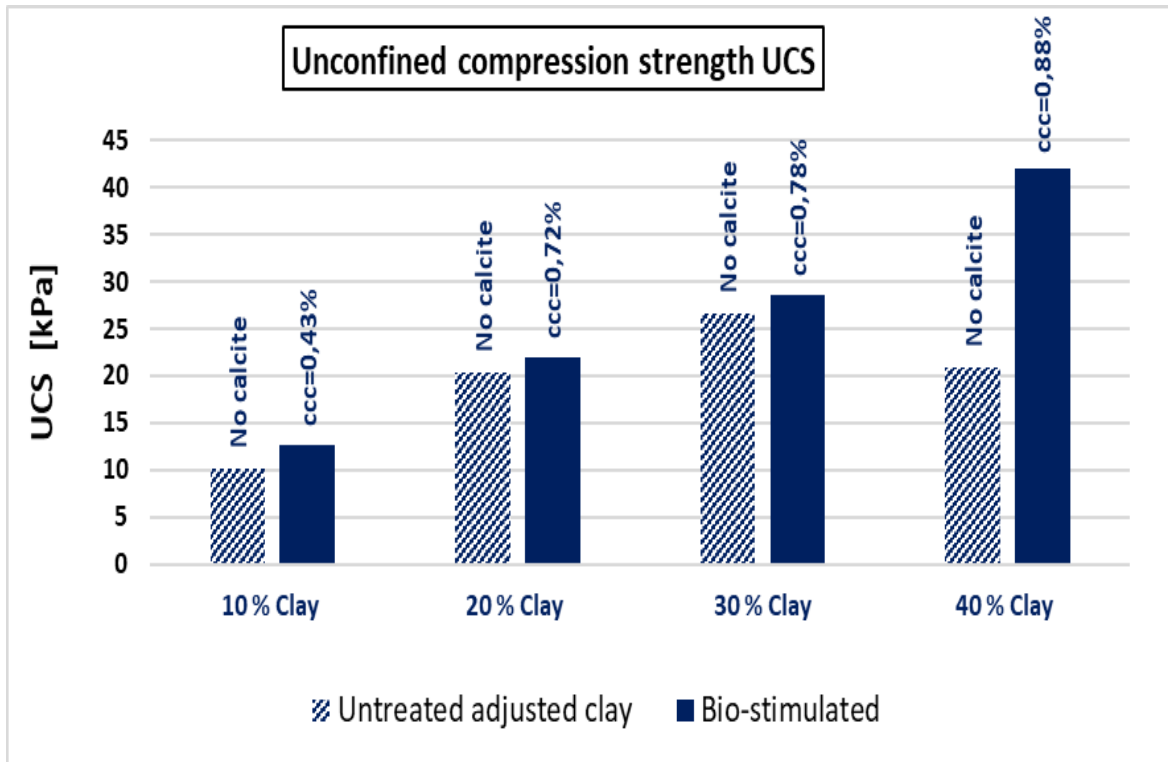


Figur 149. Show UCS as a function of pH for different volumes of bacterial suspension in MICP-treated clay (*S.pasteurii*). Data adapted from (Keykha et al., 2017)

(Behzadipour et al., 2019) reported that increased share of fines in MICP-treated sandy soil reduced the degree of enhancement, compared to lower share of fines. The observed improvement in shear strength, was suggested to be due to an increase in cohesion. (Kannan et al., 2020) reported on 148% increase in undrained shear strength (S_u) and a reduction in liquid limit (L_L) and plasticity index (I_p) for MICP-treated marine clay.

In their work, (Islam et al., 2020) used bio-stimulation as MICP treatment, where indigenous bacteria in the soil are stimulated with nutrients and cementation solution ($\text{CaCl}_2/\text{urea}$), for soils adjusted with 10, 20, 30 and 40% clay.

Almost no CaCO_3 was found in the untreated control samples, while the MICP-treated samples obtained very low CCC, where UCS increased with increasing clay content. However, the difference in UCS for untreated and treated samples at similar clay content, was only distinct in samples with the highest clay content. The results are presented in the diagram below.



Figur 150. Show UCS as a function of clay content for different CCC in soil treated by stimulating indigenous bacteria in the soil (bio-stimulation). Data adapted from (Islam et al., 2020).

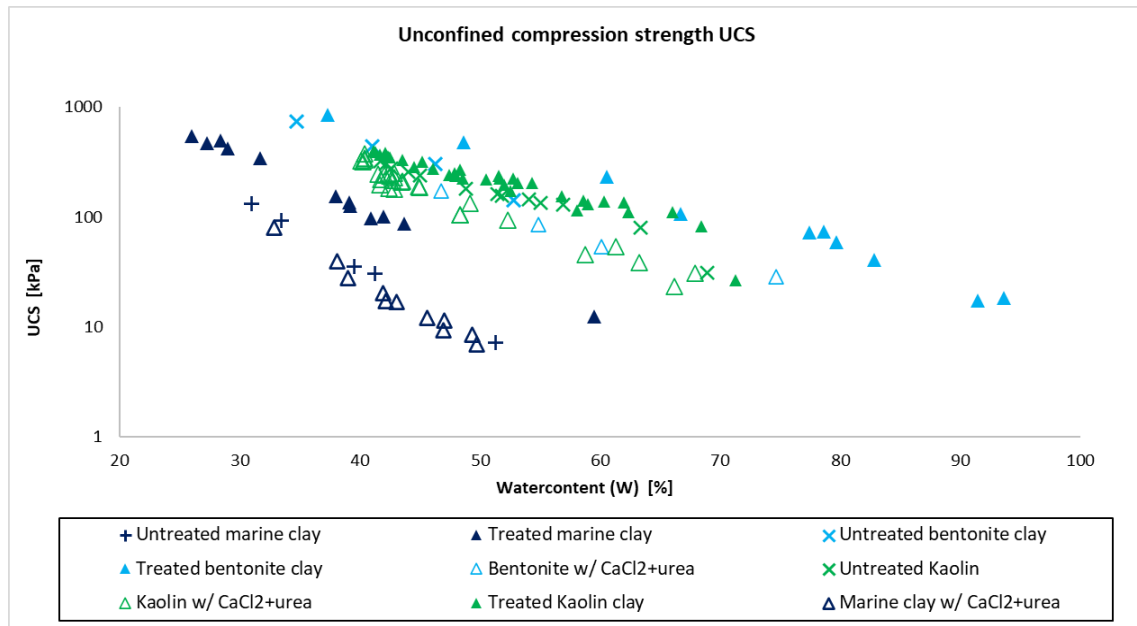
As part of a thesis by (Bing, 2015), three types of clay were MICP-treated with *B. sphaericus*. The properties of the clays in the study are listed in the table below.

Tabell 18. Lists properties of the clays used in the study. Data adapted from (Bing, 2015).

Property		Kaolin clay	Marine clay	Bentonite clay
Plasticity index	[%]	42,8	21,7	371,9
Fine content	[%]	100	72,3	100

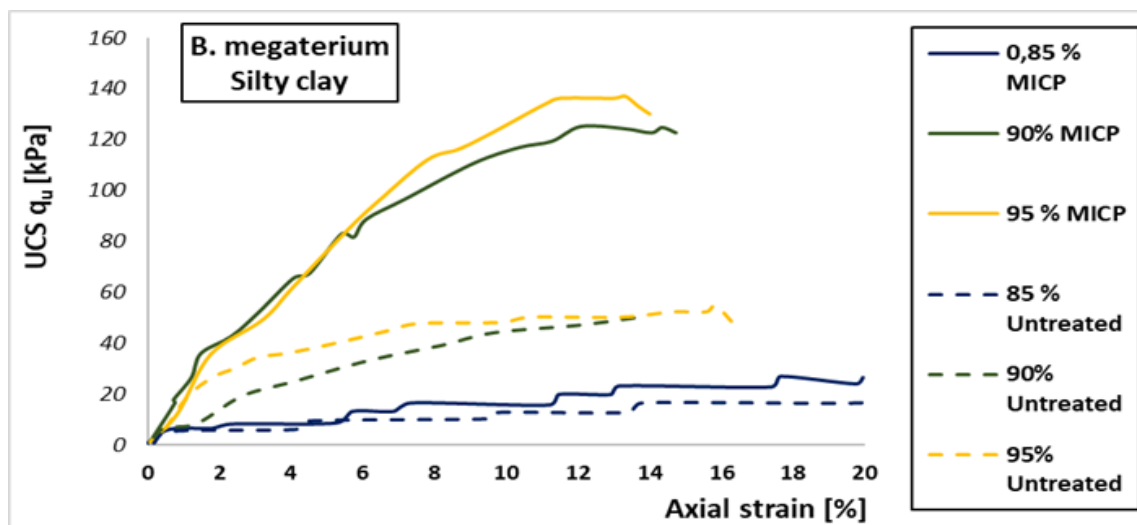
The results show generally higher achieved UCS with lower water content (W), where the highest (400%) increment in UCS from untreated to treated state for same W, is found for the marine clay, while the Kaolin clay achieve a 150% increase in UCS. Samples with similar W and treated with (bacteria+ CaCl_2 /urea), achieve a significantly higher UCS than control samples treated with only cementation solution (CaCl_2 + urea). This suggest that the added bacteria have a

significant influence on the increased UCS. The results are presented in the plot below.



Figur 151. Show UCS as a function of water content in MICP-treated clay and clay treted with only cementation solution ($\text{CaCl}_2/\text{urea}$).. Data adapted from (Bing, 2015).

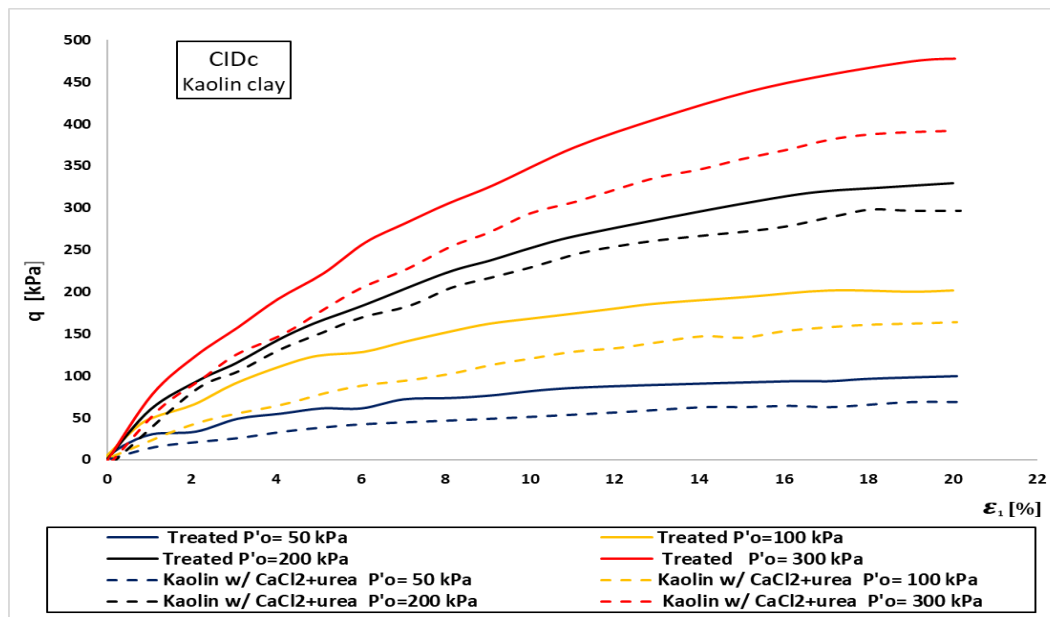
A study by (Soon et al., 2013), used *B. Megaterium* for MICP-treatment of medium plasticity silty clay with 29% sand, 55% silt and 16% clay, compacted to different percentage (85, 90, 95%) of maximum dry density for both untreated and treated samples. The results show increased UCS and strain-hardening behaviour with increasing dry density for samples compacted to 90 and 95 % of max dry density, whereas sample at 85% show negligible changes in shear strength or stress-strain response. The results are presented in the plot below.



Figur 152. Show UCS for MICP-treated clayey silt at different percentage of max dry density. Data adapted from (Soon et al., 2013)

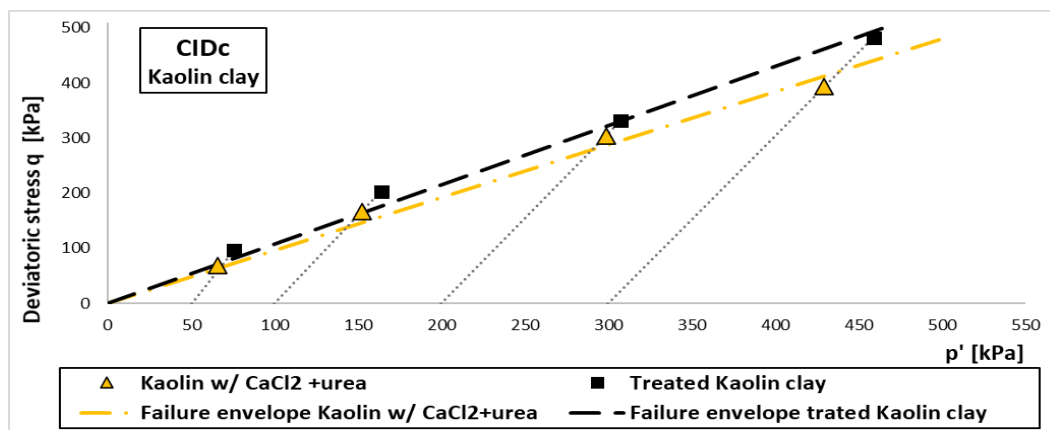
4.2.2 Shear strength and volumetric response

Work by (Bing, 2015) conducted drained triaxial tests on MICP-treated (B. sphaericus) Kaolin clay and Kaolin clay treated only with cementation solution ($\text{CaCl}_2/\text{urea}$), where P'_o was varied in the range 50-300 kPa. The results show increased shear strength with increasing P'_o and higher achieved shear strength at similar P'_o for MICP-treated samples, compared to samples only treated with cementation solution. All samples show increased strain-hardening after treatment. The drained stress-strain curves are presented in the plot below.



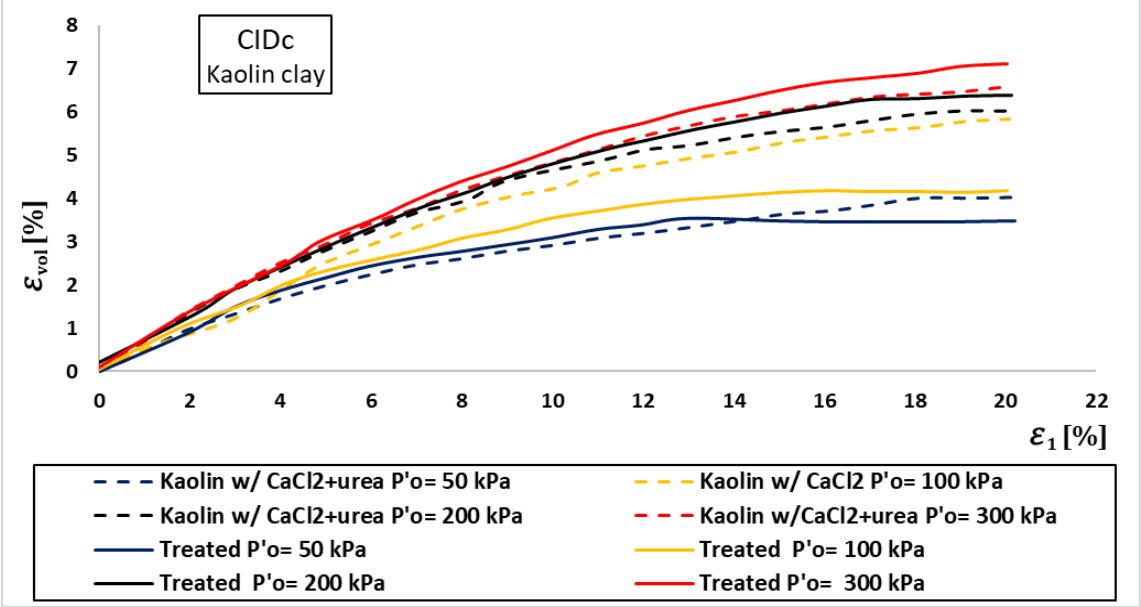
Figur 153. Show drained shear strength and strain response for MICP-treated clay and clay treated with only cementation solution ($\text{CaCl}_2/\text{urea}$) for different confining pressure. Data adapted from (Bing, 2015)

The q - p plot below show a moderately steeper failure envelope and increased friction angle for MICP-treated samples, compared to samples treated with only cementation solution. The results are presented below.



Figur 154. Show drained failure envelope for MICP-treated clay and clay treated with only cementation solution ($\text{CaCl}_2/\text{urea}$). Data adapted from (Bing, 2015).

As can be seen in the plot below, both samples treated with bacteria and cementation solution as well as samples treated with only cementation, show a dilative behaviour. All samples display small contraction before dilating at low strain, which is not visible in the plot presented below.



Figur 155. Show drained volumetric response for MICP-treated clay and clay treated with only cementation solution (CaCl_2 /urea) for different confining pressure. Data adapted from (Bing, 2015)

5. Discussion

5.1 Factors affecting MICP

Part of the objectives of this thesis is to research the factors affecting the MICP process. The findings are:

Cell growth

- *The research demonstrate that *S. pasteurii* can be cultivated with exponential aerobical growth on a large scale at lower cost, where batches should be stored at late exponential or early stationary stage of growth.*
- *The research indicate that *S. pasteurii* cell cultivated under oxic conditions, is an efficient and robust nucleation site for precipitation of CaCO_3*
- *The findings further indicate that the cell growth is affected by nutrients, temperature, oxygen and pH. It is uncertain whether *S. pasteurii* can grow into healthy cells under anoxic conditions.*
- *High bacterial density or repeated cycles of injections with fresh bacteria, could possibly exclude reliance on further cell growth post-injection in anoxic conditions.*

Urease activity

- *The research demonstrate that *S. pasteurii* can sustain urease activity under oxic conditions at pH 6-9 and within a broad range in temperatures (4-50°C). *S. pasteurii*s capacity for sustaining urease activity over time under anoxic conditions is unclear, but unlikely.*
- *The findings indicate a prolonged duration of urease activity with increased concentrations of urea in suspension. Low temperatures are indicated to cause a slower initiation of ureolysis but longer duration, whereas higher (20-30°C) temperatures leads to faster initiation and shorter duration. Correlations between bacterial density and urease activity if any, is unclear due to inconsistent findings.*

- *The findings further indicate that concentrations $\leq 0,5$ M of cementation solution ($\text{CaCl}_2/\text{urea}$) are favorable for precipitation, where increased share of urea is suggested to have a positive effect on urease activity, whereas increased share of CaCl_2 is suggested to have an adverse effect.*
- *Clay minerals could possibly have an adverse effect on urease activity, whereas the effect of restricted pore space in fine grained cohesive soils on the metabolism of ureolytic bacteria, is uncertain.*

Ammonium as a by-product

- *Hydrolysis of urea (ureolysis) during MICP leads to the release of both ammonium (NH_4^+) and ammonia (NH_3), which will have to be removed from the soil post-treatment.*
- *The research indicate that removal of NH_4^+ in granular soils is feasible using a high pH and high ionic strength rinse solution. However, studies show a small share of sorbed NH_4^+ remaining in the treated soil after rinsing. Further work on removal of residual NH_4^+ as well as removal of NH_4^+ in fine grained soils, is needed.*
- *Ammonia (NH_3) is volatile and can be released as foul smelling and potentially toxic gas. Research indicate that a significant reduction of NH_3 may be achieved using the one-phase low pH solution proposed by (Cheng et al., 2019).*

Geometric compatibility

- *The research suggest that increasing depth and content of fines would reduce the microbial activity in a soil profile.*
- *Bacteria is suggested to be transported within the soil either by self-propelled movement or through passive diffusion between pores*
- *The transport distance of bacteria is increased by fresh water due to a reduction in attractive forces acting upon bacteria from particle surfaces or through water flow generated by hydraulic boundaries.*
- *The findings indicate that pores larger than the bacteria size ($0,5\text{-}3\ \mu\text{m}$) are favorable for bacterial movement.*
- *Fully saturated pores are indicated to be favorable for movement between pores, whereas partially saturated pores reduce this mobility.*

- *Bacteria located in pores with size close to or equal to the size of bacteria, are suggested by the literature to be trapped or inactive.*
- *The findings further indicate that most of the pores in clays are too small to provide bacterial movement, but studies show that bacteria which are manually mixed into cohesive soils precipitate CaCO_3 , suggesting sustained metabolic activity of bacteria, even when located in very small voids.*

Precipitation of CaCO_3

- *The research shows that *S. pasteurii* have high capacity for precipitation in sand, but indicate a lower capacity in silt and clay.*
- *The findings indicate that increased rate of ureolysis and concentration at supersaturation, increases the precipitation rate, while amount of urea may prolong the urease activity and consequently the duration of precipitation.*
- *The findings further indicate that *S. pasteurii*'s capacity for precipitation is sustained between 4-50°C and at pH 7-9, while efficient between 4°C and 30°C, where concentrations $\leq 0,5$ M of cementation solution ($\text{CaCl}_2/\text{urea}$), is indicated to be most favorable for precipitation.*
- *The crystal quality and size of the precipitated calcium carbonate and generated cementation pattern, is indicated to be directly affected by the precipitation rate and concentration at supersaturation, and indirectly by temperature and urease activity.*
- *Effective cementation (particle bonding) and higher residual permeability post-treatment, is demonstrated at 4 and 25°C. However, further studies are needed for demonstration of reproducibility of the results.*

CaCO_3 crystals

- *The CaCO_3 binder is indicated to have an estimated service life above 50 years, under favorable ground conditions.*
- *Acidic environments could be a concern regarding corrosion on CaCO_3 mass, where findings indicate that loss of shear strength due to corrosion of CaCO_3 , is governed by CCC of the MICP-treated soil.*

- Findings further suggest that temperature and pH through the resulting level of urease activity and precipitation rate, may affect the crystal growth and morphology during MICP.
- Fewer and larger crystals providing effective particle bonding are demonstrated at 4 and 25°C and lower urease activity, while numerous and smaller crystal with less particle bonding, are generated at 50°C and higher urease activity.
- Findings suggest a need for further work on the effect of low temperatures and low urease activity, on the crystalline quality of CaCO₃ crystals.
- The output mineral at precipitation is suggested to be affected by the concentration of ions at superstauration, where high concentrations generate metastable vaterite, whereas low concentrations generate the more stable calcite.
- The findings do not provide any certainty on determining factors for the generated shape of the crystal, nor on any direct correlation between bacterial concentration and crystal growth. However, less space between cells during precipitation is suggested to generate spherical crystals, wile larger space generate cubic shape.
- The research further indicate that concentration as well as share of urea and CaCl₂ in the cementation solution, have an effect on crystal growth, where increasing shear of urea is favorable compared to increased share of CaCl₂. High concentrations of Mg²⁺ is found to adversely alter the morphology.

Effect of particle characteristics

- The research indicate that particle shape and size, affect the acheived cementation with MICP.
- Findings indicate that angular particles in the range coarse silt to medium sand are favorable, while a higher number of contact points per soil volume and increasing density prior to treatment, increases the acheived shear strength post-treatment in granular soils.
- Uniform soils of angular particles acheive a higher increment in increased shear strength post-treatment, compared to uniform soils of round particles.

Cementation pattern

- *The research indicate that different cementation patterns can be generated during precipitation, where type of pattern may affect the degree of achieved shear strength, residual permeability or reduction of porosity in MICP-treated soils.*
- *Findings indicate that cementation at the particle contacts are predominant at lower precipitation rates, while higher precipitation rates generate further crystal growth around the contact points, leading to reduced void size and lower residual permeability.*
- *Fully saturated pores are indicated to lead to more precipitation in the center of the voids reducing the residual permeability, whereas partially saturated pores lead to cementation at particle contacts and higher residual permeability.*
- *Control of cementation pattern through control of urease activity and precipitation rate, is indicated to be feasible. However, further work is needed on the predictability of the control as well as the effect of saturation which is indicated to have an effect on the cementation pattern, independent from controlling factors for the precipitation rate.*

Flow and bacterial retention

- *A reduction of bacterial and substrate density along flowpath should be expected during injections in situ, hence strategies addressing this issue, should be integrated into potential injection methods in situ.*
- *High salinity solutions drive flocculation of bacteria, which could cause stagnation in flow paths due to accumulated CaCO_3 . However, such solutions increases attractive forces on the bacteria, which increases retention of bacteria within the target area.*
- *Flocculation from high salinity solutions, could possibly be reduced by utilizing low pH solutions that delay precipitation.*
- *Stagnation in flow could possibly be addressed with the use of constant pressure instead of constant flow rate during injections.*

Injection strategies and spatial distribution of CaCO₃ binder

- *The research show that several strategies have been applied in order to optimize the achieved spatial distribution of binder post-treatment.*
- *The surface percolation method could possibly be a suitable method for increasing the erosion resistance of surface layers in slopes, reducing permeability in porous deposits or strengthen the base layers of shallow foundations.*
- *The research indicate that low pressure injections are viable in granular soils and that distribution of CaCO₃ binder within target area is achievable, where the one-phase low pH solution proposed by (Cheng et al., 2019), is evaluated to have the greatest potential for achieving increased uniformity in the spatial distribution of CaCO₃ in granular soils.*
- *The research indicate that low pressure injections are not viable in fine silt and clay due to low permeability, where achieving distribution of CaCO₃ across low permeability layers within stratified soil deposits with varying permeability, is unlikely.*
- *The utilization of injection and extraction wells in a grid pattern, have been demonstrated as effective in large scale MICP-treatment of granular soils and is evaluated as the most suitable injection method for MICP in granular soils.*

5.1.1 Cell growth

- ***S. pasteurii as a causative agent for MICP in soils.***
- ***Challenges for the implementation of MICP in situ***
- ***Factors affecting the MICP process***

Ureolytic bacteria utilized in MICP, should among other factors stated in chapter 3.4, have capacity for exponential growth under cost effective cultivation, have high urease capacity under oxic as well as anoxic conditions under a broad range of temperatures, tolerate harsh and alkaline environments and have a highly negatively charged and robust cell surface.

The viability of MICP is dependent on cost efficient large scale batch cultivation, where (Griffiths, 1986) reported that for scale up of cell cultivation, the cost of cultivation medium increases proportionally with the decline in total product and labour cost. To address this issue, (Whiffin, 2004) managed to reduce costs of cultivation medium by 95% by replacing the most expensive components, where the cells still obtained a high urease activity. This indicates that the urease capacity of cultivated bacteria could be sustained, even under large scale cultivation.

Work by (Nayanthara et al., 2019, Stocks-Fischer et al., 1999, Whiffin, 2004), demonstrated that *S.pasteurii* show an exponential increase in growth up to a maximum and then a stationary phase followed by a gradual fall. This is important for securing a rapid growth during cultivation, but could also impact further growth in the sub-surface, if the ground conditions would allow for such growth.

(Van Paassen, 2009a) reported that batch cultivation of bacteria stored at late exponential growth state or early stationary growth, obtained maximum growth yield and that the degree of growth could be influenced by the composition of nutrients, temperature and pH. (Ng et al. 2012 ; Nayanthara et al. 2019) found favorable growth conditions between 20-30°C, whereas (Kim et al., 2018) found optimal pH (pH_{opt}) 7-9 for cell growth.

To store the batch at high bacterial density before lysis and depletion of nutrients can initiate at the late stationary stage, seems reasonable. The suggested influence on degree of growth, could possibly suggest that the rate of growth could be controlled by adjusting factors in the suspension. This is important for balancing the bacterial density and the available nutrients and oxygen at a given time, to delay depletion and the consequent lysis and decline in urease activity as observed in work by (Stocks-Fischer et al., 1999).

Work by (Harkes et al., 2010b) reported that *S.pasteurii* can be grown under limited oxygen levels, while increased levels of oxygen during growth were more favorable, whereas (Martin et al., 2012) found that *S. pasteurii* was not capable of anaerobic growth. The aspect of capacity for anaerobic growth is relevant for applications of MICP in soils below the water table, where the research is contradicting on *S. pasteurii*'s capacity for such growth. However, the findings indicate that degree of available oxygen does have an effect on the growth. Further growth in the sub-surface post-injection where oxygen levels are low or none, suggest the need for high bacterial density in the injected suspension, which could cause

an earlier depletion and lysis or repeated injection cycles of fresh bacteria or oxygenated fluids.

(Mitchell et al., 2019) state that under anoxic conditions, facultative anaerobic bacteria such as *S. pasteurii*, use other compounds besides O_2 as terminal electron acceptors. They reported lower growth under anoxic conditions than under aerobic growth, where the anaerobic growth did not sustain over time, regardless of added ETAs. However, the growth did show a rapid increase when oxygen (O_2) was allowed to enter the system. This could indicate that *S. pasteurii* have capacity for low initial anaerobic growth, where the bacteria can survive for a short time by using ETAs, but can not further grow in to high densities utilizing ETAs as a substitute for O_2 . This is supported by the observation of the rapid and exponential growth occurring at the introduction of O_2 in the system.

In their work, (Williams et al., 2017) found that *S. pasteurii* could sustain negative cell charge during exposure to stressors such as heat, nutrient depletion and high pH, where the highest negative zeta potential was registered in the culture with the highest urease activity. However, no trend of increase in potential with increasing level of urease activity, could be registered for the rest of the cultures. Work by (Ma et al., 2020b) reported that an increased negative surface charge is favorable for binding positively charged ions such as Ca^{2+} and Mg^{2+} , where *S. pasteurii* showed higher negative potential than other comparable ureolytic bacteria and where adding urea to the culture increased the cell surface charge, while (Keykha et al., 2017) found an increase in negative potential of *S. pasteurii* with increasing pH.

The findings indicate that *S. pasteurii* seem to have a robust cell structure with high negative surface charge even when subjected to stressors, suggesting it to be an effective nucleation site for precipitation, even under challenging ground conditions. The lack of correlation between urease activity and magnitude of negative cell charge could however suggest that other factors than urease activity, govern the magnitude of the cell charge. However, the addition of urea to the culture which would increase the urease activity, seem to boost the potential.

The results do not give a clear indication on governing factors for magnitude of cell charge. The findings on rising negative potential with increasing pH, seem reasonable given that low pH increase the voltage at opposite polarity.

(Ma et al., 2020b) further reported that *S. pasteurii*, remained in good physical shape, despite being surrounded by compact CaCO_3 crystals, as opposed to *B. subtilis* that was damaged and lysed. These findings are in line with those of (Williams et al., 2017) and suggest that *S. pasteurii* could have the capacity to sustain precipitation during early stages of CaCO_3 encapsulation. Lysis due to restricted access to oxygen or nutrients, would however most likely occur at complete encapsulation.

5.1.2 Urease activity

- ***S. pasteurii* as a causative agent for MICP in soils.**
- ***Factors affecting the MICP process***
- ***Challenges for the implementation of MICP in situ***

The level of urease activity is related to the end product in MICP, which is precipitation of CaCO_3 . The bacteria utilized in MICP, should be able to initiate and sustain high urease activity over time under conditions with limited access to oxygen or dissolved oxygen as well as under a broad range of temperature and pH. For MICP to be viable as method for ground improvement it is necessary to identify the factors that affect the urease activity, so that regulation of these factors can be utilized to steer the process towards the desired outcome, which for example could be amount, rate or pattern of precipitation.

Work by (Bhadur et al., 2016), found that *S. pasteurii* can secrete large amounts of the urease enzyme, where Duraisamy (2016) reported that *S. pasteurii* show a high urease activity, compared to other ureolytic bacteria. This suggests that *S. pasteurii* could sustain the capacity to produce urease enzyme in sufficient quantity, which is essential to the following precipitation of CaCO_3 .

(Okwadha and Li, 2010, Teng et al., 2020) reported on results that indicated that rate of ureolysis increased with bacterial concentration. However, (Teng et al., 2020) found that the increased urease activity with increasing bacterial concentration, was just initial and hence temporarily and a limiting factor for sustained urease activity. (Whiffin, 2004) found no correlation between bacterial concentration and urease activity and (Stocks-Fischer et al., 1999) reported on a reduction in the precipitation when bacterial concentrations exceeded 10^8 cells/ml.

(Okwadha and Li, 2010) found that bacterial concentration had greater influence on the rate of ureolysis than the initial concentrations of urea, while (Stocks-Fischer et al., 1999) note that the rate of ureolysis depend on the concentration of urea.

The litterature is contradicting on whether the number of cells in suspension affect the specific urease activity. It is reasonable to think that the specific urease activity per cell is dependent on the concentration of urea and nutrition available per cell, which could possibly explain the findings of (Teng et al., 2020, Stocks-Fischer et al., 1999). It is further possible that the rate of ureolysis have an upper limit where abundance of urea would not increase the rate beyond its maximum, while a reduction in urea would reduce the rate. However, given that the degradation of urea is dependent on the availability of urea, the concentration of urea would most likely affect the urease activity.

Work by (El Mountassir et al., 2018) found that the rate of ureolysis is strongly influenced by the urease activity, which in turn is suggested to be governed by the amount of urea in the solution. (Moyo et al., 1989) observed a rapid initial increase in urease activity at increasing concentration of urea from 0 to 0,02 M, where the activity then stagnated when concentration of urea was further increased from 0,02 to 0,06 M. It is not clear whether an increasing number of cells would have a collective effect on the urease activity or whether amount of urea available per cell, is the determinig factor. Initially, concentration of urea do seem to have an effect on the urease activity, but above a certain treshold, the activity do not seem to be influenced by a further increase in concentrations of urea. This could possibly suggest that as previously discussed, there is a limit to the rate of ureolysis and that the available urea and oxygen per cell is a limiting factor for the urease activity. One could however assume that amount of urea in the suspension, could contribute to increase the duration of the urease activity.

For geotechnical applications of MICP, it will often be the case that the target soil is located below the groundwater table, where (Inglett et al., 2005) note that once a soil is saturated, the availability of oxygen is reduced due to the displacement of oxygen in the pore space. Saturated soil below the water table, will generally have a limited availability of dissolved oxygen decreasing with depth

from the water table. MICP needs to be operational under such conditions, in order to be a viable solution for ground improvement.

In their work, (Hamdan et al., 2011) state that *S. pasteurii* uses aerobic respiration during ureolysis which would restrict urease activity at low levels of oxygen. (Jain and Arnepalli, 2019) found that the urease activity of *S. pasteurii* under anoxic conditions was very low, where (Teng et al., 2020, DeJong et al., 2010) stated that *S. pasteurii* can survive in anoxic environments, but the capacity to produce urease in the absence of oxygen, is time limited. On the contrary, (Tobler et al., 2011, Mortensen et al., 2011b, Mitchell et al., 2019) reported that anoxic conditions did not significantly inhibit the urease activity of *S. pasteurii*.

The findings on *S. pasteurii*'s capacity for sustaining urease activity under anoxic conditions are inconsistent. The findings suggesting that oxygen levels have a minor effect on the urease activity, could be due to the cells already having developed urease enzyme during aerobic growth, as noted in work by (Martin et al., 2012). This is in line with findings of (Teng et al., 2020, DeJong et al., 2010) and could suggest that initial urease activity could be sufficient with limited available oxygen, whereas no new urease enzyme would be produced, thus shortening the duration of the urease activity. Further studies on the duration of urease activity under anoxic conditions could clarify. One of the studies that found no negative effect of anoxic conditions on the urease activity, based their assumption on a rising pH which according to (Jain and Arnepalli, 2019), could be due to the breakdown of complex proteins in the stationary growth phase, rather than an indication of urease activity.

Work by (Mitchell et al., 2019), suggested resuscitation and re-stimulation of the injected bacteria, through cyclic injections of oxygenated fluids, while (Chen et al., 2012) developed an injectable solution, with high initial oxygen retention and a slowly declining oxygen release rate, to address these challenges. A solution to the uncertainty tied to anaerobic cell growth as well as sustainability of urease activity under anoxic conditions, could be to either supply the target soil with multiple injections of fresh bacteria, injecting oxygenated fluids as proposed by (Mitchell et al., 2019) or by injecting compounds with delayed oxygen release as

suggested by (Chen et al., 2012). To verify the effect of such solutions, further studies should be conducted below the watertable in situ.

The sub-surface temperature in cold climate regions are often low (4-8°C) and for MICP to be a viable method for ground improvement in such areas, the bacteria needs to be able to initiate and sustain urease activity under such conditions. In work by (Gillman et al., 1995), it was reported on 3,1-12,4 times higher natural occurring urease activity at 37°C than at 5°C, from indigenous ureolytic bacteria in different type of soils. All soil types showed an increase in urease activity with increasing carbon content at 37°C, but none at 6 °C, where (Vahed et al., 2011) observed a positive correlation between carbon content and urease activity at higher temperatures, but not at lower temperatures.

The findings show that urease activity occur by indigenous bacteria in soils with temperatures down to 6°C. However, the urease activity is much lower at 6°C than at higher temperature. Increased carbon content only correlated with increased urease activity at higher temperatures, suggesting a much slower ureolysis at low temperatures. This could indicate that temperature have a strong influence on naturally occurring urease activity in soil, while organic content in the soil have less influence on the urease activity. This assumption is further supported by the findings of (Vahed et al., 2011), where the natural occurring urease activity in soils at 24°C was higher than at 16°C, while (Moyo et al., 1989) observed an exponential increase in urease activity of indigenous bacteria with increasing temperature in the range 5-50°C.

(Cacchio et al., 2003) reported on slow initiation of ureolysis at low temperatures and a faster initiation with increasing temperature. (Ng et al., 2012b) reported on marginally higher rate of ureolysis at 30°C compared to 20°C, while (Gillman et al., 1995) observed a significant increase (1800%) in rate of ureolysis when temperature was increased from 5 to 20°C, whereas further increase above 30° C, did not increase the rate.

The findings indicate that temperature have an influence on how fast ureolysis is initiated, which could possibly be due to low bacterial metabolism at low temperatures, which is in line with findings of (Peng and Liu, 2019a, Nayanthara et al., 2019), where a faster initiation of ureolysis between 20-30°C compared to 10°C

was observed. The limited range (5 to 20°C) where temperature seem to have an impact on the rate in the findings of (Gillman et al., 1995), could suggest an optimal rate of ureolysis at a certain temperature, as suggested in work by (Stocks-Fischer et al., 1999).

(Whiffin, 2004) reported high urease activity for *S. pasteurii* in the range 30-70°C and no activity under 5°C, while (Cheng et al., 2016) found that *S. pasteurii* showed low urease activity at 4°C which generated effective cementation, while (Nayanthara et al., 2019) found optimal urease activity for *S. pasteurii* at 25°C and (Kim et al., 2018) at 30°C and lowest at 50°C. Work by (Peng and Liu, 2019a) reported on increased urease activity within the range 10-30°C, where increasing temprature decreased the duration of sustained urease activity.

Precipitation of effective CaCO₃ crystals by *S. pasteurii*, occured at temperatures down to 4°C, where the urease activity also was lower than at higher temperatures. However, the lower urease activity observed by (Cheng et al., 2016) at 4°C was demonstrated to generate effective cementation, which contradict the reports of no urease activity at 5°C by (Whiffin, 2004). This suggests a need for further studies on MICP at low temperatures to verify the reproducibility of the results acheived at 4°C. However, the findings of sustained urease activity and actual precipitation at low temperature, are significant.

The research suggests high urease activity for *S. pasteurii* at 20-30°C. However, the duration of the urease activity is also of great importance, where the findings of (Peng and Liu, 2019a) suggest a faster initiation and higher peak between 20-30°C, while (Nayanthara et al., 2019) found a slower initiation, lower peak and longer duration at 10°C. This observation is in line with work of (Whiffin, 2004), who found that cell lysis (death) is slow around 10°C and where increased temperature will accelerate the cell lysis.

These results together with the demonstrated sustained urease activity and consequent precipitation at 4°C, excluding other factors affecting the process, support an evaluation of MICP with *S. pasteurii* as viable in cold climate ground conditions. However, further studies on the effect of low temperatures on the metabolism and urease activity, are needed.

The pH can vary in different sub-surface environments depending on soil minerals and groundwater. In their work, (Tang et al., 2020, Stocks-Fischer et al., 1999) state that the pH value can affect urease activity through the metabolism of ureolytic bacteria, where (Stocks-Fischer et al., 1999) state that level of pH will govern the bacterias ability to decompose urea. This could suggest that too alkaline or too acidic ground conditions, may have an inhibitory effect on initiation of ureolysis.

S. pasteurii is according to the litterature alkaphile and resistant too high pH (Wiffin, 2004, Hsu et al., 2017, Rahman et al., 2020b). However, this is related to its ability to survive and does not exclude adverse affects on the metabolism and capacity for ureolysis under such conditions, where (Stocks-Fischer et al., 1999) found that the rate of ureolysis is low at both acidic (pH < 6) and alkaline (pH > 10) environments.

As noted by (Ng et al., 2012a), ammonium (NH_4^+) generated during ureolysis will increase the pH of the medium, while the generated carbon dioxide (CO_2) from ureolysis and microbial respiration, slows or counteract the rapid increase in pH. This could possibly mean that high bacterial density in suspension could slow the rise of pH through increased release of CO_2 during ureolysis. However, it is not clear how large the contribution of CO_2 is from the process, compared to the released NH_4^+ from the degraded urea.

A study by (Gillman et al., 1995) observed that urease activity occurred naturally in soils, at pH ranging from 5,3 to 7,1, while (Vahed et al., 2011) reported on moderate correlation between pH and urease activity in indogenous ureolytic bacteria, whith optimal pH around 7. These observations suggest that naturally occurring ureolysis in situ is affected by the level of pH, where optimal pH for indogenous bacteria seem to be in the lower range of that found for *S. pasteurii* during lab studies.

Work by (Kim et al., 2018) suggest that *S. pasteurii* is sensitive to change in pH and have an optimal urease activity at pH 7, while (Nayanthara et al., 2019) observed a rapid increase in urease activity between pH 6,0-9,0 and an optimum at 9,0 for *S. pasteurii*. Further, work by (Stocks-Fischer et al., 1999) reported an

optimum rate of ureolysis for *S. pasteurii* at pH 8,5, while (Whiffin et al., 2007) found that *S. pasteurii* reached peak rate of ureolysis after 5 hours at pH 7-8.

The research indicate that the optimal pH for urease activity for *S. pasteurii*, ranges between 7 and 9. The reason for this variation could be variations in temperature, concentration of urea or availability of oxygen, among others. The research further describe cases of natural occurring urease activity in soils with pH down to 5,3, which suggest sustained urease activity under a broad range in pH, but a rise and decline in level of urease activity within this range, as suggested in work by (Stocks-Fischer et al., 1999).

However, the pH of the target soil in situ could be lowered or increased with solutions prior to treatment. However, very acidic ground conditions may not be a good candidate for MICP due to the long-term adverse effects of corrosion on the CaCO_3 binder, while the long-term effects of highly alkaline ground conditions on the CaCO_3 binder, is unclear.

Soils rich in organic matter and soft clays and clayey soils with high watercontent, can cause larger settlements and have low bearing capacity for foundations, while leached marine clays are unstable and could cause large landslides if located on inclined ground and they are disturbed. Ground improvement is often applied when stabilizing or building on such conditions. Clarifying the effect of organic matter and clay minerals on the urease activity, is for this reason important.

Studies indicate that soil properties such as organic content and clay minerals, can affect the levels of urease activity (Makboul and Ottow, 1979, Sun et al., 2019b, Vahed et al., 2011). In their work, (Makboul and Ottow, 1979) found that illite clay minerals have a greater adverse impact on urease activity than montmorillonite and kaolinite. (Sun et al., 2019c) found that inhibitory effect on the urease activity of *S. pasteurii* increased with increasing share of added clay. When added individually, FeCl_3 showed a higher reduction in urease activity than Al_2O_3 , while (Montoya, 2012) reported on a much lower precipitation rate for MICP-treated sand rich in Fe_2O_3 , compared to sand rich in quartz, feldspar or calcite.

The research suggest that some clay minerals may have an inhibitory effect on the urease activity of *S. pasteurii* with a varying effect depending on the mineral.

Minerals containing iron (Fe) seem to have a more adverse effect on the urease activity and consequently the rate of precipitation, than others.

(Gillman et al., 1995, Vahed et al., 2011) found a strong correlation between level of nitrogen in the soil and urease activity. (Gillman et al., 1995) reported on a weak correlation between share of clay and urease activity and (Vahed et al., 2011) found a moderate correlation, while the correlation for share of silt or sand was found to be weak.

Limited pore space in fine soils could possibly affect the metabolism of the bacteria, thus reducing the urease activity. The findings of (Makboul and Ottow, 1979, Sun et al., 2019c, Montoya, 2012) may however suggest that certain clay minerals have an adverse effect on the urease activity, independent of potential effects from small pore space in clays. The findings of (Gillman et al., 1995, Vahed et al., 2011) are not consistent and do not differentiate between effect from minerals and effects from limited pore space, where one or both could have an adverse effect on the urease activity. The findings suggest a need for further studies.

The findings of (Vahed et al., 2011) do not suggest any correlation between silt or sand particles and urease activity, while (Montoya, 2012) reported on an effect from predominant minerals in sands on precipitation rate and hence the urease activity. The strong correlation between nitrogen or organic content and urease activity observed by (Vahed et al., 2011, Gillman et al., 1995), was however not independent of temperature, which makes it difficult to isolate nitrogen as the reason for the correlation.

(Sidik et al., 2014) found that urease activity was sustained over time and CaCO_3 was precipitated in organic soil (60% OC), where the amount of CaCO_3 was much smaller than that of similar studies in sandy soils. They suggest a possible inhibitory effect on the crystal growth from organic matter, but not the urease activity itself, while (O'Toole and Morgan, 1984) note that variations in organic content will have an impact on the urease capacity. The findings are inconsistent, where the low amount of precipitated CaCO_3 could be due to low urease activity or as a consequence of the organic content interfering in the crystal growth. The available research on these topics is limited and further studies should be conducted to clarify the effect of organic content on urease activity and crystal growth.

Work by (Van Paassen, 2009b), note that precipitation during MICP narrows the flow channels, which increase the flow velocity and reduce the residence time of injected substrates within the target area. This would likely reduce the urease activity per soil volume, which could indicate a need for a delay in the precipitation, where both bacterial suspension and cementation solution is distributed within the target area, before precipitation is initiated.

The CaCl_2 in the cementation solution ($\text{CaCl}_2/\text{urea}$) most commonly used in MICP, provide calcium ions and buffer the pH, whereas the urea increases the pH through the byproducts generated during ureolysis. In their work, (Tang et al., 2020) state that the concentration and proportion of cementation solution have a significant influence on the urease activity. (Whiffin, 2004) reported that concentrations of CaCl_2 exceeding 0,5M had an inhibitory effect on the urease activity of *S. pasteurii*, whereas concentrations $\leq 0,5\text{M}$ did not adversely affect the urease activity.

If a direct or indirect relation between urease activity and precipitation rate is assumed, the findings of (Whiffin, 2004) are consistent with studies that found optimal precipitation with concentrations of $\text{CaCl}_2/\text{urea}$ below 0,5 M (Cheng et al., 2016, Nemati and Voordouw, 2003, QABANY and Soga, 2014). The assumption of a relation between urease activity and precipitation, is in line with findings of (Nemati and Voordouw, 2003, Hammad et al., 2013), where the results show increased precipitation rate with increasing urease activity.

However, (Shahrokhi-Shahraki et al., 2015) achieved highest UCS at concentrations above 0,5 M, where share of urea had greater impact than share of CaCl_2 . This contradiction could be because the study used 85% and 100 % higher share of urea than CaCl_2 for those results. The high share of urea could generate a prolonged urease activity and a higher CCC. Grain size distribution and relative density of sample prior to treatment, could also be factors affecting the achieved UCS. However, a major part of the studies find that concentration $\leq 0,5\text{M}$, is favorable.

The urease of *S. pasteurii* is according to (Gorospe et al., 2013) sensitive to environmental stresses, where specific conditions promote optimal urease performance. However, the affecting factors have a limit where if exceeded, the enzyme performance is reduced. This suggests that knowledge of the limits of

affecting factors, could possibly be utilized to optimize cost of solution to achievable gain as well as sustaining optimal performance over time during treatment.

In their work (Shahrokhi-Shahraki et al., 2015), found that for same concentrations of urea/CaCl₂, increasing concentration of bacteria reduced the UCS. However, the levels of urease activity were not registered. The research previously discussed in this chapter is not conclusive on whether bacterial concentration can be directly correlated with level of urease activity. However, it is possible that increased density of bacteria could lead to a shorter duration of the urease activity, due to depletion of urea, oxygen or nutrients.

Work by (Gorospe et al., 2013) observed a decrease in urease activity, relative to pure urease enzyme when 0,5 mM of varying types of salts (incl. CaCl₂) were added to the urease, whereas (Hammes et al., 2003) found that adding 30 mM CaCl₂ to solution of urease enzyme increased the urease activity by 10 times. Given the data available from the studies, it is difficult to see an obvious reason for this contradiction. The extreme increase in urease activity due to CaCl₂ observed by (Hammes et al., 2003) is particularly surprising, given that CaCl₂ would lower the pH, which in turn would reduce the urease activity.

5.1.3 Ammonium as a byproduct

- **Challenges for the implementation of MICP in situ**
- **Factors affecting the MICP process**

For MICP to be a viable method for ground improvement, the dissolved ammonium (NH₄⁺) needs to be removed from the treated soil, while the volatile ammonia (NH₃) needs to be reduced or eliminated from the process.

(Lee et al., 2019a) state that high concentrations of NH₄⁺ in surface waters, decreases the pH and could stimulate growth of toxic algae and decrease amount of dissolved oxygen, produce toxins, and contribute to bacterial growth. The adverse effects of NH₄⁺ and NH₃ which in gas form is considered toxic under long-term exposure, emphasize the importance of developing a capacity for removal of these by-products post-treatment. The capacity and predictability of such a removal, is crucial for the viability of MICP as method for ground improvement.

In a large scale (1000 m³) MICP-treatment of sandy gravel, (Van der Star et al., 2011) managed to successfully remove the released NH₄⁺ with a high pH and high ionic strength rinse solution, while (Lee et al., 2019b) achieved over 90,6% removal of NH₄⁺, in MICP-treated sand columns (3,7m x 0,2 m x 0,2m). However, some residual adsorbed NH₄⁺ was found in the treated sand, where concentration (< 10%) of both sorbed and remaining aqueous NH₄⁺, increased with distance from injection point of rinse solution.

The findings suggest that removal of NH₄⁺ can be achieved in sand and gravel. However, further work is needed on 100% removal, residual sorbed NH₄⁺ and the decline in removal by distance from injection point. Low degree of remaining NH₄⁺ could possibly be acceptable, however the extended effect of low concentrations on the environment and ground water, is not clear.

(Van der Star et al., 2011, Van Paassen, 2009a) used sets of injection and extraction wells, creating a strong artificial flow to transport the rinse solution through the treated soil. It is possible that given a strong enough flow and shorter distances between injection and extraction, an acceptable degree of NH₄⁺ removal could be achieved. This suggestion is in line with findings of (Lee et al., 2019b), where treated soil less than 2,8 m from injection point achieved more than 98% final NH₄⁺ removal..

In their work, (Cheng et al., 2019) demonstrated with the one-phase low pH injection method, that the NH₃ released in the MICP process, can be significantly reduced. The findings of (Van der Star et al., 2011, Van Paassen, 2009a, Cheng et al., 2019) demonstrate that removal of NH₄⁺ can be achieved in both sand and gravel on larger scale in situ, where the demonstration of reduction in NH₃ by (Cheng et al., 2019) could possibly be directly transferable to viability in the field, due to the reduction being tied to the injected solution itself and not rinsing of mass. However, due to few field studies on NH₄⁺ removal, further work on in situ removal in granular soils, fine grained soils and granular soils with fines, is needed.

5.1.4 Geometric compatibility

- ***S. pasteurii as a causative agent for MICP in soils.***
- ***Factors affecting the MICP process***
- ***Challenges for the implementation of MICP in situ***

Understanding the compatibility between bacteria and a given soils pore size distribution, is important when evaluating the suitability of MICP as a method for ground improvement in different types of soil. Decreasing particle size and increasing density, lowers the compatibility i.e restrict the mobility of the bacteria within the soil.

Work by (Ingham, 2021) state that bacteria are 1 μm wide and somewhat longer in length, whereas (Mitchell and Santamarina, 2005a) note that they have a cell diameter in the range of 0.5–3 μm , where *S. pasteurii* usually is between 0,5-1,2 in diameter and 1,3-4 μm in length. (Ng et al., 2012a, Lin, 2016, Rebata-Landa, 2007) note that bacteria move through the soil via the pore throats between soil particles, either by self-induced movement or by passive diffusion, where they according to (El Mountassir et al., 2018) can attach themselves to particle contacts, pore throats or particle surfaces due to electrostatic net attractive forces.

(Rebata-Landa, 2007) note that habitable and traversable pores are found in coarse soils and in some clayey soils at shallow depth, where (Yang and van Elsas, 2018) note that they can find shelter inside pores in the range 0,2-6 μm , whereas porethroats with size equal to or lower than the cells size, will restrict any movement. The lower part of the range (0,2-6 μm) described by (Yang and van Elsas, 2018) could possibly include bacteria that are smaller than *S. pasteurii* (0,5-1,2 μm) in size.

In their work, (Ng et al., 2012a) state that bacteria up to 2 μm in size, can move freely within coarse silt to coarse sand ($d=0.05\text{-}2.0\text{ mm}$), where increasing share of fines in the soil, would limit or block the movement of bacteria within the soil. This is in line with several studies acheiving increased shear strength or reduction of porosity due to precipitated CaCO_3 in MICP-treated fine sands to coarse sands (Choi et al., 2020a, Rahman et al., 2020a, Cheng et al., 2013, Shahrokhi-Shahraki et al., 2015, Cheng et al., 2016). However, these result do not confirm self induced bacterial movement within the soil, where some studies applied drying of the cohesive soil before mixing, while mode of mixing is unclear in

others. It should be noted that most of these samples do not achieve uniform distribution of CaCO_3 within the sample despite the manual mixing of fluid into the soil. This underscores the challenge of injection and distribution of fluids in and within cohesive soils.

Bacteria that are manually mixed into a fine grained soil, could possibly be placed in a small pore (habitable pore space), but not be able to relocate from that space. It is not clear whether bacteria have the capacity to push on pore walls to expand the pore space, but it is unlikely. It is reasonable to assume that ureolytic bacteria such as *S. pasteurii*, will have difficulty in finding shelter within pores that are smaller than its own size. This would exclude a large share of pores in cohesive soils such as clays, where (Zaffar and Sheng-Gao, 2015) found 50% of pores in tested clay to be $< 0,01 \mu\text{m}$ and (Yang and van Elsas, 2018) 64,6-80,8% to be $< 2,5 \mu\text{m}$.

Work by (Lin, 2016) state that lack of habitable pore space and limited mobility between pores lead to a decrease in microbial presence with decreasing particle size and soil density, where (Mitchell and Santamarina, 2005a, Lin, 2016) suggest that limiting effective particle size (d_{10}) for bacterial mobility at 5 m depth is $1,03 \mu\text{m}$, $1,22 \mu\text{m}$ at 10 m and $1,5 \mu\text{m}$ at 20 m. The findings suggest that the cells would be trapped or inactive if placed in smaller pores, where increasing depth and content of fines would reduce the microbial activity.

The research further suggest that d_{10} of soil suitable for mobility, increases with depth. This could be due to higher overburden stress with depth, resulting in increased density with depth. The increased density with depth could suggest that the application of MICP in deeper sediments with increasing content of fines, could be a challenge. However, the increase in d_{10} ($\Delta d_{10}=0,47\mu\text{m}$) from 5 to 20m due to increased overburden stress or increased density, could possibly indicate a smaller effect on the geometric compatibility for the intended depth range for MICP.

(Rebata-Landa, 2007) note that bacteria in the soil are considered "active and motile" when the size of pores and pore throats are large enough to allow for cell movement, "trapped " when pore throats are too small to move within and "dead" when confining pressure due to depth in the soil profile, exceeds the resistance of the cell structure.

In the diagram for geometric compatibility proposed by (Mitchell and Santamarina, 2005a), very fine or very coarse soils fall outside the range of compatibility. However, successful dispersion of bacteria and precipitation in coarse gravel through MICP have been demonstrated by (Van der Star et al., 2011), while MICP in fine soils for the most part have been achieved with manual mixing i.e the fluid containing bacteria could not be dispersed by flow (Xiao et al., 2020, Cheng and Shahin, 2015, Kannan et al., 2020, Bing, 2015, Teng et al., 2020, Godavarthi Rajani, 2020).

The effect of constricted pore space on the bacteria's metabolic activity is an important aspect within the evaluation of the suitability of MICP in fine soils. Studies where clay is treated by manually mixing and where precipitated CaCO_3 is observed and increased strength is achieved, suggest that metabolic activity can be sustained in small pores (Xiao et al., 2020, Kannan et al., 2020, Islam et al., 2020, Bing, 2015). However, the issue of sustained metabolic activity within limited pore space, should be investigated further.

In their work, (Schijven et al., 2017) note that the macropores have more influence on the transport of bacteria within soil than the soil texture, where (Yang and van Elsas, 2018) state that pore to pore movement is easier for bacteria in fully saturated pores, compared to partially saturated pores, where the air in the pores hinders or reduces ability for microbial transfer. (Lamka et al., 1980, Zyman and Sorber, 1988) found that bacterial transport through soil is accelerated by heavy rainfall where the ionic strength of the pore water is reduced, thus reducing attractive forces from particles upon bacteria.

The research shows that macropores connected to the pore channels as well as saturated ground conditions, enhance the mobility of the bacteria within a pore system, where reduced attachment of bacteria as well as water flow caused by hydraulic boundaries, can increase the transport distance. The findings suggest that grain size distribution, depth and flow rate and salinity of injected suspension during MICP, could have a significant impact on the attachment and distribution of injected bacteria during MICP.

In work by (Lin, 2016), it is stated that pore and porethroat sizes correlate with particle size in silts and sands, whereas (Nimmo, 2004) state that the pores in clayey soils can be several times larger than the particles themselves and still be relatively enclosed. Through their work, (Zaffar and Sheng-Gao, 2015) found

that in three different clays with high (43-50,7%) clay content, 58% of the pores were below 5 μm and 24,3% below 0,1 μm , while (Chen et al., 2019) reported that in three different clays, 64,6-80,8% of the pores were below 2,5 μm , 11,6 - 21,3% between 2,5-10 μm and 4,2-13,6% above 10 μm .

The research indicate that a large part of the pores in cohesive soils such as clays, generally are too small to allow for microbial movement, whereas entrapment of cells within pores might be possible, where viability of precipitation in such conditions is unclear, but according to results from (Xiao et al., 2020, Kannan et al., 2020, Islam et al., 2020, Bing, 2015), it could be viable. This could suggest that excluding other factors such as the bacterias resistance to high shear forces and pressure, the ureolytic activity could be sustained if bacteria are mechanically mixed into the clay under high pressure.

5.1.5 Precipitation of CaCO_3

- ***S. pasteurii as a causative agent for MICP in soils.***
- ***Factors affecting the MICP process***
- ***Challenges for the implementation of MICP in situ***

The ureolytic bacteria produce urease enzyme that degrade urea through ureolysis, which generate dissolved ammonium and increases the pH of the solution, where the generated CO_3^{2-} together with supplied Ca^{2+} feeds the concentration until it reaches supersaturation and CaCO_3 is precipitated.

The concentration at supersaturation is suggested to affect the precipitation rate, which in turn is suggested to affect the cementation pattern and crystal morphology. Knowledge of how these and other factors such as temperature, concentration of cementation solution, bacterial density, level of saturation and particle size distribution affect the precipitation, is important for evaluating the choice of parameters during application of MICP, such that desired outcome post-treatment can be obtained.

In work by (Zhang et al., 2016a), it is noted that the Bacillus species, which *S. pasteurii* is a part of, displayed the most effective precipitation, whereas (Oliveira et al., 2015) reported that the *I. insulsalsae* bacteria generated more CaCO_3 than *S.pasteurii*. Work by (Liu et al., 2019) reported that *S.pasteurii* had more effective precipitation in an artificial soil than in a natural soil containing indigenous bacteria, while (Tobler et al., 2014) observed that *S. pasteurii* was capable of

consistent calcite precipitation, even if the indigenous environment lacked prior urease activity.

The research indicate that *S. pasteurii* have a high capacity for precipitation and that ureolysis is viable in soils without pre-existing CaCO_3 . Regarding the higher precipitation for *I. insulsalae*, it is unclear if other factors such as concentration of cementation solution, temperature or pH was more favorable for *I. insulsalae*, compared to *S. pasteurii* and if this affected the outcome. The more effective precipitation in artificial soil for *S. pasteurii* could be due to competing indigenous bacteria in the natural soil. This is important when considering MICP-treatment in a given soil, where high densities of indigenous populations could shorten the time before depletion of nutrients is reached.

The temperature have an effect on the urease activity, which in turn affect precipitation (Nemati and Voordouw, 2003, Hammad et al., 2013, Cheng et al., 2016, Konstantinou et al., 2021). In their work, (Nayanthara et al., 2019) found that *S. pasteurii* precipitated much higher amounts of CaCO_3 than several other ureolytic bacteria at 25 °C, while (Peng and Liu, 2019a) reported that *S. pasteurii* demonstrated effective precipitation in the range 10-30 °C, where the amount of precipitated CaCO_3 decreased with increasing temperature. (Cheng et al., 2016) reported that crystals at 25°C and 4°C generated more effective bonding, compared to those at 50°C. The effective crystals (4°C and 25°C) were precipitated at and around particle contacts, whereas the crystals at 50°C, mostly covered the grain surface.

The research show that *S. pasteurii* is capable of precipitation in the range 4°C-50°C. However, the amount and quality of precipitated CaCO_3 varies within that range. Results indicate a more effective bonding or higher effect per unit of CaCO_3 , at lower (4-25°C) temperatures. The findings suggest that the amount of precipitation is directly or more likely indirectly through level of urease activity, affected by the temperature. The decrease in amount of precipitated CaCO_3 with increasing temperature within the range 10-30°C, could suggest a decline in precipitation rate with increasing temperature. However this is not in line with findings of (Cheng et al., 2016), where precipitation at 50°C generated larger amounts of small crystals covering the particle surfaces. Increased amounts of small CaCO_3 crystals would most likely be due to increased precipitation rate or prolonged urease activity and precipitation. The findings are however not

conclusive and further work on the direct or indirect effect of temperature on precipitation rate and effect of precipitation rate on cementation pattern, are needed.

(Montoya, 2012) found that in MICP-treated (*S. pasteurii*) sands differentiated as rich in quartz, calcite, feldspar and iron oxide, the sand rich in calcite (CaCO_3) showed the fastest precipitation rate, whereas the sand rich in Iron (Fe) obtained the lowest rate. The findings indicate an effect from minerals on either urease activity and consequent precipitation or an interference from the minerals on the crystal growth, where (Sun et al., 2019c) found that clay minerals containing have an adverse effect on the urease activity. High concentrations of calcite could suggest that previous precipitation have taken place in the sand and that the mineral conditions are favorable. However, the calcite could also have its origin from weathered bedrock in limestone or from corals or shells.

Studies indicate that the degree of precipitation is affected by the level of urease activity, where an increase in urease activity leads to increased precipitation rate (Nemati and Voordouw, 2003, Hammad et al., 2013, Cheng et al., 2016, Konstantinou et al., 2021). The correlation between temperature and urease activity (Stocks-Fischer et al., 1999, Nayanthara et al., 2019, Gillman et al., 1995, Cacchio et al., 2003) could in extension most likely be transferred to correlation between urease activity and precipitation rate. Lower temperatures are associated with lower urease activity, slower precipitation rate and fewer but larger crystals, while higher temperatures with higher precipitation rate and a higher number of smaller crystals.

The fewer but larger crystals yields more effective cementation than the larger amount of smaller crystals. Effective in this context would be the achieved increase in effective bonding between particles per unit CaCO_3 , i.e precipitation at and around particle contacts and less in centre of the voids. However, one could argue that precipitation in the centre of the voids is favorable for geotechnical applications, where reduction of porosity or permeability is the only objective. On the other hand, increased effective strength through particle to particle cementation, would be favorable for applications where increased effective strength and residual permeability post-treatment, is the objective.

(Stocks-Fischer et al., 1999) found that the degree of precipitation was reduced for bacterial concentrations above 10^8 cells/ml. This suggests that the cell density might need to be balanced with available urea, oxygen and nutrients, so that the demand for nutrients do not exceed the availability, which could cause a decline in urease activity due to cell lysis and consequently a decline in precipitation. Balancing the demand (cell density) and availability could provide a prolonged and sustained urease activity and precipitation during MICP-treatment.

In their work, (Stocks-Fischer et al., 1999) further state that the higher the concentration at critical saturation, the higher the precipitation rate. It would be reasonable to think that the concentrations of CO_3^{2-} at supersaturation could be affected by the urease activity, given that it is the ureolysis that generate CO_3^{2-} , whereas Ca^{2+} is supplied through calcium in the soil or injected CaCl_2 .

The grain size distribution in a given soil could possibly affect the ease of flow for injected solutions, where work by (Kim et al., 2014) found that *S. pasteurii* generated about two times more CaCO_3 in sand than silt. The findings could possibly be due to the smaller sized pores in the silts affecting the metabolism or movement of the bacteria or clay minerals affecting the urease activity of the bacteria.

Precipitation occur when critical supersaturation driven by increasing pH, is reached (Paassen, 2009, Al-Thawadi and Cord-Ruwisch, 2012). In work by (El Mountassir et al., 2018), it is noted that due to reduced solubility of CaCO_3 with increasing pH, precipitation of CaCO_3 increases with rising pH, where (Kim et al., 2018) found optimal pH for precipitation by *S. pasteurii* to be between 7-9. The reason for the variation in optimal pH could possibly be due to variations in concentrations of Ca^{2+} , given that point of precipitation is a function of concentration of Ca^{2+} and pH, where (Stocks-Fischer et al., 1999) note that pH at critical supersaturation or equilibrium, is higher for water with lower calcium content such as soft water and lower for water with higher calcium content such as hard water.

The concentration of cementation solution (CaCl_2 /urea) can affect the precipitation, where (Stocks-Fischer et al., 1999) found an inhibitory effect on the urease activity from concentrations of CaCl_2 /urea above 0,5 M. (Cheng et al., 2016) observed peak amount of precipitated CaCO_3 with 0,4 M CaCl_2 /urea, whereas (Nemati and Voordouw, 2003) reported higher amounts of precipitated CaCO_3 by increasing the share of CaCl_2 from 0,045 to 0,27 M.

Major part of the studies described in this thesis, found concentrations $\leq 0,5$ M $\text{CaCl}_2/\text{urea}$, to be favorable for precipitation (Whiffin, 2004, Cheng et al., 2016, Nemati and Voordouw, 2003, QABANY and Soga, 2014, Stocks-Fischer et al., 1999). However, (Shahrokhi-Shahraki et al., 2015) achieved highest UCS with concentrations above 0,5 M, where the share of urea was larger than share of CaCl_2 . The reason for these results could possibly be due to the increased share of urea prolonging the duration of the urease activity, thus increasing the precipitation. However, variations in density in the samples prior to treatment or fluid distribution within the sample during treatment, could also have affected the achieved UCS.

Precipitation of CaCO_3 by ureolysis can utilize Mg^{2+} , in the same way as Ca^{2+} . It is noted by (Aamodt and Dahl, 2016) that Norway has lower concentrations of Mg^{2+} in the groundwater due to less soluble sedimentary rockbed in the subsurface. However, other regions can have groundwater which is rich in Mg^{2+} , and the effect of Mg^{2+} on the MICP process, is for that reason important to address.

Work by (Sun et al., 2019a) found that Mg^{2+} yielded a lower amount of precipitated CaCO_3 than Ca^{2+} under similar conditions, while work by (Nayanthara et al., 2019) found that optimal ratio ($\text{Mg}^{2+} : \text{Ca}^{2+}$) for precipitated amount of CaCO_3 for *S. pasteurii*, was 0,5:1 followed by 1:1, where 1:1 showed adverse effects on the morphology (long needle shaped) of the crystals. A high share of Mg^{2+} , could possibly be effective for reduction of permeability due to the larger amount of precipitated CaCO_3 and the larger size of the crystals, whereas they would most likely not contribute much to the effective bonding of the particles.

Soils rich in organic matter have high compressibility and are in general not suitable construction ground. In most cases where the organic deposits are shallow, they are removed and replaced by soil of better quality before construction. Replacement of soil masses is however expensive and contribute to increased heavy transport along the roads, depending on location of the replacing soil. However, organic content can be present in smaller amounts in sands, silts and clays. In their work (Sidik et al., 2014) found that urease activity was sustained over time and CaCO_3 was precipitated in organic soil (60%), where the amount of precipitated CaCO_3 was small, compared to similar studies in sandy soils. This is suggested to be due to an inhibitory effect of organic matter on continuous crystal growth.

The findings suggest that organic matter could disturb the crystal growth when adsorbed to the crystal surface, which could result in smaller crystals of poor structural quality. Further work is needed on the effects of lower organic content in granular and cohesive soils on the urease activity as well as crystal growth.

5.1.6 Calcium carbonate crystals

- ***S. pasteurii as a causative agent for MICP in soils.***
- ***Factors affecting the MICP process.***
- ***Challenges for the implementation of MICP in situ***

The quality, size and shape of the precipitated crystal can affect the cementation pattern, which govern the achieved alteration or improvement of the soils properties. Several factors such as cementation solution, organic matter, concentration at supersaturation and precipitation rate, can affect the morphology and crystalline qualities of the precipitated CaCO_3 . Knowledge of the factors affecting the crystal growth, is important for evaluating choice of parameters during MICP, such that adverse effects on crystal quality can be avoided and favorable or desired qualities, can be obtained.

The durability of the calcium carbonate (CaCO_3) binder is important when considering the intended service life of a geotechnical design, where (Bindu J, 2017) note that CaCO_3 crystals, will dissolve very slowly, either when continuously flushed by buffered acidic groundwater or as a result of acidifying processes in the pores. In that regard, (Gowthaman et al., 2020) found that the corrosion rate of CaCO_3 due to acidic rainfall, depend on the intensity and pH of the flushing rain, where the loss of shear strength is governed by CCC of the MICP-treated soil. They further found that loss of mass due to cyclic (up to 50 cycles) wetting and drying (WD), induced greater erosion in samples with the lowest CCC, where initial cycles and cycles above the 30th cycle, generated the greatest loss of mass per WD cycle.

The findings suggest that higher degrees of CCC in MICP-treated soils, could reduce loss of mass or shear strength due to corrosion or erosion. There is little that can be done with the occurrence of acidic rain or rain in general, but acidic ground conditions could be stabilized with lime. However, one of the objectives for developing MICP is to reduce the use of such products. Testing of pH in local groundwater, could possibly be required when evaluating the suitability of MICP

in a given area. The findings of (Gowthaman et al., 2021), suggest that a higher degree of erosion occur in the CaCO_3 mass at initial cycles and after 30 WD cycles, which could possibly be due to poorer crystallization of the outer mass and more cycles needed to wear down the mass, once this layer is eroded. However, the rate of erosion and the affecting factors are unclear.

(DeJong et al., 2009) suggest that pre-existing stable CaCO_3 in the target soil, could indicate favorable ground conditions for durability of CaCO_3 which have an expected design life above 50 years, under favorable soil conditions.

The findings indicate that in favorable ground condition, the expected design life of the CaCO_3 binder is comparable to cement and lime based binders. The comparability of the CaCO_3 binders durability with that of other cement based binders, is an important finding in respect to the competitiveness of MICP as an alternative method for ground improvement.

The effect of curing time on achieved shear strength in MICP-treated soil, is important for the determination of time for sampling for comparison of achieved shear strength up against the geotechnical design criteria, during quality control post-treatment.

Work by (Teng et al., 2020), reported on an increase in UCS with increasing curing time (1 to 7 days) in MICP-treated silty clay, while (Godavarthi Rajani, 2020) found a greater increment of increase in UCS for MICP-treated high plasticity clay from 14 to 28 days of curing than from 3-14 days of curing. (Oyediran and Ayeni, 2020) found that CCC determined the initial and final shear strength (1-7 days) in MICP-treated sandy silt, while the rate of increase in shear strength with curing time, was similar for different CCC i.e independent of degree of cementation.

The findings indicate that significant increase in shear strength can occur between 14-28 days of curing in cohesive soils, whereas curing time in granular soils is unclear. This could suggest the need for up to a 4 week time span before final tested shear strength is compared up against design criteria. However, due to lack of findings on curing time in sands, the effect of curing on shear strength in such soils is unclear and should be investigated.

In their work, (Tang et al., 2020) notes that due to different ureolytic bacteria depositing different extracellular polymeric substances (EPS) on the cell surface, precipitated crystal type (CaCO_3) and morphology will vary, depending on type of bacteria strain. (Zehner et al., 2020) state that CaCO_3 can crystallize in different polymorphs such as calcite, vaterite and aragonite, where calcite is the most common, due to its low solubility in water (Stocks-Fischer et al., 1999, Okwadha and Li, 2010). (Paassen, 2009) found that high rates of ureolysis produced spherical vaterite, while lower rates generated mostly rhomboidal calcite crystals.

The vaterite being predominant at high rates of ureolysis, could be due to an extended period of supersturation, as noted in work by (Paassen, 2009). Higher rates of ureolysis is likely to increase the concentration of supersaturation in the solution, which is prolonged due to a continuous generation of CO_3^{2-} , as long as urea is available. Consequently, precipitation of metastable precursors such as vaterite, is the most likely outcome, whereas a decline in rate of ureolysis with reduced availability of urea (depletion), would lower the concentration of supersaturation, resulting in kinetically favoured precipitation of calcite over vaterite

Work by (Cheng et al., 2016) found that high temperature and high urease activity (*S.pasteurii*) formed small crystals, whereas low temperature and low urease activity formed clusters of larger crystals. In their work, (Xu et al., 2017) observed increasing crystal size and change in crystal shape with increasing concentrations of Ca^{2+} , while (Nayanthara et al., 2019) found that increasing the $\text{Mg}^{2+}/\text{Ca}^{2+}$ ratio from 0.43 to 1 in the cementation solution, generated long needle shaped crystals, which filled the voids.

The findings of (Xu et al., 2017) suggest that Ca^{2+} concentration have a significant effect on crystal growth, which is plausible given that Ca^{2+} is a main component of the precipitated mineral. Increased concentrations of Mg^{2+} seem to generate a crystal morphology, which most likely will have a lower resistance to compressive forces than square or spherical crystals.

(Al-Thawadi and Cord-Ruwisch, 2012) found that increasing bacterial density increased the size of precipitated crystals, while (Xu et al., 2017) suggested that the bacterial density was related to the surface structure and less to the crystal size. (Cheng et al., 2007) found that low bacterial concentrations generate cubic crystals, whereas high cell concentration lead to the formation of spherical crystals.

The findings suggest an effect from bacterial density on crystal growth, but is not converging on what aspect of the crystal growth it affects. As noted by (Cheng et al., 2007), the available space between nucleation sites (cells) could affect the crystal shape. It is possible that lower bacterial density would provide greater space between nucleation sites (cell surfaces), while higher density would lead to less space, where cubical crystals would acquire more space than spherical. This could possibly explain the changes in shape occurring due to change in bacterial density.

In work by Whiffin (2004), a lower precipitation rate and larger crystals at pH below 8 was observed, while (Cheng et al., 2007) found that precipitation by *S. pasteurii* generated spherical shaped crystals at pH 8.0 and square shaped crystals at pH 9, where both generated calcite as output mineral.

The findings indicate that pH may affect the size and shape of precipitated crystals. The temperature and amount of available urea will affect the rate of ureolysis, which in turn will affect pH and concentration at supersaturation. It is for this reason, difficult to isolate the effect of pH on the crystal morphology.

Work by (Jianyun, 2005) reported on precipitated calcite at 5°C and 25°C, while calcite and vaterite was precipitated at 50 °C, where the crystals at 5°C and 50°C were amorphous, while crystalline at 25°C. The reason for the amorphous mineral structure observed by (Jianyun, 2005) at 5 °C and 50°C, is not clear. It would be reasonable to expect similar mineral structure for crystals at 5°C and 25°C and possibly a deviation from that at 50°C, given the similar larger crystal size of good quality reported by (Cheng et al., 2016) at 4°C and 25°C and smaller crystals of poorer quality at 50°C. The urease activity was most likely higher at 25°C than at 5°C, which could have generated higher concentrations at supersaturation and affect the mineral structure of the precipitated CaCO₃. An amorphous structure would likely translate to ductile properties in the cementation bond, while the crystalline structure could be assumed to be harder but generate a more brittle behaviour in the bond during applied stress.

(Wang et al., 2019) reported that longer intervals between injection cycles of cementation solution (CaCl₂/urea), generated larger crystals, compared to shorter intervals. (Al-Thawadi and Cord-Ruwisch, 2012) found a sharp rise in crystal size when concentration of cementation solution (CaCl₂/urea [1:1]) was raised

from 0,055 M to 0,258 M and a flattening in crystal size, when further increased from 0,258 M to 1,255 M.

The findings indicate that cementation solution may have an effect on the crystal growth. This is a reasonable assumption, given that urea would increase the level of urease activity and concentrations of generated CO_3^{2-} , while CaCl_2 would increase concentrations of Ca^{2+} , leading to increased concentrations at supersaturation and consequently increased precipitation rate. Increased rates would most likely generate smaller crystals, while lower rates would generate larger crystals. The flattening of crystal growth (size) observed when a certain concentration was exceeded, is in line with findings of (Stocks-Fischer et al., 1999, Al-Thawadi and Cord-Ruwisch, 2012), where concentrations of $\text{CaCl}_2/\text{urea}$ above 0,5 M was found to have an inhibitory effect which is tied to increasing concentrations of CaCl_2 and not urea. The larger size of crystals observed at longer intervals between injection cycles ($\text{CaCl}_2/\text{urea}$), could possibly be due to the crystals having sufficient time to grow before new supply of Ca^{2+} is introduced.

5.1.7 Effect of particle characteristics

- ***S. pasteurii as a causative agent for MICP in soils.***
- ***Factors affecting the MICP process.***
- ***Challenges for the implementation of MICP in situ***

Particle shape, size and surface roughness have an effect on the mechanical properties of untreated granular soils. It is important to evaluate any transferability of such characteristics onto cementation post-treatment, or if the characteristics themselves, affect the level of increment in shear strength achieved in the soil post-treatment.

As noted by (Sandven et al., 2017, Alshibli and Alsaleh, 2004), the mineral type, particle shape and surface roughness effect the effective shear strength of granular soils, due to the internal friction caused during shear. In their work, (Alshibli and Alsaleh, 2003) note that angular particles yield greater internal friction than rounded particles, where the internal friction angle increases with increasing angularity. The findings are reasonable. Surface roughness and particle angularity would cause higher friction and resistance than smooth particles, when they slide against each other under pressure, thus a higher friction angle with increasing angularity and surface roughness, is as expected. However, increased friction in

granular soils can be affected by the state of density prior to and during shear, where (Mitchell and Santamarina, 2005a) note that soils with angular shaped particles, tend to be less dense than soils with more rounded particles.

Work by (Rebata-Landa, 2007) reported that particle sizes between 0,01-0,1 mm achieve the most effective cementation, while (Mortensen et al., 2011b) suggested that the high number of contact points in well graded and compacted soils, are favorable for achieving effective cementation. In their work, (Ismail et al., 2002) reported on better particle bonding through cementation in fine rounded particles, than in coarse round particles.

The findings by (Rebata-Landa, 2007) suggest effective cementation for particles in the range medium silt to fine sand. It is possible that the number of contact points per soil volume i.e particle size and degree of compaction, have more impact than the particle size itself. However, one could argue that increased degree of compaction would reduce the voids, thus reducing the flow and distribution of injected liquids in the soil, which would lead to lower degree of spatial distribution of CaCO_3 binder within the soil.

Uniform fine particled granular soils will have more particle contacts per volume than coarser uniform granular soil. In well graded soils the finer particles would fill the voids between larger particles, which also would increase number of contact points per volume. At similar particle size, a loose uniform fine sand could be expected to achieve lower degree of cementation or shear strength post-treatment than a dense uniform fine sand.

It is not clear whether the effect of particle characteristics on shear strength in untreated granular soil, can be directly transferred onto the increased achieved shear strength in treated soils. However, if the increment in increased shear strength post-treatment is greater for some particular particle characteristics, they would likely have an influence on the degree of cementation or pattern of cementation.

In their work, (Nafisi et al., 2018) found that MICP-treated coarse angular sand, achieved a higher degree (50%) of improvement in shear strength than treated coarse round sand (35%). They further found that the interparticle cementation was more effective in the angular coarse particles, than in round coarse particles. The findings suggest that the particle shape have an influence on the achieved

effect in shear strength post-treatment, in granular soils. It would be reasonable to assume that cementation at and around particle contacts would be favorable for increased shear strength. It is not clear whether increased particle angularity would provide more contactpoints, where (Mitchell and Santamarina, 2005a) found round particles to provide a higher density than angular particles. However, cementation on rough surfaces such as in angular particles, could possibly yield higher friction during shear than cementation on smoother surfaces such as in round particles.

In their work, (Nafisi et al., 2018) further used numerical modelling (Discrete Element modelling) to investigate the effect of particle shape on cementation, in triaxial shear. The results showed that angular particles are favorable and that degree of improved shear strength in cemented soil is determined by the bonding radius of the particle contacts. The findings suggest that increased radius of the parallel bond in cemented particles, increases the strength of the bond. The findings can be considered as reasonable, due to a wider bond being more stable and more resistant to shear or tensile forces acting upon the bond.

5.1.8 Cementation pattern

- ***Factors affecting the MICP process.***
- ***Challenges for the implementation of MICP in situ***

The cementation pattern may influence the strength and hydraulic properties of the soil post-treatment. Different geotechnical applications will have different requirements in properties and for this reason it is important to identify factors affecting the cementation pattern, so that these factors can be considered when utilizing MICP in a given soil. For the evaluation of the viability of MICP as a method for ground improvement, it is also important to investigate if the research indicate that cementation pattern and residual permeability can be controlled with a degree of predictability.

In their work, (Cheng et al., 2016, Al Qabany et al., 2012) note that the cementation pattern influence the flow properties of porous media, where (Al Qabany et al., 2012) state that it also affects the stress or load transfer between particles. (Rong and Qian, 2012) state that cementation patterns can occur as crystal growth on particle surfaces, at or near particle contacts, in voids with bridging of particles or in voids without bridging of particles.

The findings suggest that several cementation patterns can occur as a result of precipitation during MICP in soils. It would be reasonable to assume that the patterns acceptable for geotechnical applications, would be crystal growth in voids with or without bridging for reduction of porosity, crystal growth in voids with bridging for improvement of compressibility with no concerns regarding residual permeability and particle contact cementation for improvement of shear strength and stiffness, where residual permeability post-treatment is critical.

(Cui et al., 2017a) note that the crystal growth can be classified as either effective or non-effective crystals, where effective crystals can be further classified as particle-contact cementation and crystal-crystal cementation, where parts of the areas around the particle contacts as well as the particle contacts themselves, are cemented. They further note that, at lower cementation level, the effective crystals are mainly precipitated as particle-contact cementation, while at increased cementation level, effective crystals are precipitated as crystal-crystal cementation.

The findings suggest that cementation of the particle contacts are predominant at lower precipitation rates, whereas higher rates generate crystal to crystal cementation, i.e particle contact cementation with further growth occurring. This kind of precipitation pattern would likely also fill into the void space around the contact points, reducing the residual permeability.

In work by (Cheng et al., 2013), they found that lower degree of saturation in fine and coarse MICP-treated sand, was favorable for obtaining residual permeability post-treatment. It is reasonable to assume that level of saturation in the soil could also affect the cementation pattern, where air in partially saturated pores would push injected solutions against the particle contacts, whereas the injected solution in saturated pores would be distributed evenly in the pore, resulting in a higher degree of reduction of the pore space.

Given that the generated cementation pattern could affect the achieved particle bonding and residual permeability post-treatment, the ability to control the precipitation rate through regulation of affecting factors, might be required to achieve a cementation pattern which is suitable for a given geotechnical application of MICP. The findings indicate potential for control of cementation pattern through the control of precipitation rate. However, the reproducibility and predictability

of the results behind this indication, suggest further work on the matter, where the effect of saturation on the cementation pattern, should be included.

5.1.9 Flow and bacterial retention

- ***Factors affecting the MICP process.***
- ***Challenges for the implementation of MICP in situ***

To ensure an adequate spatial distribution of CaCO_3 binder within the target area during MICP-treatment, the flow velocity need to be compatible with the objectives of long reach and sufficient attachment of bacteria within the target area. A too low velocity could result in clogging around the injection point and a short reach, while too high velocity could flush the bacteria past the target area. High salinity solutions could lead to flocculation of bacteria and accumulation of CaCO_3 which reduce the flow, but enhance the bacterial attachment by increasing the attractive forces from particle surfaces acting upon the bacteria. The evaluation of proposed strategies for fluid flow and bacterial attachment or retention, is important in order to ensure an approach adapted towards obtaining adequate spatial distribution of the alteration or enhancement of the soils properties, across the target area.

High salinity fluids such as CaCl_2 causes due to attractive forces, the bacteria to attach to the soil particles, whereas low salinity fluids such as rainwater will reduce these forces. (Cheng et al., 2016) found that flushing MICP-treated sand with fresh water (simulation of heavy rain fall), decreased the efficiency of urea conversion down to less than 5%, which consequently yielded a very low precipitation ($\text{CCC} < 0,3\%$), whereas the control sample achieved 10 times higher CCC. The low CCC for flushed samples is suggested to be due to washing out of bacteria and substrates during flushing, where (Cheng et al., 2016) state that insufficient bacteria retention could lead to the bacteria being flushed away or detached by cyclic injections.

The attachment of bacteria along the flow paths post-injection is of great importance for the consequent distribution of CaCO_3 binder in the soil. The findings could suggest that MICP-treatment during heavy rainfall in permeable soils should be avoided, or could possibly require an increase in the concentration of fixation fluids, so that the attractive forces acting upon the bacteria from the particle

surfaces are intensified. However, it is unclear if this would have any effect on the retention of injected substrates.

(Ng et al., 2012a, Harkes et al., 2010b) note that high salinity solution drives bacterial flocculation, which supports the adsorption and retention of bacteria, where (Ng et al., 2012a) adds that low salinity solutions such as fresh water, reduce the degree of bacterial attachment along a flowpath, while (Harkes et al., 2010b) suggest that both adsorption (high salinity) and increased transport distance (low salinity), can be achieved by controlling salinity in fixation fluids.

It is reasonable to think that flocculation of bacteria could result in points with accumulated CaCO_3 crystals along the flow paths, causing stagnation in the flow. This could possibly be avoided by using low pH solutions that delay the precipitation. However, the findings of (Cheng et al., 2016) suggest a very low attachment of bacteria during flow of solutions with low pH.

The retention of bacteria along the flow path is crucial and the use of low salinity solutions might be problematic in achieving this objective, while increased injection pressure in combination with high salinity fixation fluids could possibly enable the fluids to reach far enough into the target area with sufficient bacteria retention along the flowpath. However, a reduction of bacterial and substrate density along flowpath should be expected at any flow rate and strategies that address this issue, should be integrated into potential injection methods in situ.

(El Mountassir et al., 2018) note that high flow velocity can reduce bacterial attachment, while (Minto et al., 2019, Van Paassen, 2009a) suggest that flow velocity can be used to control the location of precipitation. (Minto et al., 2019) suggest that constant pressure rather than constant flow rate, or sequentially decreasing the flow rate for each injection cycle, may enhance the spatial distribution of bacteria within the target area.

Controlling the distribution by regulating the flow velocity is a plausible approach to ensure adequate spatial distribution of liquids. The use of constant pressure during injection instead of constant flow rate, could possibly counteract stagnation in flow due to narrowing of flow paths by precipitated CaCO_3 . The reasoning behind a sequential decrease in flow rate per injection cycle, is not clear. However, if one assumes a decline in density of both bacteria and cementation solution with distance from injection point, such an approach could lead to a higher

density close to injection points, compared to further away from the injection points.

In their work, (Cuthbert et al., 2013) proposed to mix CaCl_2 :urea (0,2 M:0,4M) into the bacterial suspension before injection, to achieve adequate retention of bacteria in a desired area. This approach would most likely create problems with clogging around the injection point due to early initiation of precipitation.

5.1.10 Injection strategies and spatial distribution of CaCO_3 binder

- ***Factors affecting the MICP process.***
- ***Challenges for the implementation of MICP in situ***

When designing geotechnical solutions, the engineer needs to rely on a given shear strength or parameter, being well distributed throughout the treated soil volume. For MICP to be a competitive and viable method for ground improvement, it is necessary to achieve a satisfactory spatial distribution of the precipitated CaCO_3 binder within the target soil. To achieve this, injection strategies need to be adapted such that both concentration of bacteria and cementation solution are approximately equally distributed within the target area.

(Knappett and Craig, 2012) note that in stratified soil deposits, the permeability for flow parallel to the direction of stratification, is higher than for flow perpendicular to the direction of stratification. This could suggest a need for shorter vertical distance between injection points on injection wells with multiple injection valves with depth.

In their work, (Whiffin et al., 2007) developed the two-phase injection method, where an injection of bacterial culture is followed by an injection of cementation solution, while (Cheng and Cord-Ruwisch, 2012) proposed a modified two-phase method, integrating a retention period between the injection of bacteria suspension and the following injection of cementation solution. (Harkes et al., 2010a) introduced a multi-phased procedure, where first a bacterial suspension is injected, then a fixation solution is injected followed by injection of cementation solution.

The strategies proposed by (Whiffin et al., 2007, Cheng and Cord-Ruwisch, 2012) applied the same injection direction for both bacterial suspension and cementation solution, where the achieved spatial distribution was non-uniform.

However, the strategy proposed by (Harkes et al., 2010a), using fixation fluids during a retention period, could possibly be beneficial to enhance the uniformity of the distribution by reducing the number of bacteria that are flushed past the target area in porous soils, during injection cycles of cementation solution. The retention period would most likely give time for bacteria to disperse and attach within the soil structure before precipitation is initiated upon supply of cementation solution. However, these procedures are extensive and would increase the cost of the treatment.

Due to rapid precipitation causing clogging around the injection point (Harkes et al., 2010a), work by (Al Qabany et al., 2012) modified the approach by slowing the flow rate of injected bacterial solution, whereas (Whiffin et al., 2007) suggested increasing the flow rate of injected cementation solution.

It is reasonable to assume that higher flow rate, if applied to both injection of bacteria as well as injection of cementation solution, could increase the distance of liquid into the target area. However, it could also reduce bacterial attachment along flow path, where an increase in the concentration of the fixation solution to increase attractive forces acting upon the bacteria from the particles, could be required.

Even in porous soil, the movement of bacteria is slow. Distribution of bacteria in the target area would be dependent on transportation through the flow of the injected liquid or assisted flow through hydraulic gradients in the sub-surface. However, minor movement locally in macropores could possibly occur within the time frame of the treatment. The approach of slowing the injection rate of the bacterial solution could possibly be favorable for a more even distribution of bacteria along the flowpath. However, the bacterial density will most likely decline with distance from injection point at any flow rate.

In their work, (Cheng et al., 2014) applied surface percolation in coarse and highly permeable soil by trickling bacterial suspension and cementation solution alternately on the soil surface. This approach could possibly be viable for applications targeting surface erosions in slopes with granular surface layers, reduction of porosity at shallow depths or strengthening base layers for foundations. The approach would be particularly dependent on adequate permeability in the surface layer, due to the fluid flow not being controlled or regulated, as in the

case of injections. Surface percolation would most likely not be applicable in low permeability soils.

(Zhao et al., 2014, Xiao et al., 2020) used mechanically mixing of bacteria and cementation into sand and clay in small scale samples, while (Gomez et al., 2018) used stimulation of existing ureolytic bacteria in the sub-surface (biostimulation), where nutrients and cementation solution is injected. The method showed varying results, but did successfully induce precipitation in samples of granular soil extracted from up to 12 m depth. (Kannan et al., 2020, Islam et al., 2020) used bio-stimulation in marine clay and clayey soil to clay, where (Kannan et al., 2020) reported on unsuccessful bio-stimulation but successful bioaugmentation in marine clay, while (Islam et al., 2020) reported on varying degree of cementation for different shares of fines in clayey soil to clay.

The approach of stimulating pre-existing ureolytic bacteria in the sub-surface could be considered a more economically viable method compared to other injection methods, given the cost of cultivating bacteria. However, it is dependent upon sufficient amounts and distribution of bacteria in the soil volume. Further, it is also dependent on an exponential growth occurring in the soil when nutrients are introduced, where capacity for anoxic growth below the watertable is unclear, but unlikely. It is difficult to see this approach as a dependable, consistent and reproducible method for ground improvement.

When considering bio-stimulation in the context of ground improvement in cohesive soils, one could entertain the idea of stimulating trapped bacteria within the small pores. However, the injection of nutrients or cementation solution would meet the same challenges as the other strategies such as low permeability causing the intrusion and flow to be very difficult and time consuming. Further, the work by (Kannan et al., 2020) suggest few or no bacteria in the clay. This could of course vary with location and depth, but it underscores the uncertainty and lack of predictability of this approach.

Work by (Cheng and Shahin, 2015) found that low pressure injection was only suitable for sand with less than 5% clay, whereas manually mixing of bacterial suspension followed by injection of cementation solution in sand with up to 10% clay, resulted in good distribution of cementation. The findings might indicate that the flow of injected fluid is restricted before the bacterial metabolism, during an increase in fines. However, due to lack of findings of any effects of limited

pore space on the bacteria's metabolism, such a correlation is still unclear. Introduction of fluids through injections in low permeability soils, would most likely require simultaneously applied, high injection pressure and mechanical mixing in situ.

In their work, (Cheng et al., 2019) developed a low pH one-phased integrated solution, where bacteria and urea/CaCl₂ was injected simultaneously, while (Van Paassen, 2009a, Van der Star et al., 2011) applied injection and extraction wells in a grid pattern, creating an artificial gradient transporting the injected solutions through a designated area. The strategy proposed by (Cheng et al., 2019), ensures a delay in the precipitation due to the initial low pH in the solution, where it should be mentioned that (El Mountassir et al., 2018) previously had suggested delaying precipitation by adding hydrochloric acid to solution for lowering the pH.

The low pH one-phase solution demonstrated by (Cheng et al., 2019), enables the injected solutions to reach further into the soil, before precipitation which could reduce the void size and limit the flowpaths, is initiated. The combination of injection and extraction wells, could enable better control of flow throughout the target area and particularly in areas where natural hydraulic boundaries are not sufficient to create a steady flow.

In their work, (Ginn et al., 2001) suggest that bacteria injected through the pore space of soils, most likely are filtered through the sand with a long-linear reduction of microbe concentration along the flow path. Work by (DeJong et al., 2009), suggested a reversed injection direction of cementation solution, relative to the direction of injected bacterial suspension. As noted by (Ginn et al., 2001), concentration of injected fluid is likely to decline with distance from injection point, where the reversed injection of cementation solution proposed by (DeJong et al., 2009), could possibly address the problem with poor spatial distribution of precipitated CaCO₃. This strategy could possibly ensure that the higher number of bacteria located at one injection point receive less cementation solution and the lower number of bacteria at opposite injection point, receive high concentrations of cementation solution.

It would further be reasonable to evaluate the possibility of applying injections of the low pH one-phase method proposed by (Cheng et al., 2019) in both directions, where the integrated solution (Bacteria + CaCl₂/urea) could be injected as a single injection first in one direction and then followed by an injection in the

opposite direction through injection and extraction wells in a grid pattern as demonstrated by (Van Paassen, 2009a, Van der Star et al., 2011). The injection and extraction wells would need pumps that can switch from push to pull in an easy and rapid manner. The low pH would delay precipitation and enable a proper dispersion of both bacteria and cementation solution in the target area, while the reversed injection would provide more uniform distribution of both bacteria and cementation solution along the flowpath.

The different injection methods discussed in this chapter show a compatibility with granular soils. However, when considering injection strategies for fine grained cohesive soils with high share of small pores, the different proposed methods for introducing bacterial and cementation fluids are due to the low permeability, most likely not applicable. Most research conducted on such soils in the context of MICP, have applied some form of mechanical dry mixing in the lab.

Simultaneously applied, high injection pressure and mechanical mixing is an appealing technique in regards to geotechnical design, due to the reliability in spatial distribution and possibility for reaching deeper layers in the sub-surface. Such an approach, would however require a better knowledge on the particular ureolytic bacterias ability to endure high pressures and shear forces as well as the effect of clay minerals and small voids on the metabolic activity of the bacteria. This approach would eliminate the dependency on flow and bacterial transport, given a sustained urease activity of trapped bacteria.

The available research describes manually mixing of the solutions into the cohesive soil, hence it is not applicable for evaluating the approach of simultaneously applied, high injection pressure and mechanical mixing in situ. This approach could most likely use the one-phase low pH solution proposed by (Cheng et al., 2019). However, it is unclear if strategies such as injections of retarded oxygen releasers due to anoxic conditions, is compatible with this approach.

Two of the drivers for developing MICP as an alternative ground improvement method, is to reduce the footprint of heavy machinery on the ground surface, reducing the disturbance to the soil due to high injection pressures and reducing noise pollution. The high pressure mixing approach would most likely require the use of loud and heavy machinery and definitely high injection pressure, which would counteract three of the objectives with developing the method. However, this

approach is only suggested for MICP in cohesive soils and it would reduce the use of cement, which is a very important incentive and objective.

5.1.11 Comparison of methods

The competitiveness of MICP in respect to other methods utilizing cement, lime and ash products will have an effect on whether MICP will be adopted as a new method for ground improvement in the industry. Work by (Umar et al., 2019) compared MICP-treatment with lime treatment in residual soil, where the sample treated with only MICP, achieved lower UCS than sample treated with lime and sample treated with MICP and lime. The samples treated with only lime and lime and MICP, increased the UCS significantly over time, whereas the sample treated with only MICP, lost shear strength over time.

The findings suggest both an initially higher shear strength post-treatment as well as higher rate of increase in shear strength with curing time, for samples treated with lime and MICP and lime compared to sample treated with only MICP, where the productive curing time for this sample was significantly shorter. However, the residual soil used in the study contained high share of fines as well as high share of very coarse soil (gravel), which both have been associated with lower cementation effect during MICP. Due to lack of findings on such a comparison in sand, it is unclear whether the gap between MICP treated sample and samples treated with lime would have been smaller, given the higher achieved shear strength in MICP-treated sands, demonstrated in the literature.

(Oyediran and Ayeni, 2020) compared the use of Portland cement, Ash and MICP in highly plastic weathered soil consisting of 55,8% fines, 35,9 % sand and 8,3% gravel. The results showed slightly higher UCS for samples treated with cement compared to samples treated with MICP or ash, but the UCS is higher for samples treated with ash or MICP after 3 days of curing, but higher at 7 and 28 days of curing. The rate of increase in shear strength is similar for cement and MICP in the range of 5-10% in additives, whereas the rate of increase is significantly higher for samples treated with cement when percentage additives, is increased from 10 to 15%.

Contrary to findings by (Umar et al., 2019), the gap between initial shear strength post-treatment for samples treated with MICP and cement is smaller. This could possibly be due to the smaller share of gravel in this study compared to

that of (Umar et al., 2019), where the share of fines and sand are similar for the two studies. The reason for the difference in effect of additives above 10 %, is unclear, but could possibly be due to longer hydration process in cement, compared to conversion of urea during MICP.

5.2 MICP-treated granular soils

Part of the objectives of this thesis is to research the factors affecting the MICP process. The findings are:

Unconfined compression strength

- *The research show that UCS increases exponentially with increasing CCC for $CCC \geq 5\%$.*
- *Findings are not conclusive regarding the effect of urease activity on achieved UCS, but lower levels of urease activity and temperatures (4 and 25°C) are indicated to generate effective particle bonding i.e increased effective shear strength.*
- *Findings indicate that fine sand with lower porosity have greater resistance to FT cycles, compared to coarse sand with higher porosity, where findings suggest a 1% reduction in UCS per FT cycle up to 10 FT cycles. It is not clear whether the rate of reduction is linear with number of FT cycles, where further research using a higher number of FT cycles, is needed to evaluate the effect of long-term exposure on the binder.*
- *The findings indicate that concentrations $\leq 0,5$ M of cementation solution ($\text{CaCl}_2/\text{urea}$), are favorable for achieved UCS post-treatment, where increased share of urea is indicated to have a positive effect, while increased share of CaCl_2 is indicated to have an adverse effect.*

Triaxial shear strength and volumetric response

- *The research show that the shear strength of MICP-treated sands, increase with increasing CCC, where increasing initial D_r and P'_o is indicated to be favorable for achieved shear strength post-treatment.*

- *The main contribution to the increased shear strength in granular soils, is indicated to be due to increased cohesion generated by the cementation of the particles. A contribution to a higher friction angle in smooth round particles, could however be possible due to increased surface roughness of cemented particles post-treatment.*
- *The findings further suggest that MICP-treatment of sands lead to an increase in brittleness, an increase in dilatancy under drained shear, an increase in peak and critical shear strength and a reduction in generated excess pore pressure during undrained shear.*
- *Low levels of cementation (CCC < 3%) in MICP-treated sands, are indicated to not provide any significant change in drained volumetric response from untreated to treated state.*
- *MICP-treated silty sand (25-35%) showed an increase in peak and critical shear strength with increasing silt content, improved resistance to liquefaction and a reduction in excess pore pressure generated during undrained shear. However, the increment in reduction of excess pore pressure was lower for silty sand than sand.*

Reduction of porosity and residual permeability

- *The findings show that reduction of permeability due to precipitated CaCO_3 in granular soils, is closely related to CCC, where MICP-treated coarse sand is indicated to achieve a greater degree of reduction in permeability with increasing CCC, compared to fine sand.*
- *The residual permeability in MICP-treated fine to coarse sand is comparable to that of untreated coarse silt to fine sand.*
- *Partial pore saturation and coarser sands is indicated to be favorable for achieving enhanced strength, while sustaining residual permeability post-treatment. Further research on the effect of saturation level on precipitation pattern, is needed.*
- *The findings suggest an increased precipitation rate, increased CCC and an increasing increment in reduction of permeability with increasing concentration of cementation solution ($\text{CaCl}_2/\text{urea}$), where increased share of urea is found to be favorable for longer and faster precipitation, resulting in higher CCC.*
- *Grain size and density prior to treatment can affect the magnitude of the increment in reduction of permeability.*

- *Findings regarding the effect of urease activity on reduction of permeability in MICP-treated sand, are inconsistent. However, findings indicate that high urease activity lead to higher precipitation rate and CCC, where higher precipitation rate can lead to more precipitation in the voids and consequently a greater reduction of permeability.*
- *The control of residual permeability is indicated to be feasible through control of precipitation rate, which affect the cementation pattern. However, degree of saturation could have an effect on the cementation pattern, independent of the controlling factors on precipitation rate. This suggest a need for further research for a proper evaluation of controllability and predictability of residual permeability during MICP-treatment.*

5.2.1 Unconfined compression strength

- ***Acheived enhancement of shear strength in MICP-treated granular soils***
- ***Challenges for the implementation of MICP in situ***

Through their own research or through reviews of previous studies, (Choi et al., 2020a, Rahman et al., 2020a, Cheng et al., 2013) found exponentially increasing UCS with increasing CCC in MICP-treated sands. However, (Rahman et al., 2020a) reported on high variability in the exponential trend for CCC less than 5%.

The findings show that CCC is closely related to acheived UCS in MICP-treated sands. It is not clear whether the variation in the findings for $CCC \leq 5\%$, are due to the lower CCC or poor spatial distribution of the CCC. The CCC adresses the amount of $CaCO_3$ per volume and not the spatial distribution, crystal quality, crystal size, cementation pattern or the morpholgy of the precipitated crystals. However, the increase in UCS can give an indication of the quality, distribution and pattern of the cementation. Long and needle shaped crystals would most likely offer little resistance to compression, whereas shorter cubical or spherical crystals cemented in a contact-contact or crystal-crystal pattern, would likely offer significantly higher resistance. Unconfined compression induces shear in the sample and it would be reasonable to assume that cementation in the form of

filled voids without particle bridging, would display less shear resistance compared to bridged particle cementation.

In a review on MICP by (Choi et al., 2020b), it is noted that some studies reported higher effect on UCS from lower urease activity, while others reported higher effect from higher urease activity. The findings regarding the effect of urease activity on UCS, are contradictory. It would, given the previously discussed findings on urease activity and precipitation in chapter 5.1.2 and 5.1.5, be reasonable to assume that lower urease activity would lead to a lower precipitation rate. This in turn would generate fewer but larger crystals, resulting in precipitation at and around the particle contacts i.e higher resistance to induced shear. However, it is not clear if the studies described by (Choi et al., 2020b), applied urease activity as the only variable through their research. Variation in affecting factors could possibly be the reason for the diverging results.

In their work, (Shahrokhi-Shahraki et al., 2015) found increased brittleness and UCS with increasing concentrations of ($\text{CaCl}_2/\text{urea}$) in the cementation solution for MICP-treated (*S. pasteurii*) sands, where increased share of CaCl_2 showed an adverse effect, while increased share of urea had a positive effect on the achieved UCS. They further report that for similar concentrations of urea/ CaCl_2 , increased bacterial concentration resulted in decreased brittleness.

The reason for the increase in UCS with increasing concentrations of $\text{CaCl}_2/\text{urea}$, could be due to (Shahrokhi-Shahraki et al., 2015) using 100% higher share of urea than CaCl_2 in the solution. Higher share of urea would possibly prolong the urease activity and the following supersaturation, resulting in higher total amounts of precipitated CaCO_3 . However, higher amounts of CaCO_3 do not necessarily correlate directly with higher UCS.

Increased brittleness is due to cohesion or cementation. The decrease in brittleness with increasing bacterial density, could indicate as previously discussed in chapter 5.1.2, that bacterial density becomes adverse to the urease activity when exceeding a certain density, due to depletion of oxygen, nutrients or urea. An other factor could be as previously discussed in chapter 5.1.6, that high bacterial density do not provide enough space between the nucleation sites (cells)

for cubic crystal growth. Spherical or elongated crystals grown under limited space between cells, may result in poorer cementation at the particle contacts.

Work by (Cheng et al., 2016, Sharma et al., 2021), found a decrease in the UCS with increasing freeze and thaw (FT) cycles for MICP-treated sand, where (Cheng et al., 2016) found that fine uniform sand with lower porosity showed more durability during FT cycles, compared to coarse sand with higher porosity, whereas FT cycles had a minor impact on well graded sand. The findings of (Cheng et al., 2016) suggest that the porosity of the soil prior to treatment, affects the resistance of the particle bonding to FT cycles. One would assume that small voids (low porosity) rather than large voids particularly if saturated, would be more vulnerable to volume expansion during freeze. However, at the same level of saturation the magnitude of expansion would most likely be proportional. It could be due to a more effective cementation in denser soils due to a higher number of contact points between particles per soil volume, yielding higher resistance in the particle bonding.

Cold climate regions can experience a high number of FT cycles in the span of a winter season and the long-term resistance of the CaCO_3 binder is of great importance when considering MICP in cold climate ground conditions. Work by (Sharma et al., 2021), reported on 5% reduction in UCS for 5 FT cycles and 10% reduction in UCS for 10 FT cycles. The results suggests a 1% reduction in UCS per cycle, which indicate a vulnerability of CaCO_3 binder to FT cycles long-term. However, it is not clear if this rate of reduction is linear with number of cycles or if the outer material is more sensitive to erosion than inner parts of the CaCO_3 mass.

In cold climate regions the temperature can fluctuate above and below zero multiple times per season. However, it is the upper 0-3 m below the ground surface, depending on the particle size and porosity, that will experience freezing. It would be reasonable to think that the upper layer close to the surface would experience more frequent FT cycles than the soil deeper down. This suggests that the use of MICP at shallow depth and applications such as increase of the surface resistance to erosion in slopes and increasing stiffness of base layers below shallow foundations, could be particularly affected by frequent FT cycles

long-term. Further studies should be conducted on the effect of a higher number of FT cycles on the CaCO_3 binder.

In their work, (Cheng et al., 2013) found that in MICP-treated coarse sand with the same CCC, UCS increased with decreasing soil saturation. However, saturation above 80% was found to have little impact on UCS in the coarse sand.

The findings suggest that level of saturation have an affect on the particle cementation. The sample with 20% saturation acheived the same UCS as sample at 100% saturation, which acheived higher amounts of CaCO_3 than that at 20%. This could possibly be due to the cementation solution in partiallly saturated soils being pushed into the particle contacts by the air in the pores, thus effective cementation occur at and around the particle contacts. In fully saturated soils the solution is all around the grains and precipitated amount of CaCO_3 could be greater, but concentrated as void fill with less effective bonding.

5.2.2 Triaxial shear strength and volumetric response

- ***Acheived enhancement of shear strength in MICP-treated granular soils***

In their work, (Cui et al., 2017b, Rahman et al., 2020b) note that the shear behaviour of MICP-treated soils, is generally affected by the relative density (D_r), initial confining pressure (p'_o) and CCC, where several studies found that for similar P'_o , the shear strength in MICP-treated sands, increased with increasing CCC (Cui et al., 2017b, Cheng et al., 2013, Rahman et al., 2020a, Bing, 2015, Choi et al., 2020a).

The elimination of D_r and P'_o as variables in the studies, strengthen the significance of the findings. However, it is reasonable to asume that the cementation pattern and distribution of the CaCO_3 binder within the sample, would be more correlated to an increase in shear strength, than the amount of CaCO_3 precipitated per volume soil.

Work by (Nafisi et al., 2018), found a higher increment in shear strength and more pronounced change in drained triaxial volumetric response post-treatment for MICP-treated uniform coarse angular sand ($\Delta q_{\text{dev}} = +50\%$), than in uniform

coarse round sand ($\Delta q_{dev}=+35\%$) of similar particle size. The treatment increased the brittleness and dilatancy in all samples, but induced a more pronounced strain-softening at low strain for the fine round sand, which also achieved the highest increment in peak shear strength and most pronounced change in volumetric response of the three sands.

The results could possibly suggest a higher degree of particle cementation in the fine sand i.e a larger increase in cohesion, which would cause increased brittleness at low strains during shear. The results for higher increment in shear strength for the sand with angular particles, could as previously discussed in chapter 5.1.7, be due to higher friction during shear for cemented particles with a more angular shape and rougher surface, compared to particles with a more round shape and smoother surface.

Work by (Bing, 2015), observed that the effective stress failure envelope in drained triaxial shear of MICP-treated sand, moved upward parallel to the untreated failure envelope, with increasing CCC. (Cheng et al., 2013, Cui et al., 2017a) reported that both cohesion (c) and friction angle (φ) increased with increasing CCC, in fine and coarse sand, where (Cheng et al., 2013) add that c and φ increased with increasing CCC at all degrees of saturation, for both fine and coarse sand. However, at the same saturation and CCC, the coarse sand achieved higher φ compared to the fine sand, which showed significantly higher values of c than the coarse sand. (Cui et al., 2017a) reported on an approximate linear relation between increased φ and increasing CCC and an exponential increase in cohesion with increasing CCC in the fine sand. Similar φ for untreated dense sand and sand with CCC of 6%, suggest that degree of compaction prior to treatment, could affect the achieved shear strength post-treatment.

The higher φ achieved in the coarse sand compared to fine sand in work by (Cheng et al., 2013), could possibly be due to coarse sand generally having higher φ , than fine sand in untreated state, where the study is not clear on the magnitude of increment in φ for the two sands. The higher cohesion in treated fine sand compared to coarse sand, could possibly be due to a higher number particle contacts in the fine sand, compared to the coarse sand.

The findings of (Bing, 2015), suggest that increased cohesion is the major contribution to the increase in shear strength, rather than an increased internal frict-

ion. However, findings of (Cheng et al., 2013, Cui et al., 2017a) suggest that there is a contribution from the cementation to the friction angle. This could possibly be true in round and smooth surfaced particles, which could achieve an increased roughness and angularity due to the cementation, where the friction during shear would increase. However, increased brittleness at low strain in findings of (Rahman et al., 2020a, Nafisi et al., 2018) suggest an increase in cohesion due to cementation, where (Cui et al., 2017a) observed a much higher increment in cohesion per unit CaCO_3 than the increment in friction.

(Rahman et al., 2020a) found that drained triaxial shear in MICP-treated medium and coarse sand at similar p'_o and D_r , showed an increase in brittleness as well as peak and critical shear strength with increasing CCC. The treated samples displayed less initial contraction at small strains before dilating at larger strains. The reduction in initial contraction at low strains could possibly be due to the particles having less room to rearrange due to the added cementation, thus the drained volumetric response is more rapidly forced towards expansion (dilation).

Work by (Cui et al., 2017a) reported that $\text{CCC} < 3\%$ in MICP-treated medium to coarse sand, lead to a bulging of sample under shear, while samples with higher level of cementation, showed a more defined failure plane during shear. The findings could suggest that lower levels of cementation do not alter the behaviour of the treated sand. The bulging sample with an undefined failure plane during shear, observed at both untreated and treated state with $\text{CCC} < 3\%$, supports this assumption.

In their work (Zamani and Montoya, 2015) added 0, 10, 25 and 35% of silt to fine sand prior to MICP treatment (*S. pasteurii*), where increased shear strength with increasing share of silt under undrained direct shear was observed, except for a sample with 10% silt. The excess pore pressures (Δu) generated during shear, decreased due to the cementation. However, the decrease post-treatment, was lower in the silty soil than in the sand, which in untreated state generated significant negative porepressure during shear.

The findings suggest that shear strength can be improved in silty soils by MICP and that excess pore pressure (Δu) during shear is reduced. The undrained response of the pure sand changed from a tendency towards contraction and positive

(Δu), which is typical for loose sands, into a tendency towards dilation and negative (Δu) similar to that of a dense sand, post-treatment.

The undrained response of the silty soil showed tendency towards contraction and positive (Δu) both pre- and post-treatment. The increase in shear strength with increasing share (20-35%) of silt could be due to the finer particles (silt) filling the voids between the sand particles. This could have generated more contact points per soil volume available for cementation. However, the reason for the deviation in the trend for sample with 10% silt is not clear.

5.2.3 Permeability

- ***Residual permeability in MICP-treated granular soils***
- ***Challenges for the implementation of MICP in situ***

Depending on the intended geotechnical function of the MICP-treated soil, a greater reduction of permeability post-treatment could either be a desired outcome or critical to avoid. For applications where the objectives are reduction of water flow through constructions or blockage of fluid dispersion from polluted deposits, a greater reduction in permeability would be desirable. However, for applications where maintaining adequate residual permeability in the soil while achieving increased shear strength and stiffness is the objective, the degree of reduction in permeability need to be controllable and predictable for MICP to be available as a method for ground improvement. It is for this reason important to investigate the factors that affect the degree of reduction in permeability in MICP-treated soils

The research show that reduction of permeability due to precipitated CaCO_3 in granular soils, is closely related to CCC, where the residual permeability in MICP-treated fine to coarse sand is comparable to that of untreated coarse silts to fine sand.

Findings further show an increased reduction of permeability with increasing CCC (Choi et al., 2020a, Rahman et al., 2020a, QABANY and Soga, 2014, Cheng et al., 2016, Shahrokhi-Shahraki et al., 2015, Cheng et al., 2013). In their work, (Rahman et al., 2020a) note that achieved permeability in MICP-treated sands ranged from 0.01×10^{-5} to 66×10^{-5} m/s with CCC ranging from 2-14.8%, while Choi et al., 2020b) found that $\text{CCC} \geq 10\%$, was needed for a

reduction in permeability by two orders of magnitude. In their work, (Cheng et al., 2013) found a smaller range in reduction of permeability with increasing CCC in MICP-treated fine sand, than in coarse sand. The larger increment in reduction with increasing CCC for the coarse sand, could be due to larger initial pore voids in the coarse sand, where smaller initial void space in the fine sand, leave less pore volume that is available for reduction by precipitation. The final permeability post-treatment was still lower in the fine sand, compared to the coarse sand. They (Cheng et al., 2013) further observed that lower degree of saturation in the sample yielded a smaller reduction of permeability post-treatment, compared to samples with a higher degree of saturation. It is not clear whether the effect of saturation is related to the increment, or if initial larger pores in the coarse sand is the reason for the greater increment.

Increasing degree of saturation in partially saturated pores, could increase the distribution of injected solutions within the pore. Fully saturated pores would cause the injected fluids to be evenly dispersed within the pore, generating precipitation in the whole pore and significantly reduce the fluid flow. Low degree of saturation would cause the injected fluids to be pushed by the air towards the walls of the pores, thus resulting in less precipitation in the middle of the pore and more at the particle contacts leading to higher residual permeability while increasing the shear strength and stiffness of the treated soil. This could suggest that low degree of saturation and particle size in the range fine to coarse sand, are favorable for applications of MICP, where residual permeability post-treatment is critical for the geotechnical design or purpose.

In their work, (Choi et al., 2020b) note that the degree of urease activity have less influence on the reduction of permeability in MICP-treated sand, whereas (Cheng et al., 2016) found that the high urease activity resulted in the largest reduction of permeability.

The findings on the effect of urease activity are inconsistent. It would be reasonable to assume that the main factors controlling the degree of reduction would be the initial porosity, degree of saturation, grain size distribution, cementation pattern, CCC and the distribution of CCC within the soil. The cementation pattern

and CCC could be more directly affected by the level of urease activity through concentration at supersaturation and hence precipitation rate.

Work by (Shahrokhi-Shahraki et al., 2015) found that increased concentrations of cementation solution ($\text{CaCl}_2/\text{urea}$) led to greater reduction of permeability, while (QABANY and Soga, 2014) found that using 1 M cementation solution ($\text{CaCl}_2/\text{urea}$) in MICP treatment of sand, caused a more rapid reduction of permeability than 0,25 M. (Cui et al., 2017a) reported on a linear relationship between increasing treatment cycles ($\text{urea}+\text{CaCl}_2$) and an increase in dry density of MICP-treated sand.

The findings might suggest an increased precipitation rate with increasing concentration of cementation solution. However, the share of urea compared to CaCl_2 and vice versa within the solution, might according to previously discussed findings in chapter 5.1.2 and 5.1.5, have a greater effect on the intensity and duration of the urease activity and consequently the precipitation rate and amount of precipitated CaCO_3 . It is further reasonable that an increased number of treatment cycles would provide either added growth on previously precipitated crystals or new crystal growth, depending on the cell density i.e availability of nucleation sites as discussed in chapter 5.1.6.

5.3 MICP-treated cohesive soils

Part of the objectives of this thesis is to research previous findings on achieved shear strength in MICP-treated cohesive soils. The findings are:

- *Far more studies on MICP have been conducted on granular soils, compared to cohesive soils.*
- *Most studies on MICP-treated cohesive soils apply manual mixing of bacteria and cementation solution into the soil, rather than injection under low pressure frequently applied for MICP studies on sand.*

Unconfined compression strength

- *The findings are not conclusive on whether increased share of fines are favorable or unfavorable for achieved UCS in clays and clayey soils.*
- *The research indicate that UCS of different types of clays can be significantly increased (up to 400%).*

Triaxial shear strength and volumetric response

- *The basis for an evaluation on triaxial shear and volumetric response in MICP-treated cohesive soils, is limited due to only one study.*
- *The study show increased strain-hardening rather than increased brittleness in MICP-treated clay, where UCS stress-strain curves also show increased strain-hardening for treated clay, while increased brittleness and strain-softening in treated silty clay. This could possibly suggest a different effect on cemented behaviour with variations in share of coarse particles in cohesive soils. Further research is needed to clarify the difference in stress induced behaviour, which is of great geotechnical importance.*

5.3.1 Unconfined compression strength

- ***Achieved shear strength in MICP-treated cohesive soils.***

In their work, (Islam et al., 2020) used bio-stimulation in soils with different share of clay (10-40%) and achieved 3-96% increase in UCS from untreated to treated state. No correlation between share of fines and increase in UCS was observed and the CCC post-treatment, was relatively low for all samples. There was some success with bio-stimulation for soils with 10 and 40% clay, but not for samples with 20 and 30% clay. It is difficult to find a reasonable explanation for this discrepancy, where both low and high share of fines seem to be favorable, while shares in between, seem to be highly unfavorable. Different density of indigenous bacteria populations in the samples, could possibly be the reason.

In their work, (Sharma and Ramkrishnan, 2016, Behzadipour et al., 2019) found decreasing UCS with increasing share of fines in the soil, where (Sharma and Ramkrishnan, 2016) observed a larger increase in UCS for sample with 53,6% fines (silt+clay) compared to sample with 82,3% fines. (Behzadipour et al., 2019) observed that increased share of fines in MICP-treated sandy soil reduced the UCS, compared to lower share of fines. Results on MICP-treated soft clay reported by (Xiao et al., 2020), showed a 242% increase in UCS from untreated to treated state, while (Cheng and Shahin, 2015) achieved a 150% increase in UCS for MICP-treated clayey soil (10% clay).

Work by (Kannan et al., 2020) reported a 148% increase in undrained shear strength (S_u) of MICP-treated marine clay, while (Bing, 2015) reported on up to 400% increase in UCS for MICP-treated marine clay and 150% increase in Kaolin clay. In work by (Godavarthi Rajani, 2020), a 150-250% increase in UCS for MICP-treated high plasticity clay cured up to 28 days, was registered.

The findings of (Sharma and Ramkrishnan, 2016, Behzadipour et al., 2019), where increased share of fines is suggested to have an adverse affect on achieved UCS, are not in line with findings of (Xiao et al., 2020, Cheng and Shahin, 2015, Kannan et al., 2020, Bing, 2015, Godavarthi Rajani, 2020) which suggest a high increase of UCS in clays with a high share of fines.

The results suggesting an adverse effect on cementation by increasing share of fines, could be due to declining permeability with increasing share of fines lead-

ing to poorer distribution of fluids or due to adverse effects of clay minerals on the urease activity and hence the precipitation. The samples are manually mixed, which would suggest a degree of control on the distribution of fluids within the sample, compared to injection methods. However, the results showing high UCS in soils with high share of fines, do not include samples with lower share of fines for comparison.

(Teng et al., 2020) reported on increased UCS with increasing bacterial concentration up to 0,8 OD₆₀₀ in MICP-treated silty clay, where a decrease in UCS was observed when OD₆₀₀, was further increased. In their work, (Keykha et al., 2017) found that the highest UCS in MICP-treated kaolin clay (50% clay+ 50% silt) was achieved with 50 ml bacterial suspension at pH equal to 9, compared to 30 ml, 70 ml.

The findings of (Keykha et al., 2017) could possibly be due to competition for nutrients between the bacteria at high volumes (> 50 ml) of bacteria suspension. When depletion of nutrients, urea or oxygen initiate the urease activity will possibly decline as previously discussed in chapter 5.1.2. However, this reasoning would be more applicable to the density of bacteria such as in the case of (Teng et al., 2020) and not necessarily the volume of suspension. (Keykha et al., 2017) did however vary the bacterial density between 10⁷ to 10⁸ cells ml⁻¹, which could possibly have affected the results.

5.3.2 Triaxial shear strength and volumetric response

- ***Achieved shear strength in MICP-treated cohesive soils.***

In work by (Bing, 2015), a higher shear strength for similar P'_o, was found for MICP-treated Kaolin clay in drained triaxial shear, compared to sample treated with only cementation solution (CaCl₂/urea). However, both the MICP-treated samples and samples treated with only CaCl₂/urea, showed increased strain-hardening behaviour post-treatment. All samples showed increasing shear strength with increasing P'_o, while the MICP-treated samples achieved a slightly higher friction angle compared to samples only treated with CaCl₂/urea. All samples showed increasing shear strength with increasing P'_o.

The findings indicate that the inclusion of ureolytic bacteria (MICP) in the treatment, have a significant effect compared to the effect of treatment with only cementation solution ($\text{CaCl}_2/\text{urea}$). The increased shear strength in samples treated with only cementation solution, could possibly be due to indigenous bacteria in the sample or increase in magnitude of electrostatic forces acting between the clay particles, due to increased salinity.

The increasing shear strength with increasing P'_o , could be expected from increased consolidation prior to shear. However, the increased strain-hardening and lack of increase in brittleness in the cemented clay, could possibly suggest a different effect of cementation in cohesive soils compared to granular soils, where most will show an increased brittleness post-treatment. The observed strain response is typical for a normally consolidated clay, whereas the observed drained volumetric response (dilative), is typical of an overconsolidated clay. However, the treated clay did initially contract as the strain-hardening would suggest, before dilating.

The higher friction angle (ϕ) in the MICP-treated clay and same volumetric response for both types of treatment, could suggest that the higher effective shear strength in the MICP-treated clay, is due to increased cohesion. However, increased cohesion would suggest an increase in brittleness. An other possible cause, could be increased roughness of particle surfaces due to cementation, creating increased friction at shear.

The effect of increased strain-hardening during triaxial shear in the cemented clay rather than increased brittleness such as observed in MICP-treated sands, was compared to UCS stress-strain curves for cohesive soils in results from (Xiao et al., 2020, Soon et al., 2013, Teng et al., 2020, Godavarthi Rajani, 2020). The UCS curves for MICP-treated silty clay from (Teng et al., 2020, Soon et al., 2013) showed increased brittleness, while curves for MICP-treated clay from (Xiao et al., 2020, Godavarthi Rajani, 2020) show increased strain-hardening.

This could suggest that the share of coarser particles in the clay, could possibly affect the strain response in cemented cohesive soils. Further research is needed for a more informed evaluation.

5.4 *S.pasteurii* as a causative agent for MICP in soils

*Part of the objectives for this thesis is to research and evaluate *S. pasteurii* suitability as a causative agent for MICP in soils. The findings are:*

***S. pasteurii* in MICP:**

- *S.pasteurii* follows an exponential growth curve and can be cultivated on large scale with exponential growth and intact ureolytic capacity at lower cost.
- *S.pasteurii* is non-pathogenic, have high negative cell charge and can tolerate highly alkaline environments as well as harsh conditions when situated in between precipitating CaCO₃ minerals.
- Findings indicate that *S. pasteurii* can not sustain growth or urease activity over time under conditions with limited or no dissolved oxygen. However, due to findings suggesting the contrary, further research is needed.
- *S. pasteurii* can sustain a sufficient urease activity both under high (up to 50°C) as well as low temperatures (down to 4°C) in oxic conditions with pH in the range 6-9.
- *S. pasteurii* is 0,5-1,2 µm in width and can move freely within sandy soils with particles in the range 0.05 to 2.0 mm, whereas movement into or through a large share of the pores in clay, is not possible. In coarser silts and silty to clayey sands, movement could perhaps be possible, whereas free movement within pores in fine silts and clayey silts, is less likely.
- *S. pasteurii* have a high capacity for precipitation in sand, but indicate a lower capacity for precipitation in fine grained soils.
- The use of *S. pasteurii* for MICP-treatment in cohesive soils under oxic conditions and through manual mixing, have been demonstrated to significantly increase the shear strength of silt and clays.
- *S. pasteurii* have been demonstrated to increase shear strength and reduce the porosity and permeability in MICP-treated sands.

The topics that are described in this chapter are discussed in detail in chapters 5.1.1-5.1.2 and 5.1.4-5.1.5. The suitability of a bacteria as a causative agent for MICP, should be evaluated on its performance or capacity regarding the deciding factors for the desired outcome of the MICP process. For ureolytic bacteria utilized in MICP, the following factors are important:

- Cost effective and exponential growth
- Non-repressive response to ammonium
- High urease capacity sustained under:
 - *oxic and anoxic conditions*
 - *presence of ammonium*
 - *a broad range in temperatures*
 - *alkaline conditions*
- Robust cell surface with high negative charge
- Compatibility of bacterias size and pore size distribution in target soil
- Be non-pathogenic and have no transferable elements

The research show that *S.pasteurii* is non-pathogenic, have high negative cell charge and can tolerate highly alkaline environments as well as harsh conditions when situated in between precipitating CaCO_3 minerals. Findings demonstrate that *S.pasteurii* can be cultivated on large scale with exponential growth and intact ureolytic capacity at lower cost, by replacing expensive components with cheaper ones. The bacteria follows an exponential growth curve, where the growth is affected by nutrients, temperature, oxygen and pH. The cultivated batches, should be stored at late exponential or early stationary stage of growth.

The findings indicate that *S. pasteurii* cells cultivated under oxic conditions, develop a robust nucleation site for precipitation of CaCO_3 , while it is uncertain whether it can obtain healthy growth under under oxic conditions, but unlikely. However, high bacterial density in the injected suspension or repeated injections of fresh bacteria, could possibly exclude reliance on further anaerobic cell growth during treatment below the water table.

S. pasteurii's ability to sustain urease activity under conditions with limited oxygen is unclear, while the research indicate that *S. pasteurii* can sustain a sufficient urease activity both under high (up to 50°C) as well as low temperatures

(down to 4°C) in oxic conditions, while precipitation is found to be efficient between 4°C and 30°C and pH between 7 and 9. Concentrations $\leq 0,5$ M of cementation solution ($\text{CaCl}_2/\text{urea}$), is indicated to be most favorable for precipitation with *S. pasteurii*. The findings further indicate a possible prolonged duration of urease activity with increased concentrations of urea in suspension, whereas a clear correlation between bacterial concentration and level of urease activity, can not be observed.

Bacteria with size ranging from 0.3 to 2 μm can move freely within sandy soils with particles in the range 0.05 to 2.0 mm. Increased share of fine particles in a soil would limit or block the bacteria's movement within the soil matrix, where clays can have more than 50% of pores $< 0,01$ μm , while *S. pasteurii* is 0,5-1,2 μm in width. This makes bacterial movement into or through a large share of the clays pores impossible for *S. pasteurii*. In coarser silts and silty to clayey sands, movement could perhaps be possible, whereas free movement within pores in fine silts and clayey silts, is less likely. The findings further indicate that bacterial movement from pore to pore is facilitated in fully saturated pores and reduced between partially saturated pores, whereas bacteria located in pores of size close to its own, are suggested to be trapped or inactive.

The research show that *S. pasteurii* have a high capacity for precipitation in sand, but indicate a lower capacity in fine grained soils. The reason for the difference is not clear, but could possibly be due to effects of clay minerals on urease activity, uneven distribution of injected fluids and consequently precipitated CaCO_3 or variation in affecting variables in the different studies.

The use of *S. pasteurii* in sand have achieved significant increase in shear strength as well as reduction in porosity and permeability. Although to a lesser degree than in sands, treatment with *S. pasteurii* and cementation solution have achieved significant increase in shear strength of silt and clay.

5.5 Viability and challenges for MICP as a method for ground improvement

*The research aim of this thesis, is to evaluate through the research objectives discussed in chapters 5.1-5.4, the viability and challenges of MICP with *S. pasteurii* as a method for ground improvement. Requirements for viability are described in chapter 3.14. The findings are:*

- The research show that *S. pasteurii* can be cultivated under oxic conditions on a large scale and at low cost, while sustaining exponential growth and ureolytic capacity. Cell growth, sustained ureolytic capacity over time and precipitation under anoxic conditions for *S. pasteurii* are uncertain, but unlikely.*
- MICP is demonstrated as viable in granular soils under oxic conditions, where ureolysis and consequent precipitation of CaCO_3 is found to be effective for temperatures in the range 4-30°C and pH in the range 6-9.*
- The research indicate that cementation pattern which affect acheived shear strength as well as the residual permeability post-treatment, could be influenced through control of the precipitation rate. However, the indicated independent effect of saturation on cementation pattern, need to be further investigated for a proper evaluation on controllability and predictability of the residual permeability of treated during MICP.*
- MICP is found to significantly increase the shear strength and reduce permeability with increasing CCC under oxic conditions in sands.*
- Effective particle bonding and higher residual permeability, have been demonstrated at 4 and 25°C, lower urease activity and lower consequent precipitation rate. However, further studies are needed to determine the reproducibility of these results.*
- The research demonstrate that low pressure injections using injection and extraction wells in a grid pattern are viable and distribution of CaCO_3 binder within the target area is acheivable, in granular soils. The one-phase low pH solution proposed by (Cheng et al., 2019), is evaluated to have the greatest potential for acheiving increased uniformity in spatial distribution.*

- *Findings indicate a greater reduction of void size in MICP-treated granular soils with fully saturated pores, while partially saturated pores are indicated to yield a higher residual permeability.*
- *The research indicate that low pressure injections are not viable in fine silt and clay due to low permeability, where acheiving spatial distribution of binder across low permeability layers within stratified soil deposits with varying permeability, is unlikely.*
- *Manual or mechanical mixing is found to be necessary to acheive distribution of bacteria and cementation solution within clay and fine silt.*
- *Sustained urease activity and consequent precipitation is demonstrated as possible in cohesive soils. However, amount of precipitated CaCO_3 in cohesive soils is found to be smaller than in granular soils.*
- *The removal of ammonium post-treatment using injection and extraction of rinse solutions is demonstrated as viable in granular soil, while assumed to not be acheivable in cohesive soils due to the low permeability. This affects the viability of MICP in cohesive soils and suggest the need for a different approach for removal in such soils.*
- *The one-phase low pH solution is found to significantly reduce the generated ammonia (NH_3) during ureolysis.*
- *The findings suggest possible adverse effects of some clay minerals on the urease activity, while organic matter could possibly have an inhibitory effect on crystal growth. Further research is needed on these aspects.*

- *Findings suggest lower achieved shear strength post-treatment for MICP-treated fine grained soil with high share of gravel, compared to lime or cement treatment, but similar to ash treatment. The gap in achieved shear strength between cement and MICP, is significantly reduced when share of gravel in fine grained soil is reduced.*
- *Bio-augmentation is found to be a more predictable implementation of MICP than bio-stimulation.*
- *Increase in shear strength throughout curing period of up to 28 days post-treatment is demonstrated in fine grained soils, while the effect of curing time on shear strength in granular soils, is unclear.*
- *Durability of CaCO₃ binder is found to be affected by acidic rain, where intensity and pH, determine the degree of corrosion of mass and CCC determine the loss of shear strength due to corrosion.*
- *The estimated service life of the CaCO₃ binder, is estimated to be above 50 years, under favorable ground conditions.*

The topics described in this chapter are based on the detailed discussions in chapters 5.1.1 to 5.3.2 and are a summary of the findings related to the viability of MICP as well as the challenges facing the implementation of the method in situ.

There have been conducted a much higher number of lab studies on MICP treatment of granular soils than cohesive soils. Controlled lab experiments can however never fully simulate in situ conditions, where a high number of combinations in variables affecting the MICP process, can be expected. In nature, most soil deposits are heterogenous, where varying permeability and pore size distribution across soil layers as well as hydraulic boundary conditions, could affect the transport of injected solutions and consequently the spatial distribution of CaCO_3 within the target area.

A few large scale field studies have been conducted on sand and gravel, whereas none large scale studies conducted in cohesive soils, have been found during the work on this thesis. For the MICP method to be viable as an alternative ground improvement method applied in the industry, certain requirements need to be met:

- Provide a uniform distribution of CaCO_3 binder in the target area
- CaCO_3 binder needs to be resistant to erosion and corrosion, where the service life of binder should be equal to or exceed common designlife for geotechnical design.
- Be applicable in stratified soils with layers of different permeability and pore size distribution or grain size distribution
- Be applicable under conditions with limited dissolved oxygen and under a broad range of ground temperatures
- Provide means for control of crystal morphology, crystal size and cementation pattern
- Provide method for obtaining residual permeability, while increasing strength and stiffness of soil
- Provide a method for reducing NH_3 and removal of aqueous and adsorbed NH_4^+

Main challenges facing the implementation of MICP in granular and cohesive soils, are:

- Uniform spatial distribution of CaCO_3 binder in granular soils and injection and distribution of fluids in cohesive soils

- Geometric compatibility in low permeability cohesive soils
- Cell growth and urease activity under anoxic conditions
- Controllability and predictability of cementation pattern and residual permeability

MICP is found to be a viable method in sands under oxic conditions under a broad range of temperature, where sustained urease activity and consequent precipitation have been demonstrated. The results show a significant increase in shear strength as well as significant reduction in porosity with increasing CCC (Choi et al., 2020a, Rahman et al., 2020a, Cheng et al., 2013, Shahrokhi-Shahraki et al., 2015, Cheng et al., 2016).

The viability of MICP in fine silt and clay is uncertain, where some studies suggest an inhibitory effect from some clay minerals on the urease activity, while the low permeability renders injections of fluids in situ, ineffective. The large share of pores smaller than the bacteria size, renders entrance into or transport through such pores, not feasible. However, sustained urease activity and consequent precipitation with 150-400% increase in shear strength is demonstrated in MICP-treatment of clays and silts under oxic conditions, when bacteria and cementation solution is manually mixed into the soil. (Xiao et al., 2020, Cheng and Shahin, 2015, Kannan et al., 2020, Bing, 2015, Teng et al., 2020, Godavarthi Rajani, 2020). The viability of MICP in organic soils is uncertain, where findings suggest that organic matter can have an adverse effect on crystal growth.

Methods such as surface percolation are cost-effective and could be suitable for increasing resistance to surface erosion in slopes, reducing permeability in porous shallow deposits or strengthen the base layers of shallow foundations. For low permeability soils such as clays and fine silts, the research conducted in this thesis have not found any findings that suggest that current strategies such as low pressure injections, can be viable. Further, uniform spatial distribution of CaCO_3 across impermeable layers within stratified granular soil deposits, would be difficult and unlikely to achieve, with the strategies suggested up until now.

The utilization of injection and extraction wells in a grid pattern have proven to be effective in large scale field studies in granular soils (Van Paassen, 2009a, Van der Star et al., 2011), and is found to be the most suitable approach for

injection with MICP in permeable soils. The one-phase low pH solution proposed by (Cheng et al., 2019) and $\leq 0,5$ M $\text{CaCl}_2/\text{urea}$, is found to be the most suitable injection solution, due to delayed precipitation which enables proper distribution of injected fluids within the target area, before precipitation is initiated. This approach also significantly reduce the generation of NH_3 (g). Given an expected decline in density of injected solution with distance from injection point, applying a strategy of injections with the one-phase solution in both opposite directions of the target area could ensure a better distribution of bacteria and reactants along the flow path. However, any adverse effect on bacterial attachment from the low pH solution needs to be investigated.

This thesis proposes two different approaches to be evaluated through further research as potential strategies for implementing MICP in granular soils and cohesive soils. The suggested approach for granular soils consist of combining independent methods proposed individually and demonstrated to be viable by other researchers into one integrated approach:

- *For MICP in granular soils, the integrated one-phase low pH solution proposed by (Cheng et al., 2019) described in chapter 5.1.10, applied through grids of injection and extraction wells with $< 2,8$ m spacing utilized by (Van Paassen, 2009a, Van der Star et al., 2011) and described in 5.1.10, should be tested with the use of one-phase low pH injection solution in both directions of the flowfield. The injection and extraction wells would need pumps that can switch from injection to extraction in an easy and rapid manner. Effects of low pH on bacterial attachment would need to be investigated, but injections in both directions could ensure adequate distribution along flow path.*
- *Removal of NH_4^+ can be achieved with the extraction wells as demonstrated in granular soil by (Van Paassen, 2009a, Van der Star et al., 2011)*

The suggested approach for cohesive soils is based on the same principles as implementation of MSM or DSM:

- *For MICP in fine silt and clay, mechanical mixing in situ under high injection pressure with a low pH one-phase solution should be evaluated.*
- *This approach would require investigations on the ureolytic bacterias capacity to endure high pressures, where (grouting, 2021) suggest that*

100-600 bar in injection pressure is applied during jet grouting in cohesive soils, while (Mitchell and Santamarina, 2005a) note that bacteria can tolerate > 100 bar of pressure, whereas the bacterias tolerance for high shear forces, is unclear.

- *The approach suggests a need for further studies on urease capacity in the presence of clay minerals and the effect of small voids on metabolic activity.*
- *The removal of NH_4^+ post-treatment in cohesive soils will due to the low permeability, likely encounter the same challenges as injections. This suggest a need for a different approach for removal in cohesive soils.*

Studies showing effective particle bonding as well as adequate residual permeability post-treatment at 4°C in sands, indicate that lower temperature and consequently a lower urease activity, is favorable for obtaining residual permeability while improving shear strength. However, MICP-treatment of soil with fully saturated pores are indicated to promote a greater reduction of void size, whereas partially saturated pores are indicated to lead to higher residual permeability and more effective cementation at and around particle contacts.

Although temperature dependent, the research demonstrate that urease activity can be sustained and precipitation of CaCO_3 at supersaturation occur, in temperatures from 4°C to 50°C. Effective precipitation is found to occur in the range 4-30°C, where the urease activity increases with increasing temperature and 25°C is considered optimal. The sub-surface temperature of most climatic regions, falls within this range. However, due to a result that showed no urease activity below 5°C, further studies on the effect of low temperatures on urease activity are needed.

Findings indicate that lower temperatures and consequently lower urease activity and precipitation rate, generate less amounts of CaCO_3 , larger crystals but more effective particle bonding, whereas temperatures above 30°C are indicated to increase the urease activity and hence the precipitation rate, generate larger amounts of CaCO_3 and smaller crystals with less effective particle bonding.

Higher rates of ureolysis are indicated to lead to higher concentrations at supersaturation and increased rate of precipitation, which would favor precipitation of meta stable output mineral (vaterite), whereas lower precipitation rates are indicated to favor precipitation of more stable mineral (calcite). Further research on

the effect of temperature on the mineral structure of the CaCO_3 crystals as well as the effect of ductile or brittle crystal properties on shear strength in MICP-treated soil, are needed.

The research is not clear, but findings suggest that cell growth, urease activity and ureolysis can not be sustained over time under conditions with limited availability of dissolved oxygen, such as below the water table. However, there are studies which indicate that this issue could be addressed with repeated injections of highly oxygenated fluids or injections of oxygen releasing compounds with a declining rate of release.

The research show that ureolysis and precipitation is effective and sustained at pH between 7 and 9, where pH 8,5 is optimal for *S. pasteurii*. Soils in wet areas would generally have a pH in the range 5-7, while soils in drier areas would generally have a pH in the range 6,5-9, whereas most groundwater systems would have pH within the range 6-8,5.

(Stocks-Fischer et al., 1999) found that pH causes significant changes in the bacterial metabolism and will govern the capacity for ureolysis. The research is not clear on the bacterias capacity to initiate ureolysis under highly alkaline or very acidic conditions, but highly alkaline ground conditions could possibly be addressed with low pH solutions injected pre-treatment, to buffer the pH.

However, acidic ground conditions would most likely not be a good candidate for MICP treatment, particularly due to the adverse effect of corrosion on the CaCO_3 binder, where the research indicate that loss of shear strength due to corrosion on the CaCO_3 binder, is determined by the CCC in the MICP-treated soil volume. The loss of CaCO_3 mass due to erosion, can occur due to cyclic wetting and drying of CaCO_3 binder in the unsaturated zone. The design life of the CaCO_3 binder is estimated to be above 50 years, under favorable ground conditions

Ground water rich in calcium or magnesium could possibly increase concentration at supersaturation, where high concentrations in magnesium ions at supersaturation is suggested to generate CaCO_3 crystals of poor compressive strength, while organic content is indicated to adversely interfere with the crystal growth during precipitation.

The findings do not provide any certainty on determining factors for the generated shape of the crystal, nor on any direct correlation between bacterial

concentration and crystal growth. However, findings indicate that concentration as well as share of urea and CaCl_2 in the cementation solution have an effect on crystal growth, where increasing share of urea is favorable compared to increased share of CaCl_2 .

MICP leads to the release of both ammonium (NH_4^+) and ammonia (NH_3), which needs to be removed from the MICP-treated soil post-treatment. The research demonstrate that removal of NH_4^+ in granular soils is feasible using a high pH and high ionic strength rinse solutions. However, the results show small amounts of residual sorbed ammonium in the treated soil, which needs to be addressed. Research indicate that a significant reduction of NH_3 may be achieved using the one phase low pH injection method. The removal of NH_4^+ post-treatment in cohesive soils will likely encounter the same challenges as injections, due to the low permeability. This suggest that the approach applied in granular soils, where injection and extraction of rinsing fluids are utilized, would most likely be unsuccessful in cohesive soils. Further work on new approaches for removal of NH_4^+ in cohesive soils as well as removal of residual NH_4^+ in granular soils, is needed.

The competitiveness of MICP in respect to methods utilizing cement and lime products, will have an effect on whether MICP will be adopted as a new method for ground improvement in the industry. MICP-treatment of fine grained soil with gravel achieve lower shear strength than treatment with cement or lime, but similar to that of treatment with ash. The gap in achieved shear strength between cement and MICP is significantly reduced when share of gravel in fine grained soil is reduced. Comparison of methods for achieved shear strength in sand, is unclear due to lack of findings in the littertaure.

MICP would require a system for performance monitoring before, during and after treatment. Before treatment, an integration of pH measurement of groundwater and testing for pre-existing CaCO_3 during laboratory investigations, could possibly be required. During treatment, field tracers could possibly be used to verify the reach of injected fluids by depth or width from induced flow field. However the use of equally distanced injection and extraction well in a grid with multiple injection and extraction points with depth should provide adequate spatial coverage of fluid flow.

Short-term after treatment, the binder distribution and magnitude of desired properties needs to be verified through sampling and geophysical tests and compared up against the design criteria, where findings indicate that significant increase in shear strength can occur between 14-28 days of curing in cohesive soils, whereas curing time in granular soils is unclear. This could suggest a period of up to 4 weeks before final comparison of shear strength up against the set design criteria in cohesive soils.

Long-term after treatment, the owner of the project should conduct periodical controls of the binder (CaCO_3) quality in the soil throughout the service life as well as pH measurements of groundwater if treated soil is located below the watertable. In areas with frequent and heavy rainfalls and areas which experience cyclic freeze and thaw, the control intervalls should be shorter to assure early detection of erosion in the binder material.

The performance monitoring can be achieved through rigorous and standardised schematic quality control conducted by the contractor and later the owner. The testing scheme could specify the minimal number of samples to be obtained, tests to be conducted on samples etc.

5.6 Viability of MICP in cold climate ground conditions

*Part of the research goal of this thesis is to evaluate the viability of MICP with *S. pasteurii* as a method for ground improvement in cold climate ground conditions. Requirements for viability specific to cold climate ground conditions are addressed in this chapter, while general requirements for viability are addressed in chapter 5.5. The findings are:*

- Further work is needed on the effect of long-term cyclic FT for a proper evaluation on the viability of MICP in cold climate ground conditions.*
- The work on this thesis have not obtained any results on the effect of FT cycles on cohesive soils.*
- The research indicate that crushing of particles during cyclic FT, is associated with granular soil and not clays.*
- Sustained urease activity and consequent precipitation have been demonstrated under oxic conditions at temperatures down to 4°C in sand.*
- Findings indicate effective particle bonding and higher residual permeability post-treatment at 4°C and low urease activity in sand, where UCS increased exponentially with increasing CCC.*
- The findings suggest that CaCO₃ binder at shallow depths, could be vulnerable for long-term cyclic FT.*
- The findings show a decrease in shear strength with increasing FT cycles (up to 10 cycles) in MICP-treated sand. It is unclear whether the erosion of CaCO₃ is linear with increasing FT cycles or if the porous material in the periphery of the crystal mass have a higher rate of erosion than the rest of the mass.*

The topics that are described in this chapter are discussed in detail in chapters 5.2.1. The findings and evaluation in 6.5 cover most of the requirements for viability of MICP as a method for ground improvement in cold climate regions. In this chapter additional requirements that are specific to cold climate regions and listed below, are evaluated:

- Bacteria must be able to initiate hydrolysis of urea (urolysis) and sustain urease activity in temperatures down to 4°C.
- Ability to generate CaCO₃ crystals of quality and size that promote effective particle to particle bonding and sufficient residual permeability in temperatures down to 4°C.
- Sufficient erosion resistance in CaCO₃ binder when exposed to long-term cyclic freeze and thaw.

Sub-surface temperatures in cold climate regions such as Norway range between 4-8°C. The temperatures during the cold season can fluctuate above and below zero, where the frost depth is 0-3 m, where coarse surface layer would lead to deeper frost and finer layers would experience a more shallow freeze.

Findings indicate that precipitation is achieved at temperatures down to 4°C, where lower temperatures lead to lower urease activity and precipitation rate, which generate fewer but larger CaCO₃ larger crystals that provide efficient particle to particle bonding and higher residual permeability. However, due to a result that showed no urease activity below 5°C, further studies on the effect of low temperatures on urease activity should be conducted. The capacity for further cell growth post-injection under low temperatures is not clear.

There is a study, where the results suggest that the mineral structure of the precipitated crystal could be affected by temperature, where crystals at 5°C were characterized as amorphous. Such mineral structure would likely translate to ductile properties. The effect of temperature on crystal properties as well as the effect of crystal properties onto the shear resistance during shear, should be investigated further.

Findings indicate that fine sand with lower porosity have greater resistance to FT cycles, compared to coarse sand with higher porosity, where findings suggest a 1% reduction in UCS per FT cycle up to 10 FT cycles. However, it is not clear

whether the rate of reduction is linear. It is reasonable to assume that the highest frequency in FT cycles within the range of frost depth, would occur in the soil close (0-0,5m) to the surface. The findings suggest that MICP applications at shallow depths, for increasing erosion resistance of slope surfaces and strengthening base layers below shallow foundations, might be particularly vulnerable for FT cycles in the long term. Further research is needed to evaluate the effect of long-term exposure (multiple FT cycles) on the CaCO_3 binder in both granular and cohesive soils.

6. Conclusions

6.1 Research objectives

MICP have the potential to be an alternative and sustainable method for ground improvement. The method can reduce the use of cement products during ground improvement, is less intrusive to the soil and have a lighter footprint on the terrain. For the past 13 years, the number of publications on MICP have according to (Rahman et al., 2020b), increased exponentially. This reflects a strong interest for more sustainable methods for ground improvement, where MICP is evaluated by researchers to have potential. The research aim of this thesis is to evaluate the viability of and challenges for MICP with *S. pasteurii* as a method for ground improvement in granular and cohesive soils, including its viability in cold climate ground conditions. The evaluation is conducted on the basis of the results from the following research objectives:

- ***Factors affecting the MICP process***

A high number of studies addressing the core factors affecting MICP such as pH, temperature, urease activity and precipitation, have provided a sufficient basis for the evaluation of most of the affecting factors. However, inconsistent findings on ureolytic capacity under anoxic conditions as well as few findings on the effect of low temperature, clay minerals, organic matter and restricted pore space on the ureolytic activity, have limited the evaluation. Further research on cell growth and ureolysis under anoxic conditions, is needed for a proper evaluation on the viability of MICP-treatment below the watertable.

The research show that the factors listed in chapter 5.1, all affect the MICP process, where factors such as pH, urease activity, precipitation rate and cementation pattern are indicated to be controllable. The spatial distribution of CaCO₃ binder post-treatment is determined by the permeability of the soil, but can be enhanced in granular soils, through proper strategies for injections in situ. However, residual permeability which is determined by the generated precipitation pattern, is indicated to be affected by degree of saturation, independent of the other factors that are indicated to control the cementation pattern. This suggest a need for further research on the effect of saturation.

Ureolysis and consequent precipitation of CaCO₃ binder, is demonstrated to be viable for a range in temperature that cover the sub-surface temperatures in most climatic regions without permafrost. This thesis find that factors affecting the MICP process such as pH, urease activity, precipitation rate and cementation pattern, most likely can be controlled, while others such as spatial distribution and bacterial retention can be affected, whereas varying pore size distribution, saturation, varying permeability in stratified soil deposits or low permeability in cohesive soils, can not be controlled nor affected and hence need to be adressed through trial and error in larger scale field studies.

- **S. pasteurii as a causative agent for MICP in soils**

A high number of studies on MICP-treatment of granular soils using *S. pasteurii*, have provided a sufficient basis for the evaluation of it as a causative agent with MICP. *S. pasteurii* is found to meet most of the requirements set in chapter 3.4 and 5.4 for viability of ureolytic bacteria used in MICP. However, contradictive findings on ureolytic capacity under anoxic conditions and few findings on the effects of low temperature, clay minerals, organic matter or restricted pore space on the ureolytic capacity of *S. pasteurii*, have limited the evaluation. Relatively few studies on MICP in fine silt and clays, have limited the basis for the evaluation of the suitability of *S. pasteurii* in such soils.

As presented in chapter 5.4, the ureolytic capacity of *S. pasteurii* and consequent precipitation at 4 -50°C under oxic conditions, have been demonstrated as effective. *S. pasteurii* is found to precipitate under oxic conditions in both granular and cohesive soils. However, its size (width) is larger than a major part of the pores in clays, thus restricting its movement within such soils or soils with incre-

asing share of fines. *S. pasteurii*s cell growth and capacity for producing urease enzyme over time in anoxic conditions is found to be uncertain, but unlikely. Further research on ureolytic capacity under anoxic conditions is needed.

- **Achieved enhancement of shear strength and reduction of permeability in MICP-treated granular soils.**

A high number of studies on MICP in sand, have provided the work conducted on this thesis, with a strong basis for a conclusive evaluation of achieved improvement in shear strength as well as reduction in permeability of MICP-treated sands.

As presented in chapter 5.2, the research demonstrate that the shear strength increase and the permeability decrease, exponentially with increasing CCC for higher levels of cementation ($CCC \geq 3\%$). Lower ($CCC < 3\%$) levels of cementation is indicated to not alter the drained volumetric response or failure mode from untreated to treated state, in sands. The research further indicate that maintaining residual permeability in sands while achieving increased shear strength during MICP treatment, is feasible. This thesis find that these results, support the evaluation of MICP as viable in granular soils under oxic conditions.

- **Achieved enhancement of shear strength in MICP-treated cohesive soils.**

Limited results for triaxial shear strength and volumetric response in MICP-treated fine silt and clay, have limited the basis for the evaluation. However an adequate number of studies addressing UCS in cohesive soils have been obtained during the work on this thesis. The research demonstrate viable urease activity and consequent precipitation under oxic conditions in cohesive soils, where the findings converge on increased shear strength in MICP-treated silt and clay, while diverge on the effect of increasing share of fines in the soil. The findings suggest a possible different effect of cementation on the stress-strain response during shear in clays with high share of clay particles (fat clay), compared to silty clays with higher share of more coarse particles. This is of significant geotechnical importance and need to be further studied.

6.2 Viability of MICP with *S. pasteurii*

The evaluation of MICPs viability as a method for ground improvement, have been restricted by insufficient number of studies on MICP in cohesive soils as well as bacterias ureolytic capacity under anoxic conditions. However, the work conducted in this thesis have provided sufficient basis for evaluation of some of the requirements for viability set in chapter 3.14 and 5.5, while insufficient for others. Further work is needed on the long-term effect of corrosion due to acidic conditions, erosion due to cyclic FT and cyclic WD on the CaCO_3 binder, the effect of low temperatures on urease activity, crystal quality and cementation pattern, the effect of saturation on cementation pattern and residual permeability as well as the effect of clay minerals or small pore space on urease activity.

Ureolytic capacity is found to be functional under a broad range of temperature, while such capacity over time in anoxic conditions is uncertain, but unlikely. Ureolysis under low temperatures in cohesive soils have not been demonstrated, but indications are that other factors specific to the cohesive soil could affect the ureolysis, independent of the temperature.

MICP is found to reduce permeability in granular soils, increase shear strength in both granular and cohesive soils, where control of residual permeability in granular soils post-treatment, is found to be feasible by adjusting the factors governing the precipitation rate and hence the cementation pattern. However, a possible independent effect from saturation on the cementation pattern and hence the residual permeability suggest a need for further research.

The removal of the byproducts such as ammonium and ammonia have been considered a problematic issue for the viability of MICP, where this thesis finds that removal of ammonium post-treatment in granular soils have been demonstrated as viable in the field and that generated ammonia can be reduced by the use of a proper solution. Such removal in cohesive soil have not been evaluated in the research and would probably encounter the same challenges as injections in such soils, due to the low permeability. This means that the approach with injection and extraction of rinsing solution applied for NH_4^+ removal in granular soils, most likely will be ineffective in cohesive soils.

Achieving a degree of spatial distribution of CaCO_3 and control of crystal size and cementation pattern is found to be feasible in granular soils by adjusting affec-

ting factors during treatment, whereas uniform spatial distribution in granular soils could possibly be achieved by the approach proposed in this thesis and presented in chapter 5.5. Achieving distribution by using low pressure injections in cohesive soil or distribution across low permeability layers within stratified soil deposits with varying permeability, is found to be unlikely. However, this thesis proposes the evaluation of an approach for MICP-treatment in cohesive soils as presented in chapter 5.5.

The current uncertainty regarding sustained ureolytic activity under anoxic conditions limits the application of MICP to the unsaturated zone or in soils close to the phreatic line or watertable. However, solutions for supplying oxygen to the saturated zone have been proposed, but still not demonstrated on larger scale in the field. Due to the heterogeneity of physical, environmental and chemical properties of ground conditions in situ, more studies implemented as large scale field studies should be conducted. Such studies in varying ground conditions would encounter a variation in affecting variables, where the gained data and experience can be utilized to adapt strategies which can enable MICP to be more adaptive and predictable in the presence of different ground conditions.

The studies used as basis for an evaluation of the effect of FT cycles on the CaCO_3 binder, only applied up to 10 cycles. Given an estimated service life of 50 years and a high number of FT cycles per year, studies with a much higher number of FT cycles are needed for an proper evaluation of MICP in cold climate ground conditions.

This thesis finds that the greatest challenges facing MICP as a method for ground improvement are uniform distribution of CaCO_3 , predictability and controllability of residual permeability in granular soils, injection and distribution of fluids and removal of byproducts in cohesive soils, deep soil treatment and distribution of CaCO_3 binder across layers of low permeability in stratified soils with varying permeability. The findings of this thesis supports viability of MICP with *S. pasteurii* in areas without cyclic FT under oxic conditions in granular soils. It further finds that ureolysis and consequent precipitation under oxic conditions is viable in cohesive soils. However, MICP is at the current stage of development evaluated to not be viable in cohesive soils due to the lack of strategies that can enable injection and distribution of fluids in and within low permeability soils as well as the challenge in removing the byproducts from cohesive soils through injection and extraction of rinsing solutions.

6.3 Further work

This thesis proposes two different approaches to be evaluated through further research as potential strategies for implementing MICP in granular soils and fine grained soils. The approach for granular soils consist of combining independent methods demonstrated to be viable by other researchers into one integrated approach, while the proposal for injection in fine soils is based on the same principals as MSM or DSM, replacing cement and lime products with bacteria and cementation solution in one integrated solution.

Suggested approach for MICP-treatment in granular soils:

- For field application of MICP in granular soils, the one-phase low pH solution proposed by (Cheng et al., 2019) containing both CaCl_2 /urea and bacteria, applied through grids of injection and extraction wells with spacing < 2,8 m utilized by (Van Paassen, 2009a, Van der Star et al., 2011) with injections in both directions of the flowfield, should be evaluated as an integrated solution. The injection and extraction wells would need pumps that can switch from injection to extraction in an easy and rapid manner.
- The individual methods have been proposed and tested individually with promising results, but not all together as a combined approach. The low pH of the solution, delay the precipitation, enabling the solution to reach further into the soil before precipitation is initiated and the reversed injections enhances distribution with distance from injection point in both directions.

Suggested approach for MICP-treatment in fine silt and clay:

- For field application of MICP in fine silt and clay, mechanical mixing in situ under high injection pressure with a low pH one-phase solution should be evaluated. This would require a study on the ureolytic bacterias resistance to lysis when exposed to high pressures and shear forces as well as the effect of clay minerals and small pore space on urease activity.
- NH_4^+ removal post-treatment in cohesive soils with this approach, will likely encounter the same challenges as injections in low permeability soils

and need to be addressed with a different approach than the approach with injection and extraction of rinsing solution, applied in granular soils.

Further research is needed on:

- Urease activity under anoxic conditions
- Bacterial metabolism when located in small pore space
- Effect of saturation on cementation pattern and residual permeability
- Urease activity in the presence of clay minerals
- Crystal growth in the presence of organic matter
- Effect from share of coarse particles on stress-strain behaviour of MICP-treated cohesive soils

7. Bibliography

2021. NORSK KLIMASERVICE SENTER. Available:
<https://klimaservicesenter.no/faces/desktop/article.xhtml?uri=klimaservicesenteret/Klimanormaler> [Accessed 01 30].
- AL-ANI, T. & SARAPÄÄ, O. 2008. Clay and clay mineralogy. *Physical-chemical properties and industrial uses*.
- AL-THAWADI, S. & CORD-RUWISCH, R. 2012. Calcium carbonate crystals formation by ureolytic bacteria isolated from Australian soil and sludge. *J Adv Sci Eng Res*, 2, 12-26.
- AL QABANY, A., SOGA, K. & SANTAMARINA, C. 2012. Factors affecting efficiency of microbially induced calcite precipitation. *Journal of Geotechnical and Geoenvironmental Engineering*, 138, 992-1001.
- ALSHIBLI, KHALID A. & ALSALEH, M. I. 2003. Characterizing Surface Roughness and Shape of Sands Using Digital Microscopy. baton rouge: Louisiana State University.
- ALSHIBLI, K. A. & ALSALEH, M. I. 2004. Characterizing surface roughness and shape of sands using digital microscopy. *Journal of computing in civil engineering*, 18, 36-45.
- ANDREW, R. M. 2019. Global CO₂ emissions from cement production, 1928–2018. CICERO Center for International Climate Research, Oslo 0349, Norway.
- ARUNACHALAM, K. D., SATHYANARAYANAN, K., DARSHAN, B. & RAJA, R. B. 2010. Studies on the characterisation of Biosealant properties of *Bacillus sphaericus*. *International Journal of Engineering Science and Technology*, 2, 270-277.
- ASGHARZADEH, M., SAMADI KAFIL, H., FAHMI, A., YOUSEFI, M., AGHAZADEH, M. & POURSTADI, M. 2016. Optimizing the use of *Sporosarcina pasteurii* bacteria for the stiffening of sand. *Asian J Microbiol Biotechnol Environ Sci*, 18, 391-394.
- BEHZADIPOUR, H., PAKBAZ, M. S. & GHEZELBASH, G. R. 2019. Effects of biocementation on strength parameters of silty and clayey sands. *Bioinspired, Biomimetic and Nanobiomaterials*, 9, 24-32.
- BHADUR, S., DEBNATH, N., MITRA, S., LIU, Y. & KUMA, A. 2016. Microbiologically Induced Calcite Precipitation Mediated by *Sporosarcina*. Department of Mechanical Engineering, University of Alberta.
- BINDU J, K. K., SAJNA S. 2017. Biocementation in Marine Clays: Effect on Grain Size Distribution *Indian Geotechnical Conference 2017 GeoNEs*. Department of Civil Engineering, College of Engineering, Trivandrum -.
- BING, L. 2015. Geotechnical properties of biocement treated sand and clay. *School of Civil and Environmental Engineering, Nanyang Technological University*.
- BITTON, G. & HARVEY, R. W. 1992. Transport of pathogens through soils and aquifers. *Environmental microbiology*, 19, 103-123.
- BORDERS, H. W. 2021. Groundwater and Geotechnical Problems.
- BUDHU, M. 2008. *SOIL MECHANICS AND FOUNDATIONS, (With CD)*, John Wiley & Sons.
- CACCHIO, P., ERCOLE, C., CAPPUCCIO, G. & LEPIDI, A. 2003. Calcium carbonate precipitation by bacterial strains isolated from a limestone cave and from a loamy soil. *Geomicrobiology Journal*, 20, 85-98.
- CHANG, N., HEYMANN, G. & CLAYTON, C. 2011. The effect of fabric on the behaviour of gold tailings. *Géotechnique*, 61, 187-197.
- CHAPARRO-ACUÑA, S. P., BECERRA-JIMÉNEZ, M. L., MARTÍNEZ-ZAMBRANO, J. J. & ROJAS-SARMIENTO, H. A. 2018. Soil bacteria that precipitate calcium carbonate: mechanism and applications of the process. *Acta Agronómica*, 67, 277-288.
- CHEN, J., FANG, Y., GU, R., SHU, H., BA, L. & LI, W. 2019. Study on pore size effect of low permeability clay seepage. *Arabian Journal of Geosciences*, 12, 1-10.

- CHEN, T., KAO, C., CHIOU, H., YU, Y. & SUNG, W. Application of oxygen-releasing material to enhance in situ aerobic bioremediation. *Advanced Materials Research*, 2012. Trans Tech Publ, 1401-1404.
- CHEN, Y.-C., ISHIBASHI, I. & JENKINS, J. 1988. Dynamic shear modulus and fabric: part I, depositional and induced anisotropy. *Géotechnique*, 38, 25-32.
- CHENG, L. & CORD-RUWISCH, R. 2012. In situ soil cementation with ureolytic bacteria by surface percolation. *Ecological Engineering*, 42, 64-72.
- CHENG, L., CORD-RUWISCH, R. & SHAHIN, M. A. 2013. Cementation of sand soil by microbially induced calcite precipitation at various degrees of saturation. *Canadian Geotechnical Journal*, 50, 81-90.
- CHENG, L., QIAN, C., WANG, R. & WANG, J. 2007. Study on the mechanism of calcium carbonate formation induced by carbonate-mineralization microbe. *Acta Chimica Sinica*, 65, 2133-2138.
- CHENG, L., SHAHIN, M. & CORD-RUWISCH, R. 2014. Bio-cementation of sandy soil using microbially induced carbonate precipitation for marine environments. *Géotechnique*, 64, 1010-1013.
- CHENG, L. & SHAHIN, M. A. Assessment of different treatment methods by microbial-induced calcite precipitation for clayey soil improvement. 68th Canadian Geotechnical Conference, GeoQuebec 2015, 2015.
- CHENG, L., SHAHIN, M. A. & CHU, J. 2019. Soil bio-cementation using a new one-phase low-pH injection method. *Acta Geotechnica*, 14, 615-626.
- CHENG, L., SHAHIN, M. A. & MUJAH, D. 2016. Influence of Key Environmental Conditions on Microbially Induced Cementation for Soil Stabilization. *Journal of Geotechnical and Geoenvironmental Engineering*.
- CHENG, L., SHAHIN, M. A. & MUJAH, D. 2017. Influence of key environmental conditions on microbially induced cementation for soil stabilization. *Journal of Geotechnical and Geoenvironmental Engineering*, 143, 04016083.
- CHOI, S.-G., CHANG, I., LEE, M., LEE, J.-H., HAN, J.-T. & KWON, T.-H. 2020a. Review on geotechnical engineering properties of sands treated by microbially induced calcium carbonate precipitation (MICP) and biopolymers. Korea Institute of Civil Engineering and Building Technology (KICT), 238 Goyangdae-ro, Ilsanseo-gu, Goyang, Republic of Korea.
- CHOI, S.-G., CHANG, I., LEE, M., LEE, J.-H., HAN, J.-T. & KWON, T.-H. 2020b. Review on geotechnical engineering properties of sands treated by microbially induced calcium carbonate precipitation (MICP) and biopolymers. *Construction and Building Materials*, 246, 118415.
- COLLINS, K. T. & MCGOWN, A. 1974. The form and function of microfabric features in a variety of natural soils. *Geotechnique*, 24, 223-254.
- CONSOLI, N., PRIETTO, P. D. M. & ULBRICH, L. A. 1998. Influence of fiber and cement addition on behavior of sandy soil. *Journal of Geotechnical and Geoenvironmental Engineering*.
- COVICORP. 2020. Accusand.
- CROWLEY, R., ZIMMERMAN, A., HUDYMA, N. & WASMAN, S. J. 2019. Application of Microbial Induced Calcite Precipitation to Stabilize Florida High-Organic Matter Soils for Roadway Construction. Florida. Department of Transportation.
- CUI, M.-J., LAI, H.-J., HOANG, T. & CHU, J. 2021. One-phase-low-pH enzyme induced carbonate precipitation (EICP) method for soil improvement. *Acta Geotechnica*, 16, 481-489.
- CUI, M.-J., ZHENG, J.-J., ZHANG, R.-J., LAI, H.-J. & ZHANG, J. 2017a. Influence of cementation level on the strength behaviour of bio-cemented sand. *Acta Geotechnica*, 12, 971-986.
- CUI, M.-J., ZHENG, J.-J., ZHANG, R.-J. & LAILAI, H. L. 2017b. Influence of cementation level on the strength behaviour of bio-cemented sand. *Acta Geotechnica* 12.
- DE MOEL, P., VAN DER HELM, A., VAN RIJN, M., VAN DIJK, J. & VAN DER MEER, W. 2013. Assessment of calculation methods for calcium carbonate saturation in drinking water for DIN 38404-10 compliance. *Drinking water engineering and science*, 6, 115-124.
- DEJONG, J., MARTINEZ, B., MORTENSEN, B., NELSON, D., WALLER, J., WEIL, M., GINN, T., WEATHERS, T., BARKOUKI, T. & FUJITA, Y. 2009. Upscaling of bio-mediated soil improvement. Idaho National Laboratory (INL).

- DEJONG, J., SOGA, K., KAVAZANJIAN, E., BURNS, S., VAN PAASSEN, L., AL QABANY, A., AYDILEK, A., BANG, S., BURBANK, M. & CASLAKE, L. F. Biogeochemical processes and geotechnical applications: progress, opportunities and challenges. *Bio-and Chemo-Mechanical Processes in Geotechnical Engineering: Géotechnique Symposium in Print 2013, 2014*. Ice Publishing, 143-157.
- DEJONG, J. T., MORTENSEN, B. M., MARTINEZ, B. C. & NELSON, D. C. 2010. Bio-mediated soil improvement. *Ecological Engineering*, 36, 197-210.
- DUPRAZ, S., PARMENTIER, M., MÉNEZ, B. & GUYOT, F. 2009. Experimental and numerical modeling of bacterially induced pH increase and calcite precipitation in saline aquifers. *Chemical Geology*, 265, 44-53.
- DURAISAMY, Y. 2016. Strength and stiffness improvement of bio-cemented Sydney sand.
- EL MOUNTASSIR, G., MINTO, J. M., VAN PAASSEN, L. A., SALIFU, E. & LUNN, R. J. 2018. Applications of microbial processes in geotechnical engineering. *Advances in applied microbiology*, 104, 39-91.
- EMDAL, A., GRANDE, L. & NORDAL, S. 2009. Geoteknikk beregningsmetoder. *Kompendium for bruk i emne TBA4105*.
- FAUSKERUD, O. A., ATHANASIU, C., HAVNEGJERDE, C. R., TØRUM, E., CHRISTENSEN, S. O. & GYLLAND, A. 2012. Bruk av anisotropiforhold i stabilitetsberegninger i sprøbruddmaterialer.
- FENG, K. & MONTOYA, B. 2016. Influence of confinement and cementation level on the behavior of microbial-induced calcite precipitated sands under monotonic drained loading. *Journal of Geotechnical and Geoenvironmental Engineering*, 142, 04015057.
- FERRICK, M. & GATTO, L. W. 2005. Quantifying the effect of a freeze–thaw cycle on soil erosion: laboratory experiments. *Earth Surface Processes and Landforms: The Journal of the British Geomorphological Research Group*, 30, 1305-1326.
- FERRIS, F. G., PHOENIX, V., FUJITA, Y. & SMITH, R. 2004. Kinetics of calcite precipitation induced by ureolytic bacteria at 10 to 20 C in artificial groundwater. *Geochimica et Cosmochimica Acta*, 68, 1701-1710.
- FUJITA, Y., REDDEN, G. D., INGRAM, J. C., CORTEZ, M. M., FERRIS, F. G. & SMITH, R. W. 2004. Strontium incorporation into calcite generated by bacterial ureolysis. *Geochimica et cosmochimica acta*, 68, 3261-3270.
- GILLMAN, E., MORGAN, M. & SHERWOOD, M. Urease activity in Irish soils at 6 C. *Biology and Environment: Proceedings of the Royal Irish Academy*, 1995. JSTOR, 19-26.
- GINN, T., MURPHY, E., CHILAKAPATI, A. & SEEBONRUANG, U. 2001. Stochastic-convective transport with nonlinear reaction and mixing: application to intermediate-scale experiments in aerobic biodegradation in saturated porous media. *Journal of contaminant hydrology*, 48, 121-149.
- GODAVARTHI RAJANI, V. R. G., ARIF ALI BAIG MOGHAL 2020. Bio-Cementation of Fat Clay using MICP. *Indian Geotechnical Conference 2020*. Visakhapatnam, India: Researchgate.
- GOMEZ, M. G., GRADDY, C. M., DEJONG, J. T., NELSON, D. C. & TSESARSKY, M. 2018. Stimulation of native microorganisms for biocementation in samples recovered from field-scale treatment depths. *Journal of Geotechnical and Geoenvironmental Engineering*, 144, 04017098.
- GOROSPE, C. M., HAN, S.-H., KIM, S.-G., PARK, J.-Y., KANG, C.-H., JEONG, J.-H. & SO, J.-S. 2013. Effects of different calcium salts on calcium carbonate crystal formation by *Sporosarcina pasteurii* KCTC 3558. *Biotechnology and bioprocess engineering*, 18, 903-908.
- GOWTHAMAN, S., MOHSENZADEH, A., NAKASHIMA, K., NAKAMURA, H. & KAWASAKI, S. 2020. Evaluation on the Performance of MICP Treated Slope Soil Under Acid Rain Environment.
- GOWTHAMAN, S., NAKASHIMA, K. & KAWASAKI, S. 2021. Effect of wetting and drying cycles on the durability of bio-cemented soil of expressway slope. *International Journal of Environmental Science and Technology*, 1-14.
- GRIFFITHS, B. 1986. Can cell culture medium costs be reduced? Strategies and possibilities. *Trends in Biotechnology*, 4, 268-272.
- GROUTING, B. J. 2021. et grouting

- HAMDAN, N., KAVAZANJIAN JR, E. & RITTMANN, B. E. Sequestration of radionuclides and metal contaminants through microbially-induced carbonate precipitation. Proc. 14th Pan American Conf. Soil Mech. Geotech. Engng, Toronto, 2011.
- HAMMAD, I. A., TALKHAN, F. & ZOHEIR, A. 2013. Urease activity and induction of calcium carbonate precipitation by *Sporosarcina pasteurii* NCIMB 8841. *Journal of Applied Sciences Research*, 9, 1525-1533.
- HAMMES, F., BOON, N., DE VILLIERS, J., VERSTRAETE, W. & SICILIANO, S. D. 2003. Strain-specific ureolytic microbial calcium carbonate precipitation. *Applied and environmental microbiology*, 69, 4901-4909.
- HAMZA, M. A. & ANDERSON, W. 2005. Soil compaction in cropping systems: A review of the nature, causes and possible solutions. *Soil and Tillage Research* 82(2):121–145.
- HARKES, M. P., VAN PAASSEN, L. A., BOOSTER, J. L., WHIFFIN, V. S. & VAN LOOSDRECH, M. C. M. 2010a. Fixation and distribution of bacterial activity in sand to induce carbonate precipitation for ground reinforcement. *Ecol.Eng.*, vol. 36,.
- HARKES, M. P., VAN PAASSEN, L. A., BOOSTER, J. L., WHIFFIN, V. S. & VAN LOOSDRECHT, M. C. 2010b. Fixation and distribution of bacterial activity in sand to induce carbonate precipitation for ground reinforcement. *Ecological Engineering*, 36, 112-117.
- HOLTZ, R. D., KOVACS, W. D. & SHEAHAN, T. C. 1981. *An introduction to geotechnical engineering*, Prentice-Hall Englewood Cliffs.
- HSU, C.-M., HUANG, Y.-H., NIMJE, V. R., LEE, W.-C., CHEN, H.-J., KUO, Y.-H., HUANG, C.-H., CHEN, C.-C. & CHEN, C.-Y. 2017. Comparative Study on the Sand Bioconsolidation through Calcium Carbonate Precipitation by *Sporosarcina pasteurii* and *Bacillus subtilis*. Crystals.
- INGHAM, E. R. 2021. Soil Bacteria.
- INGLETT, P., REDDY, K. & CORSTANJE, R. 2005. Anaerobic soils.
- ISLAM, M. T., CHITTOORI, B. C. & BURBANK, M. 2020. Evaluating the applicability of biostimulated calcium carbonate precipitation to stabilize clayey soils. *Journal of Materials in Civil Engineering*, 32, 04019369.
- ISMAIL, M., JOER, H., RANDOLPH, M. & MERITT, A. 2002. Cementation of porous materials using calcite. *Géotechnique* 52(5):313-324.
- JAIN, S. & ARNEPALLI, D. 2019. Biochemically induced carbonate precipitation in aerobic and anaerobic environments by *Sporosarcina pasteurii*. *Geomicrobiology Journal*, 36, 443-451.
- JIANYUN, W. R. Q. C. W. 2005. Study on microbiological precipitation of CaCO₃. *Journal of Southeast University (Natural Science Edition)*, S1.
- K:R, A. 2004. *Soil mechanics and foundation engineering*, New Delhi, Standard Publishers Distribution.
- KANNAN, K., BINDU, J. & VINOD, P. 2020. Engineering behaviour of MICP treated marine clays. *Marine Georesources & Geotechnology*, 38, 761-769.
- KEYKHA, H. A., ASADI, A. & ZAREIAN, M. 2017. Environmental factors affecting the compressive strength of microbially induced calcite precipitation-treated soil. *Geomicrobiology Journal*, 34, 889-894.
- KHAN, J. A. 2011. Biodegradation of azo dye by moderately halotolerant *Bacillus megaterium* and study of enzyme azoreductase involved in degradation. *Advanced Biotech*, 10, 21-27.
- KIM, D., PARK, K. & KIM, D. 2014. Effects of ground conditions on microbial cementation in soils. *Materials*, 7, 143-156.
- KIM, G., KIM, J. & YOUN, H. 2018. Effect of temperature, pH, and reaction duration on microbially induced calcite precipitation. *Applied Sciences*, 8, 1277.
- KNAPPETT, J. & CRAIG, R. F. 2012. *Craig's soil mechanics*, CRC press.
- KONSTANTINOUC, C., WANG, Y., BISCONTIN, G. & SOGA, K. 2021. The role of bacterial urease activity on the uniformity of carbonate precipitation profiles of bio-treated coarse sand specimens. *Scientific reports*, 11, 1-17.

- KRALJ, D., BREČEVIĆ, L. & NIELSEN, A. E. 1994. Vaterite growth and dissolution in aqueous solution II. Kinetics of dissolution. *Journal of crystal growth*, 143, 269-276.
- KUILA, U. & PRASAD, M. 2013. Specific surface area and pore-size distribution in clays and shales. *Geophysical Prospecting*, 61, 341-362.
- LAMKA, K. G., LECHEVALLIER, M. W. & SEIDLER, R. J. 1980. Bacterial contamination of drinking water supplies in a modern rural neighborhood. *Applied and Environmental Microbiology*, 39, 734-738.
- LEE, M., GOMEZ, M. G., SAN PABLO, A. C., KOLBUS, C. M., GRADDY, C. M., DEJONG, J. T. & NELSON, D. C. 2019a. Investigating ammonium by-product removal for ureolytic bio-cementation using meter-scale experiments. *Scientific reports*, 9, 1-15.
- LEE, M., GOMEZ, M. G., SAN PABLO, A. C. M., KOLBUS, C. M., GRADDY, C. M. R., DEJONG, J. T. & NELSON, D. C. 2019b. Investigating Ammonium Byproduct Removal for Ureolytic Biocementation Using Meter-scale Experiments. *Scientific Reports* | (2019) 9:18313.
- LI, J., VASANTHAN, T. & BRESSLER, D. C. 2012. Improved cold starch hydrolysis with urea addition and heat treatment at subgelatinization temperature. *Carbohydrate Polymers*, 87, 1649-1656.
- LIN, H. 2016. *Microbial Modification of Soil for Ground Improvement*, Lehigh University.
- LIN, H., SULEIMAN, M. T., BROWN, D. G. & KAVAZANJIAN JR, E. 2016. Mechanical behavior of sands treated by microbially induced carbonate precipitation. *Journal of Geotechnical and Geoenvironmental Engineering*, 142, 04015066.
- LIU, P., SHAO, G.-H. & HUANG, R.-P. 2019. Study of the interactions between *S. pasteurii* and indigenous bacteria and the effect of these interactions on the MICP. *Arab. J. Geosci.*
- MA, L., PANG, A.-P., LUO, Y., LU, X. & LIN, F. 2020a. Beneficial factors for biomineralization by ureolytic bacterium *Sporosarcina pasteurii*. *Microbial cell factories*, 19, 1-12.
- MA, L., PANG, A. P., LUO, Y., LU, X. & LIN, F. 2020b. Beneficial factors for biomineralization by ureolytic bacterium *Sporosarcina pasteurii*. Jiangsu: State Key Laboratory of Bioelectronics, School of Biological Science and Medical Engineering, Southeast University.
- MAKBOUL, H. & OTTOW, J. 1979. Clay minerals and the Michaelis constant of urease. *Soil Biology and Biochemistry*, 11, 683-686.
- MARTIN, D., DODDS, K., NGWENYA, B. T., BUTLER, I. B. & ELPHICK, S. C. 2012. Inhibition of *Sporosarcina pasteurii* under anoxic conditions: implications for subsurface carbonate precipitation and remediation via ureolysis. *Environmental science & technology*, 46, 8351-8355.
- MINTO, J. M., EL MOUNTASSIR, G. & LUNN, R. J. Micro-continuum modelling of injection strategies for microbially induced carbonate precipitation. E3S Web of Conferences, 2019. EDP Sciences, 11019.
- MINTO, J. M., MACLACHLAN, E., EL MOUNTASSIR, G. & LUNN, R. J. 2016. Rock fracture grouting with microbially induced carbonate precipitation. *Water Resources Research*, 52, 8827-8844.
- MITCHELL, A. C., ESPINOSA-ORTIZ, E. J., PARKS, S. L., PHILLIPS, A. J., CUNNINGHAM, A. B. & GERLACH, R. 2019. Kinetics of calcite precipitation by ureolytic bacteria under aerobic and anaerobic conditions. *Biogeosciences*, 16, 2147-2161.
- MITCHELL, J. K. & SANTAMARINA, J. C. 2005a. Biological considerations in geotechnical engineering. *Journal of geotechnical and geoenvironmental engineering*, 131, 1222-1233.
- MITCHELL, J. K. & SANTAMARINA, J. C. 2005b. Biological Considerations in Geotechnical Engineering. *JOURNAL OF GEOTECHNICAL AND GEOENVIRONMENTAL ENGINEERING © ASCE / OCTOBER 2005*.
- MITCHELL, J. K. & SOGA, K. 2005. *Fundamentals of soil behavior*, John Wiley & Sons New York.
- MONTOYA, B. & DEJONG, J. 2015. Stress-strain behavior of sands cemented by microbially induced calcite precipitation. *Journal of Geotechnical and Geoenvironmental Engineering*, 141, 04015019.
- MONTOYA, B. M. 2012. *Bio-mediated soil improvement and the effect of cementation on the behavior, improvement, and performance of sand*, University of California, Davis.

- MORTENSEN, B., HABER, M., DEJONG, J., CASLAKE, L. & NELSON, D. 2011a. Effects of environmental factors on microbial induced calcium carbonate precipitation. *Journal of applied microbiology*, 111, 338-349.
- MORTENSEN, B. M., HABER, M. J., DEJONG, J. T., CASLAKE, L. F. & NELSON, D. C. 2011b. Effects of environmental factors on microbial induced calcium carbonate precipitation. Department of Civil and Environmental Engineering, University of California.
- MOYO, C., KISSEL, D. & CABRERA, M. 1989. Temperature effects on soil urease activity. *Soil Biology and Biochemistry*, 21, 935-938.
- MUIR WOOD, D., LINGS, M., NASH, D. T. & GAJO, A. Anisotropy of soils: laboratory measurements and constitutive implementation. International Conference on soil mechanics and geotechnical engineering, 2001. 321-324.
- NAEIMI, M. & HADDAD, A. Investigation on the environmental impact of soil improvement techniques: comparison of cement grouting and biocement. GeoShanghai International Conference, 2018. Springer, 483-490.
- NAFISI, A., KHOUBANI, A., MONTOYA, B. M. & EVANS, M. The effect of grain size and shape on mechanical behavior of MICP sand I: Experimental study. Proceedings of the 11th National Conf. in Earthquake Eng., Earthquake Eng. Research Ins. Los Angeles, 2018.
- NAFISI, A., KHOUBANI, A., MONTOYA, B. M. & EVANS, T. M. 2018. The effect of grain size and shape on mechanical behavior of MICP sand I: experimental study. Corvallis, Raleigh: Oregon university, North Carolina university.
- NAYANTHARA, P. G. N., DASSANAYAKE, A. B. N., NAKASHIMA, K. & KAWASAKI, S. 2019. Microbial Induced Carbonate Precipitation Using a Native Inland Bacterium for Beach Sand Stabilization in Nearshore Areas. Faculty of Engineering, Hokkaido University.
- NAYANTHARA, P. G. N., DASSANAYAKE, A. B. N., NAKASHIMA, K. & KAWASAKI, S. 2019. Microbial induced carbonate precipitation using a native inland bacterium for beach sand stabilization in nearshore areas. *Applied Sciences*, 9, 3201.
- NEMATI, M. & VOORDOUW, G. 2003. Modification of porous media permeability, using calcium carbonate produced enzymatically in situ. *Enzyme and microbial technology*, 33, 635-642.
- NG, W.-S., LEE, M.-L. & HUI, S.-L. An overview of the factors affecting microbial-induced calcite precipitation and its potential application in soil improvement. Proceedings of World Academy of Science, Engineering and Technology, 2012a. Citeseer.
- NG, W.-S., LEE, M.-L. & HUI, S.-L. 2012b. An Overview of the Factors Affecting Microbial-Induced Calcite Precipitation and its Potential Application in Soil Improvement. World Academy of Science, Engineering and Technology International Journal of Civil and Environmental Engineering Vol:6, No:2, 2012.
- NIMMO, J. R. 2004. Porosity and pore size distribution. *Encyclopedia of Soils in the Environment*, 3, 295-303.
- NVE, N. V.-O. E. 2021. Grunn- og markvann.
- O'TOOLE, P. & MORGAN, M. 1984. Thermal stabilities of urease enzymes in some Irish soils. *Soil Biology and Biochemistry*, 16, 471-474.
- OKWADHA, G. D. & LI, J. 2010. Optimum conditions for microbial carbonate precipitation. *Chemosphere*, 81, 1143-1148.
- OKYAY, T. O., NGUYEN, H. N., CASTRO, S. L. & RODRIGUES, D. F. 2016. CO₂ sequestration by ureolytic microbial consortia through microbially-induced calcite precipitation. *Science of the Total Environment*, 572, 671-680.
- OLIVEIRA, P. J. V., DA COSTA, M. S. & COSTA, J. N. P. 2015. Comparison of the Ability of Two Bacteria to Improve the Behavior of Sandy Soil. Journal of Materials in Civil Engineering.
- OYEDIRAN, I. A. & AYENI, O. O. 2020. Comparative effect of microbial induced calcite precipitate, cement and rice husk ash on the geotechnical properties of soils. *SN Applied Sciences*, 2, 1-12.
- PENG, J. & LIU, Z. 2019a. Influence of temperature on microbially induced calcium carbonate precipitation for soil treatment. *PloS one*, 14, e0218396.

- PENG, J. & LIU, Z. 2019b. Influence of temperature on microbially induced calcium carbonate precipitation for soil treatment. Varenyam Achal, Guangdong Technion Israel Institute of Technology, CHINA.
- POWERS, M. 1953. A new roundness scale for sedimentary particles: *Journal Sedimentary Petrology*, v. 23.
- PAASSEN, L. V. 2009. Ground Improvement by Microbially Induced Carbonate Precipitation Delft university.
- QABANY, A. A. & SOGA, K. Effect of chemical treatment used in MICP on engineering properties of cemented soils. *Bio-and Chemo-Mechanical Processes in Geotechnical Engineering: Géotechnique Symposium in Print 2013, 2014*. ICE Publishing, 107-115.
- RAHMAN, M., HORA, R. N., AHENKORAH, I., BEECHAM, S., KARIM, R. & IQBAL, A. 2020a. State-of-the-Art Review of Microbial-Induced Calcite Precipitation and Its Sustainability in Engineering Applications. Mawson Lakes: Geotechnical Engineering, University of South Australia, UniSA STEM.
- RAHMAN, M. M., HORA, R. N., AHENKORAH, I., BEECHAM, S., KARIM, M. R. & IQBAL, A. 2020b. State-of-the-art review of microbial-induced calcite precipitation and its sustainability in engineering applications. *Sustainability*, 12, 6281.
- REBATA-LANDA, V. 2007. *Microbial activity in sediments: effects on soil behavior*. Georgia Institute of Technology.
- RONG, H. & QIAN, C. 2012. Characterization of microbe cementitious materials. *Chinese science bulletin*, 57, 1333-1338.
- SAHRAWAT, K. L. 1984. Effects of temperature and moisture on urease activity in semi-arid tropical soils. *Plant and Soil* 78(3):401-408.
- SANDVEN, R., SENNESET, K., EMDAL, A., NORDAL, S., JANBU, N., GRANDE, L. & KORNBRERKE, H. 2012. Geotechnics, field and laboratory investigations. *Norwegian University of Science and Technology (NTNU), Geotechnical Division, Trondheim. Lecture notes: Part, 1*.
- SANDVEN, R., SENNESET, K. A., EMDAL, A., NORDAL, S., JANBU, N., GRANDE, L. & AMUNDSEN, H. A. 2017. *Geotechnics, Field and Laboratory Investigations*, Trondheim, NTNU.
- SANTAMARINA, J. C. 2003. Soil behavior at the microscale: particle forces. *Soil behavior and soft ground construction*.
- SCHIJVEN, J., PANG, L. & YING, G. 2017. Evaluation of subsurface microbial transport using microbial indicators, surrogates and tracers. *Global Water Pathogen Project. Michigan State University*.
- SENER, N. K. 2021. klimanormaler.
- SHAHROKHI-SHAHRAKI, R., ZOMORODIAN, S. M. A., NIAZI, A. & O'KELLY, B. C. 2015. Improving sand with microbial-induced carbonate precipitation. *Proceedings of the Institution of Civil Engineers-Ground Improvement*, 168, 217-230.
- SHARMA, A. & RAMKRISHNAN, R. 2016. Study on effect of microbial induced calcite precipitates on strength of fine grained soils. *Perspectives in Science*, 8, 198-202.
- SHARMA, M., SATYAM, N. & REDDY, K. R. 2021. Effect of freeze-thaw cycles on engineering properties of biocemented sand under different treatment conditions. *Engineering Geology*, 284, 106022.
- SIDIK, W. S., CANAKCI, H., KILIC, I. H. & CELIK, F. 2014. Applicability of biocementation for organic soil and its effect on permeability. *Geomechanics and Engineering*, 7, 649-663.
- SOON, N. W., LEE, L. M., KHUN, T. C. & LING, H. S. 2013. Improvements in engineering properties of soils through microbial-induced calcite precipitation. *KSCE Journal of Civil Engineering*, 17, 718-728.
- SOON, N. W., LEE, L. M., KHUN, T. C. & LING, H. S. 2014. Factors affecting improvement in engineering properties of residual soil through microbial-induced calcite precipitation. *Journal of Geotechnical and Geoenvironmental Engineering*, 140, 04014006.
- STOCKS-FISCHER, S., GALINAT, J. K. & BANG, S. S. 1999. Microbiological precipitation of CaCO₃. *Soil Biology and Biochemistry*, 31, 1563-1571.

- SUN, X., LINCHANG, M., WU, L. & WANG, C. 2019a. Study of magnesium precipitation based on biocementation. *Marine Georesources & Geotechnology*, Volume 37, 2019 - Issue 10.
- SUN, X., MIAO, L. & CHEN, R. 2019b. Effects of different clay's percentages on improvement of sand-clay mixtures with microbially induced calcite precipitation. *Geomicrobiology Journal*, 36, 810-818.
- SUN, X., MIAO, L., WU, L. & WANG, C. 2019c. Study of magnesium precipitation based on biocementation. *Marine Georesources & Geotechnology*, 37, 1257-1266.
- TANG, C.-S., YIN, L.-Y., JIANG, N.-J., ZHU, C., ZENG, H., LI, H. & SHI, B. 2020. Factors affecting the performance of microbial-induced carbonate precipitation (MICP) treated soil: a review. *Environmental Earth Sciences*, 79, 1-23.
- TENG, F., OUEDRAOGO, C. & SIE, Y.-C. 2020. Strength improvement of a silty clay with microbiologically induced process and coir fiber. *J. Geoengin*, 15, 79-88.
- TOBLER, D. J., CUTHBERT, M. O., GRESWELL, R. B., RILEY, M. S., RENSHAW, J. C., HANDLEY-SIDHU, S. & PHOENIX, V. R. 2011. Comparison of rates of ureolysis between *Sporosarcina pasteurii* and an indigenous groundwater community under conditions required to precipitate large volumes of calcite. *Geochimica et Cosmochimica Acta*, 75, 3290-3301.
- TOBLER, L. J., CUTHBERT, M. O. & PHOENIX, V. R. 2014. Transport of *Sporosarcina pasteurii* in sandstone and its significance for subsurface engineering technologies. *Applied Geochemistry*.
- UMAR, M., KASSIM, K., ZANGO, M. & MUHAMMED, A. Performance evaluation of lime and microbial cementation in residual soil improvement. IOP Conference Series: Materials Science and Engineering, 2019. IOP Publishing, 012005.
- VAHED, H. S., SHAHINROKHSAR, P. & REZAEI, M. 2011. Influence of some soil properties and temperature on urease activity in wetland rice soils. *American-Eurasian Journal of Agricultural and Environmental Sciences*, 11, 310-313.
- VAN DER STAR, W., VAN WIJNGAARDEN, W., VAN PAASSEN, L., VAN BAALEN, L. & ZWIETEN, G. Stabilization of gravel deposits using microorganisms. Proceedings of the 15th European Conference on Soil Mechanics and Geotechnical Engineering, Athens, Greece, 5-9 October 2011, 2011. IOS Press.
- VAN ELSAS, J. & PENIDO, E. 1982. Characterization of a new *Bacillus megaterium* bacteriophage, MJ-1, from tropical soil. *Antonie van Leeuwenhoek*, 48, 365-371.
- VAN PASSEN, L. A., GHOS, R., VAN DER LINDEN, T. J. M., VAN DER STAR, W. R. L. & VAN LOOSDRECHT, M. C. M. 2010. Quantifying biomediated ground improvement by ureolysis: Large-scale biogROUT experiment. *Journal of Geotechnical and Geoenvironmental Engineering*.
- VAN PAASSEN, L. A. 2009a. BiogROUT, ground improvement by microbial induced carbonate precipitation.
- VAN PAASSEN, L. A. 2009b. Ground Improvement by tMicrobially Induced Carbonate Precipitation. Delft university.
- VERBA, C., THURBER, A., ALLEAU, Y., KOLEY, D., COLWELL, F. & TORRES, M. 2016. Mineral changes in cement-sandstone matrices induced by biocementation. *International Journal of Greenhouse Gas Control*, 49, 312-322.
- WANG, Y., SOGA, K., DEJONG, J. T. & KABLA, A. J. 2019. Microscale visualization of microbial-induced calcium carbonate precipitation processes. *Journal of Geotechnical and Geoenvironmental Engineering*, 145, 04019045.
- WHIFFIN, V. S. 2004. *Microbial CaCO₃ precipitation for the production of biocement*. Murdoch University.
- WHIFFIN, V. S., VAN PAASSEN, L. A. & HARKES, M. P. 2007. Microbial carbonate precipitation as a soil improvement technique. *Geomicrobiology Journal*, 24, 417-423.
- WHIFFIN, V. S. 2004. *Microbial CaCO₃ precipitation for the production of biocement*. Sdne: Murdoch university.
- WILEY, W. & STOKES, J. 1962. Requirement of an alkaline pH and ammonia for substrate oxidation by *Bacillus pasteurii*. *Journal of bacteriology*, 84, 730-734.

- WILLIAMS, S. L., KIRISITS, M. J. & FERRON, R. D. 2017. Influence of concrete-related environmental stressors on biomineralizing bacteria used in self-healing concrete. *Construction and Building Materials*, 139, 611-618.
- XIAO, J., WEI, Y., CAI, H., WANG, Z., YANG, T., WANG, Q. & WU, S. 2020. Microbial-Induced Carbonate Precipitation for Strengthening Soft Clay. *Advances in Materials Science and Engineering*, 2020.
- XU, G., TANG, Y., LIAN, J., YAN, Y. & FU, D. 2017. Mineralization process of biocemented sand and impact of bacteria and calcium ions concentrations on crystal morphology. *Advances in Materials Science and Engineering*, 2017.
- YANG, D., XU, G. & DUAN, Y. 2020. Effect of Particle Size on Mechanical Property of Bio-Treated Sand Foundation. Tianjin: State Key Laboratory of Hydraulic Engineering Simulation and Safety, Tianjin University.
- YANG, P. & VAN ELSAS, J. D. 2018. Mechanisms and ecological implications of the movement of bacteria in soil. *Applied Soil Ecology*, 129, 112-120.
- YANG, S., SANDVEN, R. & GRANDE, L. Undrained behaviour of silt. International Conference on soil mechanics and geotechnical engineering, 2001. 2265-2270.
- ZAFFAR, M. & SHENG-GAO, L. 2015. Pore size distribution of clayey soils and its correlation with soil organic matter. *Pedosphere*, 25, 240-249.
- ZAMANI, A. & MONTOYA, B. Undrained behavior of silty soil improved with microbial induced cementation. 6th international conference on earthquake geotechnical engineering, 2015. 1-4.
- ZEHNER, J., RØYNE, A., WENTZEL, A. & SIKORSK, P. 2020. Microbial-induced calcium carbonate precipitation: an experimental toolbox for in situ and real time investigation of micro-scale pH evolution. Royal society of Chemistry.
- ZHANG, J. L., WU, R. S., LI, Y. M., ZHONG, J. Y., DENG, X., LIU, B., HAN, N. X. & XING, F. 2016a. Screening of bacteria for self-healing of concrete cracks and optimization of the microbial calcium precipitation process. *Biotechnological products and process engineering*.
- ZHANG, Z., WEI, M., WENJIE, F., DONGHUI, X. & XIN, H. 2016b. Reconstruction of soil particle composition during freeze-thaw cycling: a review. *Pedosphere*, 26, 167-179.
- ZHAO, Q., LI, L., LI, C., LI, M., AMINI, F. & ZHANG, H. 2014. Factors affecting improvement of engineering properties of MICP-treated soil catalyzed by bacteria and urease. *Journal of Materials in Civil Engineering*, 26, 04014094.
- ZYMAN, J. & SORBER, C. 1988. Influence of simulated rainfall on the transport and survival of selected indicator organisms in sludge-amended soils. *Journal (Water Pollution Control Federation)*, 2105-2110.
- AAMODT, G. & DAHL, C. 2016. Magnesium i drikkevannet—Kan rørhelse og folkehelse bli ett?

